PB80-225071

Chemically Active Fluid Bed for SOx Control Volume II. Spent Sorbent Processing for Disposal/Utilization

Westinghouse Research and Development Center
Pittsburgh, PA

Prepared for

Industrial Environmental Research Lab.
Cincinnati, OH

Dec 79

U.S. Department of Commerce
National Technical Information Service
NTIS

TECHNICAL REPORT DATA

(Please read Instructions on the reverse before completing)

1. REPORT NO. EPA-600/7-79-158b	2.	3. RECIPIENT'S ACCESSION NO. PB80 225071
4. TITLE AND SUBTITLE Chemically Active Fluid Bed for SOx Control: Volume II. Spent Sorbent Processing for Disposal/Utilization		5. REPORT DATE December 1979
		6. PERFORMING ORGANIZATION CODE
7. AUTHOR(S) C.H. Peterson		8. PERFORMING ORGANIZATION REPORT NO.
9. PERFORMING ORGANIZATION NAME AND ADDRESS Westinghouse Research and Development Center 1310 Beulah Road Pittsburgh, Pennsylvania 15235		10. PROGRAM ELEMENT NO. EHB536
		11. CONTRACT/GRANT NO. 68-02-2142
12. SPONSORING AGENCY NAME AND ADDRESS EPA, Office of Research and Development Industrial Environmental Research Laboratory Research Triangle Park, NC 27711		13. TYPE OF REPORT AND PERIOD COVERED Final; 7/75-10/79
		14. SPONSORING AGENCY CODE EPA/600/13

15. SUPPLEMENTARY NOTES IERL-RTP project officer is Samuel L. Rakes, Mail Drop 61, 919/541-2825.

16. ABSTRACT The report describes the processing of spent calcium-based sulfur sorbents (limestones or dolomites) from an atmospheric-pressure, chemically active fluid bed (CAFB) gasification process, using a regenerative sulfur sorbent process that produces low- to intermediate-Btu gas. Data are developed to provide a basis for evaluating process concepts to minimize the environmental impact (heat release, H_2S release, and potential leachates) or possibly for spent sorbent utilization. Flow diagrams and cost estimates were prepared for five processing options. A dry sulfation process operating at 850 C to produce spent solids containing $CaSO_4$ acceptable for disposal and low-temperature ash blending to produce a material for disposal or utilization is recommended for further development. A concept for briquetting to produce aggregate is presented as a low-temperature blending option based on laboratory tests that produced compacts with compressive strengths up to 80 MPa. Direct disposal, dead-burning for disposal by heating at 1250 C and reducing the sulfide content to $< 0.03\%$, and sintering at 1550 C to release the sulfur for recovery and produce a possible source of lime containing $< 0.15\%$ sulfur are also investigated. Processing sorbent from a once-through sorbent process containing CaS is also considered.

17. KEY WORDS AND DOCUMENT ANALYSIS

a. DESCRIPTORS		b. IDENTIFIERS/OPEN ENDED TERMS	c. COSATI Field/Group	
Pollution	Aggregates	Pollution Control	13B	11G
Fluidized Bed Processing		Stationary Sources	13H, 07A	
Coal Gasification	Briquetting	Chemically Active Fluid Bed Process		
Calcium Carbonates	Waste Disposal			
Regeneration	Combustion	Spent Sorbent Processing		21B
Sulfation		Dead Burning	07C, 07B	

18. DISTRIBUTION STATEMENT Release to Public	19. SECURITY CLASS *(This Report)* Unclassified	21. NO. OF PAGES
	20. SECURITY CLASS *(This page)* Unclassified	22. PRICE

EPA Form 2220-1 (9-73)

PB80-225071

United States
Environmental Protection
Agency

Industrial Environmental Research
Laboratory
Research Triangle Park NC 27711

EPA-600/7-79-158b
December 1979

EPA

Chemically Active Fluid Bed for SO_x Control: Volume II. Spent Sorbent Processing for Disposal/Utilization

Interagency Energy/Environment R&D Program Report

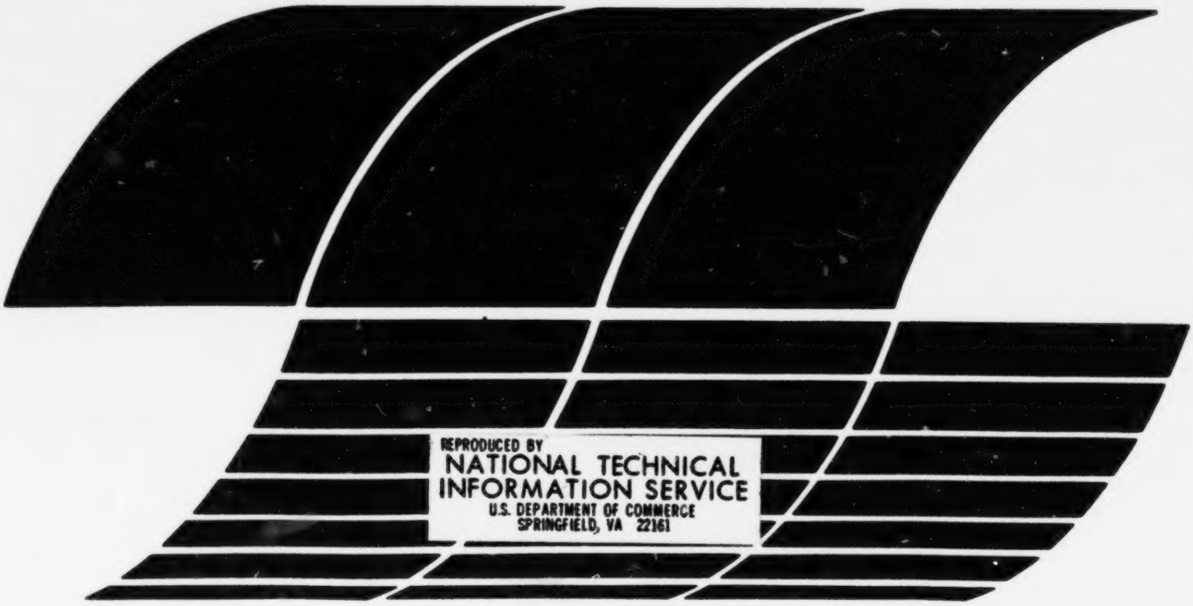

REPRODUCED BY
NATIONAL TECHNICAL
INFORMATION SERVICE
U.S. DEPARTMENT OF COMMERCE
SPRINGFIELD, VA 22161

RESEARCH REPORTING SERIES

Research reports of the Office of Research and Development, U.S. Environmental Protection Agency, have been grouped into nine series. These nine broad categories were established to facilitate further development and application of environmental technology. Elimination of traditional grouping was consciously planned to foster technology transfer and a maximum interface in related fields. The nine series are:

1. Environmental Health Effects Research
2. Environmental Protection Technology
3. Ecological Research
4. Environmental Monitoring
5. Socioeconomic Environmental Studies
6. Scientific and Technical Assessment Reports (STAR)
7. Interagency Energy-Environment Research and Development
8. "Special" Reports
9. Miscellaneous Reports

This report has been assigned to the INTERAGENCY ENERGY-ENVIRONMENT RESEARCH AND DEVELOPMENT series. Reports in this series result from the effort funded under the 17-agency Federal Energy/Environment Research and Development Program. These studies relate to EPA's mission to protect the public health and welfare from adverse effects of pollutants associated with energy systems. The goal of the Program is to assure the rapid development of domestic energy supplies in an environmentally-compatible manner by providing the necessary environmental data and control technology. Investigations include analyses of the transport of energy-related pollutants and their health and ecological effects; assessments of, and development of, control technologies for energy systems; and integrated assessments of a wide range of energy-related environmental issues.

EPA REVIEW NOTICE

This report has been reviewed by the participating Federal Agencies, and approved for publication. Mention of trade names or commercial products does not constitute endorsement or recommendation for use.

This document is available to the public through the National Technical Information Service, Springfield, Virginia 22161.

EPA-600/7-79-158b

December 1979

Chemically Active Fluid Bed for SO_x Control: Volume II. Spent Sorbent Processing for Disposal/Utilization

by

C.H. Peterson

Westinghouse Research and Development Center
1310 Beulah Road
Pittsburgh, Pennsylvania 15235

Contract No. 68-02-2142
Program Element No. EHB536

EPA Project Officer: Samuel L. Rakes

Industrial Environmental Research Laboratory
Office of Environmental Engineering and Technology
Research Triangle Park, NC 27711

Prepared for

U.S. ENVIRONMENTAL PROTECTION AGENCY
Office of Research and Development
Washington, DC 20460

PREFACE

The Westinghouse Research and Development Center is carrying out a program under contract to the United States Environmental Protection Agency (EPA) to provide experimental and engineering support for the development of the Chemically Active Fluid-Bed (CAFB) process. The process was originally conceived at the Esso Research Centre, Abingdon, UK (ERCA), as a fluidized-bed gasification process to convert heavy fuel oils to a clean, medium heating-value fuel gas for firing in a conventional boiler. Westinghouse, under contract to EPA, completed an initial evaluation of the process in 1971.[1] Conceptual designs and cost estimates were prepared for new and retrofit utility boiler applications using heavy fuel oil. Westinghouse continued the process evaluation from 1971 to 1973 and formulated an atmospheric pollution control demonstration plant program for retrofit of a utility boiler utilizing a high-sulfur, high metals-content fuel oil (for example, vacuum bottoms).[2] The CAFB process represented an attractive option for use of these low-grade fuels for which pollution control using hydrodesulfurization or stack-gas cleaning was not economical. Application of a pressurized CAFB concept with combined-cycle power plants was also assessed.[2] Experimental support work was initiated between 1971 and 1973 to investigate two areas of concern - sorbent selection and spent sorbent processing - to achieve an acceptable material for disposal or utilization. The preliminary design and cost estimate for a 50 MWe demonstration plant at the New England Electric System (NEES) Manchester Street Station in Providence, RI were completed in 1975.[3] Commercial plant costs were projected and development requirements identified. Experimental support of the sulfur removal system continued in order to provide a basis for the detailed plant design. A number of design and operating parameters from the preliminary design study that required further development were identified. The disposal of the spent limestone sorbent requires a solution that is economical and environmentally acceptable if the CAFB process is to be commercialized. Westinghouse has processed spent sorbent to produce a material that will meet environmental requirements for disposal or that can be utilized as a resource. This report presents the results of experimental studies and process analyses carried out from 1976 to June 1979 to provide perspective on alternative spent sorbent processing options. Perspective on the relative environmental impact of the processing options is presented in Volume 3 of this report.[4]

Additional support work carried out under the present contract (68-02-2142) includes:

- Sorbent selection[5]
- Solids transport between adjacent CAFB fluidized beds[6]
- Engineering evaluation of the CAFB process.[7]

ABSTRACT

Processing spent calcium-based sulfur sorbents (limestones or dolomites) from an atmospheric-pressure fluidized-bed gasification (Chemically Active Fluid Bed [CAFB]) process is reported. The concept uses a regenerative sulfur sorbent process and produces low- to intermediate-Btu gas. Data are developed to provide a basis for evaluating process concepts to minimize the environmental impact (heat release, H_2S release, and potential leachates) or possibly for utilizing spent sorbent. Flow diagrams and cost estimates were prepared for five processing options. A dry sulfation process operating at 850°C to produce spent solids containing $CaSO_4$ acceptable for disposal and low-temperature ash blending to produce a material for disposal or utilization are recommended for further development. A concept for briquetting to produce aggregate is presented as a low-temperature blending option based on laboratory tests that produced compacts with compressive strengths up to 80 MPa. Direct disposal, deadburning for disposal by heating at 1250°C and reducing the sulfide content to $< 0.03\%$, and sintering at 1550°C to release the sulfur for recovery and produce a possible source of lime containing $< 0.15\%$ sulfur are also investigated. Processing sorbent from a once-through sorbent process containing CaS is also considered. Environmental impact tests on the processed materials are reported in EPA-600/7-79-158c and show that the processing options will reduce the environmental impact of residue disposal and will be required for nonhazardous disposal.

TABLE OF CONTENTS

		Page
	PREFACE	iii
1.	INTRODUCTION	1
2.	SUMMARY AND CONCLUSIONS	3
3.	SPENT SORBENT DISPOSITION	6
	Statement of the Problem	6
	Status of the Investigation	7
	Perspective on the Disposal Problem	7
4.	SPENT SORBENT UTILIZATION	10
	Lime Source	10
	Agriculture	10
	Municipal Sludge Treatment	13
	Acid Mine Drainage	14
	Industrial Applications	15
	Calcium Sulfate Source	18
	Construction Uses	20
	Aggregate	20
	Cement	23
5.	SPENT SORBENT PROCESSING	24
	Direct Disposal	24
	Dead-Burning	28
	Sintering	30
	Dry Sulfation	32
	Fly Ash Blending - Low Temperature	40
	Fly Ash Blending - High Temperature	43
	Calcium Sulfide Processing	43

Preceding page blank

TABLE OF CONTENTS (Cont)

Page

Miscellaneous Equipment Sizing 44
- Storage Silos 44
- Kilns 44
- Solids Cooler 45
- Holoflite Cooler 46
- Steam Generation 46

6. ECONOMIC EVALUATION 47

Perspective 47
Basis for Cost Data 47
Capital Cost 48
Assessment 48
- Capital Investment 48
- Environmental Impact 69
- Effect of By-Product Credits 69
- Variations 70

Conclusions 71

7. OCEAN DISPOSAL 72

Background 72
Experimental Work 72
Initial Tests 73
Tests with Seawater 73
Results from Seawater Tests 74
Assessment 77
Conclusions 78

8. REFERENCES 79

APPENDICES

A. Preliminary Dead-Burning/Sintering Studies 83
B. Fluidized-Bed Test Facility 94
C. Fluidization Studies 101

TABLE OF CONTENTS (Cont)

Page

D. Dry Sulfation Studies 108

E. Pore Volume Studies 158

EA. Attachment 204

F. Low-Temperature Fly Ash Blending 218

G. High-Temperature Fly Ash Blending 233

H. Calcium Sulfide Studies 266

I. Test Procedures for in Situ Leaching of Spent Sorbents with Seawater 274

J. Analytical Procedures Used on Samples from Ocean Dumping Tests 277

K. Extraction of Selected Trace Elements by Seawater from Spent Sorbents 282

LIST OF TABLES

Page

1. Crushed Stone Sold or Used by Producers in the United States in 1975 9
2. Lime Sold or Used by Producers in the United States in 1975 11
3. Energy Consumption of the Cement Industry 16
4. Gypsum Supply and Demand in the United States 19
5. Market Data on Selected Construction Materials 21
6. Gas Velocities in the Dry Sulfation of Regenerator Stone in Run CAFB-905 37
7. Comparison of Investments in Stone Processing Options in Oil Gasification 49
8. Equipment List for Direct Disposal Option for Processing Spent CAFB Regenerator Stone 50
9. Equipment List for Dead-Burning Option for Processing Spent CAFB Regenerator Stone 52
10. Equipment List for Sintering Option for Processing Spent CAFB Regenerator Stone 54
11. Equipment List for Dry Sulfation, Absorber Option, for Processing Spent CAFB Regenerator Stone 56
12. Equipment List for Dry Sulfation, Kiln Option, for Processing Spent CAFB Regenerator Stone 58
13. Equipment List for Briquetting Option for Processing Spent CAFB Regenerator Stone 60
14. Equipment Costs for Direct Disposal Options for Processing Spent CAFB Regenerator Stone 62

LIST OF TABLES (CONT'D)

Page

15. Comparison of Investments Required for Dead-Burning and Sintering Options for Processing Spent CAFB Regenerator Stone 63

16. Comparison of Investments Required for Dry Sulfation of Spent CAFB Regenerator Stone 65

17. Investment Required for Briquetting Options for Processing Spent CAFB Regenerator Stone 68

18. Comparison of Trace Elements in Maryland Bay Water with Established Drinking Water Standards 74

19. Comparison of Trace Element Concentration Produced from Spent Sorbents with Established Criteria 77

LIST OF FIGURES

Page

1. Price Index for Selected Commodities 21
2. Direct Disposal of Spent Sorbent from a 200 MW CAFB Plant 25
3. Disposal of Spent Regenerator Stone from a 200 MW CAFB Plant by Dead-Burning 29
4. Disposal of Spent Regenerator Stone from a 200 MW CAFB Plant by Sintering 31
5. Disposal of Spent Regenerator Stone from a 200 MW CAFB Plant by Dry Sulfation with Rotary Kiln 33
6. Disposal of Spent Regenerator Stone from 200 MW CAFB Plant by Dry Sulfation with Absorber 34
7. Sulfur Capture in CAFB Absorber vs. Overall Sulfur Capture at 10% Recycle of Boiler Flue Gas 37
8. Effect of Boiler Flue Gas Recycle on Sulfur Capture Required in CAFB Absorber at 90% Overall Sulfur Capture 37
9. Aggregate Production by Briquetting Spent Sorbent from a 200 MW CAFB Plant-Feed Separation Section 41
10. Aggregate Production by Briquetting Spent Sorbent from a 200 MW CAFB Plant - Briquetting Section 42

NOMENCLATURE

ANL	Argonne National Laboratory
BFW	boiler feedwater
BOP	basic oxygen process
CAFB	chemically active fluidized bed
EPA	Environmental Protection Agency
ERCA	Esso Research Centre, Abingdon, UK
NEES	New England Electric System
PDQS	proprietary equipment and design quote service
PROVES	proprietary service related to PDQS (Project Valuation and Estimation System)
a	ratio of sulfur in regenerator stone and total sulfur leaving regenerator in the spent stone and the off-gas
D_p	particle diameter
G	mass flow rate of gas
h	heat transfer film coefficient
k	thermal inactivity of a particle
Nu_p	Nusselt Number of a particle
Pr	Prandtl Number
R	fraction of boiler flue gas recycled to gasifier
Re_p	Reynolds Number of a particle
S_A	Sulfur content of absorber off-gas recycled to gasifier, moles/hr
S_R	sulfur content of regenerator off-gas fed to absorber, moles/hr
U	heat transfer coefficient
U_{mf}	minimum fluidization velocity
U_o	superficial velocity
V	particle velocity
X_o	overall sulfur capture
X_G	Gasifier sulfur capture

X_A	absorber sulfur capture
μ	gas viscosity
ρ	gas density

ACKNOWLEDGMENT

Many have contributed to the preparation of this report and it is a pleasure to acknowledge as co-workers Drs. M. Gunasekaran and T. K. Gupta of R. B. Grekila's Ceramics and Glasses Department. W. D. Straub performed the sintering and hot-pressing experiments, while G. M. Halgas and S. C. Stroz prepared specimens for the low-temperature studies. Members of F. J. Byrne's Analytical Chemistry Department made a substantial contribution: J. Penkrot and R. J. Nadalin, wet chemistry; J. S. Rudolph, x-ray analyses for total sulfur; C. L. Page and M. B. Theodore, trace element determinations. J. M. Forns of Westinghouse Oceanic Division devised test procedures and was responsible for execution of the tests on the feasibility of disposal of spent sorbent in the ocean. Within the Fossil Fuels and Fluidized Bed Processes Department, D. L. Keairns provided valuable guidance in the management of the project while C. C. Sun provided data on the environmental impact of processed residues. A. C. Gasparovic carried out the fluidization experiments and the various high-temperature experiments in the 10-cm laboratory test unit. Both he and L. M. Thomas were responsible for assembling this apparatus. L. M. Thomas also carried out low-temperature experiments. R. E. Brinza and J. T. McAdams did the numerous sulfate and sulfide determinations. C. W. Beck of Physical Metallurgy made porosimetry measurements, while D. P. Wei of the Computer Department provided a plotting routine for pore volume results. The Research Library under A. Newell was very helpful in obtaining documents from other investigators. Test quantities of spent sorbent were obtained from the pilot plant at Abingdon, UK, through the cooperative efforts of Esso Research Centre personnel, and samples of spent dolomite were obtained from Argonne National Laboratories.

We especially appreciate the support and guidance of the EPA through its project officer, S. L. Rakes.

1. INTRODUCTION

The CAFB (Chemically Active Fluidized Bed) gasification process, in which limestone or dolomite removes the sulfur from fuel gas during the gasification process, was developed to permit the utilization of high-sulfur residual fuel oil or refinery bottoms in conventional boilers by producing a low-sulfur fuel gas. Coal is also being investigated as a fuel. The process can be operated as a once-through limestone sorbent system, a sorbent regeneration/sulfur recovery system, or a sorbent regeneration system without sulfur recovery by capturing the sulfur-rich gas from the regenerator with the spent stone. The spent stone from each system alternative can be processed to minimize the environmental impact of the waste stone for disposal or to provide material for potential market utilization.[3,8]

Under contract to the U. S. Environmental Protection Agency (EPA), Westinghouse has carried out laboratory support work on sulfur removal, solid transport, processing of spent sorbent for disposal or utilization, and the environmental impact of processed and unprocessed residue disposal.[3,8] Esso Research Centre, Abingdon, England (ERCA) has carried out pilot-scale tests to investigate sulfur removal.[9] At San Benito, Texas, a 10 MW demonstration plant has been retrofitted by Foster Wheeler Energy Corporation and Central Power and Light Co. and is being tested.[10]

The CAFB gasification/desulfurization process produces a dry, partially utilized limestone (or dolomite) with particles up to 6000 μm in size. The composition of the sorbent for disposition will depend on the characteristics of the original stone, the fuel feed, the selection of the sorbent processing system, and the process operating conditions. Spent sorbent compositions for the once-through and regenerative operating modes are:

	Solids Composition, wt %	
	Regenerative (regenerator solids)	Once-through (gasifier solids)
CaO	85-95	50-75
CaS	2-5	25-50
$CaSO_4$	2-4	∿1
Inerts	1-10	1-10

Spent sorbent processing to produce a material suitable for disposal or for utilization as a resource is evaluated in the current report. The previous work Westinghouse carried out to identify alternative processing options and to provide a reference plant design and cost has been utilized to guide the experimental and process analysis work reported. On the basis of this information and an assessment of the potential market for alternative products, we have identified priority spent sorbent processing options for study and have obtained experimental data to permit technical evaluation of these options. These analyses and data provide a basis for the development of process flowsheets and a technical evaluation of each spent sorbent processing option. Relative subsystem costs have been prepared to provide a basis for a comparison of the economics of spent sorbent processing options.

2. SUMMARY AND CONCLUSIONS

This evaluation and the experimental screening tests are based on a CAFB plant using a low-grade petroleum residue, such as vacuum bottoms, as fuel. This application of the concept has technical merit and is potentially economical. Spent sorbent from residual oil firing was available for testing; subsequent work has investigated the use of coal as a fuel. The conclusions on spent sorbent processing would generally apply to a coal-fired CAFB, subject to acceptable performance of the system.

The CAFB process generates solid residues comprised of spent sorbent and fuel ash. The spent sorbent used in the development work was a calcium-based material, mainly limestone, which has been shown to require processing to be acceptable for disposal. This report is a continuation of previous studies of residue disposal in which twenty conceptual possibilities were screened on the basis of technical and qualitative factors. Five of these were selected for more detailed evaluation through development of process flowsheets and capital cost requirements.

Laboratory data were obtained to provide the technical basis for the various process designs. Cost data were obtained from a proprietary service, from scale-ups and updates from previous estimates, and from direct quotations from vendors. All such data have been adjusted to July 1978. Market data for various commercial utilizations were obtained from government statistics.

The investigations and evaluations reported herein show that the dry sulfation option for spent sorbent disposal is the most attractive of the five examined. As a subsystem, it is the most expensive, either as percent of plant cost or relatively, but its ultimate cost advantage results from elimination of a sulfur recovery plant. The latter by itself costs three to eight times as much as the stone processing subsystem. The estimated cost for the dry sulfation subsystem represents about 15 percent of the CAFB plant cost proper, as was shown in the 1975 report.[3] Backup options are direct disposal, which is attractive if a consumer is able to utilize the material, and briquetting. The direct disposal option, with utilization of the material in building block, is an option for the CAFB demonstration plant in San Benito, Texas.

Further data on the environmental impact of ocean disposal of CAFB residues are presented. We conclude that ocean disposal may be a practicable option, although present requirements are stringent and current EPA policy is to phase out this practice.

RECOMMENDATIONS

We recommend that development work be continued on three of the options studied:

- Dry sulfation (absorber option)
- Direct disposal, with specific focus on direct use in building block
- Briquetting.

Specific technical questions that merit attention include:

- Dry sulfation
  - Calcium utilization as function of particle size
  - Sulfur capture
  - Properties of sulfated residues versus possible commercial uses
  - Maximum gas velocity in the absorber

- Direct disposal
  - Calcium sulfide (CaS) inactivation
  - Slaking process details
  - Reuse possibilities
  - Fixation possibilities
  - Ocean disposal or utilization in reefs
- Briquetting
  - Process simplification through substitution of direct casting
  - Commercial attractiveness of pressed compact properties.
  - Further mechanical and stability tests on the compacts.

In addition, we recommend study of the potential for reducing the cost of sulfur recovery processes.

3. SPENT SORBENT DISPOSITION

STATEMENT OF THE PROBLEM

The use of solid sorbents to capture fossil fuel sulfur during the CAFB gasification process requires the continual withdrawal of the spent sorbent produced through gradual loss of activity and attrition. Twenty alternatives for disposal of this spent sorbent were identified in a prior contract report.[3] The disposal problem is multifaceted, involving considerations of spent sorbent quantities, final chemical form, potential market sizes, available technology, and governmental regulations, especially those regarding environmental impact.

We concluded that, from the standpoint of solubility, the final chemical form for a calcium-based sorbent should be carbonate, silicate, or sulfate if the material is to be exposed to the environment. Phosphate was ruled out because a low-cost source of this ion was, in general, not readily available.

Subsequent work singled out dry sulfation as the most promising of the alternatives. Its major advantage was the elimination of the sulfur recovery plant, thus reducing capital and operating costs and eliminating the problems of coupling a chemical plant to an electric utility. Other processes considered competitive were direct disposal, wet carbonation, dead-burning and oxidation-plus-carbonation.

No option, including sulfur recovery, could count on by-product credits for the near term, and therefore disposal of the sulfur in a form other than sulfur or sulfuric acid (H_2SO_4) was indicated. Finally, ocean dumping, while greatly restricted by existing regulations, was worth exploring, at least for coastal areas.

Although the problem of reducing the spent sorbent production rate was studied, available information indicated the limestone molar makeup rate would be as high as 1:1 on sulfur. It is unlikely that complete elimination of makeup will be achieved.

Specific environmental concerns are:

- Dusting
- The potential leaching of calcium hydroxide ($Ca(OH)_2$), CaS, calcium sulfate ($CaSO_4$), and trace elements
- The heat release on hydration of the calcium oxide (CaO) that typically makes up 85 weight percent of the spent sorbent
- Prevention of hydrogen sulfide (H_2S) release from residual CaS.

Other concerns arise from the quantities involved for even a 200 MWe plant - namely, the size of the disposal site required and the supply of a suitable quality limestone makeup.

STATUS OF THE INVESTIGATION

The current report covers work performed since the 1975 Report.[3] It provides the background data on which to base an evaluation of various conceptual processes for disposing of spent sorbent. The scope of this report is limited to presentation and analysis of the data with, in some cases, qualitative conclusions and preliminary economic comparisons.

The alternative disposal methods currently under active investigation include direct disposal, dry sulfation, dead-burning, sintering, and fly-ash blending. Work has concentrated on the regenerative CAFB process, although the possibility of a once-through process in which spent sorbent is withdrawn from the gasifier has been kept open. This sorbent would contain CaS, ideally to 100 percent utilization of the calcium.

PERSPECTIVE ON THE DISPOSAL PROBLEM

We estimate that a 200 MWe plant using the CAFB process burning a 3 percent sulfur fuel oil and having a sorbent molar makeup rate of 1:1

(Ca/S) would produce about 21,800 Mg/yr (24,000 ton/yr) of spent sorbent containing 91 weight percent CaO, 3 weight percent CaS, and 2.5 weight percent of $CaSO_4$. The balance is impurities from the original limestone and those picked up from the fuel oil.

Estimates of new power generation facilities required in the coming decade vary. Consumption of electric power is currently of the order of 42 million MWh/week, which represents at least 250,000 MW of existing generating capacity. At a growth rate of only 2 percent/yr, new capacity of 22 percent or at least 54,700 MW would be needed in 10 years. If all the new plants included sulfur removal facilities based on limestone technology such as the CAFB process, the spent sorbent output would be 5.4 million Mg/yr (nearly 6 million tons/yr).

The need to dispose of large quantities of sorbent directs attention toward those industries that have the potential for general, mass utilization, such as construction, agriculture, and water treatment. It is therefore of interest to review statistics on the stone industry, which includes limestone and dolomite, as well as statistics on chemical forms of calcium such as lime and gypsum. Table 1 is a condensation of several tables from preprints from the 1975 Minerals Yearbook of the Bureau of Mines.[11] It shows that, of 902 million tons of crushed stone used in 1975, 74 percent was limestone and dolomite. Construction uses (road base stone, road stone, aggregate, concrete aggregate, fill), in which the limestone and dolomite is used for its volume rather than its chemical properties, accounted for 70 percent of the limestone and dolomite uses. The average value of crushed stone was \$2.47/Mg (\$2.24/ton), which is assumed to be f.o.b. the quarry. Special uses may command prices as high as \$11.02/Mg (\$10/ton), but the basis on which value information is being reported remains a question to be checked later. Further discussion will be found in the individual sections following.

Table 1

Dwg. 1701850

CRUSHED STONE SOLD OR USED BY PRODUCERS IN THE UNITED STATES IN 1975, THOUSANDS OF TONS/YEAR[a]

Utilization	Stone										
	Limestone and Dolomite	Granite	Traprock	Sandstone Quartz and Quartzite	Marble	Calcareous			Miscellaneous Stone	Total	Average Value, $/ton
						Shell	Marl	Slate			
Dense-Graded Roadbase Stone	151760	30139	19152	6401		3486			5571	216509	2.04
Roadstone	73097	12409	17258	5588		6182			2465	111699	2.26
Aggregate	120554	23450	22740	4913	281	252		510	2920	175620	2.42
Concrete Aggregate	94305	15900	6880	2185		10			386	119660	2.18
Cement	88326			718		3725	2690			95459	1.75
Agriculture	33947						486			34433	2.60
Fill	29657	11386	11408	3805					2877	59133	2.05
Lime	27663					993				28656	2.15
Flux	22756			1063						23819	2.29
Special Uses	3294				747					4041	10.37
Other Special Uses	3292	4	57	979						4332	4.27
Alkali Manufacture	3209									3209	2.19
Food Industry	2779	81								2860	4.81
Dead-Burned Dolomite	1967									1967	1.99
Coal Mine Dusting	1149									1149	5.23
Drain Fields, etc.	457		27							484	1.29
Filter Stone	294	147	222	37					27	727	2.60
Paper Industry	135									135	4.53
Refractories	76			889						965	6.87
Acid Neutralization	55									55	3.27
Unspecified Uses	7539	742	699	542	433	806	353	251	182	11547	2.57
	666311	94258	78443	27120	1461	15454	3529	761	14428	901765	2.24

[a] Source: Preprint from the 1975 Bureau of Mines Minerals Yearbook.

4. SPENT SORBENT UTILIZATION

Three classes of utilization are considered for the spent sorbent: as a source of lime, a source of $CaSO_4$, and a resource for construction use.

LIME SOURCE

Table 2, condensed from a Bureau of Mines preprint,[12] summarizes domestic lime usage in 1975. The steel industry is shown to be the major user. In particular, the basic oxygen process (BOP) uses one-third of the lime. Alkali manufacture and various applications in water treatment use about one-sixth each. Agriculture uses 0.5 percent.

All except agricultural users showed average values for lime in a very narrow range, $29.32 to 31.06/Mg ($26.60 to 28.18/ton). The agricultural use averaged $38.30/Mg (34.75/ton) for lime versus $3.16/Mg ($2.87/ton) for limestone (Table 1). The difference is probably due mainly to the cost of calcination.

Agriculture

Limestone and lime have been used for centuries to improve agricultural yields.[13] Their effects are achieved in several ways: neutralizing soil acidity, providing some plant nutrients directly, aiding in absorption of other nutrients, increasing organic matter, increasing soil microorganisms and earthworms, improving soil tilth, providing trace elements, and improving the effectiveness of fertilizers. Crops generally remove only minor amounts of calcium and magnesium from the soil, so the pH adjustment appears to be the more important function of liming. About 0.56 to 2.2 Mg CaO/ha* (0.25 to 1.0 ton/acre) are required to raise the pH of the soil by one unit, depending on local conditions.

---

*1 ha = 1 hectare = 2.471 acres.

Dwg. 1701849

Table 2

LIME SOLD OR USED BY PRODUCERS IN THE UNITED STATES IN 1975,[a] THOUSANDS OF TONS/YEAR

	Usage	Average Value, $/ton
Agriculture	97	34.75
Construction		
Soil Stabilization	750	
Other	541	
Subtotal	1291	28.18
Chemical and Industrial		
Steel - BOF	6542	
Electric	663	
Open hearth	511	
Subtotal	7716	27.05
Ore Concentration	690	26.94
Other Metallurgy	368	27.00
Environment		
Water purification	1403	
Sewage treatment	681	
Acid mine water	50	
Sulfur removal	3	
Subtotal	2137	27.01
Petroleum	135	27.04
Alkalis	2100	27.00
Glass	261	27.01
Calcium Carbide	205	26.98
Food Industry	977	27.02
Paper and Pulp	921	27.03
Precipitated Calcium Carbonate	65	26.95
Miscellaneous Uses	77	26.95
Unspecified Uses	1206	26.60
	18246	
Refractory Dolomite	914	34.13
Total	19160	27.46

[a] Source: Preprint from the 1975 Bureau of Mines Minerals Yearbook.

To check the market potential for limestone in agriculture, we assembled several facts. First, of 4.30 x 10^8 ha (1063 million acres) of land in farms, only 1.55 to 10^8 ha (384 million) or 36.1 percent are in cropland.[14] Next, the national average application rate in 1962 is calculated as 0.134 Mg/ha (0.060 tons/acre). Western soils, however, are normally alkaline and do not require liming. For the ten states using the most limestone, the application rate in 1962 was 0.177 Mg/ha (0.079 tons/acre) of land in farms.[13] Correcting this for the percentage of land in crops, the rate was 0.491 Mg/ha (0.219 tons/acre). In contrast, the rate for all the rest of the United States was 0.052 Mg/ha (0.023 tons/acre). Since total consumption has increased 21 million Mg (23 million tons) in 1962 versus 31 million Mg (34 million tons) in 1975, and cropland acreage has not, the average rate has increased to 0.197 Mg/ha (0.088 tons/acre), or by 47 percent. This is a growth rate of 3 percent/yr, although there are in fact fluctuations in the trend which undoubtedly reflect several factors. Moreover, although liming can be done every year, high labor costs favor spreading larger amounts every two to three years. Limestone usage is projected to 64 million Mg (70 million tons) by the year 2000, a growth rate of 2.9 percent/yr. Lime usage adds about 181,000 Mg/yr (200,000 tons/yr).

Use of lime has declined because of its higher price and considerably lower Federal subsidy per Mg.[13] According to the Agriculture Stabilization and Conservation Service at Pittsburgh, PA,[15] the subsidy varies by county, but 50 percent of the average price of limestone is representative. In practice, the land is treated and sown with grass. After two years, the farmer can plow under the grass and then plant crops. Table 1 shows the average price of limestone used in agriculture in 1975 was \$2.87/Mg (\$2.60/ton). This is f.o.b. the quarry. Crushing, sizing, transportation, and spreading costs bring the total to about \$19.84/Mg (\$18.00/ton). The limestone must be crushed to -149 μm (-100 mesh) to increase the rate at which it reacts in the soil. The CAFB stone, on the other hand, is already in a reactive form: granular CaO. A nominal crushing for ease of handling would probably be sufficient. The outlook for using CAFB stone in agriculture, therefore, on the basis of the preceding considerations appears good.

A further consideration, however, is the impact of trace elements. Nearly all the vanadium (V) and 75 percent of the nickel (Ni) from the fuel oil exit with the spent sorbent. Assuming 400 ppm vanadium and 50 ppm nickel in the fuel oil, the concentrations of these elements in the spent sorbent will be about 1.0 and 0.1 weight percent respectively. Although the earth's crust contains about 130 ppmw of vanadium and 80 ppmw of nickel,[16,17] some soils may contain over ten times these levels. Repeated applications of CAFB spent stone would probably result in a buildup of these elements in the top layer of soil.[18] Some plants are extremely sensitive to heavy metals. Since the pH of the soil affects the uptake of heavy metals, a potential hazard exists because, even if uptake were controlled by maintaining proper pH, in some year inadequate liming could result in an uptake of amounts toxic either to the plants or to human or animal consumers of the plants.

In summary, this use of CAFB spent sorbent from gasification of fossil fuels with high vanadium or nickel contents appears to be a practice that cannot be recommended as unconditionally safe over the long range. Control of trace element concentrations would be a necessary quality restriction.

Municipal Sludge Treatment

Municipal sludge treatment represents a small market of only about 181,440 Mg (200,000 tons) of lime/yr and, therefore, is not considered a significant outlet for CAFB stone. Other reasons include the fact that the problem of disposal is simply transferred to another location and that soluble substances will be discharged from the treatment system into a water course that may become a source of drinking water for downstream communities.

Although the usage of lime in water treatment is about four times as great as in sludge treatment, the hazard of introducing such trace elements as vanadium and nickel picked up from the fuel appears to oppose this application.

Acid Mine Drainage

Pyritic minerals associated with coal deposits hydrolyze and oxidize upon exposure to air, water, and microbial activity[19] to form H_2SO_4. This in turn solubilizes iron (Fe), aluminum (Al), manganese (Mn), and other elements, adding to the total environmental pollution.

Treatment consists of neutralizing the acid to at least pH 6.0 with some form of lime and oxidizing the iron with air. While limestone is the cheapest form normally, it is also less reactive, may have to be ground to 37 µm (400 mesh) to achieve high utilization, but produces a dense, rapidly settling dewaterable sludge. On the other hand, pH above 7, needed for rapid iron oxidation, is apparently impossible to attain with limestone. For a ferrous iron concentration below 100 mg/dm^3, acid mine drainage can be effectively treated with limestone without including facilities for iron oxidation. Between 100 and 500 mg/dm^3 postneutralization aeration is needed, while above 500 mg/dm^3 preneutralization aeration is indicated.[20] The chemical reactions involved may be expressed as:

$$H_2SO_4 + CaCO_3 \rightarrow CaSO_4 + H_2O + CO_2 \qquad (1)$$

$$2\ FeSO_4 + 2\ CaCO_3 + 3\ HOH + \frac{1}{2}\ O_2 \rightarrow 2\ Fe(OH)_3 + 2\ CaSO_4 + 2\ CO_2 \qquad (2)$$

The acid mine drainage may have a pH of 2.6 to 5.0 and a ferrous iron concentration of 0 to 10,000 mg/dm^3. At 100 percent utilization of limestone, to raise the pH from 2.0 to 6.0 would require 0.50 kg $CaCO_3$/1000 dm^3 (4.2 lb $CaCO_3$/1000 gal). To treat acid mine drainage with 1000 mg ferrous iron/dm^3 would require another 1.8 kg $CaCO_3$/1000 dm^3 (15 lb $CaCO_3$/1000 gal). The total is about 2.4 kg/m^3 (20 lb/1000 gal). The actual total may be considerably higher because the utilization may be as low as 35 percent.[21]

Spent CAFB sorbent may be useful in the treatment of acid mine drainage. As in the treatment of municipal sludge, however, one would be merely transferring and modifying the solids disposal problem. No general, ultimate disposal for acid mine drainage treatment sludge has been identified. It would appear that its use as a fill in mining operations is the most likely disposition of it.[22] Yet, if treatment of acid mine drainage is practical on a larger scale, the spent CAFB sorbent might prove attractive. An alternative to treatment would be better mining practices to minimize exposure of pyritic materials.

Industrial Applications

As noted in Table 2, the main consumer of lime is the steel industry. At least one company chooses to handle limestone, probably for a combination of cost, health, and stability reasons. It is calcined on site and fed to steel processing in enclosed equipment. Current information is that the sulfur content of the limestone fed should be no higher than 0.03 to 0.06 percent (0.053 to 0.106 percent on CaO). The usage is large: 0.30 Mg limestone/Mg pig iron (0.30 ton limestone/ton of pig iron) and 0.13 Mg lime/Mg BOP steel (0.13 ton lime/ton BOP steel). The latter is six times the lime requirement of the open hearth process.[13]

Tests described later in this report (Appendix A) showed that heating spent CAFB sorbent of 1500°C for at least two hours reduced the sulfur content to about 0.17 percent, present mainly as the sulfate. It would appear that a potential exists for utilizing the spent sorbent in the steel industry. Trace elements, such as nickel and vanadium, should not present a problem since steel manufacture involves charging scrap that contains similar elements.

Of other industrial applications, the cement industry appears especially interesting. Calcium oxide is the major constituent of cement, typically lying in the range of 61.2 to 63.8 weight percent. To achieve this content about (1.1 Mg (1.2 tons) of limestone are charged to the kiln/Mg (ton) of cement produced. About 32 kg (70 lb) of gypsum are intergound with the cooled cement to serve as a retarder in setting.[23] The immediate advantages of using the CAFB stone are that the stone has already been calcined and the preliminary size has been reduced. Table 3 shows figures for the energy consumption in the cement industry.* If we combine the different forms of energy input using [illegible] x 10^6 Btu/ton of coal, 6.3 x 10^6 Btu/bbl oil, 1000 Btu/CF gas and 10,000 Btu/kWh, the energy requirement works out to 1,376,000 Btu/bbl cement for dry processes and 1,423,000 for wet processes. For comparison, the FEA[24] has estimated the average energy requirement at 1,391,000. The Conference Board[25] arrived at 1,318,000 for 1967, which has since declined through technological improvements to 1,218,000 in 1971. The Board did not include a breakdown, but the kiln itself may consume 700,000 Btu/bbl for the dry process, of which 95 percent is required for heating from ambient temperature to 900°C and calcining the calcium carbonate ($CaCO_3$) and magnesium carbonate ($MgCO_3$) in the limestone. Additional heat is required to get to the clinkering temperature of about 1430°C but is largely offset by exothermic clinkering reactions.

---

*Because both the cement and the oil industry use barrels and Btus, we have not converted these figures to SI units.

Table 3

ENERGY CONSUMPTION OF THE CEMENT INDUSTRY[a,b]

	Energy Source			
	Coal, short tons	Oil, bbls	Gas, CF	Electricity, kWh
Dry Processes				
Total annual usage[c]	3.957	0.775	62,484	3,948
Per bbl cement	0.02547	0.00499	402	25.42
Per ton cement	0.1355	0.0265	2140	135.2
Wet Processes				
Total annual usage[c]	5.551	4.987	140,436	5,621
Per bbl cement	0.02317	0.02082	586	23.46
Per ton cement	0.1232	0.1107	3118	124.8

[a] Source: Minerals Yearbook, 1968[26]

[b] Unit quantities based on 155.3[illegible]7 million barrels of cement produced by dry processes and 239.572 million by wet processes. One barrel of cement contains 376 pounds of cement.

[c] All total quantities in millions of indicated units.

Two possibilities for integration with the CAFB process arise. Close integration would feature transfer of the hot spent sorbent directly to a cement process. The Trief process[27] probably would be best suited to this approach since the charge is fully melted rather than merely clinkered. Whether the dust problems of a cement plant are compatible with the air requirements for a large power plant needs careful review. Alternatively, the spent sorbent would be cooled and shipped to a cement plant at another location. There it would be ground to at least 74 μm (200 mesh) and used as the CaO source. In this case the saving in energy for the cement operation is only the calcination energy, which is about 54 percent of the kiln energy requirement. If applied to the entire production of 395 million bbl of cement, the saving amounts to about 65,000 bbl of fuel oil equivalent (FOE)/day. This does not have tremendous national significance when compared to the daily demand of 17,000,000 bbl of petroleum in the United States or even to the heavy fuel oil demand of 2,400,000 bbl/day. Its importance, therefore, is, indirect, since cutting the operating costs of cement manufacture would help keep down construction costs. At 378,000 Btu/bbl fuel consumption would be reduced from 0.218 bbl FOE/bbl cement to 0.158, a reduction of 27 percent. With cement at $4.50/bbl and fuel oil at $10/bbl, the fuel cost represents half the cement price and the saving is about 14 percent. Equally important factors may be the supply of limestone of a quality suitable for fluid-bed combustion and the economics of transportation.

Cement production requires about 0.21 Mg (0.23 tons) of limestone/bbl of cement or 33 million Mg (36 million tons) of limestone/year, which, by reference to the section in this report on market data, would correspond to the output of spent sorbent from about 920 200-MWe plants using limestone. The minimum-size cement plant in 1971 appears to have produced about 1,000,000 bbl/year, with 16 percent being over 5,000,000. A 3 million bbl plant could take the output from a 1000 MWe power plant. Electrical requirements would be 76,000 MWh/yr, or about 230 MW, based on a 330-day operating year. Thus, an interesting possibility is for cement plants to generate their own electricity via a CAFB plant. A larger plant could practice blending of the CAFB spent sorbent with fresh limestone if there were technical reasons why the spent sorbent could not be used alone. A further projection is that, by 1980, 60 percent of the energy requirement of the cement industry will be coal, with another 8 percent from purchased electricity. In 1971, coal provided 35 percent and gas 45 percent of the energy requirement. Along with the higher consumption of coal is the higher production of coal ash, a potential source of pozzolan. A more detailed study of the profitability of the cement business, however, is needed to clarify the potential CAFB market. The long-term growth rate has been about 2.8 percent/yr from 1909 to about 1967. While this growth rate is expected to slow down, partly because imports will increase to 50,000,000 bbl/yr, there could be 100,000,000 bbl of domestic capacity required by 1980. Demand for hydraulic cement is expected to increase in this same period at the rate of 3.0 percent/year.

CALCIUM SULFATE SOURCE

Calcium sulfate is used mainly in one of two forms: the dihydrate (gypsum) or the hemihydrate (plaster). Table 4 summarizes statistics on these uses.[26,28] As much as one-third of the gypsum can be imported economically. About one-third of the total consumption is used uncalcined, divided about 3:1 between use as a cement retarder and in agriculture. The largest use (92 percent) for the calcined form is in prefabricated products, mainly gypsum board (also about 92 percent).

Thus far only two of the CAFB spent stone processing options would yield a product with a significant content of $CaSO_4$. Dry sulfation would yield anhydrous $CaSO_4$, and wet sulfation would produce gypsum. An important question is whether the uses for gypsum really require that form. In agriculture gypsum is used as a soil conditioner; perhaps the anhydrous form would prove satisfactory there. In cement the anhydrous form

Table 4

Dwg. 6451A70

GPYSUM SUPPLY AND DEMAND IN THE UNITED STATES

Supply Sources and Final Uses	1968			1973		
	Quantity, 1000 Mg	Value		Quantity, 1000 Mg	Value	
		10^6 \$	\$/Mg		10^6 \$	\$/Mg
Supply						
Mined	9088	36.8	4.04	12300	56.6	4.61
Imports	4948			6950		
	14036			19250		
Uses						
Uncalcined						
Cement retarder	3120	16.0	5.14	3763	22.2	5.90
Agriculture	1259	6.2	4.94	1318	7.4	5.61
Other	98	0.9	8.04	106	1.5	13.93
	4477	23.1	5.17[a]	5187	31.1	5.98[a]
Calcined						
Industrial	273	8.9	32.64	320	14.2	44.28
Plasters	1192	30.0	25.18	699	24.0	34.26
Prefabricated products	7961[b]	342.7	43.04	12513	563.6	45.04
	9426	381.6	40.48[a]	13532	601.8	44.67[a]

[a] These figures are overall average values.

[b] Prefabricated product weights include paper, metal, and other materials.

(anhydrite) can replace 25 to 75 percent of the gypsum without affecting the setting time, the strength, or the volume changes of concrete made from such cements.[13] The market, however, is small. ASTM Specification C-150, Portland Cement,[29] calls for an upper limit of 3.0 weight percent on SO_3 in Type I when the tricalcium aluminate ($3\ CaO \cdot Al_2O_3$) content is not more than 8 percent. This corresponds to 6.4 percent $CaSO_2 \cdot 2\ H_2O$, 5.4 percent $CaSO_4 \cdot 1/2\ H_2O$, or 5.1 percent $CaSO_4$. Whether the CAFB product is equivalent to natural anhydrite would have to be shown by appropriate tests. In prefabricated products CAFB gypsum is probably at a disadvantage with respect to natural gypsum. Product quality is a factor inasmuch as vanadium, nickel, and sodium would be picked up from heavy fuel oil.

Similar considerations apply in the case of a modification of the CAFB process in which the regeneration is replaced by an oxidizer and the desulfurizer is operated to produce a spent sorbent with a high content of CaS. Oxidation of CaS to $CaSO_4$ is highly exothermic, and an adequate method of temperature control must be devised. Further, the particles may develop an outer shell of $CaSO_4$ that might slow down the diffusion rate of oxygen to a commercially impractical level.

CONSTRUCTION USES

The sheer volume of spent sorbent to be produced from CAFB plants will probably direct major attention to disposal/utilization in some section of the construction industry. This could mean landfill or road construction or, at upgraded levels of utilization, cement, concrete, and aggregate. Some statistics are given in Table 5.[26,28] Ordinary commodities like sand and gravel are no longer inexpensive. The higher prices for these appear to be for metropolitan areas which are exhausting local supplies of acceptable quality aggregates. Figure 1 shows the doubling of the price index for selected commodities over a recent four-year period.[30] This increase is attributed to the step change in fuel prices in 1973.

Aggregate

ASTM Standard D8-71 defines an aggregate as a granular material of mineral composition, such as sand, gravel, shell, slag, or crushed stone, used with a cementing medium to form mortars or concrete or alone, as in base courses, railroad ballasts, and the like.[31] Concrete contains a mixture of cement, fine aggregate, and coarse aggregate. The aggregates

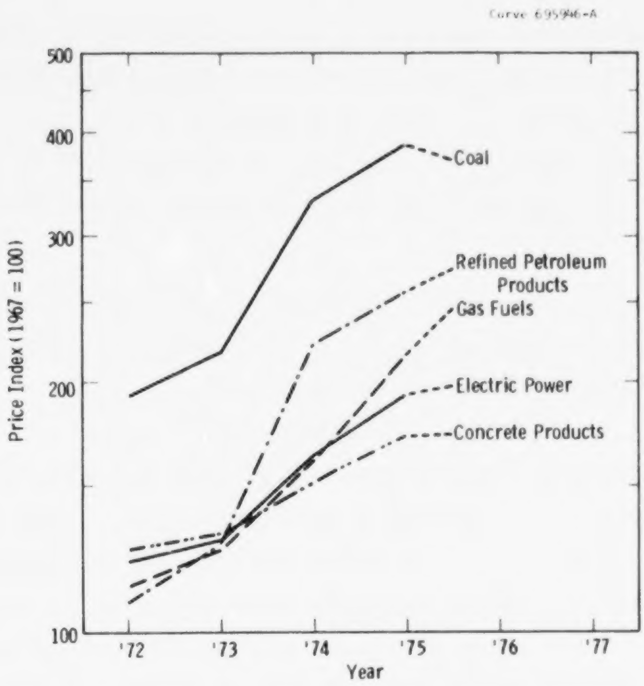

Figure 1 - Price Index for Selected Commodities

Table 5

MARKET DATA ON SELECTED CONSTRUCTION MATERIALS

Material	1968		1973	
	Quantity, 10^6 Mg/yr	Price Level, \$/Mg	Quantity, 10^6 Mg/yr	Price Level, \$/Mg
Portland cement	69	21.11-29.04	78	25.35-36.82
Sand	336	1.76- 4.74	390	1.05- 7.11
Gravel	499	1.82- 4.96	499	1.76- 6.28
Gypsum, crude	9.1	4.04	13	4.61
Gypsum, calcined	8.2	16.60	12	17.97

used are normally hard, chemically inert, resistant to deterioration by wetting and alternating freezing and thawing, and have suitable mechanical strength properties.[32] The terms gravel, stone, and rock appear to be used interchangeably, but they may be distinguished by size. In other words, stones are fragments of rock, and gravel consists of fragments of stones.

Rocks contain one or more minerals of which the more common are feldspars, ferromagnesians, micas, clays, zeolites, silicates, carbonates, sulfates, iron sulfides, and iron oxides. Chemically, the first five are silicates of aluminum, calcium, iron, or magnesium, with potassium and/or sodium present in some cases. What is of interest here is the chemical reactivity and the physical structure. Clay minerals and zeolites show large changes in volume when wetted and dried. Sulfates, as in gypsum and anhydrite, offer the risk of attack on cement. Porous cherts, shales, some limestones, and some sandstones are known to be susceptible to frost damage. Chert is a very fine-grained rock composed of silica in the form of cryptocrystalline quartz, chalcedony, opal, or combinations thereof, and may be alkali reactive. Quartz is anhydrous, opal is hydrous, and chalcedony is believed to be a mixture of the two. Other known alkali-reactive constituents are tridymite, cristobalite, zeolite, heulandite, the glassy-to-cryptocrystalline rhyolites, dacites, andesites, and certain phyllites. The deleterious expansions sometimes do not occur until two or more years after the concrete is placed.

Unconsolidated sediments include gravel, sand, silt, and clay, according to particle size. There is also, however, a trend in composition. Gravel and coarse sands are usually rock fragments. Fine sands and silt are predominantly mineral grains. Clay consists exclusively of mineral grains, largely of the clay minerals group. On consolidation, sandstones, siltstones, and claystones are formed. The cementing material may be quartz, opal, calcite, dolomite, clay, iron oxides, or other materials. Hard, platy claystones are shales. Some shales cause concrete to fail because of excessive shrinkage. Dolomite in certain carbonate rocks is present as large crystals scattered in a finer-grained matrix of calcite and clay. Such a structure leads to deleterious expansions in concrete.

Micas are subject to cleavage and also may be altered during the hydration of cement. Iron sulfides form ferrous sulfates, which in turn yield iron hydroxide and calcium sulfoaluminate. Surface staining is also possible.

With respect to the CAFB process, two possibilities for disposition of spent sorbent exist. One is utilization of the spent sorbent as fine aggregate; the other is processing it to large compacts for use as a coarse aggregate. In either case both environmental stability and environmental impact must be checked.

Cement

Chemically, cement is a material obtained by sintering substances containing CaO and silica (SiO_2) to form calcium silicates. Upon hydration a gel is formed in which various hydrated silicates of calcium, aluminum, and iron form. The compressive strength obtained is attributed to products from di- and tricalcium silicate.

High-temperature processing (over 1000°C) could convert mixtures of spent sorbent and fly ash to a material with cementlike properties. It is conceivable that processing at ambient temperature could also yield a material that would behave as a cement.

A basic question is whether the hydration product from mixtures of CaO and siliceous materials such as fly ash has a gel structure similar to that of Portland cement and also whether the mechanical properties (compressive strength and durability) are comparable.

5. SPENT SORBENT PROCESSING

INTRODUCTION

We have defined spent sorbent processing options to provide a basis for technical and economic evaluation. The options considered include:

- Minimal on-site processing prior to direct disposal to the environment or delivery to an outside consumer for use as, for example, block production
- On-site processing to minimize the environmental impact (dead-burning, sintering, and dry sulfation)
- On-site processing to produce a material suitable for utilization or acceptable for disposal (fly ash blending).

We have also considered the processing of the CaS that would result from operation as a once-through sorbent system.

Experimental screening tests were carried out to permit technical evaluation of each process. Process flowsheets that form the basis for process and economic evaluation are presented. The evaluation of the environmental impact of the products resulting from the alternative processes is presented in Volume 3 of this report.[4]

In all options the plant is a 200 MWe oil-fired regenerative CAFB plant. The oil feed contains three percent sulfur by weight, and the sorbent is limestone fed at a molar treat ratio of 1:1 calcium to sulfur (Ca/S). Each option includes on-site equipment from the regenerator outlet to the battery limits. Off-site facilities have not been included.

DIRECT DISPOSAL

Direct disposal represents a base case that should have the lowest capital and operating costs. Figure 2 shows the minimum facilities required, based on the concept that there is some ultimate disposition

Dwg. 1690B64

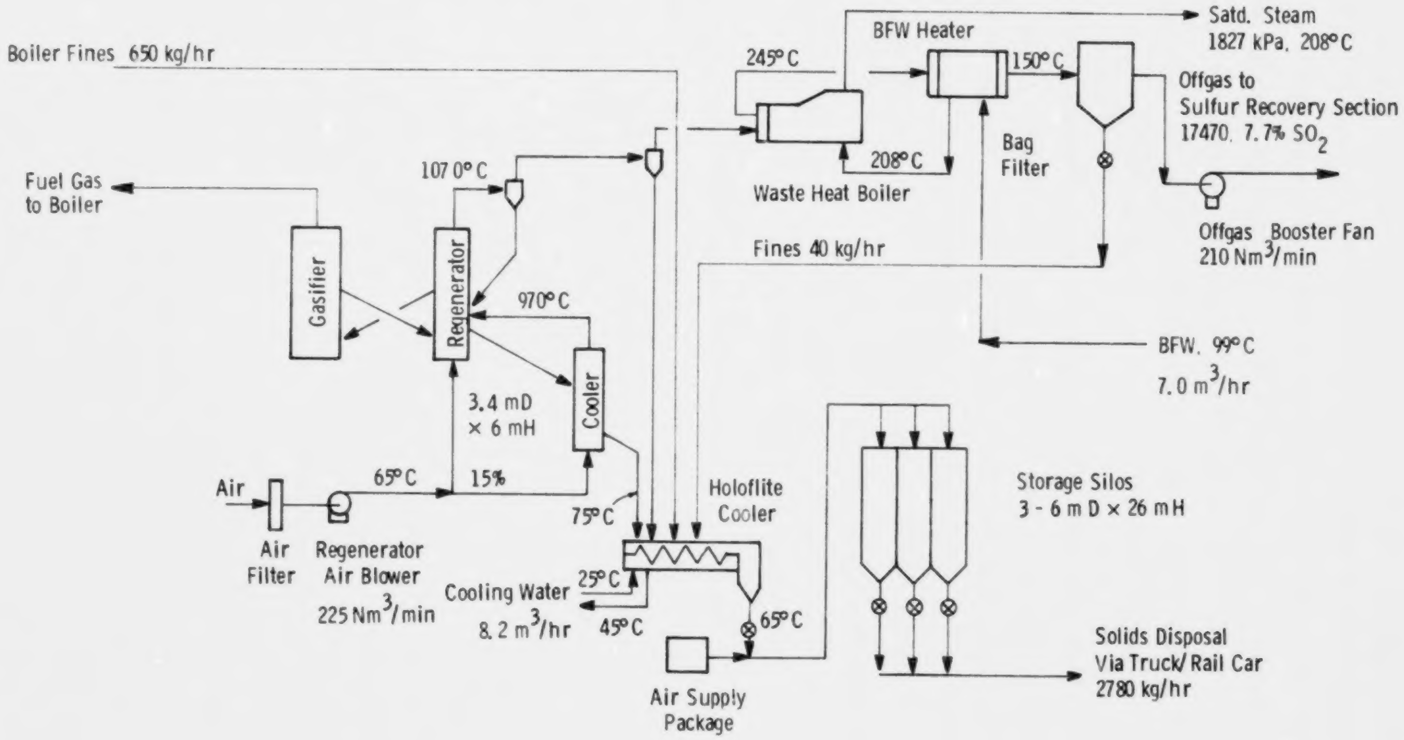
Boiler Fines 650 kg/hr
Fuel Gas to Boiler
Gasifier
Regenerator
107 0° C
970° C
Cooler
3.4 mD × 6 mH
Air
Air Filter
Regenerator Air Blower 225 Nm³/min
65° C
15%
75° C
Cooling Water 8.2 m³/hr
25° C
45° C
Holoflite Cooler
65° C
Air Supply Package
245° C
Waste Heat Boiler
208° C
BFW Heater
150° C
Bag Filter
Fines 40 kg/hr
Satd. Steam 1827 kPa, 208° C
Offgas to Sulfur Recovery Section 17470, 7.7% SO2
Offgas Booster Fan 210 Nm³/min
BFW, 99° C 7.0 m³/hr
Storage Silos 3 - 6 m D × 26 m H
Solids Disposal Via Truck/ Rail Car 2780 kg/hr

Figure 2 - Direct Disposal of Spent Sorbent from a 200 MW CAFB Plant

available such as depositing the spent sorbent in a disposal site or delivering it to a consumer. These facilities should be able to cool the spent sorbent from 1070°C to a temperature at which it could be safely handled, such as 65°C (149°F), and should include a reasonable amount of on-site enclosed storage capacity, since the spent sorbent from the CAFB process reacts vigorously with water. The storage capacity proposed amounts to 30 days' production.

The questions that arise regarding environmental impact include those about heat release, leaching ($Ca(OH_2)$, $CaSO_4$, trace elements), and odor generation due to hydrolysis of CaS. The production rate of spent sorbent is estimated as 25,800 Mg/yr (28,500 tons/yr) which will contain about 83 weight percent CaO. If deposited in an outdoor site, with an assumed 20-year project life, about 58,800 m^2 (14.5 acres) will be required, which will produce a stockpile 6 m (20 ft) high for a bulk density of 1440 kg/m^3 (90 lb/ft^3).

To treat the leaching question first, rainfall in the United States averages 15 to 150 cm/yr (6 to 60 in/yr), depending on location.[14] The upper limit would mean an average water input of 136 ℓ/min (36 gpm) to the above stockpile. At a solubility of 1.63 g $Ca(OH_2)$, only 13.3 kg $Ca(OH)_2$/hr would be leached if we assume 100 percent efficiency of contacting and an average temperature of 20°C. Solubility decreases with an increase in temperature. Thus, only 0.41 percent of the day's production of CaO could be leached. This can clearly be reduced by proper design of the stockpile.

This estimate of leachate potential is reduced by 13.1 ℓ/min (3.5 gpm), the water required to convert the day's production of CaO to the hydroxide. Two problems arise in this operation: evolution of heat and evolution of H_2S from the residual CaS in the spent sorbent. The actual heat evolution depends on how dead-burned the stone is; but if we assume it is all active, then 0.8 MJ/s (2.8×10^6 Btu/hr) would be released. Without adequate dissipation local temperatures would go at least to the boiling point of water. If sufficient water were not present to carry off the heat of hydration as steam, as in commercial slakers, then temperatures could go high enough to ignite flammable material.

The CaS content is normally no more than about 3 weight percent, which in the above 200 MWe plant would be 137 kg/hr (302 lb/hr). If all the sulfur in the CaS were released as H_2S, the volumetric production rate would be 42.6 Nm^3/hr (1504 SCFH/hr). To dilute this to 10 ppmv (the 8-hour Threshold Limit Value) in the 10-ft deep layer of air on the top surface of the stockpile would require an average wind velocity of 1.6 m/s (3.6 mph). This calculation indicates that, even if the CaS were inactivated, to dispose of the spent sorbent in a valley or to create a large disposal pile on level ground would be a mistake, because accidental H_2S evolution could generate objectionable and possibly harmful concentrations under adverse meteorological conditions.

We conclude that direct disposal to the environment must involve slaking the spent sorbent in an excess of water to cope with the above effects, although this could be done off site.

With respect to the characteristics of the leachate, saturated aqueous $Ca(OH_2)$ would have a pH of 12.64. To reduce this to a pH of 8.5, which represents a limiting requirement as the permissible criterion for public water supplies promulgated by the National Technical Advisory Committee on Water Quality Criteria through the Federal Water Pollution Control Administration, requires dilution by a factor of 14,000. If actual leachate production is, say, 6.8 m^3/hr (30 gpm), then 95,400 m^3/hr (420,000 gpm) of dilution water is required. Such a dilution would also take care of reducing $CaSO_4$ from a saturation value of 3000 ppm to 250. A sulfide, however, may have to be limited to less than 1 ppm.

The sulfide question merits further consideration. Some of the CaS will probably hydrolyze on contact with water:

$$2\ \mathrm{CaS} + 2\ \mathrm{HOH} \rightarrow \mathrm{Ca(HS)_2} + \mathrm{Ca(OH)_2}.$$

A partial pressure of H_2S over the leachate will be established, creating at least an odor nuisance. This reaction needs further study to determine the extent of the hydrolysis, whether the $Ca(HS)_2$ remains in solution, and whether H_2S can be removed from the system by simple means. If the sulfide is in solution, its concentration will be 512 ppmw, so dilution for pH control would also reduce sulfide to levels far below the maximum permitted (36 ppbw).

An on-site slaking process would produce either a dry product containing CaS or a wet product plus a recirculating stream of slaking water in which the sulfide content will build up to a level at which sulfide stripping must be provided. Details need to be worked out on the basis of future laboratory tests. If all the sulfide can be evolved, it could be disposed of by incineration since it would release only 35 ng sulfur dioxide $(SO_2)/J$ or 0.082 lb $SO_2/10^6$ Btu fired versus 516 (1.2) allowable. If necessary, the design of the main process of gasification could probably be adjusted toward a higher primary sulfur removal.

DEAD-BURNING

Figure 3 shows the facilities required to convert the CAFB spent regenerator stone to an inactive (dead-burned) form by heating it for five hours at 1250°C. The data on which this design is based are presented in Appendix A. The experimental results may be summarized as follows:

- Residual CaS in the regenerator stone can be oxidized essentially completely by heating the stone for about two hours at 1550°C or five hours at 1250°C in air.

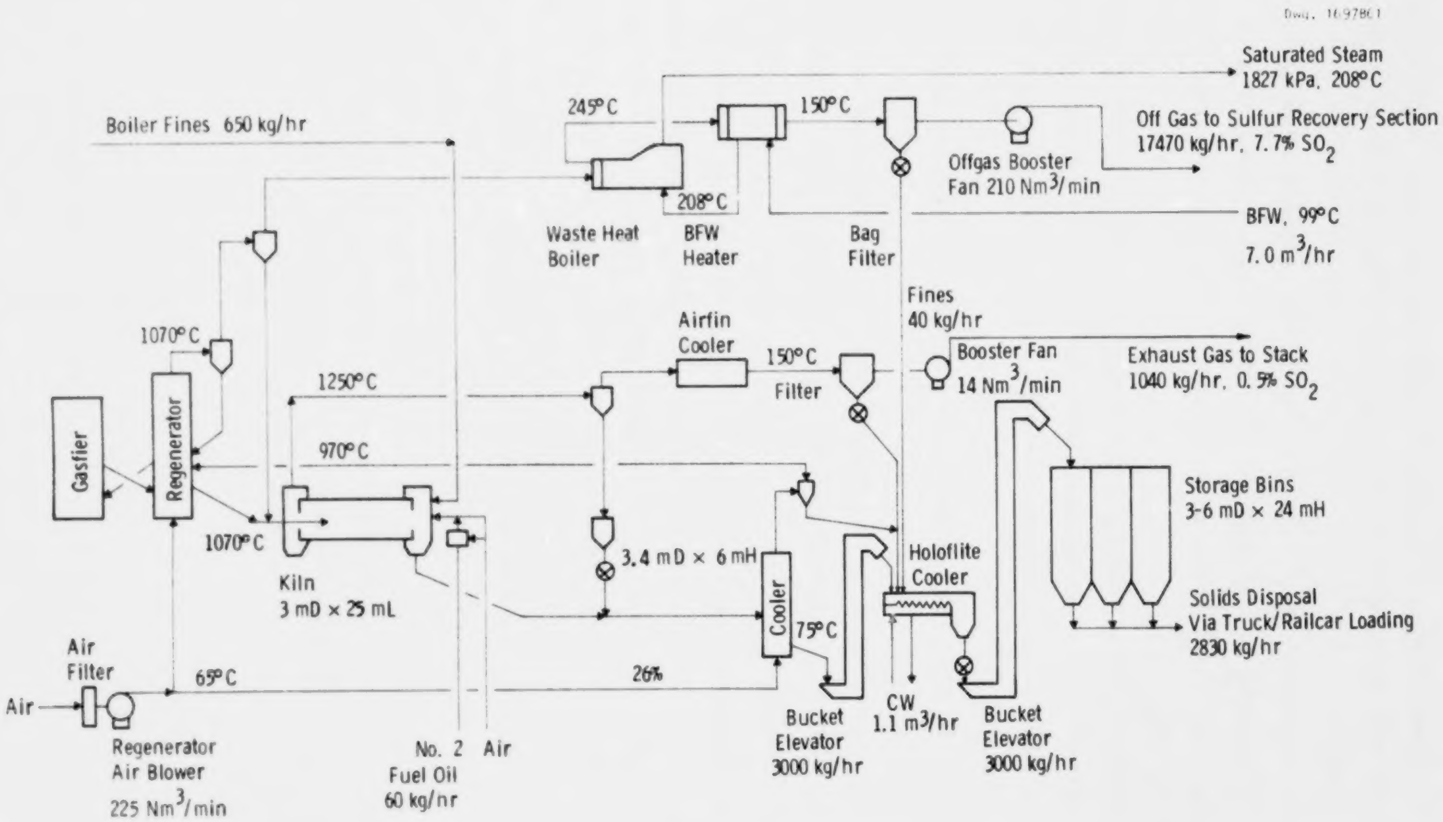
Dwg. 1697B61
Saturated Steam
1827 kPa, 208°C
Off Gas to Sulfur Recovery Section
17470 kg/hr, 7.7% SO2
Boiler Fines 650 kg/hr
245°C
150°C
Offgas Booster
Fan 210 Nm3/min
208°C
Waste Heat
Boiler
BFW
Heater
Bag
Filter
BFW, 99°C
7.0 m3/hr
Fines
40 kg/hr
Airfin
Cooler
1070°C
150°C
Filter
Booster Fan
14 Nm3/min
Exhaust Gas to Stack
1040 kg/hr, 0.5% SO2
1250°C
970°C
Gasifier
Regenerator
1070°C
Kiln
3 mD × 25 mL
3.4 mD × 6 mH
Cooler
75°C
Holoflite
Cooler
Storage Bins
3-6 mD × 24 mH
Solids Disposal
Via Truck/Railcar Loading
2830 kg/hr
Air
Air
Filter
65°C
26%
Regenerator
Air Blower
225 Nm3/min
No. 2
Fuel Oil
60 kg/hr
Air
Bucket
Elevator
3000 kg/hr
CW
1.1 m3/hr
Bucket
Elevator
3000 kg/hr

Figure 3 - Disposal of Spent Regenerator Stone from 200 MW CAFB Plant by Deadburning

- If dead-burning is judged by BET surface area, heating at 1550°C for two to five hours is required or for more than 24 hours at 1250°C.
- On the basis of its heat release when treated with water, the CAFB stone may already be 40 percent dead-burned as produced.
- Heating times required are shortened by grinding the stone to -44 μm.
- Sulfate sulfur can be reduced to the level of 0.5 to 1.0 weight percent SO_4 by heating it at 1550°C for two hours. Heating it at 1250°C for 24 hours is ineffective in reducing the SO_4 content.
- Heating the spent sorbent in a static bed results in sintering, even at 1250°C.
- On the basis of the leaching data, dead-burning at 1550°C greatly reduces the solubility of $CaSO_4$ but reduces that of CaO by only one-third.

Thus, dead-burning appears to be a relative term. There is some evidence that even CaS can be dead-burned, but CaO remains as a leachable component. The design, therefore, is constructed around the idea of dealing with the sulfide content by oxidizing the spent sorbent to $CaSO_4$, during which process about 10 percent of the sulfur is lost as SO_2. Grinding the stone prior to heating it is not recommended since no advantage was demonstrated by doing so.

As to ultimate disposition, one must assume that for the purposes of economic evaluation the dead-burned sorbent can be deposited in a disposal site. As discussed under direct disposal, however, this does not appear to be a completely acceptable method environmentally.

SINTERING

Figure 4 shows a modification of dead-burning involving use of a higher temperature to drive off the maximum amount of sulfur to permit its use as a source of lime. Experimental data (see Appendix A) showed

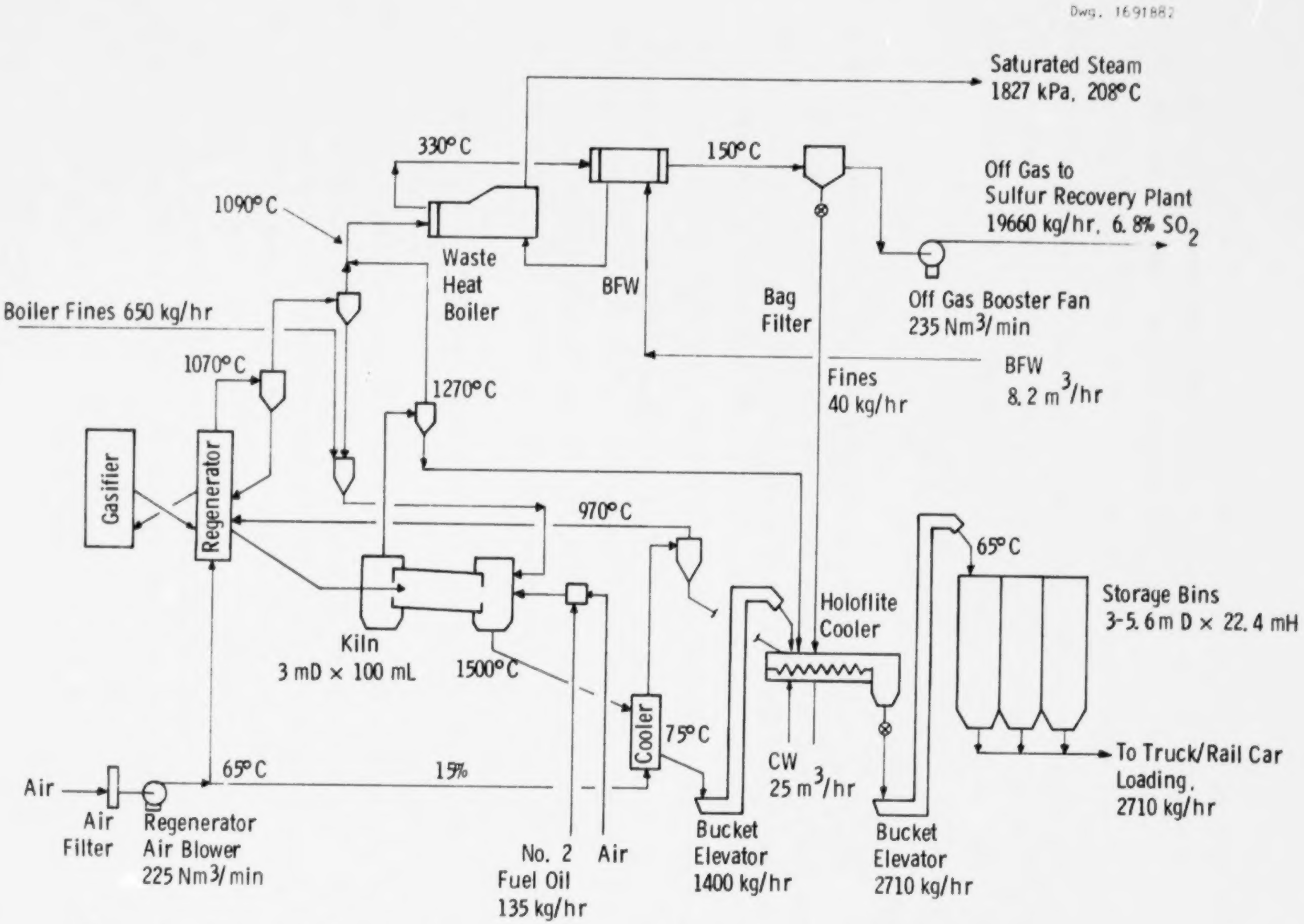
Dwg. 1691B82
Saturated Steam
1827 kPa, 208°C
330° C
150°C
1090° C
Off Gas to
Sulfur Recovery Plant
19660 kg/hr, 6.8% SO2
Waste
Heat
Boiler
BFW
Bag
Filter
Off Gas Booster Fan
235 Nm3/min
Boiler Fines 650 kg/hr
1070° C
1270° C
Fines
40 kg/hr
BFW
8.2 m3/hr
Gasifier
Regenerator
970° C
65°C
Storage Bins
3-5.6 m D × 22.4 mH
Holoflite
Cooler
Kiln
3 mD × 100 mL
1500°C
Cooler
75°C
CW
25 m3/hr
To Truck/Rail Car
Loading,
2710 kg/hr
Air
65°C
15%
Air
Filter
Regenerator
Air Blower
225 Nm3/min
No. 2
Fuel Oil
135 kg/hr
Air
Bucket
Elevator
1400 kg/hr
Bucket
Elevator
2710 kg/hr

Figure 4 - Disposal of Spent Regenerator Stone from a 200 MW CAFB Plant by Sintering

that heating at 1550°C for five hours would result in a 95 weight percent loss of sulfur. About 86 percent of the $CaSO_4$ was decomposed, and the product retained about 0.7 percent of the original CaS. If vented, the SO_2 released would amount to 52 ng SO_2/J (0.12 lb/10^6 Btu) fired.

The sintered product would contain 0.15 weight percent sulfur. The steel industry currently uses limestone with 0.03 weight percent sulfur or less. It is possible that with some modification of steel processing the product could be used in this industry.

DRY SULFATION

Figures 5 and 6 show proposed flowsheets for dry sulfation based on the design study presented in 1975[3] and updated through extensive analysis of the data collected on the dry sulfation of CAFB regenerator stone in a 10-cm fluidized bed. The bed is described in Appendix B and the results in Appendices C through E. Important conclusions are:

- It was impossible to fluidize -100 μm fines and still retain a dense bed. At the lower velocities the fluidizing medium would mostly bypass the solids in the bed through ratholes.
- Fluidization was achieved by having larger particles present in the bed.
- Sulfation temperatures in the range of 750 to 850°C appear adequate.
- Contact time is still uncertain. It appears that complete sulfation can be achieved in about 20 hours, but predictions from model developed from the data indicate a longer time is required. Data available were taken under different conditions and have not yet been reconciled.
- Maximum bed velocity should be limited to less than 25 cm/s at conditions to minimize elutriation of fines (-100 μm particles).

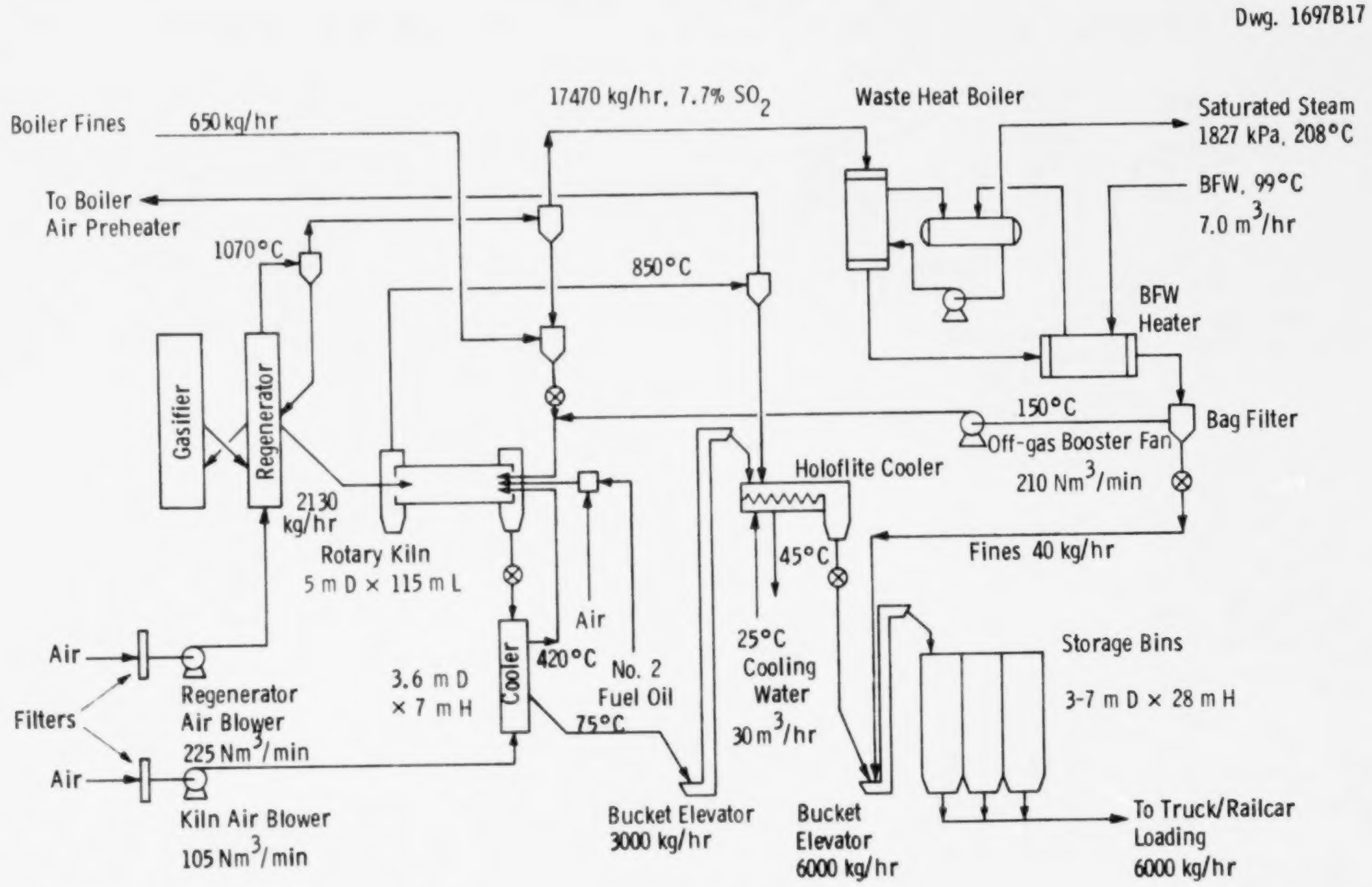

Dwg. 1697B17
Boiler Fines
650 kg/hr
To Boiler
Air Preheater
1070°C
17470 kg/hr, 7.7% SO2
850°C
Waste Heat Boiler
Saturated Steam
1827 kPa, 208°C
BFW, 99°C
7.0 m3/hr
BFW
Heater
150°C
Bag Filter
Off-gas Booster Fan
210 Nm3/min
Gasifier
Regenerator
2130
kg/hr
Rotary Kiln
5 m D × 115 m L
Holoflite Cooler
45°C
Fines 40 kg/hr
Air
Air
Filters
Air
Regenerator
Air Blower
225 Nm3/min
Kiln Air Blower
105 Nm3/min
3.6 m D
× 7 m H
Cooler
420°C
No. 2
Fuel Oil
75°C
25°C
Cooling
Water
30 m3/hr
Storage Bins
3-7 m D × 28 m H
Bucket Elevator
3000 kg/hr
Bucket
Elevator
6000 kg/hr
To Truck/Railcar
Loading
6000 kg/hr

Figure 5 - Disposal of Spent Regenerator Stone from 200 MW CAFB Plant by Dry Sulfation with Rotary Kiln

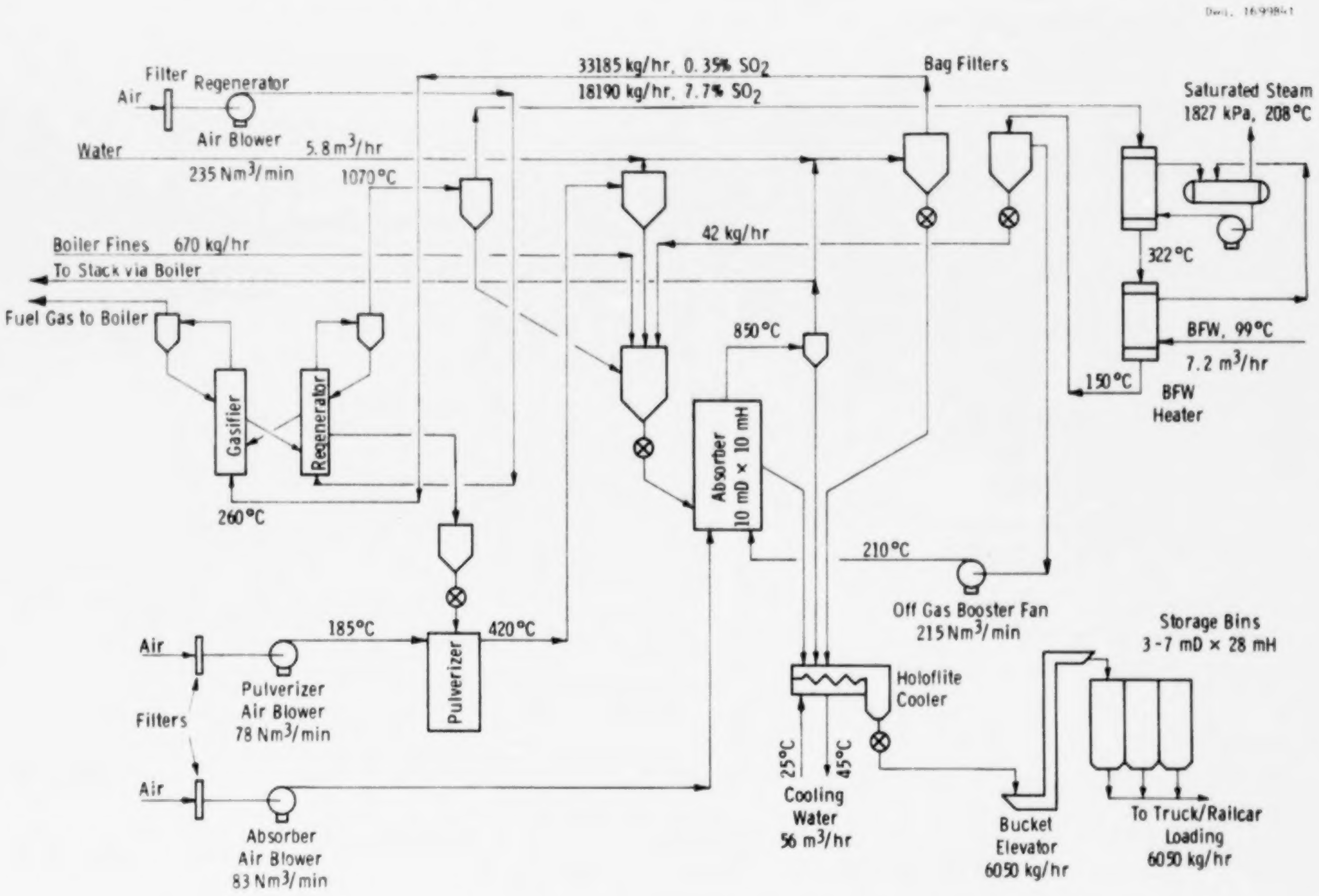
Dwg. 1699B41
Air
Filter
Regenerator
Air Blower
235 Nm³/min
Water
5.8 m³/hr
1070°C
33185 kg/hr, 0.35% SO₂
18190 kg/hr, 7.7% SO₂
Bag Filters
Saturated Steam
1827 kPa, 208°C
Boiler Fines 670 kg/hr
To Stack via Boiler
Fuel Gas to Boiler
42 kg/hr
322°C
BFW, 99°C
7.2 m³/hr
150°C
BFW
Heater
850°C
Gasifier
Regenerator
Absorber
10 mD × 10 mH
260°C
210°C
Off Gas Booster Fan
215 Nm³/min
Storage Bins
3-7 mD × 28 mH
Air
185°C
420°C
Pulverizer
Pulverizer
Air Blower
78 Nm³/min
Filters
Holoflite
Cooler
Air
Absorber
Air Blower
83 Nm³/min
25°C
45°C
Cooling
Water
56 m³/hr
Bucket
Elevator
6050 kg/hr
To Truck/Railcar
Loading
6050 kg/hr

Figure 6 - Disposal of Spent Regenerator Stone from 200 MW CAFB Plant by Dry Sulfation with Absorber

Alternatives for disposal of the absorber off-gas were explored conceptually. If one assumes a target of 90 percent overall sulfur capture, and if the absorber off-gas is vented directly to a stack, then sulfur capture in the absorber must be 94.6 percent, on the basis of the following:

- Gasifier capture is 95 percent of the gaseous sulfur fed to it.
- Sulfur introduced as an impurity in the limestone is retained.
- The sulfur in the recirculated sorbent is retained, although recycled $CaSO_4$ may be reduced in the gasifier and reoxidized in the regenerator.
- Regenerator stone composition is as per the original NEES design.

A second possibility would be to recycle the absorber off-gas to the gasifier, reducing the sulfur capture required in the absorber to 46.5 percent. As an extension of this case, the following expressions which take into account the recycle of boiler flue gas were derived for X_A, absorber capture:

$$X_A = 1 - (S_A/S_R)$$

where

S_A = sulfur content of the absorber off-gas recycled to the gasifier, moles/hr

and

S_R = sulfur content of the regenerator off-gas fed to the absorber, moles/hr.

These quantities are given in turn by:

$$S_A = \frac{S_2}{1 - R}\left\{\frac{1 - X_0}{1 - X_G} - (1 - RX_0)\right\}$$

and

$$S_R = (1 - a)\left\{S_1 + \frac{S_2}{1 - R}(1 - X_0)\frac{X_G}{1 - X_G}\right\}$$

where

S_1 = sulfur content of limestone fed to the gasifier
S_2 = sulfur content of feed oil fed to the gasifier
R = fraction of boiler flue gas recycled to the gasifier
X_0 = overall sulfur capture
X_G = gasifier sulfur capture

and

a = ratio of the sulfur in the spent regenerator stone to the total sulfur leaving the regenerator in the spent stone and the off-gas. The value of a used herein was 0.016359, derived from the NEES design.

These relations are presented in Figures 7 and 8. For 90 percent overall capture, 95 percent retention in the gasifier, and 10 percent flue gas recycle, the sulfur capture in the absorbed need be no higher than 41.8 percent.

From the design data presented in the Westinghouse March 1975 Report, Appendices D and G,[3] the 46 MW demonstration plant proposed at that time would meet the Federal standard for new fuel oil-fired boiler plants of 344 ng SO_2/J (0.8 lb $SO_2/10^6$ Btu) with an overall sulfur retention of 74 percent. This conclusion is based on a heat rate of 3.05 J/Ws and a 2.6 percent sulfur content in the fuel. With absorber off-gas recycle, given 90 percent retention in the gasifier, the absorber need retain only 27 percent of the sulfur fed to it. For a 5 percent sulfur fuel the overall retention required would increase to 86 percent, and the absorber retention would be 61 percent.

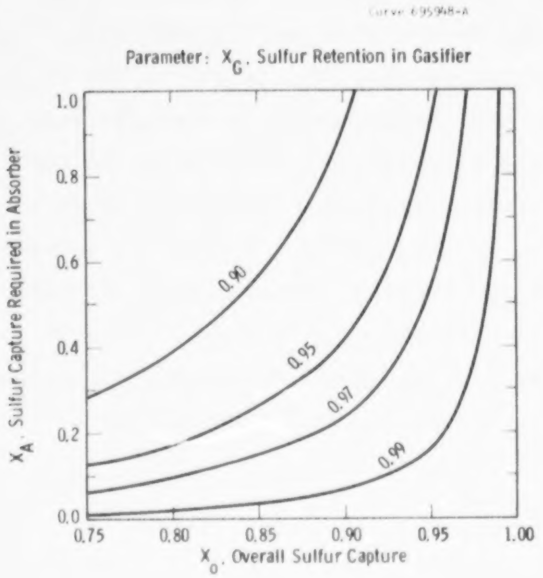

Figure 7 - Sulfur Capture in CAFB Absorber Vs Overall Sulfur Capture at 10% Recycle of Boiler Flue Gas

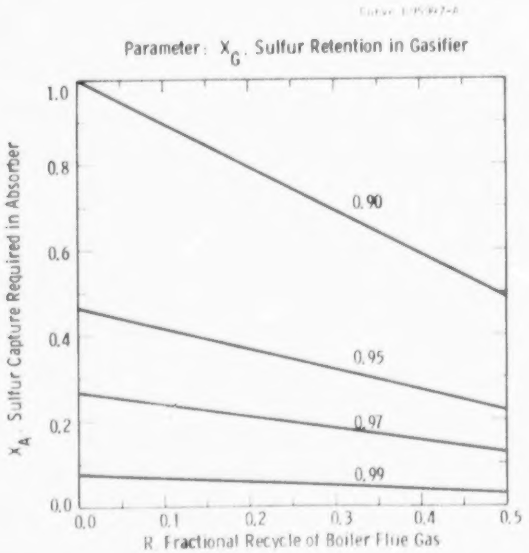

Figure 8 - Effect of Boiler Flue Gas Recycle on Sulfur Capture Required in CAFB Absorber at 90% Overall Sulfur Capture

To allow for the gas contact time required and the possibility of process upsets, the option of recycling absorber off-gas (Figure 5) was adopted. We assumed that SO_2 capture in the absorber would be 90 percent, which would increase the absorption duty in the gasifier and the spent stone circulation rate between the gasifier and the regenerator by about 10 percent. These effects were not included in the cost estimates in this report. Absorber pressure was set slightly higher than gasifier pressure to permit this off-gas recycle. As shown in Figure 6, we assumed that the kiln could be made long enough to provide the necessary contact time. This would require experimental verification but is a reasonable assumption for the purposes of economic evaluation.

With respect to the other design parameters, the experimental results supported the view that grinding the spent sorbent did not increase SO_2 absorption and it was therefore eliminated as a process step. The range of particle sizes then is so large (0-3175 μm), however, that retention of fines (-100 μm) while fluidizing the largest particles is impossible. Table 6 summarizes the fluidization conditions in Run CAFB-905. Minimum fluidization velocities were obtained from the Ergun equation using the Wen and Yu averages of 0.669 for sphericity and 0.474 for voidage.[33] We found that in some cases velocities to 200 times U_{mf}, the minimum fluidization velocity, were needed to elutriate fines. Only the -44 μm particles approached or exceeded this criterion. Better than 90 percent of the +88 μm material was retained in the bed. Thus, to retain 44 μm particles at 850°C would require a superficial gas velocity of not more than 10 cm/s, whereas to fluidize 354 μm particles would require at least 3.6 cm/s.

A moving bed, therefore, is proposed for the absorber option. The bed depth is limited to 2 m because of pressure drop considerations. The bed diameter of 10 m corresponds to a superficial velocity of 0.12 to 0.15 m/s at which particles 63 μm and larger are expected to be retained.

Table 6

GAS VELOCITIES IN THE DRY SULFATION OF REGENERATOR STONE IN RUN CAFB-905, cm/s

Condition	Phase		
	I	II	III
Temperature Level, °C	450	750	850
U_o, Superficial Velocity	24.66	13.56	9.94
U_{mf}, Minimum Fluidization Velocity			
Particle size, μm			
44 (325 mesh)	0.0748	0.0583	0.0548
88 (170 mesh)	0.299	0.233	0.220
354 (45 mesh)	4.83	3.77	3.55
500 (35 mesh)	9.56	7.50	7.06
U_o/U_{mf}			
44 μm	330	233	181
88 μm	82	58	45
354 μm	5.1	3.6	2.8
500 μm	2.6	1.8	1.4

This probably means the boiler fines will have a residence time comparable to the gas contact time of about 15 seconds. Retained solids will have a residence time of 84 hours.

Further experimental work is needed to confirm sulfur capture and calcium utilization. For the purposes of this study, the final solid effluent will be a blend of absorber product and fines from the bag-filter on the regenerator off-gas. It will contain about 5 weight percent residual CaO and about 10 mole percent of the total calcium present. Laboratory tests to evaluate the change in environmental impact following dry sulfation are reported in Volume 3 of this report.[4] Leaching results demonstrated that leachate quality was improved, reducing the potential for water pollution, and that the sulfide evolution concern could be eliminated.

The rotary kiln option was initially attractive because it offered the possibibility of process simplification. The heat balance on the resulfation reaction, however, revealed that substantial heat removal was required. A waste heat boiler was added in both the absorber and the kiln versions, and we introduced nearly three times stoichiometric air. Boiler fines as well as regenerator secondary cyclone fines were fed to the kiln to provide the CaO needed for sulfur capture. The kiln diameter was set arbitrarily at 5 m, as perhaps the largest practical for a rotating vessel. If we assume that 7 percent of the cross-sectional area was occupied by solids, the gas residence time in a 115 m kiln would be 105 seconds, while the solids residence time would be about 84 hours.

FLY ASH BLENDING - LOW TEMPERATURE

Appendix F contains the experimental data on the exploration of fixing the spent sorbent with fly ash. This can be done in a variety of ways: direct mixing, briquetting, or isostatic pressing. These variations are all based on the pozzolanic reaction between the lime in the spent sorbent and the silica in the fly ash. Figures 9 and 10 show the facilities required for the briquetting option. Grinding high lime-content spent sorbent to -125 μm, compressing it isostatically, and then curing it in water has been shown to result in compacts with compressive strengths well above the normal concrete range, 13.8 to 41.4 MPa (2000-6000 psi). Such material could be used as aggregate. We judged, however, that briquetting would probably be more economical than isostatic pressing, which is basically a batch process.

We expect that a source of coal fly ash will be available, perhaps even on site from an existing boiler. Development work is also in progress on feeding coal to the CAFB process. If the work is successful, the cost of ash silos could be deleted. A weigh system is shown, although volumetric feeding might prove satisfactory. There is some question about the mechanics of transferring the fresh briquets to the

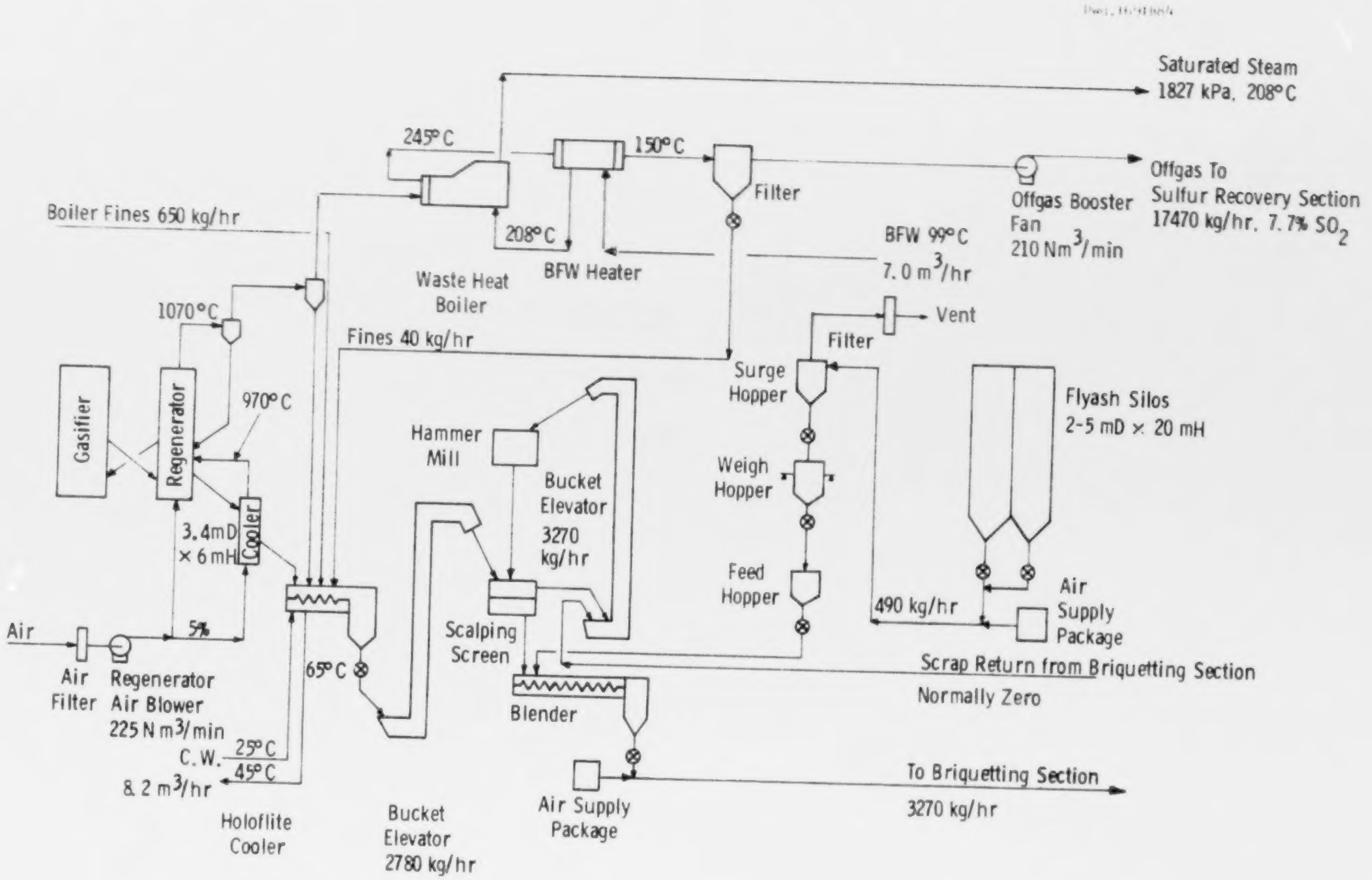
Saturated Steam
1827 kPa, 208°C
245°C
150°C
Filter
Offgas To
Sulfur Recovery Section
17470 kg/hr, 7.7% SO2
Offgas Booster
Fan
210 Nm3/min
Boiler Fines 650 kg/hr
208°C
BFW Heater
BFW 99°C
7.0 m3/hr
Waste Heat
Boiler
1070°C
Fines 40 kg/hr
Filter
Vent
Surge
Hopper
970°C
Gasifier
Regenerator
Hammer
Mill
Bucket
Elevator
3270
kg/hr
Flyash Silos
2-5 mD × 20 mH
Weigh
Hopper
3.4mD
× 6 mH
Cooler
Feed
Hopper
Air
Supply
Package
490 kg/hr
Air
5%
Scalping
Screen
Scrap Return from Briquetting Section
Normally Zero
Air
Filter
Regenerator
Air Blower
225 N m3/min
65°C
Blender
C. W.
25°C
45°C
8.2 m3/hr
To Briquetting Section
3270 kg/hr
Air Supply
Package
Holoflite
Cooler
Bucket
Elevator
2780 kg/hr

Figure 9 - Aggregate Production by Briquetting Spent Sorbent from a 200 MW CAFB Plant Feed Preparation Section

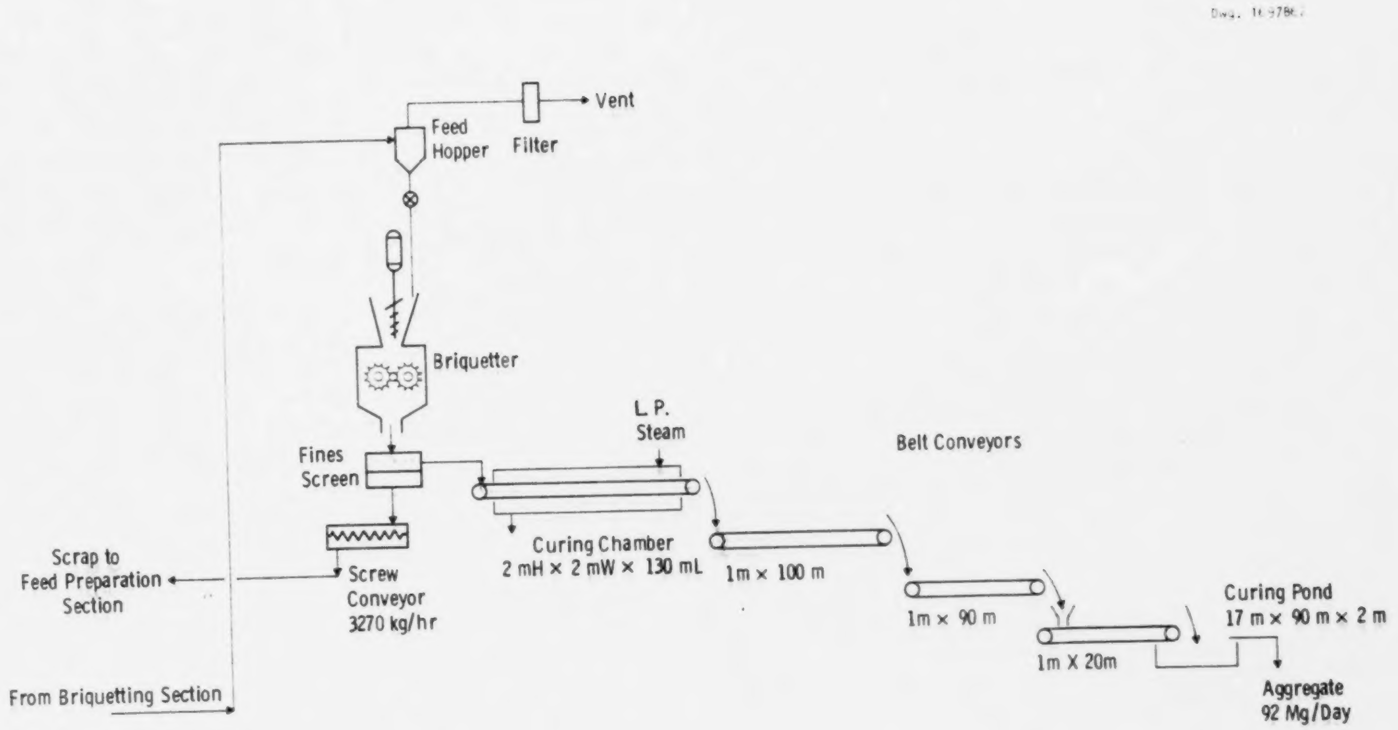

Dwg. 1697B62
Vent
Feed Hopper
Filter
Briquetter
L.P. Steam
Fines Screen
Belt Conveyors
Curing Chamber 2 mH × 2 mW × 130 mL
1m × 100 m
1m × 90 m
1m X 20m
Scrap to Feed Preparation Section
Screw Conveyor 3270 kg/hr
Curing Pond 17 m × 90 m × 2 m
Aggregate 92 Mg/Day
From Briquetting Section

Figure 10 - Aggregate Production by Briquetting Spent Sorbent from a 200 MW CAFB Plant Briquetting Section

belt conveyors in the curing chamber, but we have assumed that any additional feeding devices would have a negligible impact on cost. No commercial unit was found to carry out the initial three-hour steam cure so we estimated a cost on the basis of a system of five conveyor belts inside a single atmospheric-pressure enclosure.

The final curing pond is intended to provide 30 days of water curing. The pond will be divided into 30 cells to permit systematic loading and unloading of material. The material of construction will be the spent sorbent. About 24 days' production will be required. Initial production from the plant could be disposed of in a landfill if it is not of satisfactory quality. Winterizing may be needed, but data from another project suggest that curing continues even at temperatures below 0°C.

FLY ASH BLENDING - HIGH TEMPERATURE

Although data were obtained that showed a potential for processing spent sorbent at temperatures over 1000°C, we decided not to develop this option into a specific flowsheet since we judged it to be less favorable than low-temperature processing. The results of feasibility experiments are presented in Appendix G.

CALCIUM SULFIDE PROCESSING

An alternative to the regenerative CAFB process is a once-through operation in which the solid effluent is taken from the gasifier and contains a relatively high concentration of CaS. An attractive possibility would be the reversal of the desorption reaction to release H_2S. Evidence thus far indicates this is not favored thermodynamically (see Appendix H). Perhaps the most practical alternative is oxidation to $CaSO_4$, which would be a third process generating such a material. However, sintering with siliceous materials to make an aggregate may be possible. Further consideration of this option was deferred.

MISCELLANEOUS EQUIPMENT SIZING

Storage Silos

Inventory is based on a 30-day normal production rate. Bulk densities were 1280 kg/m^3 for regenerator stone, 1600 for sulfated stone, 1345 for dead-burned stone, 1600 for sintered stone, and 640 for fly ash. The aspect ratio for the silos was set initially at L/D of 4:1, which allowed 1 diameter for freeboard and coning at the top. In effect, this assumed a maximum angle of repose of 63°. These assumptions were modified by constraints set by commercial design practices.

Enclosed storage is recommended for at least the direct disposal case because of the high content of active lime. It is preferable in the dead-burning and sintering cases and in the dry sulfation cases to avoid any problems arising from leachate production. In general, it is not required for the briquetted product. Results of freeze-thaw tests from another project suggest that curing of compacts may continue even under freezing conditions.

Kilns

Conceptually, a rotary kiln offers a way to process materials at high temperature with a low pressure drop. For the dead-burning case, the residence time provided for solids is 5 hours; for sintering, 29 hours. Although fines from the boiler have been exposed to combustion conditions, we propose to subject them to additional exposure up to 1250°C. Because of their small particle size range, they will flow concurrently with the gas stream in the kiln. It is possible the secondary cyclone fines would be fed similarly. In the sintering and dry sulfation cases the higher gas rate definitely favors concurrent flow for fines. Heat transfer was estimated from

$$U = 0.05\ G^{0.67}$$

where

U = heat transfer coefficient, $Btu/hr\text{-}ft^2$ of kiln surface - °F and

G = gas mass flow rate, lb/hr-ft^2 kiln cross-section.[34]

Solids Cooler

Heat transfer data for gases to granular solids in beds were summarized in Kunii and Levenspiel.[35] For Reynolds numbers ($D_p V\rho/\mu$) covering the range 0.1 to 100, heat transfer coefficients (h), expressed as Nusselt numbers (hD_p/k), showed a range of five orders of magnitude. The pattern for both fixed beds and fluidized beds may be described as linear bands on log-log plots with roughly a +45° slope.

For fixed beds of coarse solids at $N_{Re} > 100$,

$$Nu_p = 2.0 + 1.8\ Pr^{1/3}\ Re_p^{1/2}$$

where

Pr is the gas Prandtl number

and

Nu_p is the particle Nusselt number.

For air at 500°C and 250 μm solids of particle density 1.3 g/cm^3, h at $Re_p = 100$ works out to 4280 W/m^2-K (755 Btu/hr-ft^2-°F). The air velocity at these conditions is 32.0 m/s. At this Reynolds number experimental data lie somewhat below the correlation. For lower Reynolds numbers the disparity between the correlation and the data increases. At $Re_p = 0.2$, Nu_p is 0.001 vs 3 for the correlation.

For fluidized beds, the data for gas back-mixing from various investigators fall along correlating lines scattered over four orders of magnitude of Nu_p. Plug flow data appear to straddle the general trend of the fixed-bed data. The spread (uncertainty), however, is larger. At 1 m/s gas superficial velocity, corresponding to $Re_p = 3.13$, h for fixed beds from the above correlation is 1160 W/m^2-K (204 Btu/hr-ft^2-°F). Plug flow fluid bed data indicate an h of only 48.4 W/m^2-K (8.54 Btu/hr-ft^2-°F) while fixed-bed data yield 14.5 W/m^2-K (2.56 Btu/hr-ft^2-°F). Since the spread in these predictions was so great, we decided to design the solids cooler on the basis of pressure drop and elutriation considerations, leaving confirmation of the heat transfer performance to a future experimental program.

Air rate through the coolers was based on a supply temperature of 65°C and a 100°C approach to the inlet stone temperature. Ambient air was set at 15°C and 50 percent relative humidity.

Holoflite Cooler

We assumed that all sorbent-derived spent solids would be disposed of in only one way and, therefore, would be combined into one stream. Heat duty on these coolers includes cooling spent regenerator bed material from 75°C, boiler fines from 150°C, regenerator secondary cyclone fines from 1070°C, and off-gas bag-filter fines from 75°C to 65°C. The cooling water inlet temperature and the allowable rise were taken to be 25°C and 20°C respectively. The size of the coolers was prorated from vendor quotations on previous jobs.

Steam Generation

All cases include facilities for recovery of heat from hot gases through use of waste heat boilers. Various configurations are possible. A reboiler is shown in four cases, while a vertical exchanger with a separate steam disengaging drum is shown in the two dry sulfation cases. Still another option is to use a horizontal exchanger plus the separate steam drum. Capital requirements are based on this third option.

Boiler feedwater (BFW) is assumed to be available from a deaerator at 99°C and is preheated to saturation temperature. Steam is not required at a high pressure so an intermediate level was shown. Heat transfer coefficients were set at 142 W/m^2-K (25 Btu/hr-ft^2°F) for the BFW preheater. Steam generators were sized on the basis of 61 m/s (200 fps) tube velocity. Heat transfer coefficients worked out to the range of 80 to 102 W/m^2-K (14 to 18 Btu/hr-ft^2-°F).

6. ECONOMIC EVALUATION

PERSPECTIVE

The previous section presented engineering details for five alternative options for processing CAFB solid residues. This information provides the technical basis for a preliminary economic comparison of these options. These options had been selected from a total of twenty bv previous technical and qualitative evaluations. The objective was to determine whether these subsystems differ significantly in cost and, if so, what components are mainly responsible for the differences. The actual costs of course, would depend on the site selected, the specific plant requirements, and many other factors. The analysis presented here assumes that the effect of these factors, within the accuracy of the information available, would be common to all options.

BASIS FOR COST DATA

The physical basis for these evaluations was given in Section 5. The cost estimates were developed from the direct equipment costs by a factored approach. All costs are referred to a base date of July 1978.

Prices for equipment items such as pressure vessels and silos were obtained with the aid of PDQS, a proprietary computerized equipment design and quote service. Blower costs were obtained from PROVES, a related proprietary service. Additional items were based on vendor estimates, literature data,[36,37] or the amount of material needed for fabrication.

Site development and auxiliary buildings have not been included. The cost of the sulfur recovery plant was scaled up from a 1974 estimate by an architect-engineering firm.

CAPITAL COST

Table 7 summarizes the total investment required in the various options. Tables 8 through 13 are equipment lists for the various options; Tables 14 through 17 are equipment cost lists.

ASSESSMENT

Capital Investment

The lowest installed cost option proved to be dry sulfation, absorber option, at \$22/kW. We wish to emphasize that this figure does not represent the actual construction cost for this option but rather a figure used to estimate the rankings of the options with regard to cost. The chief reason for this limitation is that the estimates do not include the boiler or ancillary equipment.

Even if the front end of the plant must be enlarged somewhat to handle the absorber off-gas recycle, the cost of this option is still expected to be no more than the general level of the others (\$58/kW). The kiln variation for dry sulfation is considered unattractive technically and economically.

Dead-burning and sintering require significant capital investments to produce a material which may be merely discarded. Both appear to cost about the same (\$60/kW), as does briquetting. Even direct disposal, the fifth option, is an expensive option.

What emerges is that the cost of the sulfur recovery plant overrides differences in the costs of the stone processing systems. For stone processing alone, direct disposal has the lowest cost and dry sulfation has the highest. As before, the costs for briquetting, dead-burning, and sintering are about the same (\$14/kW).

Thus, the practical alternatives to dry sulfation are the low-temperature options at a combined cost of \$52/kW for direct disposal and \$60/kW for briquetting. The latter may be reduced further if direct casting is practicable. Briquetting is particularly interesting for areas where the local supply of coarse aggregate has been depleted.

Table 7

COMPARISON OF INVESTMENTS IN STONE PROCESSING OPTIONS IN OIL GASIFICATION[a]

	Low Temperature Options		Dry Sulfation		High Temperature Options	
	Direct Disposal	Briquetting	Absorber Option	Kiln Option	Dead-burning	Sintering
Equipment Cost	$ 523	$ 1,048	$1,306	$3,868	$ 985	$ 1,282
Field Materials	83	268	625	1,130	230	335
Field Labor	142	393	697	1,062	274	367
Freight, Insurance, & Taxes	49	105	154	400	97	129
Field Indirects	96	265	470	716	185	247
Engineering	83	161	221	625	160	207
Bare module cost	976	2,240	3,473	7,801	1,931	2,567
Contingency & Fee @ 25%	244	560	868	1,950	483	642
Total installed cost	$ 1,220	$ 2,800	$4,341	$9,751	$ 2,414	$ 3,209
$/kW	6.10	14.00	21.70	48.75	12.07	16.04
Sulfur Recovery Plant	9,110[b]	9,110	--	--	9,110	9,110
Combined cost	$10,330	$11,910	$4,341	$9,751	$11,524	$12,319
$/kW	51.65	59.55	21.70	48.75	57.62	61.60

---

[a] All costs in thousands of dollars as of July 1978.

[b] Based on $3,000,000 for a 46 MW plant in 1975.

Table 8

EQUIPMENT LIST FOR DIRECT DISPOSAL OPTION FOR PROCESSING SPENT CAFB REGENERATOR STONE

Reactors

Pressure Vessels

Spent stone cooler	3.4 m D x 6 m H
Design	175 kPag @ 340°C

Other Vessels

Storage silos	3 - 6 m D x 26 m H
Design	Concrete, precast Double cone bottom Bulk density, 1280 kg/m^3 (80 lb/cf) Cast iron rotary outlet valves

Fans and Blowers

Regenerator air blower	300 Am^3/min @ 60 kPa ΔP 50% R.H. @ 15°C
Off-gas booster fan	420 Am^3/min. @ 60 kPa ΔP Suction pressure - 96.5 kPa Suction temperature - 150°C MW - 31.7

Heat Transfer Systems

Waste heat boiler	135 m^2
Design	Shell side - 2.07 MPag @ 340°C Tube side - 17.5 kPag @ 340°C Inlet gas temperature - 1070°C
Steam drum	1.2 m D x 3.6 m L
Design	2.07 MPag @ 340°C
BFW heater	80 m^2
Design	Shell side - 2.07 MPag @ 340°C Tube side - 1.04 MPag @ 340°C
Holoflite cooler	690 MJ/hr Cooling water rise 20°C

Table 8 (Cont'd)

Particulate Removal Systems	
Regenerator primary cyclones	880 Am^3/min @ 1070°C
Regenerator secondary cyclones	880 Am^3/min @ 1070°C
Off-gas bag filter	330 Am^3/min @ 150°C
Regenerator air filter	300 Am^3/min @ 15°C
Transport Systems	
Air-supply package	2780 kg spent stone/hr

Table 9

EQUIPMENT LIST FOR DEAD-BURNING OPTION FOR PROCESSING SPENT CAFB REGENERATOR STONE

Reactor	
Rotary kiln	3 m D x 25 m L Solids residence time 5.7 hr @ 1250°C
Pressure Vessels	
Spent stone cooler	(1)
Other Vessels	
Kiln cyclone seal pot	1.4 m D x 3 m H
Storage silos	(1)
Fans and Blowers	
Regenerator air blower	(1)
Off-gas booster fan	(1)
Kiln gas booster fan	30 Am^3/min @ 10 kPa ΔP
Heat Transfer Systems	
Waste heat boiler	(1)
Steam drum	(1)
BFW heater	(1)
Airfin cooler	15 m^2
Holoflite cooler	92 MJ/hr Cooling water rise 20°C
Fuel oil system	60 kg No. 2 fuel oil/hr

Table 9 (Cont)

Particulate Removal Systems	
Regenerator cyclones	(1)
Off-gas bag filter	(1)
Kiln gas bag filter	25 Am^3/min @ 159°C
Kiln cyclone	80 Am^3/min @ 1250°C
Cooler cyclone	265 Am^3/min @ 970°C
Regenerator air filter	(1)
Transport System	
Cooled stone elevator	2 - 3000 kg/hr

---

(1) As in Direct Disposal Option

Table 10

EQUIPMENT LIST FOR SINTERING OPTION FOR PROCESSING SPENT CAFB REGENERATOR STONE

Reactors	
Rotary kiln	3 m D x 100 m L Residence time - 29 hrs @ 1500°C
Pressure Vessels	
Spent stone cooler	(1)
Fines surge pot	1.4 m D x 3 m H
Other Vessels	
Storage silos	3 - 5.6 m D x 22.4 m H
Design	Concrete, precast Double cone bottom Bulk density - 1600 kg/m^3 (100 lb/cf) Cast iron rotary outlet valves
Fans and Blowers	
Regenerator air blower	(1)
Booster fan	480 Am^3/min @ 60 kPa ΔP
Heat Transfer Systems	
Waste heat boiler	150 m^2
Steam drum	(1)
BFW heater	90 m^2
Holoflite cooler	2.0 GJ/hr Cooling water rise 20°C
Fuel oil system	135 kg No. 2 fuel oil/hr
Particulate Removal Systems	
Regenerator cyclones	(1)
Off-gas bag filter	370 Am^3/min
Regenerator air filter	(1)

Table 10 (Cont)

Kiln cyclone	140 Am^3/min
Cooler cyclone	115 Am^3/min
Transport Systems	
Cooler stone elevator	1400 kg/hr
Pressed stone elevator	2710 kg/hr

---

(1) As in Direct Disposal Option.

Table 11

EQUIPMENT LIST FOR DRY SULFATION, ABSORBER OPTION, FOR PROCESSING SPENT CAFB REGENERATOR STONE

Reactors	
Absorber	10 m D x 10 m H
Design	175 kPa @ 340°C
Pressure Vessels	
Spent stone cooler	Not required
Cyclone seal pot	1.4 m D x 3 m H
Pulverizer feed	1.4 m D x 3 m H
Other Vessels	
Storage vessels	3 - 7 m D x 28 m H
Design	Concrete precast Double cone bottom Bulk density - 1600 kg/m^3 (100 lb/cf) Cast iron rotary outlet valve
Other Equipment	
Pulverizer	1420 kg/hr
Fans and Blowers	
Regenerator air blower	310 Am^3/min @ 65 kPa ΔP 50% R.H. @ 15°C
Off-gas booster fan	350 Am^3/min @ 115 kPa/ΔP MW 31.5
Absorber air blower	90 Am^3/min @ 115 kPa ΔP 50% R.H. @ 15°C
Pulverizer air blower	105 Am^3/min @ 445 kPa ΔP 50% R.H. @ 15°C

Table 11 (Cont)

Heat Transfer Systems	
Waste heat boiler	270 m^2
Steam drum	(1)
BFW heater	85 m^2
Holoflite cooler	4.70 GJ/hr
Design	Cooling water rise 20°C
Particulate Removal Systems	
Regenerator cyclones	920 Am^3/min
Absorber cyclones	710 Am^3/min
Pulverizer cyclones	125 Am^3/min
Off-gas bag filter	350 Am^3/min
Absorber off-gas bag filter	825 Am^3/min
Regenerator air filter	310 Am^3/min
Pulverizer air filter	105 Am^3/min
Absorber air filter	90 Am^3/min
Transport Systems	
Processed stone elevator	6050 kg/hr

---

(1) As in Direct Disposal Option

Table 12

EQUIPMENT LIST FOR DRY SULFATION, KILN OPTION, FOR PROCESSING SPENT CAFB REGENERATOR STONE

Reactors	
Rotary kiln	5 m D x 115 m L Residence time - 84 hr @ 850°C
Pressure Vessels	
Spent stone cooler	3.6 m D x 7 m H
Design	175 kPag @ 340°C
Fines surge pot	1.4 m D x 3 m H
Other Vessels	
Storage silos	3 - 7 m D x 28 m H Concrete, precast Double cone bottom Bulk density - 1600 kg/m^3 (100 lb/cf) Cast iron rotary outlet valves
Fans and Blowers	
Regenerator air blower	(1)
Kiln air blower	140 Am^3/min @ 60 kPa ΔP
Off-gas booster fan	420 Am^3/min @ 5 kPa ΔP
Heat Transfer System	
Waste heat boiler	(1)
Steam drum	(1)
BFW heater	(1)
Holoflite cooler	2.47 GJ/hr
Fuel oil system	(2)

Table 12 (Cont)

Particulate Removal Systems		
Regenerator cyclones		(1)
Regenerator air filter		(1)
Kiln cylinders	1210 Am^3/min	
Kiln air filter	140 Am^3/min	
Off-gas bag filter		(1)
Transport Systems		
Cooled stone elevator	3000 kg/hr	
Processed stone elevator	6000 kg/hr	

---

(1) As in direct disposal
(2) Startup only - cost not included in comparisons

Table 13

EQUIPMENT LIST FOR BRIQUETTING OPTION FOR PROCESSING SPENT CAFB REGENERATOR STONE

Reactors	None
Pressure Vessels	
Spent stone cooler	(1)
Design	
Other Vessels	
Fly ash silos	2 - 5 m D x 20 m H Concrete, precast Double cone bottom Bulk density - 640 kg/m^3 (40 lb/cf) Cast iron rotary outlet valves
Curing chamber	130 m L x 2 m W x 2 m H 5 Conveyor belts, 1 m wide x 126 m L
Curing pond	17 m x 90 m x 2 m
Fans and Blowers	
Regenerator air blower	(1)
Off-gas booster fan	(1)
Heat Transfer Systems	
Waste heat boiler	(1)
Steam drum	(1)
BFW heater	(1)
Holoflite cooler	(1)

Table 13 (Cont)

Particulate Removal Systems	
Regenerator Cyclones	(1)
Off-gas Bag filter	(1)
Regenerator air filter	(1)
Transport Systems	
Air supply packages	1 - 3270 kg mix/hr 1 - 490 kg fly ash/hr
Cooled stone elevator	2 - 2780 kg stone/hr
Screw conveyor	3270 kg scrap/hr
Belt conveyors	1 m x 100 m 1 m x 90 m 1 m x 20 m
Materials Processing	
Hammer mill	3270 kg/hr
Briquetter	3270 kg/hr
Blender	3270 kg/hr
Scalping screen	3270 kg/hr
Fines screen	3270 kg/hr
Briquetter feed hopper	2.0 m D x 2.3 m H 1 hr surge capacity
Flyash surge hopper	2.0 m D x 2.3 m H 4 hr surge capacity
Flyash weigh	0.5 m D x 1.3 m H 15 minute weigh cycle
Flyash feed hopper	0.5 m D x 2.3 m H 2 dumps from weigh hopper

---

(1) As in Direct Disposal Option

Table 14

EQUIPMENT COSTS FOR DIRECT DISPOSAL OPTIONS FOR PROCESSING SPENT CAFB REGENERATOR STONE

Vessels	
Spent stone cooler	$ 41,310
Blowers and Fans	
Regenerator air blower	52,120
Off-gas booster fan	57,420
Heat Transfer Systems	
Waste heat boiler	26,040
Steam drum	11,040
BFW heater	13,000
Holoflite cooler	19,990
Particulate Removal Systems	
Regenerator cyclones	41,670
Off-gas bag filter	11,000
Regenerator air filter	700
Subtotal	$274,290
Transport and Systems	
Air supply package	12,000
Materials Handling	
Storage silos	237,090
Total	$523,380

Table 15

COMPARISON OF INVESTMENTS REQUIRED FOR DEADBURNING AND SINTERING OPTIONS FOR PROCESSING SPENT CAFB REGENERATOR STONE

	Dead-burning	Sintering
Basic items as in direct disposal (1)	$254,300 (2)	$146,840 (3)
Reactors		
Rotary kiln	426,000	724,000
Vessels		
Fines surge pot	--	13,260
Kiln cyclone seal pot	13,260	--
Blower and Fans		
Kiln gas booster fan	2,960	--
Off-gas booster fan	(4)	62,430
Heat Transfer Systems		
Holoflite cooler	5,400	39,930
Waste heat boiler	(4)	27,550
Air fin cooler	15,970	--
BFW heater	(4)	14,040
Fuel oil system	15,560	26,360
Particulate Removal Systems		
Kiln cyclones	2,800	4,030
Kiln gas bag filter	2,060	--
Cooler cyclone	6,100	3,550
Off-gas bag filter	(4)	11,900

Table 15 (Cont)

	Dead-burning	Sintering
Transport Systems		
Cooled stone elevators	$ 3,200	$ 2,600
Materials Handling		
Storage silos	237,090	205,330
Subtotal	730,400	1,134,980
Total equipment	$984,700	$1,281,820

---

(1) Common Items with Direct Disposal

Spent Stone Cooler	41,310	41,310
Regenerator air blower	52,120	52,120
Off-gas booster fan	57,420	--
Waste heat boiler	26,040	--
Steam drum	11,040	11,040
BFW heater	13,000	--
Regenerator cyclones	41,670	41,670
Holoflite cooler	--	--
Off-gas bag filter	11,000	--
Regenerator air filter	700	700
	$254,300	$146,840

(2) 9 items
(3) 5 items
(4) Included in basic items

Table 16

COMPARISON OF INVESTMENTS REQUIRED FOR DRY SULFATION OF SPENT CAFB REGENERATOR STONE

Dry Sulfation Option	Absorber	Kiln
Basic Items, as in Direct Disposal (1)	$ 700 (2)	$ 155,570 (3)
Reactors		
Absorber	463,520	--
Rotary kiln	--	3,200,000
Vessels		
Spent stone cooler	--	46,360
Fines surge pot	--	13,260
Pulverizer feed pot	13,260	--
Cyclone seal pot	13,260	--
Blowers and Fans		
Regenerator air blower	62,290	(4)
Off-gas booster fan	15,750	15,360
Absorber air blower	26,840	--
Pulverizer air blower	29,950	--
Heat Transfer Systems		
Waste heat boiler	45,060	(4)
Steam drum	22,080	(4)
BFW heater	13,520	(4)
Fuel oil system	10,000	10,000
Holoflite cooler	69,570	45,800

Table 16 (Cont)

	Absorber	Kiln
Particulate Removal Systems		
Regenerator cyclones	$ 42,890	(4)
Absorber/kiln cyclones	36,240	51,250
Pulverizer cyclones	7,220	--
Off-gas bag filters	11,430	(4)
Absorber off-gas bag filter	19,960	--
Regenerator air filter	(4)	(4)
Absorber/kiln air filter	320	420
Pulverizer air filter	350	--
Transport Systems		
Processed stone elevator	2,900	2,900
Cooled stone elevator	--	1,200
Materials Handling		
Pulverizer	73,740	--
Storage silos	325,660	325,660
Subtotal	1,305,810	3,712,210
Total Equipment	$1,306,510	$3,867,780

---

(1) Common Items between Dry Sulfation and Direct Disposal

	Absorber	Kiln
Dry sulfation Option	--	--
Spent stone cooler	--	--
Regenerator air blower	--	52,120
Off-gas booster fan	--	--

Table 16 (Cont)

	Absorber	Kiln
Waste heat boiler	--	$ 26,040
Steam drum	--	11,040
BFW heater	--	13,000
Holoflite cooler	--	--
Regenerator cyclones	--	41,670
Off-gas bag filter	--	11,000
Regenerator air filter	700	700
	$700	$155,570

(2) 1 item
(3) 7 items
(4) Included in basic items

Table 17

INVESTMENT REQUIRED FOR BRIQUETTING OPTIONS FOR PROCESSING SPENT CAFB REGENERATOR STONE

Basic Items, as in Direct Disposal	$ 274,290 (1)
Curing Chamber	260,270
Curing Pond	48,610
Transport Systems	
Air supply packages	15,890
Cooled stone elvators	2,500
Screw conveyor	6,540
Belt conveyors	101,300
Materials Handling Systems	
Storage silos	130,890
Hammer mill	2,810
Briquettes	145,000
Blender	8,710
Fines screen	5,580
Scalping screen	12,820
Briquetter feed hopper	12,750
Flyash hoppers	19,750
Additional Items	773,420
Total Equipment	$1,047,710

---

(1) 10 items

Table 16 (Cont)

	Absorber	Kiln
Waste heat boiler	--	$ 26,040
Steam drum	--	11,040
BFW heater	--	13,000
Holoflite cooler	--	--
Regenerator cyclones	--	41,670
Off-gas bag filter	--	11,000
Regenerator air filter	700	700
	$700	$155,570

(2) 1 item
(3) 7 items
(4) Included in basic items

Table 17

INVESTMENT REQUIRED FOR BRIQUETTING OPTIONS FOR PROCESSING SPENT CAFB REGENERATOR STONE

Basic Items, as in Direct Disposal	$ 274,290 (1)
Curing Chamber	260,270
Curing Pond	48,610
Transport Systems	
Air supply packages	15,890
Cooled stone elvators	2,500
Screw conveyor	6,540
Belt conveyors	101,300
Materials Handling Systems	
Storage silos	130,890
Hammer mill	2,810
Briquettes	145,000
Blender	8,710
Fines screen	5,580
Scalping screen	12,820
Briquetter feed hopper	12,750
Flyash hoppers	19,750
Additional Items	773,420
Total Equipment	$1,047,710

---

(1) 10 items

Environmental Impact

Since all options would be designed to meet existing environmental regulations and criteria, there should be no difference in SO_2 emissions. There could be differences in the environmental impact of solid residues, however, the dry sulfation option would have a spent sorbent effluent set by the Ca/S treat ratio of about 1:1. All the other options have the theoretical possibility of a smaller spent sorbent rate because of a lower Ca/S ratio. This could result from use of more attrition-resistant limestones, modified main process conditions that degrade the sorbent activity at a lower rate, or synthetic sorbents. The first of these appears to have limited potential for reducing the generation rate of residues, but the other two are receiving some attention at the laboratory level.

In addition, all the options except dry sulfation would generate residues from the sulfur recovery plant associated with them. While different systems might be used, for the present we have concluded that the stone processing options should be debited equally for this aspect. These residues might be char, ash, and possibly chemical wastes, as from the Stretford Process.

Conclusions about leachate characteristics have been reported in Volume 3.[4] Among them was the finding that the leachate quality from processed spent sorbent was equal to or better than that from natural gypsum. Trace elements are not expected to result in environmental problems.

Effect of By-Product Credits

The effect of a by-product credit for sulfur recovery has proved to be unimportant. The 200 MW plant at 3 percent sulfur will produce about 10,770 Mg (10,600 long tons) sulfur per year at 90 percent overall recovery. The price of domestic sulfur has fluctuated roughly between \$17 and 28/Mg over the period 1950-1973.[14] In 1974, the price jumped to about \$30/Mg, and to \$45/Mg the following year.[38] It is currently about \$64/Mg.[39] Interestingly enough, while the price was increasing sharply, demand declined only slightly, which confirms the view that sulfur is an essential mineral for which industry has found no substitute. The rise in price can be attributed to the sharp increase in energy costs, since most of the domestic sulfur is Frasch sulfur. At \$64/Mg, the gross realization of recovery is \$689,000/yr which does not even cover annual capital charges of 17 percent or \$1,550,000. This reconfirms an earlier assessment that sulfur recovery is uneconomical by available processes. Further, 70 percent of the domestic sulfur is used in the southern states, with Florida taking 28 percent, the latter presumably because of the phosphate industry. The demand for electric power is nationwide, but the sulfur market is concentrated in, perhaps, five states.

A word about possible by-product credits for briquets or lime: at 92 Mg of briquets/day, the gross annual realization at \$151,800 vs. charges on incremental capital of \$268,600. Concrete block (8" x 8" x 16"), however, is quoted in the Pittsburgh area at about \$27/Mg. If we assume that block made with spent sorbent could command the same price, the gross realization would be \$820,000. Thus, the case for making cinder block appears more attractive than for making a coarse aggregate. Different equipment, however, would be required.

Variations

After further data on the residence time for gas in the dry sulfation case are obtained, the size of the absorber and the amount of gas recycled to the gasifier may prove uneconomical. This option may still be made more attractive than any with a sulfur recovery plant, however, by adding additional fresh lime either to the gasifier or to the absorber. This technique would be contrary to current efforts to reduce lime usage but is suggested as an alternative possibly more acceptable to power plants than having essentially to operate a chemical plant in the form of a sulfur recovery plant.

If dry sulfation is rejected, another possibility would be to build the CAFB plant next to an existing sulfuric acid plant and sell it the regenerator off-gas. In this case the gas would have to be cooled from 1070°C, passed through a baghouse or a high-temperature electrostatic precipitator, and boosted in pressure. The cost of these facilities should be substantially less than those for a complete sulfur recovery plant.

CONCLUSIONS

The technical and economic evaluations clearly show that a dominant factor in the CAFB process is the investment required for a sulfur recovery plant. Since this cost is eliminated in the dry sulfation process, further development work should be carried out for this process.

In parallel with such work, development of a process such as briquetting to make aggregate or direct disposal via block manufacturing should continue:

- To preserve a back-up option to either direct disposal or dry sulfation.
- To offer the possibility of by-product credits and resource conservation.

In either case these options require confirmation of the acceptability of the products.

7. OCEAN DISPOSAL

BACKGROUND

As noted in Appendix S, Spent Limestone Disposition, of the 1975 Report,[3] ultimate disposal of spent sorbent by ocean dumping was considered a possibility for locations in and near coastal areas although Federal regulations already had severely reduced the probability of obtaining a permit for a new source.[40-42] Recognizing that ocean disposal might be excluded as an option, we nevertheless considered tests to determine the technical feasibility of ocean dumping of spent sorbent to be constructive for providing a basis for evaluation. Of the five classes of permits, at least three to be available. The special permit was valid for three years, and the research permit held for only 18 months; both were renewable. Interim permits expired annually, could be reapplied for, but would not be granted for new sources unless Phase A of an implementation plan was completed. This plan would either eliminate dumping or bring it within the requirements of Section 227.3 of the Final Regulations. Utilization of spent limestone sorbents as ocean reefs may provide an attractive option. This alternative is under study by others for flue-gas desulfurization wastes.[43]

EXPERIMENTAL WORK

The facilities of the Westinghouse Ocean Research Laboratory were utilized to perform tests on three specimens of solid sorbents with actual seawater. Some of the results were reported in March 1978.[43] The stone of main interest was regenerator stone from Run 9 of ERCA's CAFB oil gasification pilot plant in Abingdon, England. The second was a spent dolomite from Argonne National Laboratories (ANL). The third was a simulated spent dolomite made at the Westinghouse R&D Center by successively calcining, sulfiding, and oxidizing Tymochtee dolomite. Analyses of these specimens are shown in Appendix D.

The compositions shown were obtained by calculation from the chemical analyses for sulfate, sulfide, calcium, and magnesium. Carbon dioxide was measured in the ANL stone but not on the other two, since they are produced under conditions such that residual CO_2 would be very low. The dolomite from Run D-2 was selected because its composition was closest to that expected for a commercial plant.

Initial Tests

Initial tests (Appendix I) measured the temperature rise and pH changes in Maryland Bay water when contacted with the spent sorbents. The sorbents are described in Table I-1.

Table I-2 shows that 90 percent of the temperature rise was produced within six hours. On the other hand, the pH showed an immediate rise for all three specimens of 30 to 60 percent of the ultimate increase, with nearly all of the total increase occurring within one hour.

Table I-3 shows somewhat lower values for temperature rise and pH for the ANL and Westinghouse stones at 100 g/ℓ. We attribute this difference to the considerably smaller degree of mechanical mixing in Test II. Increasing the treat ratio increased the ultimate pH within Test II, but the final values for ANL and Westinghouse stones were about the same as for Test I. The CAFB stone showed significantly greater pH at 400 g/ℓ treat ratio and about 10X the heat generation of the other two stones.

Tests with Seawater

Preliminary tests of leaching were done with Maryland Bay water, yielding 6-hour and 24-hour samples of filtrates and suspended floc, plus the final solids. In general, the main tests, done with seawater at an actual dump site, yielded four kinds of samples: filtrate and floc from the liquid, plus core and surface samples of the residual solids. About two-thirds of the samples were inspected, as summarized in Appendix J, by procedures described in Table J-1. Inspections included the following:

1. Spectrochemical analysis for Cr, Cu, Ni, Pb, Sn and V
2. Atomic absorption (flameless) determination of Se and Hg on three samples (IIA 400L, IIA 400CS, II SL1)
3. Weight-volume relationships of sediment in liquid samples
4. Total volume of solid-liquid samples submitted for analysis
5. Analysis of both solid and liquid fractions for the listed impurities
6. Determination of fluorine (wet chemistry) on selected samples.

Results from Seawater Tests

The untreated sample of Maryland bay water contained levels of selected trace elements relative to water standards as shown in Table 18.

Table 18

COMPARISON OF TRACE ELEMENTS IN MARYLAND BAY WATER
WITH ESTABLISHED DRINKING WATER STANDARDS

Element	US Public Health Service	Commonwealth of Pennsylvania	World Health Organization
Chromium	P	NS	DNP
Copper	P	P	P
Lead	DNP	NS	DNP
Nickel	P	NS	NS
Tin	P	NS	NS
Vanadium	NS	NS	NS

P = Passes: level found is not more than the standard

NS = No standard

DNP = Does not pass, meaning the upper limit established by spectrographic analysis is higher than the standard. Actual value in the sample may be lower than standard.

Except for lead, whose level is in the doubtful category, Maryland bay water contained tolerable levels of the above six elements.

Effect of Stirring Time in Extraction of Trace Elements from Spent Sorbents

Test I included sampling, after 6 and after 24 hours of mechanical stirring, of suspensions of seawater and spent sorbent. For all three spent sorbents there was no difference in the upper limit found in the filtrates for seven elements as a result of stirring longer than 6 hours.

Levels of these elements in the residual solids were 10 to 1000X those in the filtrates, so apparently they are present in the spent sorbents in not readily leachable forms. As expected, the CAFB stone had high levels of vanadium and nickel. The ANL stone showed 100 ppm of chromium, while Tymochtee dolomite from the Westinghouse tests had 150 ppm of chromium and 200 ppm of nickel. These levels should be checked on other samples of these stones. It may be that chromium and nickel are being picked up from the reactor systems.

Effect of Treat Ratio on Extraction of Trace Elements from Spent Sorbents

Treat ratios used ranged from 20 to 400 g/ℓ seawater. The only agitation occurring was that due to the motion of the boat at the ocean disposal test site. The results are for 24 hours of contact time. No trend due to treat ratio was detected, either in the filtrates or in the residual solids.

Extraction Rate of Trace Elements

In general, the levels of trace elements found in the filtrates were no higher than background levels. This finding also supports the conclusion that the trace elements of interest (Cr, Cu, Ni, Pb, Sn, V) are apparently present in not readily leachable forms.

Spot checks were also made of the levels of three other elements, as shown in Appendix K. Background levels of mercury and selenium in Maryland bay water (Specimen II SL 1) were below the limits of detection by flameless atomic absorption, while fluorine was found to be 0.68 ppm. Although both the CAFB and the ANL stones showed fluorine contents of the order of 40 ppm, their leachates showed values somewhat less than the background bay water. Selenium, on the other hand, was not detected in either the leachate or the residual solids from the ANL stones. Mercury was found in the ANL stone to be less than 10 ppb, while the leachate was not detectably higher than background.

Trace Element Material Balances

The accuracy of the spectrographic analysis is estimated to be within a factor of 3. A result of, say, 12 ppm is to be read as having a high probability of being in the range of 4 to 36 ppm. A spot check of one sample, IIC20L, yields the following balance for vanadium:

		Mg of V
Filtrate	1000 g @ 0.1 ppm	0.1
Floc	0.3 g @ 100 ppm	0.0084
Solids	20 g @ 2000 ppm	40.0
Total found		40.1
Feed Solids	20 g @ 1%	200.0 mg
Seawater	1000 g @ 0.1 ppm	0.1
		200.1

V recovery = (40.1/200.1) 100 = 25%

The recovery is actually higher, since the vanadium content of the residual solids was reported as more than 2000 ppm. For this initial set of tests, we considered it unnecessary to pursue this disparity further.

Comparison with Regulations

Table 19 shows a comparison of trace element concentrations arising from spent sorbents with levels promulgated under federal regulations.

Table 19

COMPARISON OF TRACE ELEMENT CONCENTRATION PRODUCED FROM SPENT SORBENTS WITH ESTABLISHED CRITERIA, ppm

	Maximum Permissible Level	Argonne Spent Dolomite	CAFB Spent Limestone
Mercury			
In solids	0.75[a]	<0.010	--
In liquids	1.5[a]; 0.0020[b]	<0.001	--
Selenium			
In solids	-	<1	--
In liquids	0.01[b]	<0.1	--
Fluorine			
In solids	-	34	46
In liquids	2.4[b]	0.23	0.41

---

[a] Source: Reference 42.

[b] Source: EPA Proposed Interim Primary Drinking Water Standards, Federal Register, 40(51): 11989-98 (March 14, 1975).

The values shown for mercury under maximum permissible levels are for solid and liquid phases of water, respectively, in the case of ocean dumping. Where blanks are shown, no standards have been promulgated. We conclude that mercury and fluorine do not constitute a problem, while a conclusion on selenium is best deferred until additional measurements are available.

ASSESSMENT

Overall, the data support the view that the leach rate of trace elements such as chromium, copper, nickel, lead, tin, vanadium, mercury, selenium, and iron are essentially zero in the first 24 hours from all three samples tested. Experience with leaching of solids in the laboratory generally shows that the leach rates decrease with time from their initial values.

CONCLUSIONS

While these test results are certainly not definitive, they suggest that ocean disposal of spent calcium-based sorbents from fluidized-bed gasification or combustion of fossil fuels may not have a deleterious impact on the ocean environment due to trace elements. The effect of major constituents such as calcium, magnesium, and sulfate ions has not been investigated here, but it is possible that additional calcium may even be beneficial to aquatic life.

An opposing conclusion was obtained from EPA as recorded in Appendix A of the 1978 report.[34] The argument was based on several factors:

- The general policy of EPA to phase out ocean dumping by 1981
- The observation that the solid wastes under consideration here may contain vanadium, mercury, and arsenic as well as being highly alkaline
- The stringent criteria to be met by those seeking a permit for ocean disposal
- The high cost.

This conclusion was directed at commercial-scale dumping and left open the possibility of dumping for research purposes or on an interim basis.

The same report contained the conclusion from the Westinghouse Ocean Research Laboratory that it may be possible to obtain interim permits, noting that the Final Regulations specify a limiting permissible concentration for selected elements in the receiving water, not in the solid waste, and implying that dumping would meet criteria on trace elements if these elements were fixed in the wastes in a nonleachable form.

8. REFERENCES

1. Archer, D. H., D. L. Keairns, J. R. Hamm, R. A. Newby, W. C. Yang, L. M. Handman, and L. Elikan, Evaluation of the Fluidized Bed Combustion Process, Vols. I, II, and III. Report to EPA, Westinghouse Research and Development Center, Pittsburgh, PA, November 1971, OAP Contract 70-9, NTIS PB 211-494, 212-916, and 213-152.

2. Keairns, D. L., D. H. Archer, R. A. Newby, E. P. O'Neill, E. J. Vidt, Evaluation of the Fluidized-Bed Combustion Process, Vol. IV, Fluidized-Bed Oil Gasification/Desulfurization. Report to EPA, Westinghouse Research and Development Center, Pittsburgh, PA, December 1973, EPA-650/2-73-048d, NTIS PB 233-101.

3. Keairns, D. L., R. A. Newby, E. J. Vidt, E. P. O'Neill, C. H. Peterson, C. C. Sun, C. D. Buscaglia, and D. H. Archer, Fluidized Bed Combustion Process Evaluation - Residual Oil Gasification/ Desulfurization Demonstration at Atmospheric Pressure. Report to EPA, Westinghouse Research and Development Center, Pittsburgh, PA, March 1975, EPA-650/2-75-027 a&b, NTIS PB 241-834 and PB 241-835.

4. Sun, C. C., Chemically Active Fluid Bed for SO_x Control: Volume 3, Sorbent Disposal. Report to EPA, Westinghouse Research and Development Center, Pittsburgh, PA, July 1979, EPA-600/7-79-158c.

5. O'Neill, E. P., D. L. Keairns, and M. A. Alvin, Sorbent Selection for the CAFB Residual Oil Gasification Demonstration Plant. Report to EPA, Westinghouse Research and Development Center, Pittsburgh, PA, March 1977, EPA-600/7-77-029, NTIS PB 266-827.

6. Bachovchin, D. M., P. R. Mulik, R. A. Newby, and D. L. Keairns, Solids Transport between Adjacent CAFB Fluidized Beds. Report to EPA, Westinghouse Research and Development Center, Pittsburgh, PA, January 1979, EPA-600/7-79-021.

7. Keairns, D. L., W. G. Vaux, N. H. Ulerich, E. J. Vidt, and R. A. Newby, Chemically Active Fluid Bed for SO_x Control: Volume 1, Process Evaluation Studies. Report to EPA, Westinghouse Research and Development Center, Pittsburgh, PA, December 1979, EPA-600/7-79-158a, to be issued.

REFERENCES (Cont)

8. Keairns, D. L., C. H. Peterson, and C. C. Sun, Disposition of Spent Calcium-Based Sorbents Used for Sulfur Removal in Fossil Fuel Gasification, Presented at the Solid Waste Management Session, 69th Annual Meeting, AIChE, November 28 - December 2, 1976, Westinghouse Scientific Paper 76-9E3-FBGAS-P1.

9. Craig, J. W. T., et al., Chemically Active Fluid Bed Process for Sulfur Removal During Gasification of Heavy Fuel Oil - Second Phase. Report to EPA, Esso Research Centre, Abingdon, UK, November 1974, EPA-650/2-74-109, NTIS PB 240-632/AS.

10. Chemically Active Fluid Bed Process (CAFB). Monthly report to EPA, Foster Wheeler Energy Corporation, Livingston, N. J. May 29 - June 25, 1978, Contract 68-02-2106.

11. Minerals Yearbook 1975, Preprint on Stone, United States Department of the Interior, Bureau of Mines, U.S. Government Printing Office, Washington, DC

12. Minerals Yearbook 1975, Preprint on Lime, United States Department of the Interior, Bureau of Mines, U.S. Government Printing Office, Washington, DC

13. Boynton, R. S., Chemistry and Technology of Lime and Limestone, New York; Interscience Publishers; February 1967.

14. Statistical Abstract of the United States, 1975, U. S. Department of Commerce, Bureau of the Census, Washington, DC

15. Agricultural Stabilization and Conservation Service, Current Bulletins and Newsletters, Beaver, PA and Washington, PA.

16. Abernethy, R. F., M. J. Peterson, and F. H. Gibson, Spectrochemical Analysis of Coal Ash for Trace Elements, R17281, Bureau of Mines, U. S. Department of the Interior, July 1969.

17. Erickson, R. L., Coastal Abundance of Elements and Mineral Reserves and Resources, United States Mineral Resources Geological Survey Professional Paper 820, D. A. Brobst and W. P. Pratt, editors, U.S. Department of the Interior, Washington, DC

18. Page, A. L. and A. C. Chang, Trace Element and Plant Nutrient Constraints of Recycling Sewage Sludges on Agricultural Land, The Second National Conference on Complete Water Use, 1975, Chicago, ILL, AIChE and Environmental Protection Agency.

REFERENCES (Cont)

19. Lovell, H. L, Appraisal of Neutralization Processes to Treat Coal Mine Drainage, Pennsylvania State University, University Park, PA., EPA-670/2-73-093, November 1973.

20. Ford, C. T., J. F. Boyer, and R. A. Glenn, Studies of Limestone Treatment of Acid Mine Drainage, Part II, Bituminous Coal Research, Inc., Monroeville, PA., Water Pollution Control Research Series Publication No. 14010 EIZ 10/71, Environmental Protection Agency, December 1971.

21. Wilmoth, R. C., "Limestone and Limestone-Lime Neutralization of Acid Mine Drainage", Industrial Waste Treatment Research Laboratory, Rivesville, W. Va., EPA-670/2-74-051, June 1974

22. Moss, E. A., "Dewatering of Mine Drainage Sludge", Coal Research Bureau, West Virginia University, Morganstown, West Virginia, Water Pollution Control Research Series Publication No. 14010 FJX 12/71. Environmental Protection Agency, December 1971.

23. Shreve, R. N., "The Chemical Process Industries, Ch. XI, Cements, Calcium and Magnesium Compounds", McGraw-Hill Book Co., Inc., New York 1945.

24. "Energy Conservation Potential in the Cement Industry", FEA Conservation Paper No. 26, 1975.

25. "Energy Consumption in Manufacturing", The Conference Board, Ballinger Publishing Co., Cambridge, Mass, 1974.

26. Minerals Yearbook 1968, Vols. I-II, U. S. Department of the Interior, Bureau of Mines, U. S. Government Printing Office, Washington, D. C.

27. "New Cement Uses Fly-ash, Cost Less to Make", Chemical and Engineering News, April 5, 1976.

28. Minerals Yearbook 1973, U. S. Department of the Interior, Bureau of Mines, U. S. Government Printing Office, Washington, D. C.

29. Annual Book of ASTM Standards, 1973, Part 9, Cement, American Society for Testing and Materials, Philadelphia, Pa.

30. Survey of Current Business, January 1976, Vol. 56, No. 1, Part 1, U. S. Department of Commerce.

31. Annual Book of ASTM Standards, 1973, Part 10, Concrete and Mineral Aggregates, American Society for Testing and Materials, Philadelphia, Pa.

REFERENCES (Cont)

32. Orchard, D. F., Concrete Technology, Vol. 3, Properties and Testing of Aggregates, Third Edition, John Wiley & Sons., New York, N. Y.

33. Kunii, D. and O. Levenspiel, Fluidization Engineering, Chapter 3, John Wiley & Sons, New York, N. Y., 1969.

34. Perry, J. H., Chemical Engineer's Handbook, 4th Ed., New York; McGraw-Hill Book Co.; 1963.

35. Kunii, D., and O. Levenspiel, Op. cit., Chapter 7.

36. Guthrie, K. M., Capital Cost Estimating, Chemical Engineering, March 24, 1969.

37. Pikulik, A., and H. E. Diaz, Cost Estimating for Major Process Equipment, Chemical Engineering, October 10, 1972.

38. Merwin, R. W., Commodity Data Summaries, 1976 - Sulfur, Bureau of Mines, U. S. Department of the Interior, U. S. Government Printing Office, Washington, DC

39. A Growing Squeeze on Sulfur, Business Week, August 22, 1977.

40. Title I, Marine Protection, Reserve and Sanctuaries Act of 1972, Public Law 92-532, 86 Stat. 1052 (33 U.S.C. 1411-1421).

41. Federal Water Pollution Control Act Amendment of 1972, Public Law 92-500, Section 403(c).

42. Title 40, Chapter I, Subchapter H - Ocean Dumping, Final Regulations and Criteria, Federal Register, Vol. 38, No. 198, October 15, 1973.

43. Santhanam, C. J., R. R. Lunt, and C. B. Cooper, Current Alternatives for Flue Gas Desulfurization (FGD) Waste Disposal--An Assessment, Proceedings of the Symposium on Flue Gas Desulfurization, Vol. I, Las Vegas, NV, March 1979, Washington, DC: Environmental Protection Agency; 1979, EPA-600/7-79-167a.

44. Sun, C. C., C. H. Peterson, R. A. Newby, W. G. Vaux, and D. L. Keairns, Disposal of Solid Residue from Fluidized Bed Combustion: Engineering and Laboratory Studies. Report to EPA, Westinghouse Research Laboratories, Pittsburgh, PA, March 1978, EPA-600/7-78-049.

APPENDIX A

PRELIMINARY DEAD-BURNING/SINTERING STUDIES

This section covers tests conducted to determine whether CAFB spent regenerator stone could be rendered environmentally inactive by subjecting it to high temperatures. In CAFB-9-DB-1* samples of spent stone were tested at three temperature levels and two time intervals, and changes in weight and BET surface area were observed.

Approximately 33 g of powder were used in each experiment. The powder was placed on an alumina boat covered with platinum foil and heat treated at temperatures of 1070, 1250, and 1550°C and for times of 2.5 and 24 hours at each temperature. The heat treatment was conducted in air with a rate of rise of temperature of approximately 100°C/hr to the test temperature. Following heat treatment the powder was furnace cooled to room temperature.

WEIGHT CHANGES

Each sample was weighed before and after heat treatment. These data are presented in Table A-1 and Figure A-1. Since the finer fractions of the powder sintered and stuck to the platinum foil, the powder was weighed along with the alumina boat and the foil. The data showed that, at the two higher temperatures, the weight gain ultimately changes to a weight loss. The weight gain of approximately 4 to 4.5 percent was complete in between 2 and 5 hours at 1070 and 1250°C, and in only 2 hours at 1550°C. Within the duration of the experiment, there was no loss in weight at 1070°C. There was a rapid weight loss, however, relative to

---

*Label means: Sample No. 1 for dead-burning test; origin CAFB Run No. 9.

Table A-1

CHANGE IN WEIGHT OF CAFB STONE WITH HEAT TREATMENT

Temperature, °C	Weight % Gain or Loss		
	2 hr	5 hr	24 hr
1070	+3.70	+3.54	+4.09
1250	+3.19	+4.59	-1.95
1550	+4.57	-4.13	-3.93

Oxidation of
CaS

Decomposition of

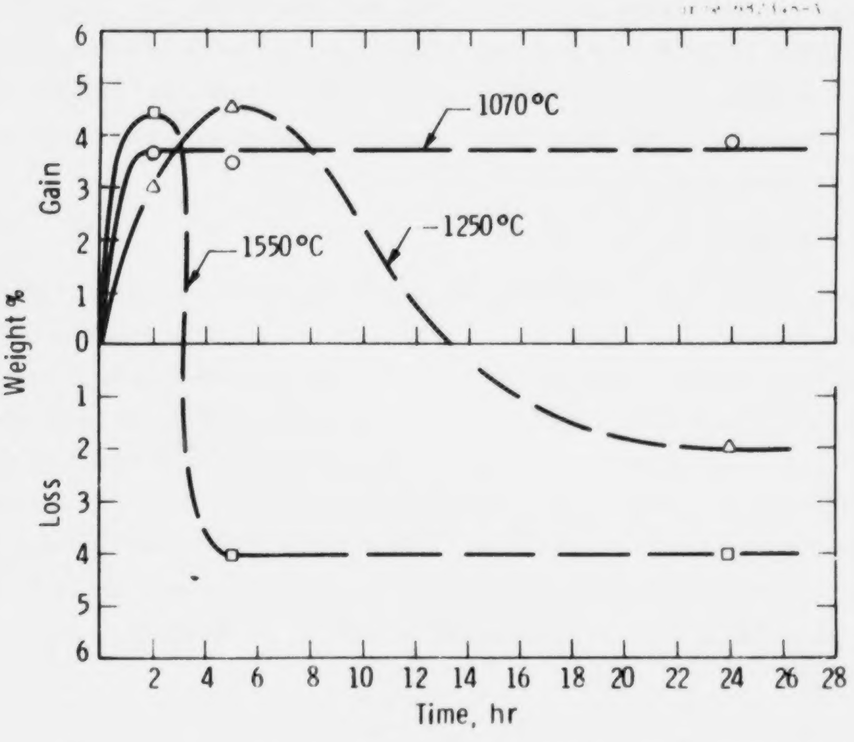

Figure A-1 - Effect of Heat Treatment on CAFB Stone in Air the initial weight of approximately 4 percent at 1550°C after 5 hours of heat treatment, and this remained nearly constant during additional heat treatment to 24 hours. The case at 1250°C was intermediate between 1070 and 1550°C.

The weight changes with temperature and time can be explained in the following way. CAFB stone contains small amounts of CaS, $CaSO_4$, and inert materils, such as iron oxide (FeO), silica, and so on. The main constituent is CaO. When the stone is heated, the following reactions can occur:

$$CaS + 2O_2 \rightarrow CaSO_4 \qquad \text{oxidation}$$

$$CaSO_4 \rightarrow CaO + SO_2 + 1/2\ O_2 \qquad \text{decomposition} \quad .$$

The weight gain may be attributed to the oxidation of CaS to $CaSO_4$ and the subsequent weight loss to the decomposition of $CaSO_4$ to CaO. As the heat treating temperature and time are increased, the decomposition is accelerated, as shown by the data at 1550°C. The predicted weight changes due to this treatment depend on the accuracy of the chemical analyses of the spent sorbent for sulfide and sulfate as well as on the variability of the sulfur content on individual particles. The fractional change in weight on oxidation, if one assumes no losses, should be

$$\frac{\Delta W}{W} = (136.14 - 72.14)\ \frac{S_1}{32.06} = 1.996\ S_1$$

where S_1 is the weight fraction of sulfide sulfur in the spent sorbent before heating. On decomposition, the fractional weight loss should be

$$\frac{\Delta W}{W} = \left(\frac{72.14 - 56.08}{32.06}\right) S_1 + \left(\frac{136.14 - 56.08}{96.06}\right) S_2 ,$$

or $\Delta W/W = 0.501\ S_1 + 0.833\ S_2$, where S_2 is the weight fraction of sulfate sulfur in the spent sorbent expressed as SO_4. Using sulfur analyses for

CAFB stone (2.24 wt % $S^=$ and 3.07 % $SO_4^=$), we calculated the maximum weight gain as 4.47 percent and the maximum weight loss as 3.68 percent. These compare very well with the observed changes.

Examination of the sulfur contents of the 5-hour samples showed sulfur losses with dead-burning as in Tables A-2 and A-3. A sulfate content greater than that in the original stone was explained by assuming that some of the CaS was oxidized to $CaSO_4$ and the balance to CaO. A smaller sulfate content meant that both the original CaS and $CaSO_4$ decomposed to CaO. The calculations showed that about 15 percent of the sulfide sulfur was lost at the lower temperatures, conceivably applicable to dead-burning, but overall only 11 percent was lost. The balance of the sulfide sulfur was oxidized to sulfate.

Table A-2

SULFUR RETENTION OF DEAD-BURNED CAFB-9 REGENERATOR STONE*

Temperature, °C	Time, hr	Composition, wt %		
		Sulfide	Sulfate	Calcium
1070	5	0.302	7.58	60.00
1250	5	0.021	8.45	62.88
1550	5	0.016	0.46	67.84

---

*Sample was CAFB-9-DB1

Raising the temperature to 1250°C did result in 99 percent conversion of the sulfide, with essentially the same overall sulfur loss. Hence, if landfill is the end disposal method, 1250°C might be adequate. At 1550°C the residual sulfide was about the same as at 1250°C, but the overall sulfur loss (95 percent) approached completion.

Table A-3

SULFUR LOSS IN DEAD-BURNING CAFB REGENERATOR STONE FOR 5 HOURS

Form of S Loss	Dead-Burning Temperature		
	1070°C	1250°C	1550°C
CaS Conversion, %			
To CaO	15.7	14.3	99.3
To $CaSO_4$	70.6	84.7	--
Unconverted	13.7	1.0	0.7
$CaSO_4$ Decomposition, %			
To CaO	--	--	85.6
Unconverted	--	--	14.4
Overall S Loss, %	10.7	9.8	95.0

We concluded that, if the CAFB stone was heated for not more than 2 hours at 1550°C or 5 hours at 1250°C, oxidation of the residual CaS would be essentially complete. The stone may still not be dead-burned.

SURFACE AREA STUDY

The results of surface area estimates by BET are shown in Table A-4. The results may be interpreted on the basis of simultaneous occurrence of oxidation, decomposition, and sintering. The greatest surface area was obtained after 2 hours of heat treatment at 1550°C, commensurate with the time required for completion of oxidation. Also, at each temperature level, there was an initial increase in BET area.

Both decomposition and sintering should decrease BET area. Since the $CaSO_4$ lattice is larger than that of CaO or CaS, however, it is conceivable that some dislocations are created on oxidation which, in effect, exposes additional surface area. The BET results suggest that, if dead-burning is indicated by minimum surface area, 1550°C for 2 to 5 hours or 1250°C for more than 24 hours is required.

Table A-4

SURFACE AREA OF THE HEAT TREATED CAFB
STONE BY BET METHOD

Temperature, °C	Surface Area, m^2/g		
	2 hr	5 hr	24 hr
1070	0.58	0.53	1.33
1250	0.13	1.35	1.05
1550	1.75	0.36	0.55

OTHER INDICATIONS

The leaching data reported in another section of this report also shed some light on the dead-burning. The heat involved in producing a suspension of $Ca(OH)_2$ from solid CaO is above 65,300 J (15,600 cal)/g mole. The 3 g samples, therefore, should release 3492 J (834 cal) if hydration is complete. The 17°C rise in 20 ml water means 1424 J (340 cal) were actually absorbed, which is only 41 percent of the theoretical maximum. This calculation neglects the heat of hydrolysis of CaS, the thermal capacity of the flask, and the fact that no stirring was used. The temperature rise observed, therefore, may be high because of the first omission, low because of the second, and high because of the third. With these reservations the stone as produced is about 40 percent dead-burned.

The 20 ml of water used is 23 times the theoretical needed for hydration of the CaO present. The actual process, therefore, could quench the CAFB spent stone in water, recycle any H_2S evolved, and dispose of the slaked stone to a user such as a municipal sludge or an acid mine drainage treatment plant. Alternatively, the stone could be oxidized with air to retain the sulfur as $CaSO_4$. Previous leaching tests have suggested that this may be done at ambient conditions.

Dead-burning of CAFB-9 regenerator stone was examined further by checking the effect of particle size on it. Two size fractions were prepared by grinding CAFB stone to -88 + 63 and -44 μm.

Samples of about 10 g each were placed in alumina boats covered with platinum foil and heat treated at 1250 and 1550°C for 2, 5, and 24 hours. The heating was done in air with a temperature rise of 50°C/hr to the test temperature. The samples were then furnace cooled to room temperature.

Figure A-2 is a photograph of the dead-burned samples. All the samples heated to 1550°C took on a yellowish color, whereas those at 1250°C remained an off-white color. Large aggregates were formed with an increase in time and temperature, as expected. Simple heating, thus, does result in sintering.

Weight changes are given in Table A-5. The gains are smaller than those obtained previously, which can be explained by considering that the decomposition of sulfate proceeded more readily with the finer particles. The magnitude of the loss on continued heating, however, is greater than expected. Some of the loss is possibly due to CO_2 and perhaps to moisture. The weight changes for the two particle sizes are comparable.

Chemical analyses as summarized in Table A-6 show that 1250°C for 2 hours is sufficient to essentially eliminate sulfide sulfur from -44 μm particles in a static bed. The larger particles (-88 + 63 μm) may require times longer than 5 hours, even at 1550°C.

Sulfate sulfur can be reduced by about one order of magnitude to the level of 0.5 to 1.0 wt % SO_4 by heating at 1550°C for 2 hours. The larger particles retain more sulfate sulfur (1% vs 0.5%) at 1550°C than the smaller particles. Heating at 1250°C results in 0 to 10 percent loss of sulfate sulfur, which may be offset by oxidation of sulfide sulfur.

Table A-5

WEIGHT CHANGES IN DEAD-BURNING OF GROUND CAFB-9 REGENERATOR STONE

Particle Size, μm		-88 + 63		-44 + 0	
Temperature, °C		1250	1550	1250	1550
Time, hr					
2	Initial wt, g	8.466	8.054	10.636	10.058
	Final wt, g	8.633	7.456	10.854	9.250
	% change	+1.98	-8.05	+2.05	-7.99
5	Initial wt, g	11.737	7.154	14.657	8.892
	Final wt, g	11.583	6.615	14.453	8.166
	% change	-1.30	-7.53	-1.39	-8.16
24	Initial wt, g	10.196	12.762	14.408	16.728
	Final wt, g	10.054	11.838	14.278	15.428
	% change	-1.39	-7.24	-0.90	-7.77

Table A-6

EFFECT OF PARTICLE SIZE ON SULFUR RETENTION IN DEAD-BURNING CAFB REGENERATOR STONE

Dead-burning Temperature, °C	1250		1550	
Particle Size, μm	-88 + 63	-44	-88 + 63	-44
Dead-burning Time, hr				
	Sulfide Sulfur			
2	0.043	0.001	0.006	0.000
5	0.022	0.000	0.019	0.000
24	0.000	0.009	0.000	0.000
	Sulfate Sulfur (as $SO_4^=$)			
2	7.30	7.08	0.96	0.48
5	7.37	8.64	1.03	0.60
24	6.55	8.52	0.98	0.48

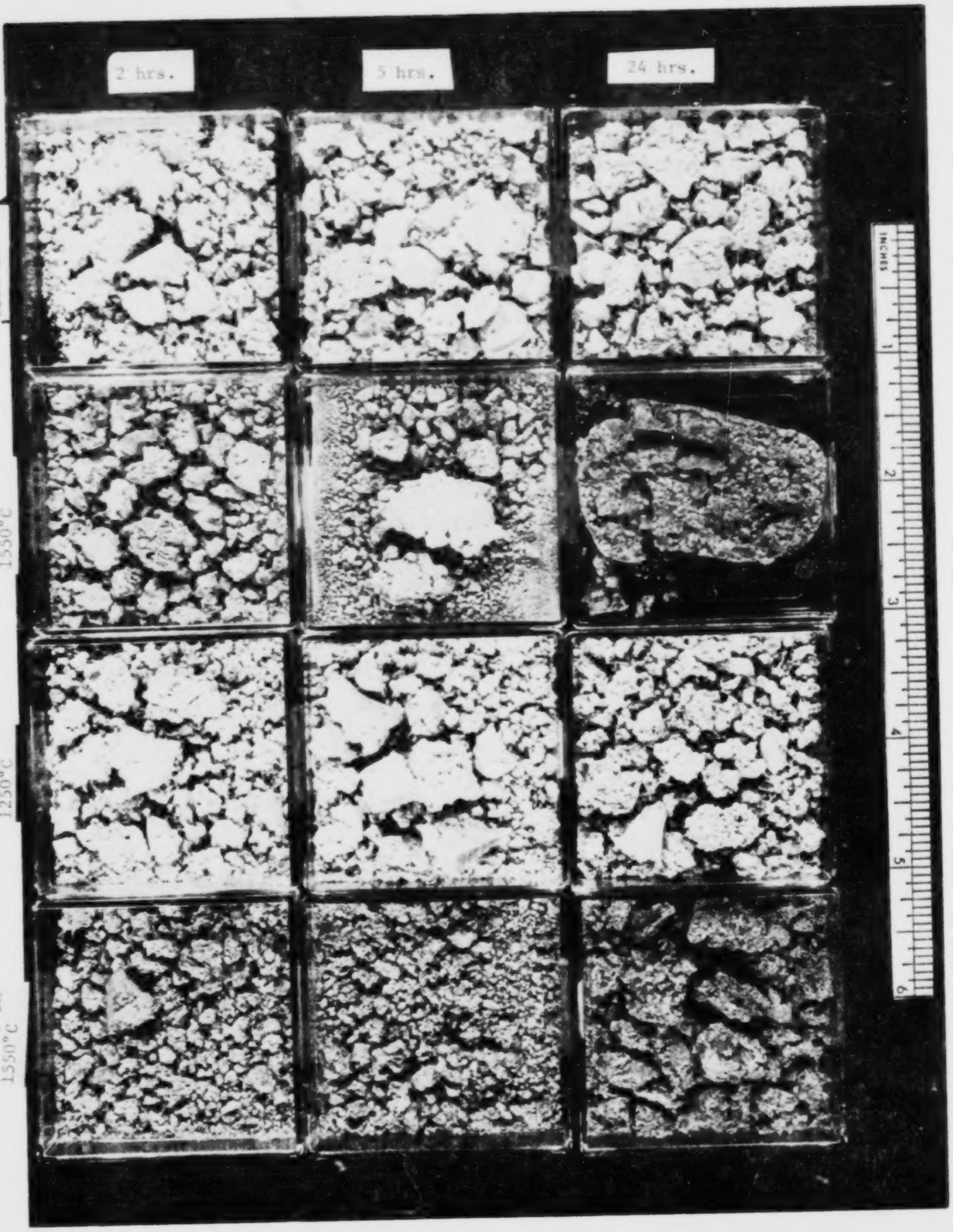
2 hrs.
5 hrs.
24 hrs.
-88 + 63 μm 1250°C
-88 +63 μm 1550°C
-44 +0 μm 1250°C
-44 +0 μm 1550°C
INCHES
1
2
3
4
5
6

Figure A-2 - Dead-Burning of Ground CAFB-9 Regenerator Stone

Overall, these results indicate that utilization of spent sorbent from the CAFB regenerator as a high purity lime after heating it to reduce sulfur appears unpromising. Heating to 1550°C from 1070°C in a 1000 MW plant burning a 3 percent sulfur fuel oil and using a limestone/sulfur molar makeup ratio of 1/1 would require about 5.6 barrels of fuel oil/hr. At $10/bbl, assuming a 20-year project life, 16 percent capital charges, and a 50 percent tax rate, the incremental alternative capital investment that could be made to avoid this fuel cost is estimated at $1,700,000. This figure is even higher when the other costs associated with installing dead-burning equipment are added in but reduced by operating costs of the alternative facilities. The energy penalty at 1550°C is at least 0.4 percent.

A further observation on dead-burning is possible through leaching tests performed on the sample included in Table A-6. These are reported in detail in another section of this report. In general, these showed that calcium and sulfate ions could be leached from the dead-burned samples, presumably as $Ca(OH)_2$ and $CaSO_4$. Table A-7 presents the calcium and sulfate results, which may be summarized as follows:

- Calcium
    - At 1250°C reduction in leaching, if dead-burning time is extended from 2 to 24 hours for both particle sizes, is negligible.
    - At 1550°C values are about two-thirds those at 1250°C, but again effect of exposure time is negligible.
- Sulfate
    - At 1250°C molar values are about one-half those of the calcium levels; the effect of exposure time at both particle sizes is negligible.
    - At 1550°C values are about one-tenth those at 1250°C and about one-twentieth of the corresponding calcium values; the effect of exposure time is negligible.

Table A-7

EFFECT OF PARTICLE SIZE ON LEACHATE COMPOSITION FROM DEAD-BURNING CAFB REGENERATOR STONE

Dead-Burning Temperature, °C	1250		1500	
Particle Size, μm	-88 + 63	-44	-33 + 63	-44
Dead-burning Time, hr				
	Calcium, m moles/ℓ			
2	34.4	24.6	20.6	31.8
5	33.0	34.0	21.0	21.4
24	32.9	34.6	21.1	21.0
	Sulfate, m moles/ℓ			
2	16.2	10.8	1.37	12.6
5	12.8	15.4	1.18	1.39
24	14.9	15.5	0.85	1.70

Saturation values for pure $Ca(OH)_2$ and $CaSO_4$ at 20°C are nearly the same - 22.0 m moles/ℓ. Dead-burning appears to significantly affect the solubility of $CaSO_4$ but not that of $Ca(OH)_2$. Since the regenerator stone is mainly a CaO, the leaching results appear to deny the technical feasibility of dead-burning as a disposal method.

APPENDIX B

FLUIDIZED-BED TEST FACILITY

A large portion of the data to evaluate the dry sulfation process in this report was obtained on specimens processed in a 10-cm diameter fluidized-bed test unit. Figures B-1 and B-2 are process flow diagrams for this unit. Basically, the unit is an apparatus for delivering mixtures of gases either from the laboratory supply or from commercial cylinders through a replaceable distributor plate to a 10-cm x 45-cm (4 in. x 18 in.) reaction chamber. The chamber is heated by external electric wraparound heaters. The feed gas mixture may also be preheated by a heating tape on the supply line.

Off-gas from the reactor is cooled by passing it through a bare U-tube gas-air exchanger. Carry-over is removed in a cyclone, and fines are caught in a sintered metal cartridge filter. When residual H_2S, H_2, or other combustibles are present, the off-gas is passed through a burner. Methane may be added to the off-gas to ensure a combustible mixture that will burn stably. The burner is an inverted, truncated, square pyramid with three levels of wire gauze screens to aid further in stabilizing flames from a wide range of gas flow rates.

A swing connection was inserted into the gas feed line to the reactor to prevent accidentally mixing fuels with air or oxygen in the feed system. This must be manually unfastened and reconnected into the desired system, oxidant or fuel. A further safety measure was the addition of small vent valves on four of the rotameters as a partial protection against overpressure. Finally, a Plexiglas plate was installed over the face of the control panel on which the rotameters were mounted.

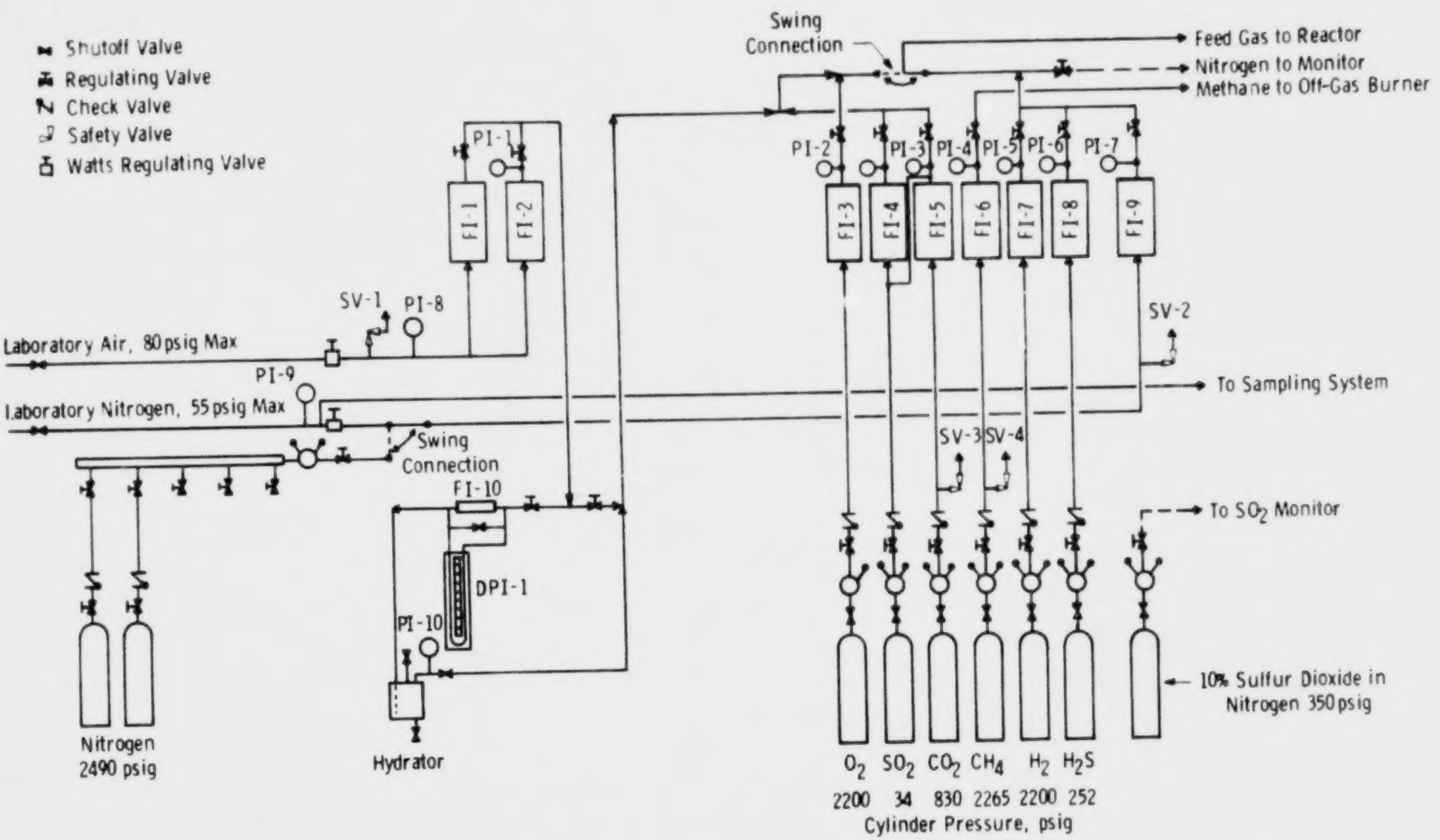

Shutoff Valve
Regulating Valve
Check Valve
Safety Valve
Watts Regulating Valve
Swing Connection
Feed Gas to Reactor
Nitrogen to Monitor
Methane to Off-Gas Burner
PI-1
FI-1
FI-2
SV-1
PI-8
Laboratory Air, 80 psig Max
PI-9
Laboratory Nitrogen, 55 psig Max
Swing Connection
FI-10
DPI-1
PI-10
Hydrator
Nitrogen
2490 psig
PI-2
PI-3
PI-4
PI-5
PI-6
PI-7
FI-3
FI-4
FI-5
FI-6
FI-7
FI-8
FI-9
SV-2
To Sampling System
SV-3
SV-4
To SO2 Monitor
10% Sulfur Dioxide in Nitrogen 350 psig
O2 SO2 CO2 CH4 H2 H2S
2200 34 830 2265 2200 252
Cylinder Pressure, psig

Figure B-1 - Process Flow Diagram for the Gas Supply Section of the 10-cm Fluidized-Bed Test Unit

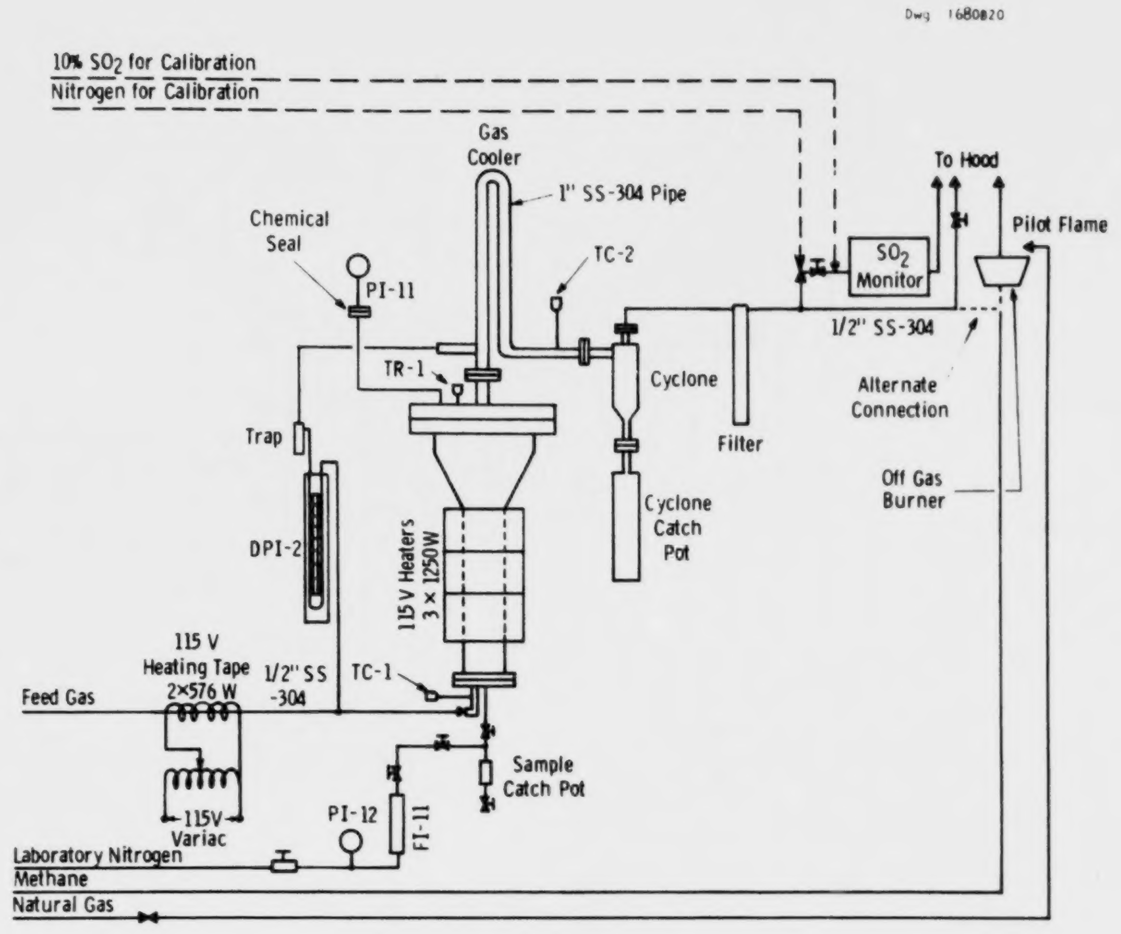
Dwg 1680820
10% SO2 for Calibration
Nitrogen for Calibration
Gas Cooler
1" SS-304 Pipe
Chemical Seal
PI-11
TC-2
TR-1
Trap
DPI-2
115 V Heaters 3 × 1250W
Cyclone
Filter
Cyclone Catch Pot
SO2 Monitor
To Hood
Pilot Flame
1/2" SS-304
Alternate Connection
Off Gas Burner
115 V Heating Tape 2×576 W
1/2" SS -304
TC-1
Feed Gas
Sample Catch Pot
115V
Variac
PI-12
FI-11
Laboratory Nitrogen
Methane
Natural Gas

Figure B-2 - Process Flow Diagram for the Reactor Section of the 10-cm Fluidized-Bed Test Unit

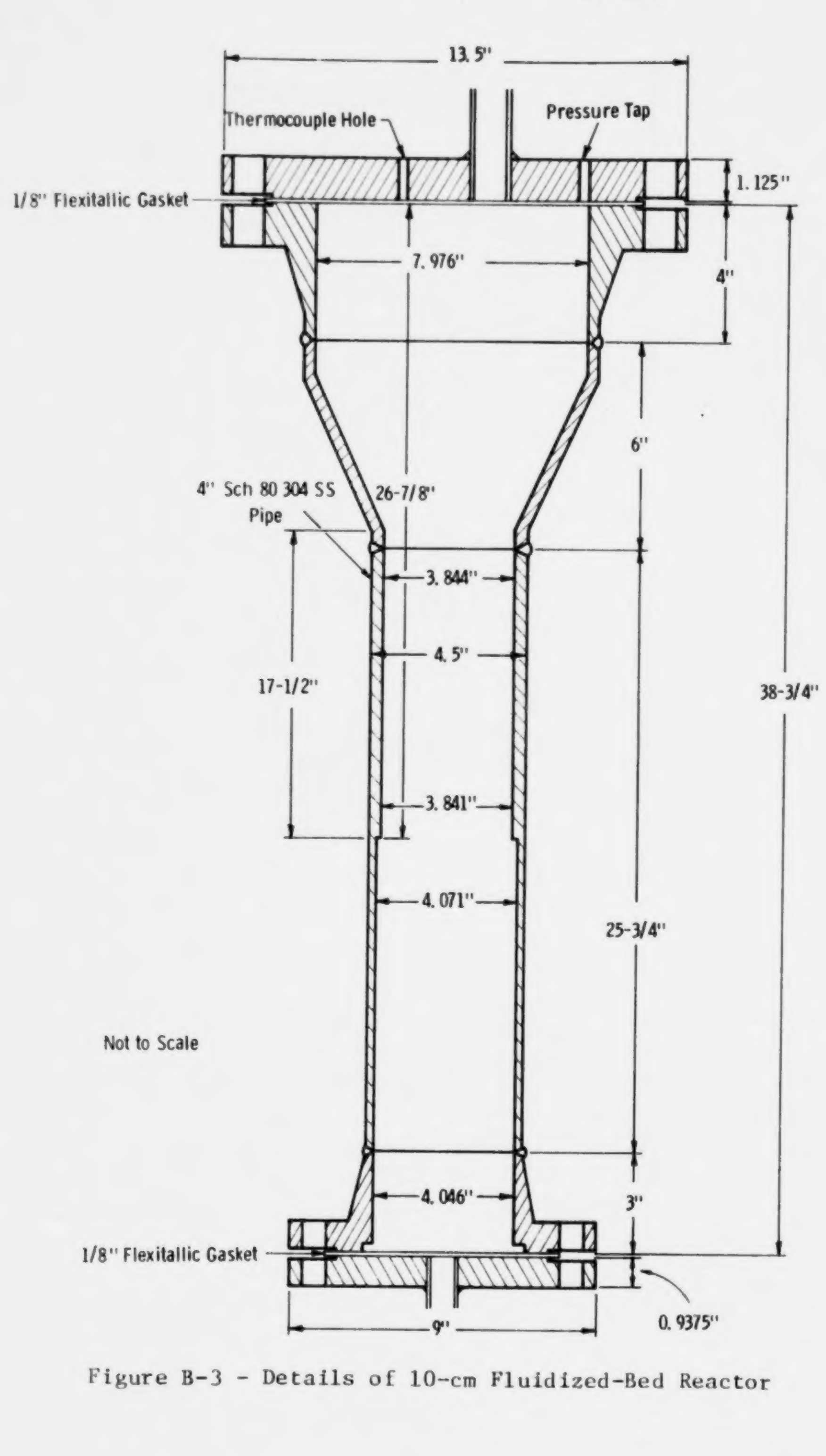
Dwg. 1701817
13.5"
Thermocouple Hole
Pressure Tap
1.125"
1/8" Flexitallic Gasket
7.976"
4"
6"
4" Sch 80 304 SS Pipe
26-7/8"
3.844"
4.5"
17-1/2"
38-3/4"
3.841"
4.071"
25-3/4"
Not to Scale
4.046"
3"
1/8" Flexitallic Gasket
9"
0.9375"

Figure B-3 - Details of 10-cm Fluidized-Bed Reactor

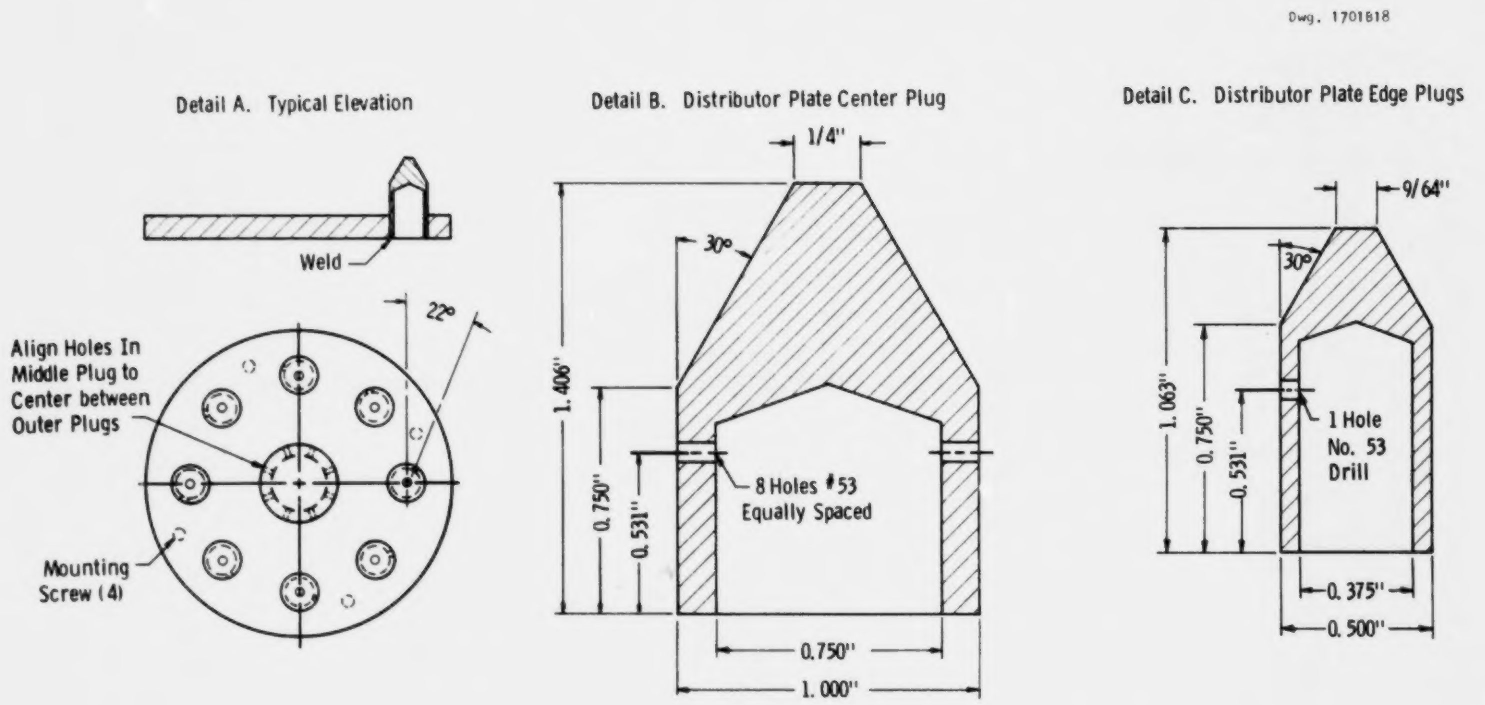
Dwg. 1701818
Detail A. Typical Elevation
Weld
22°
Align Holes In Middle Plug to Center between Outer Plugs
Mounting Screw (4)
Detail B. Distributor Plate Center Plug
1/4"
30°
1.406"
0.750"
0.531"
8 Holes #53 Equally Spaced
0.750"
1.000"
Detail C. Distributor Plate Edge Plugs
9/64"
30°
1.063"
0.750"
0.531"
1 Hole No. 53 Drill
0.375"
0.500"

Figure B-4 - Distributor Plate Assembly

Dwg. 1701B16

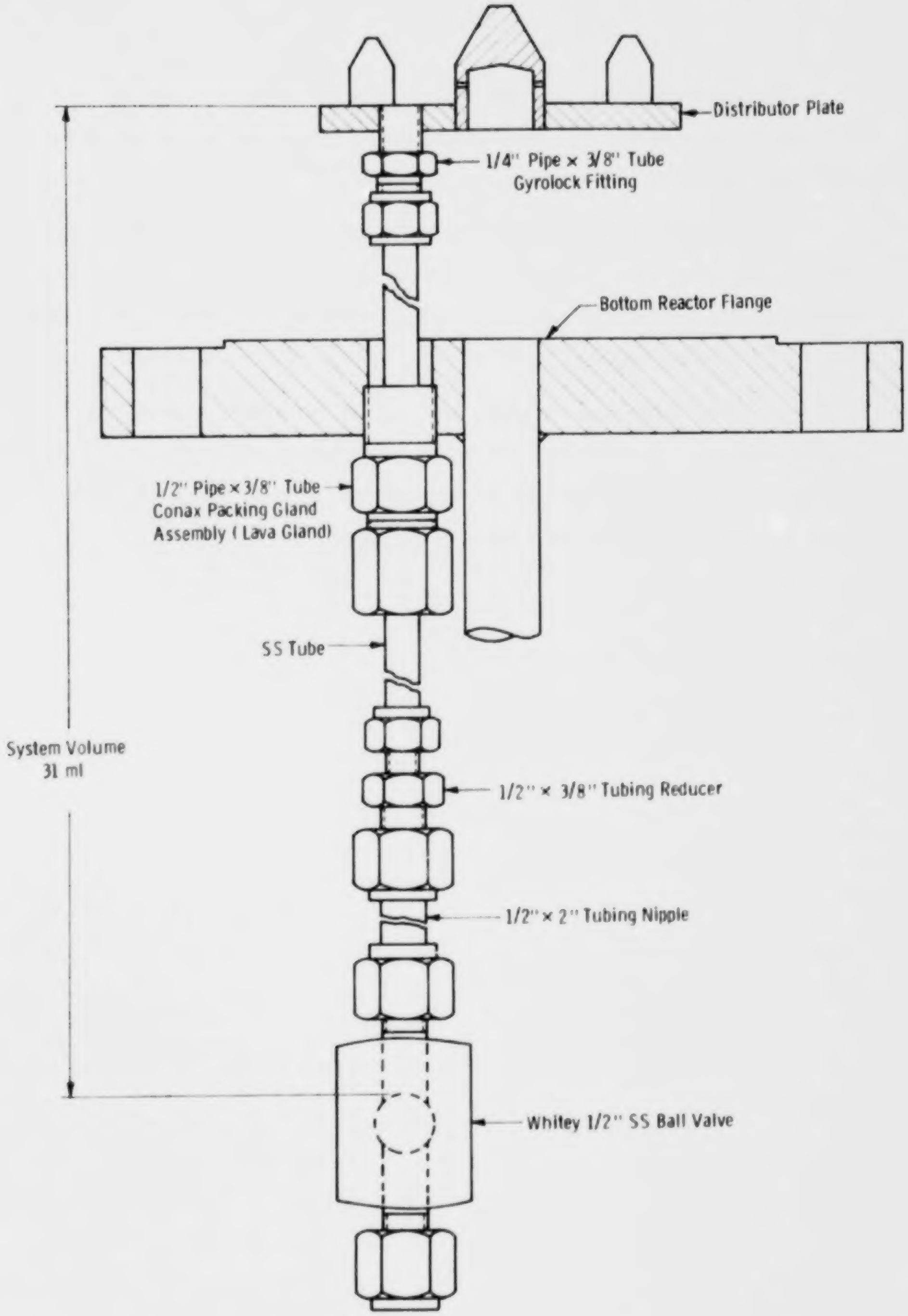
Distributor Plate
1/4" Pipe × 3/8" Tube Gyrolock Fitting
Bottom Reactor Flange
1/2" Pipe × 3/8" Tube Conax Packing Gland Assembly (Lava Gland)
SS Tube
System Volume 31 ml
1/2" × 3/8" Tubing Reducer
1/2" × 2" Tubing Nipple
Whitey 1/2" SS Ball Valve

Figure B-5 - Reactor Bed Sampling Connections

Reactor details are given in Figure B-3, distributor plate details are in Figure B-4, and bed sampling connections are in Figure B-5. The reactor and distributor plate shown were used initially on Run L-10.

The hydrator was first used on Run L-9. The information available indicated that the amount of water vapor required during dry sulfation was low but not critical. A simple system was devised to split the air feed, sending roughly half of it through the hydrator.

The bed sampling system was added on later runs. In operation this system is emptied of solids and back-blown with nitrogen, permitting a sample of bed material to be withdrawn at any desired time without the need to purge excessive amounts of previous material.

APPENDIX C

FLUIDIZATION STUDIES

Figures C-1 and C-2 show details of a 7.62-cm (3-in) Plexiglas column in which observations were made on various samples of limestone and spent sorbent in connection with the dry sulfation studies. Initially, a perforated plate distributor for the inlet air was used. The steel wool exhaust filter shown was later replaced with a cartridge-type filter.

As preparation for sulfating fine particles of CAFB regenerator stone, fluidization observations were made first on limestone and then on CAFB stone. This two-step procedure was necessitated by the limited quantity of CAFB stone available. In one test the initial charge of 500 g made a bed 10.0 cm deep with an average bulk density of 1.32 g/cm^3. Nitrogen flow was increased gradually to the maximum obtainable of 61 ℓ/min at 15°C, which is equivalent to a superficial velocity of 27.3 cm/s. At 3.4 cm/s one rathole formed but with no visible movement of the solids. At 4.0 cm/s additional ratholes formed, this time with a continual ejection of solids from the holes. A crater formed and, as the gas rate was increased, a large bubble would occasionally break through and the bed would adjust to the new rate. The area covered by the crater expanded until all of the surface was active at a gas flow of 10.6 cm/s. Further increases in gas flow resulted in an increasing fraction of the bed becoming active, although even at the highest flow rate, a portion of the solids at the wall near the distributor remained inactive. Less than 1 g of solids was blown over to the filter on the effluent line, even though bed material was ejected from the bed to a height of 17 to 34 cm above the distributor.

Fluidization was next observed with -149 + 74 μm limestone, by use of a sintered metal distributor plate. The bulk density of a 500 g bed was

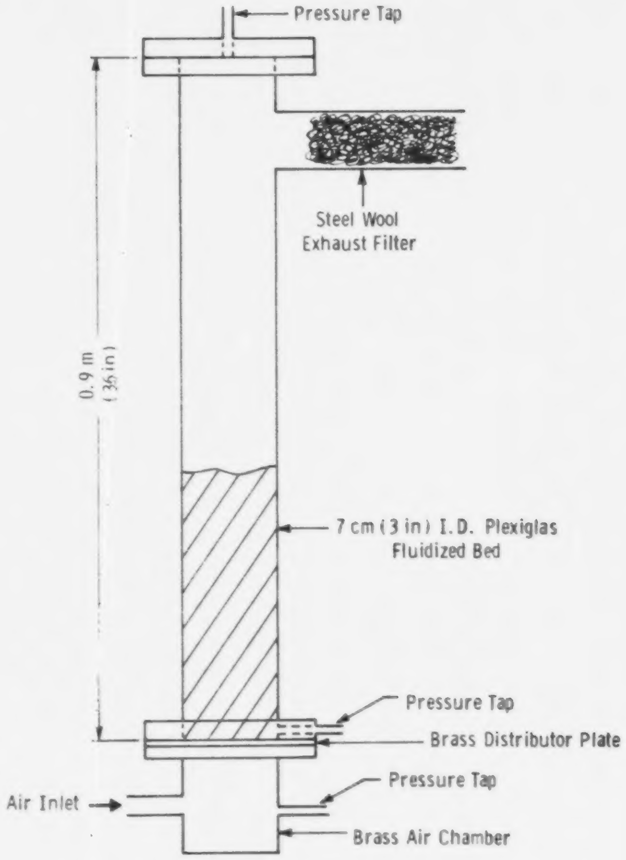
Pressure Tap
Steel Wool
Exhaust Filter
0.9 m
(36 in)
7 cm (3 in) I.D. Plexiglas
Fluidized Bed
Pressure Tap
Brass Distributor Plate
Air Inlet
Pressure Tap
Brass Air Chamber

Figure C-1 - 7.62-cm (3-in) Test Unit

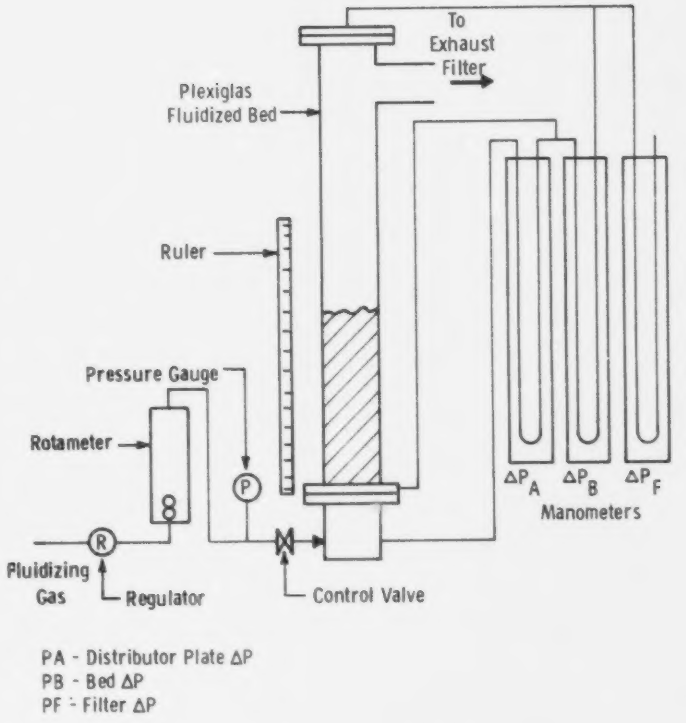
To
Exhaust
Filter
Plexiglas
Fluidized Bed
Ruler
Pressure Gauge
Rotameter
ΔP_A
ΔP_B
ΔP_F
Manometers
Fluidizing
Gas
Regulator
Control Valve
PA - Distributor Plate ΔP
PB - Bed ΔP
PF - Filter ΔP

Figure C-2 - Flow Diagram for the 7.62-cm (3-in) Test Unit

1.34 g/cm^3. At low flow rates the bed rose as an entity to about 21 cm above the distributor before collapsing. As the flow rate increased, the bed repeated this performance. Again, we found that even at maximum flow rate some of the bed (bottom 2 to 8 cm) remained inactive. Adding another 500 g of limestone yielded the same results. The distributor pressure drop was a maximum of 10 cm H_2O.

Finally, fluidization was observed with a bimodal distribution, by use of a bottom layer of 250 g of -1680 + 1190 μm limestone overlaid with 500 g of -149 + 74 μm stone. No fluidization occurred at the maximum flow when only the larger fraction was present. At the maximum flow of 22.0 cm/s, all but the bottom 6 cm were fluidized. There was no significant elutriation.

Overall, we concluded that the presence of larger particles operated to retain the fines even at flow rates considerably above the minimum fluidization velocity of the fines. Proper design of the distributor should permit all of the bed to be active.

As part of run CAFB-905, a series of tests was performed to investigate the effect of particle size distribution on the fluidization characteristics of CAFB-9 regenerator stone prior to sulfating the stone. The objective was to determine the percentage of fine particles that can be included in the bed material and still retain smooth fluidization characteristics for the bed. The testing was performed using a 7.0-cm id by 91.4-cm (2.75 in. x 36 in.) Plexiglas tube. The tube was mounted on a brass air plenum chamber, and a brass, orifice-type distributor plate with thirteen 0.81-mm holes was used throughout the testing. Compressed air, metered through standard laboratory rotameters, was used as the fluidization gas. Bed pressure drop measurements were obtained by means of water manometers connected to pressure taps along the 7.62 cm column. All testing was done at ambient temperature. The basic particle size tested was -420 + 125 μm (-40 + 120 mesh), to which various amounts of fines were added, as noted in the following tables. Tamped packing was obtained by gently tapping the loaded column until no further compaction occurred. Loose packing was produced by fluidizing the bed and then shutting off the air. The data are presented in Table C-1.

Table C-1

BED COMPOSITION FOR FLUIDIZATION STUDIES

Case	Bed Weight, g	Packing	Fines Added, g	Wt % Fines
I. No Fines Added				
I-1	900	Tamped	0	0
I-2	900	Tamped	0	0
I-3	900	Loose	0	0
II. Fines Added, -44 + 0 μm				
II-1	900	Loose	47.4	5.0
II-2	900	Loose	100.0	10.0
II-3	900	Loose	180.0	16.7
II-4	900	Loose	180.0	16.7
II-5	900	Loose	225.0	20.0
II-6	900	Loose	225.0	20.0
II-7	900	Loose	450.0	33.3
III. Fines Added, -63 + 44 μm				
III-1	900	Loose	100.0	10.0
III-2	900	Loose	100.0	10.0
III-3	900	Loose	225.0	20.0
III-4	900	Loose	225.0	20.0
III-5	900	Loose	386.0	30.0
III-6	900	Loose	386.0	30.0
IV. Fines Added, 50-50 Mixture of -63 + 44 and -44 + 0 μm				
IV-1	900	Loose	100.0	10.0
IV-2	900	Loose	100.0	10.0
IV-3	900	Loose	225.0	20.0
IV-4	900	Loose	225.0	20.0
IV-5	900	Loose	386.0	30.0

The data were reduced by a previously written computer program. Typical curves are given in Figures C-3 through C-8. These show that the addition of fines (1) increases the pressure energy needed to maintain a fluidized bed, (2) increases the maximum bed pressure drop before fluidization, and (3) produces a larger pressure drop at a lower superficial gas velocity. Also, the transition from a packed bed to a fluidized bed is less smooth and occurs over a wider range of gas velocities.

Curve 716505-A

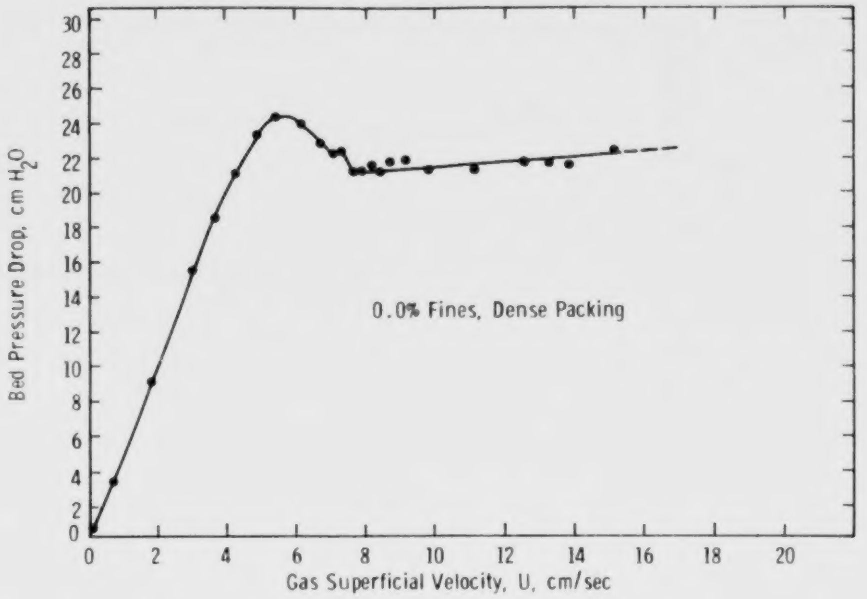

Figure C-3 - Fluidization of Ground CAFB-9 Regenerator Stone - Case I-1

716504A

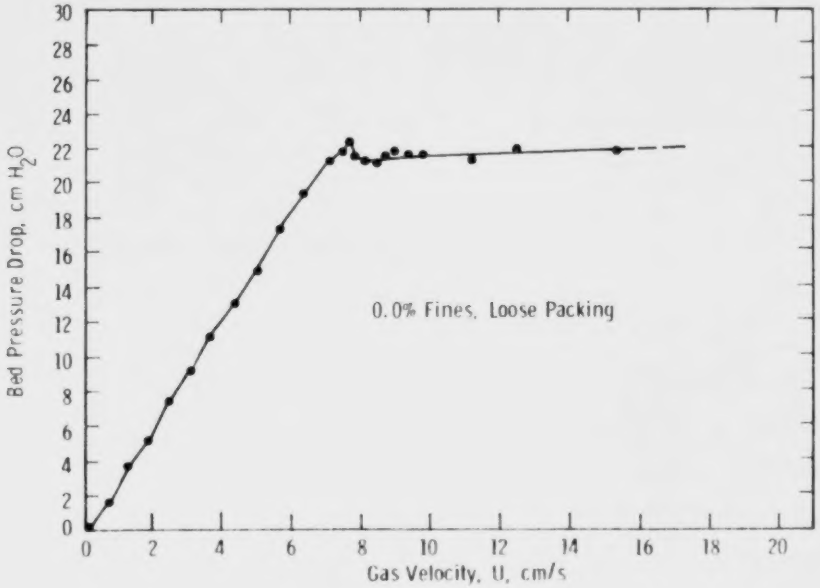

Figure C-4 - Fluidization of Ground CAFB-9 Regenerator Stone - Case I-3

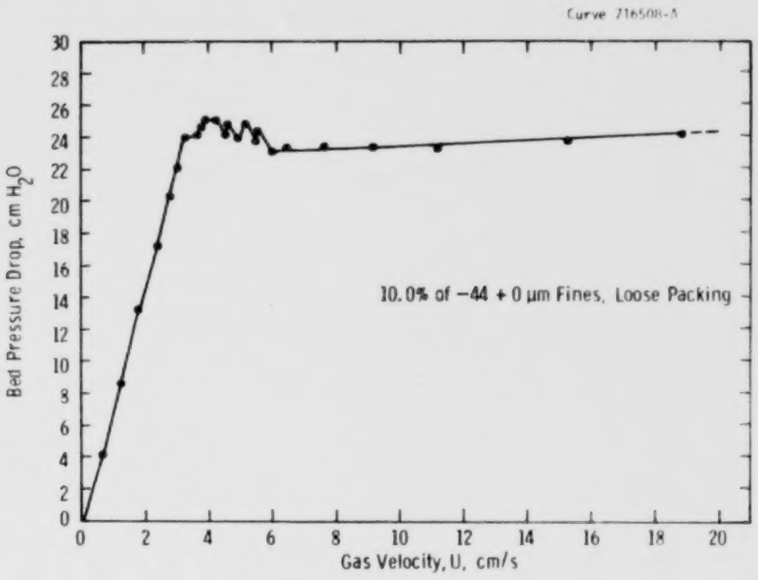

Figure C-5 - Fluidization of Ground CAFB-9 Regenerator Stone - Case II-2

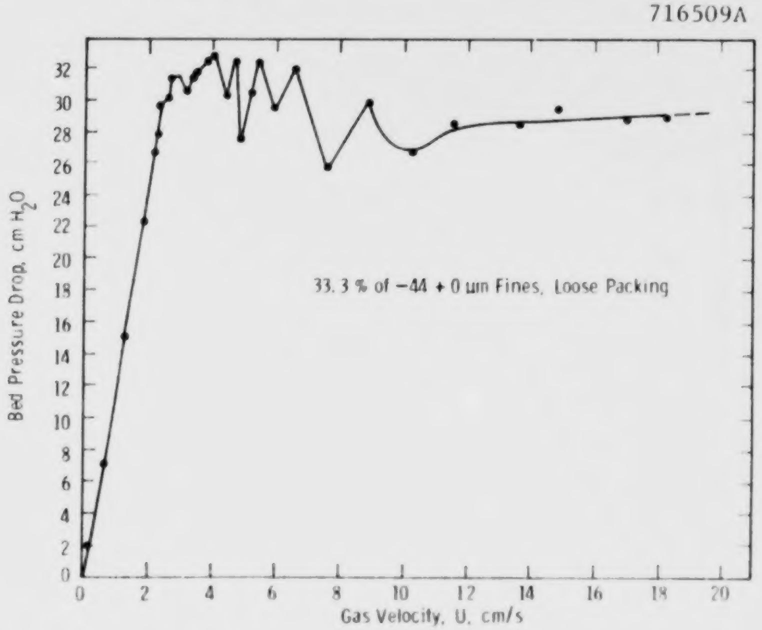

Figure C-6 - Fluidization of Ground CAFB-9 Regenerator Stone - Case II-7

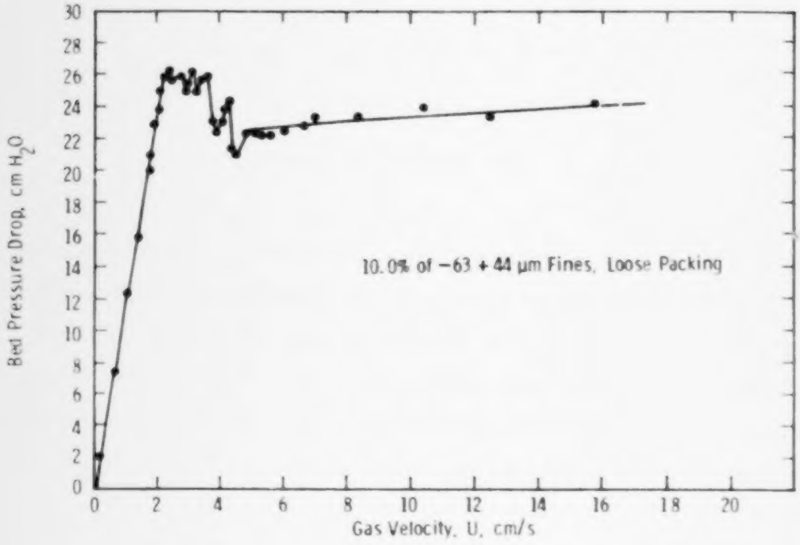

Figure C-7 - Fluidization of Ground CAFB-9 Regenerator Stone - Case III-2

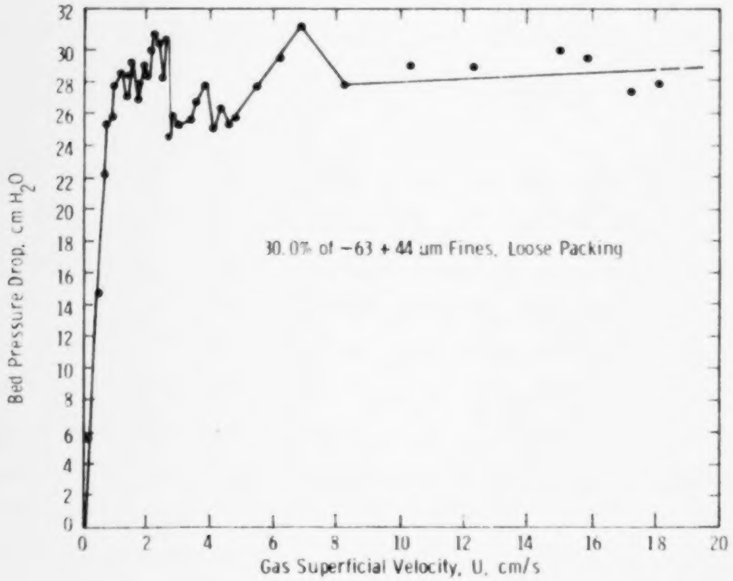

Figure C-8 - Fluidization of Ground CAFB-9 Regenerator Stone - Case III-6

APPENDIX D

DRY SULFATION STUDIES

As in the fluidization studies, we needed to conserve the available supply of CAFB regenerator stone, so we began the studies with limestone. The ultimate objective was to determine the ranges of particle size, the gas contact time, the solids residence time, and of any other factor required to achieve satisfactory resulfation of the spent stone and recapture of SO_2 in a fluidized bed. Data on the test runs are in tables at the end of this section (Tables D-1 through D-3).

INITIAL TESTS WITH LIMESTONE

The initial sulfation run, L-2, was made in the 10-cm unit using 1000 g of -149 + 74 μm limestone. This was calcined for three hours at 760 ± 10°C. The product weight was 955 g, showing less than 10 percent calcination. The reactor was charged with 300 g of this material and calcined at 900°C for 30 minutes, with a nitrogen flow of 27 ℓ/min at 15°C. The unit was cooled overnight and a 15.2 g sample removed for analysis.

The unit was brought to 870°C and the stone sulfated with a mixture of 6.5 ℓ/min of 10 percent SO_2 and 21 ℓ/min air for 30 minutes. The off-gas was monitored with a Dynasciences SO_2 monitor. Feed gas was 2.4 percent SO_2, and the O_2 supplied was about 13 times theoretical. The gas superficial velocity at operating conditions was 23.3 cm/s. The gas monitor indicated essentially no pickup of SO_2. Chemical analysis of the sulfated stone indicated 17.9 wt % $CaSO_4$. When the reactor was opened the bed appeared packed, and there was a single rathole in about the middle of the surface. Thus, inadequate fluidization caused the SO_2 to substantially bypass the bed. Table D-1 contains material balance information, Table D-2 has time-temperature data, and Table D-3 has chemical analyses.

Table D-1

MATERIAL BALANCE DATA FOR LIMESTONE SULFATION STUDIES

Batch	Gas Flow Rates (ℓ/min) at 15°C, 101.3 kPa			Batch Charge, g
	N_2	Air	SO_2/N_2	
L-2				
Calcination	27	--	--	1000
Recalcination	27	--	--	300
Sulfation	--	21	6.5[a]	
L-5				
Fluidization	91	--	--	500
	50	--	--	1000
Calcination	18	--	--	
Sulfation	18	9.0	20.8[a]	
L-7				
Calcination	18	--	--	1000
Sulfation	--	24.0	28.7[b]	
L-8				
Calcination	18	--	--	1000
Fluidization	100	--	--	
Recalcination	35	--	--	810
Sulfation	--	18.3	29.5[b]	
L-9				
Fluidization	126	--	--	786
	74	--	--	1492
Calcination	18	--	--	
Sulfation	--	18.0	1.7[c]	856
Resulfation	--	47.0	4.1[c]	
L-10				
Fluidization	--	92	--	447
	--	17-56	--	2116
Calcination	18	--	--	
Sulfation	--	17.9	1.65[c]	
L-11				
Sulfation	--	28.0-44.0	1.65[c]	1318
L-12				
Sulfation	--	26.5	2.3[c]	384

---

[a] 10 percent SO_2 in nitrogen

[b] 5 percent SO_2 in nitrogen

[c] 100 percent SO_2

Table D-2

TIME/TEMPERATURE DATA FOR LIMESTONE SULFATION STUDIES

Batch / Particle Size, μm	Heating, min at °C	Reacting, min at °C	Cooling, min at °C
L-2 (-149 + 74 μm)			
Calcination	45/533-730	185/730-765	60/765-579
Recalcination	45/561-730	145/730-902	65/902-533
Sulfation	300/ 25-835	105/835-872	35/872-629
L-5 (-149 + 74 μm)			
Calcination	160/ 25-730	125/730-906	55/906-602
Sulfation	130/515-845	120/845-879	50/879-589
L-7 (-149 + 74 μm)			
Calcination	80/473-717	205/717-901	95/901-543
Sulfation	205/602-809	198/809-850	23/850-705
L-8 (-177 + 44 μm)			
Calcination	75/594-766	145/766-910	195/910-285
Recalcination	55/556-740	105/740-908	230/908-151
Sulfation	260/551-852	124/852-870	116/870-374
L-9 (-250 + 44 μm)			
Calcination	140/ 42-720	145/720-847	20/847-623
Sulfation	159/499-854	194/854-873	122/873-437
Resulfation	213/488-843	77/843-934	100/848-319
L-10 (-250 + 63 μm)			
Calcination	215/ 45-735	1123/735-832	--
	--	108/832-872	100/690-371
Sulfation	295/604-893	192/893-872	23/872-849
L-11 (-250 + 0 μm)			
Sulfation	268/ 28-599	334/599-866	10/846-740
L-12 (-177 + 0 μm)			
Sulfation	90/ 91-518	190/518-843	--
	70/843-907	60/890-846	78/846-720

Batch L-5 was the second sulfation run. Prior to charging, the reactor was fitted with a stainless steel ring to block off the middle ring of holes in the distributor plate. Fluidization was observed by use of nitrogen. When the gas flow increased, the bed became ratholed but finally appeared completely fluidized at 91 ℓ/min or 19.3 cm/s. Doubling the bed depth by adding the balance of the charge of limestone resulted in apparent fluidization at 50 ℓ/min or 10.6 cm/s. The minimum fluidization velocity calculated from the Ergun equation was 0.5 to 1.9 cm/s. Elutriation was tolerably low. The bulk density of the slumped bed was 1.09 g/cc. The jet velocities through the 22-1.5 mm holes in the distribution plate were 3900 cm/s (128.0 fps) and 2143 cm/s (70.3 fps), respectively. One explanation for the disparity was that the apparent fluidization was really multiple jet penetration of the bed for the half charge, whereas the bed activity for the full charge was characterized by bubble formation.

On completion of sulfation, the bed was observed to be crusted, packed, and to have several channels extending the full depth of the bed. The particle size distribution showed 11 percent +149 μm and 10 percent -74 μm, neither of which was observed in the original charge. The carryover was 0.3 percent of the total reactor product. The level of sulfation achieved was higher than in L-2, as shown in Table D-1. The +149 μm fraction contained 37 wt % $CaSO_4$ versus about half this amount for the other fractions. Previous findings suggested that the reverse effect of particle size should have been obtained. We concluded that the fines were not effectively fluidized in this run. The nominal gas contact time based on superficial velocity was 0.24 s.

Batch L-7 also used -149 +74 μm limestone but at a gas flow rate 20 percent higher than in Batch L-5 as an attempt to further improve fluidization. A pressure build-up during the run to 6.3 psig was observed. The gas rate was reduced to 10 percent over L-5, the reactor pressure stabilized at 4.5 psig. When the run was completed, 18 ml of a water/solids suspension was found in the filter, and the filter surface

Table D-3

CHEMICAL ANALYSES OF STONE SAMPLES FROM LIMESTONE SULFATION STUDIES

Batch	Component, wt %			
	Ca	CO_2	$SO_4^=$	Total Sulfur
L-2				
Calcined	39.6	41.8	--	--
Recalcined	41.9	36.2	--	--
Sulfated	44.2	24.7	8.9	--
L-5				
Sulfated				
+100	--	--	27.37	--
+140	43.9	--	14.00	4.26
+200	--	--	13.58	--
-200	--	--	14.51	--
L-7				
Feed	39.8	43.4	--	--
Sulfated	40.9	21.3	--	3.33
L-8				
Feed	39.2	43.4	--	--
Calcined	46.0	32.2	--	--
Recalcined				
+80	--	--	3.00	--
+120	46.9	22.4	0.62	--
+170	--	--	0.51	--
+230	--	--	0.48	--
+325	--	--	0.39	--
-325	--	--	0.99	--
Sulfated				
Composite				
+80	41.5	14.5	14.3	--
+120	46.9	22.4	23.2	--
+170	--	--	26.7	--
+230	--	--	26.1	--
+325	--	--	23.7	--
-325	--	--	23.5	--
L-9				
Feed	40.8	--	13.1	--
Sulfated	60.8	--	--	3.41
Resulfated				
Composite	40.1	--	51.51	16.53
+60	--	--	52.8	--
+80	32.9	1.56	50.3	--

Table D-3 (Cont'd)

Batch	Component, wt %			
	Ca	CO_2	$SO_4^=$	Total Sulfur
L-9 (Cont'd)				
+120	--	0.14	51.6	--
+170	--	--	40.5	--
+230	--	--	27.4	--
+325	--	--	27.5	--
-320	--	--	28.8	--
L-10				
Sulfated				
Top of bed	--	--	36.4	--
Edge of bed	--	--	14.1	--
Center of bed	--	--	42.7	--
Bottom of bed	--	--	43.5	--
Cyclone	--	--	6.4	--
Fitter	--	--	11.6	--
L-11				
Sulfated				
+60	25.7	1.30	56.0	--
-325	31.1	10.5	32.7	--
L-12				
Sulfated				
+60	26.6	6.10	35.7	--
-325	27.1	1.51	34.0	--

was nearly all covered with a layer of wet powder. The origin of the water was not identified. Extensive scaling corrosion was found in the reactor and was attributed to the effects of the previous sulfidation run.

In Batch L-8 the initial step was to observe fluidization of the -177 + 44 μm material. Flow rates of nitrogen at ambient conditions were used, at which either 1) the entire surface of the bed appeared active, or 2) the bed material was being thrown to the level of the outlet flange.

Satisfactory fluidization without excessive elutriation was obtained at 100 ℓ/min.

The purpose of this run was to determine whether use of a wide particle size distribution would lead to 90 percent sulfation. We had also intended to use a hydrator on the air supply, but it had not yet been fabricated. The 975 g charge used was an arbitrary blend containing equal weights of -177 + 125 μm, -125 + 88 μm, -88 + 63 μm, and -63 + 44 μm Limestone 1359. Following calcination at 900°C in a flow of 18 ℓ N_2/min, the reactor was cooled to ambient temperature and opened for inspection. We observed that the bed was lightly packed and had a single 5 mm diameter rathole. Carry-over to the cyclone was 0.2 g.

Nitrogen was used to observe the fluidization character of this material. At 27 ℓ/min the rathole became an active crater; at 45 ℓ/min about 25 percent of the surface was active. We observed no further change in the quality of fluidization up to the maximum nitrogen flow available (137 ℓ/min).

The flow of gas was shut off and the bed stirred thoroughly with a metal rod. We saw no evidence of sintering, and the contents felt like a bed of granular material. Fluidization was observed again. The first active crater appeared at 18 ℓ/min; at 100 ℓ/min the whole surface was active. A thin cloud of fines was elutriated, but the bed was still visible through it.

The reactor contents weighed 835.8 g, corresponding to 34.2 percent calcination, if one assumes 5 percent inerts. Actual chemical analysis for calcium yielded 36.3 percent calcination and 3.4 percent inerts. The inference was that the bed was not adequately fluidized at 18 ℓ/min. The superficial velocity was 15.6 cm/s, which was theoretically enough to fluidize 707 μm particles, whereas the largest ones used were only 177 μm.

The material was recalcined with a flow of 35 ℓ N_2/min; allowing for samples, the actual charge of partially calcined material was 809.7 g. The weight of recalcined material was 738.5 g. After studying the data, we concluded that the calcium analysis of the recalcined material was probably low by about 7 percent. From the bed weight and the inert content estimated from the calcine charged, we calculated the extent of calcination as 50.4 percent. Carry-over to the cyclone and to the filter was negligible. The particle size distribution of the recalcined material was as follows:

Size, μm	Weight %
+177	12.4
+125	22.1
+88	23.6
+63	21.6
+44	16.6
-44	3.7
	100.0

Fines production in 11.5 hours of fluidization amounted to 3.7 percent of the product, corresponding to a rate of 0.0032 g/hr/g of final product. It is of interest that all the fines were retained by the bed. Also, some particle growth occurred: +177 μm formation was 0.011 g/hr/g final product.

The reactor was recharged with 653 g of the recalcined stone and sulfated at 870°C for two hours by using 46.8 ℓ/min of 3.1 percent SO_2 in nitrogen. Airflow was continued until the bed had cooled to 600°C. The bed was cooled further with nitrogen to 400°C, then allowed to cool overnight to ambient temperature at no flow. The product was a white powder with no evidence of sintering or packing. Fluidization was checked again using nitrogen. The bed fluidized readily; a flow of 86 ℓ/min was needed to keep all of the top surface active, somewhat less than for the partially calcined stone, suggesting incomplete sulfation. The reactor product was 706 g; carry-over was negligible. The percent sulfation by calculation was 12.8 percent. Sulfate analyses by size fraction showed more sulfation: 14 to 27 percent. This increase can be accounted for by considering the CO_2 analysis of the sulfated material as high. The test showed that adequate fluidization alone was not enough to achieve the high degree of resulfation desired.

Batch L-9 was run next, using 1466 g of the following distribution:

Size, μm	Weight %
-250	36.6
-177	30.6
-125	10.4
-88	11.3
-63	11.1
-44	0.0
	100.0

Fluidization was observed at half charge and at full charge. The bulk density of 786 g tapped to constant volume in a 1-liter graduate was 1.59 g/cc. To get the whole surface active with this amount of charge required 126 ℓ/min of nitrogen. For the full charge of 1466 g, only 74 ℓ/min was needed. At 105 ℓ/min, material was being thrown up to the level of the outlet flange.

The stone was calcined in 18 ℓ/min of nitrogen at 800 to 850°C. Significant carry-over occurred:

Material	Weight, g
Reactor product	856
Reactor piping	25
Cyclone catch	86
Filter catch	22
	989

This corresponds to 78.0 percent calcined. The total carry-over of 133 g occurred in four hours; the carry-over rate was thus 0.034 g/hr/g product.

The 856 g was charged to the reactor and stored under nitrogen until the hydrator could be installed. This was pressure tested satisfactorily with air at 15 psig.

The calcined stone was then sulfated at 870 to 880°C for 195 minutes with a gas flow of 18 ℓ/min of air plus 1.7 ℓ/min of pure SO_2. The concentration of SO_2 was thus 8.6 percent. At the end of this time, airflow was continued until the bed temperature dropped to 437°C. When the system was inspected, carry-over was found to be negligible. The reactor product was white, slightly packed, and showed one large rathole. Its fluidization behavior was again observed while still in the reactor, with nitrogen as the fluidizing medium. At 102 ℓ/min, all the surface was active, but it was clear that one side of the bed below the surface was inactive. The bed was stirred and the whole bed became active. The pressure drop across the distributor plate and the bed dropped from 29.5 to 14.8 cm of H_2O (11.6 to 5.8 in of H_2O). At 141 ℓ/min, material was thrown to the top of the 10-cm diameter section. The bed was still active at a flow rate of 91 ℓ/min, for which the pressure drop was 12.2 cm H_2O (4.8 in). A sample was taken before continuing with the sulfation. Conditions used were 47 ℓ air/min plus 3.8 ℓ 100% SO_2/min for 25 minutes. The bed temperature was at 843°C when the SO_2 was cut in and rose rapidly to 980°C. Temperature thereafter was in the range of 805 to 850°C.

The reactor product yield was 928 g, while cyclone catch plus carry-over in the piping was 112 g. The filter contained 11 cm^3 of slurry with about 1 cc solids. The reactor product size distribution and calcium sulfate content were as follows:

Size, μm	Weight %	Weight % $CaSO_4$
+250	1.1	74.8
+177	45.5	71.2
+125	42.2	72.4
+88	5.0	57.4
+63	2.0	38.3
+44	2.0	39.0
-44	2.2	40.8
	100.0	

Thus, about half of the -125 + 88 μm fraction was retained in the bed while about 80 percent of the fines fraction was elutriated. Sulfate analyses were very encouraging, although again the large particles showed significantly higher levels of sulfation. The higher degree of sulfation in this run was attributed to the use of the hydrator. The moisture content of the air corresponds to saturation at ambient temperature and 5 psig and is equivalent to 2.4 mol %.

Dry sulfation test L-10 was carried out with a modified gas distributor to obtain improved fluidization. Test conditions were: bed temperature 870°C, particle size -250 + 44 μm, reaction time 2 times stoichiometric, and 8 percent SO_2 concentration. Approximately 1.4 vol % water vapor was added to the gas.

The time to breakthrough was 53 minutes. The charge was 2117 g of -250 + 63 μm limestone and contained 40 wt % calcium or 15.10 g moles. The SO_2 feed was 1.65 ℓ/min or 0.0698 g moles/min. The sulfation was thus 24.5 mol % at breakthrough. The SO_2 content of the off-gas rose rapidly (within 20 minutes to the 7 percent level and then over a period of 2-1/2 hours to the feed level of 8.5 percent). There was still a discrepancy between the SO_2 monitor indication and the gas concentration derived from rotameter readings, one possible explanation for which was a lag in monitor response.

These results were not encouraging. We therefore decided to return to tests with smaller particle sizes, since TGA work had shown over 90 percent sulfation could be obtained below 74 μm.

As preparation for Batch L-11, fluidization observations were made on various particle size distributions in the 10-cm unit. First, 225 g of -88 + 0 μm Limestone 1359 was charged, producing a shallow bed about 2.3 cm deep. A fines return system was added so that, if elutriation did occur, the contact time of the fines could be increased by recirculating them from the cyclone to the reactor. When the system was tested to the maximum air feed rate available, however, no circulation was observed. The gas cooler and cyclone contained 21 g of fines, and the downstream filter had 3.5 g. The carry-over was close to the 25 g of -44 + 0 μm in the original charge.

Velocity conditions relative to U_{mf}, the minimum fluidization velocity estimated by the Ergun equation, were as follows:

Mesh size	170	230	325
Particle diameter, μm	88	63	44
U_{mf}	0.67	0.34	0.17
U_o/U_{mf}	37	73	149

Since the theoretical terminal velocity for the fines was 80 - 93 x U_{mf}, these observations are in accord with predictions.

The total solids were sieved, and, after adjusting the screen analysis to a common basis, we made the following comparison:

Particle Size, μm	Feed	Product
+88	0	5
-88 + 63	106.5	70
-63 + 44	85.2	113
-44 + 0	21.3	18
	213.0	206
Loss in sieving		7
	TOTAL	213

The +88 μm fraction found was considered within the variability of sampling and analysis. Some grinding apparently occurred in the -88 + 63 μm fraction since there was a reduction of 36.5 g (34 percent) along with an increase in the -63 + 44 m fraction of 27.8 g (32 percent). This size change occurred in the test period of about 30 minutes. An alternative explanation, which is probably more reasonable, is that sieve analyses are difficult to make for the small particle sizes, which tend to stick to the larger particles.

A second try was made using 200 g of -88 + 44 μm plus 615 g of -44 + 0 μm to test the hypothesis that there may not have been enough fines present to permit the return system to become effective. The design was based on picking up the cyclone catch in a jet of air and conveying it back to the reactor. Fluidization at ambient temperature was carried out. When high gas flow rates were reached, a cloud of fines began elutriating. The system was closed up and circulation of fines attempted. Again no circulation was observed, even though the system was heated to 305°C, and the combined air and nitrogen flow was 145 ℓ/min at 15°C, corresponding to a superficial velocity of 42.7 cm/s. The ratio U_o/U_{mf} was

255 for 44 μm particles. Assuming all the carry-over was -44 μm, only 4 percent of this fraction fed was elutriated. When the reactor was opened, the bed was observed to have ratholed.

Fluidization was again observed at ambient conditions. At 142 ℓ/min gas flow, the pressure drop across the distributor and the bed was (9.7 in) of oil (S.G. 2.95) or 72.7 cm of water. Deducting the bed pressure drop, estimated at 8.4 cm at a bulk density of 1.3 g/cc leaves a 61.8-cm water drop across the distributor. This yields an orifice coefficient of 0.82, which appears reasonable for a submerged orifice. The jet velocity from the distributor holes was 8250 cm/s (270 fps).

These observations led to the conclusion that a different particle size distribution was needed to achieve fluidization at reasonably low gas velocities while retaining fines in the bed. Accordingly, Batch 11 was prepared by adding 528 g of -250 + 88 μm stone to the reactor. Fluidization was observed at ambient conditions. Fluidization was considered achieved at an airflow of 80 ℓ/min, corresponding to a superficial velocity of 17.8 cm/s. This is about 3 x U_{mf} for 250 μm particles and 107 x U_{mf} for 44 μm particles. No significant elutriation occurred. Increasing the gas flow to 35 cm/s resulted in elutriation: this was at 209 x U_{mf} for 44 μm particles. The bed was thus acting as a sand filter to retain fines at gas velocities twice the terminal velocities.

The stone was then sulfated at 630 to 865°C with a nominal 8-percent SO_2 in air for 5 hours, 34 minutes. At the completion of the run, the bed was found to be caked. The bed material was sieved. Lumps that could not be broken easily by hand were included in the +250 μm fraction.

Mesh Size, μm	Feed	Reactor Product
+250	0	224
+177	213	242
+125	181	290
+88	134	232
+63	87	152
+44	113	139
-44	590	134
	1318	1313

There was no carry-over to any of the downstream equipment. Superficial velocity at maximum bed temperatures was 18.0 cm/s, which may be compared with the U_{mf} of 44 μm particles of 0.067 cm/s at 86.5°C. Chemical analysis showed the +250 μm fraction contained 56.0 wt % sulfur as SO_4, while the -44 μm fraction had 52.7 percent. If one assumes pure limestone and complete calcination of unsulfated stone, these figures correspond to 79.4 and 74.7 mol % sulfation to $CaSO_4$, respectively. Again, the CO_2 analyses seem discrepant, but sulfation appears to have been at least 70 mol % when $CaCO_3$ was taken into account. The higher sulfation compared to previous results was encouraging relative to lime utilization, but the caking of the bed was a negative factor. Fluidizing velocities would be maintained for a longer portion of the cooldown period in subsequent runs.

To improve fluidization further, Batch 12 was run with a relatively smaller content of -44 μm - namely, 7 percent. Even at 106 ℓ/min, however, the bed was not completely fluidized, although fines were being elutriated. Although we felt that heating to reaction temperature would result in satisfactory fluidization, on the basis of observations thus far, we arbitrarily adjusted the bed composition by adding 96 g (25 percent) of -250 + 177 μm stone, bringing the total charge to 480 g. The gas flow rates used corresponded to about 3 x U_{mf} for the largest particles in the bed (250 μm) and 95 x U_{mf} for the 44 μm. After sulfation the bed was again found to be packed, crusted, and ratholed. The top flange was coated with 0.6 g of a greenish-yellow powder. This was subsequently found to be insoluble in warm carbon disulfide (CS_2). Carry-over was negligible, and the reactor product weight was 490 g.

Chemical analyses showed relatively low sulfate content with essentially no difference between the +250 and -44 μm fractions. Calcium was also low, however, so sulfation was again better than 73 mol %.

Before proceeding to tests with actual CAFB spent sorbent, fluidization of this material was studied in more detail, as reported in another section of this report (Appendix C).

A summary of the test data with CAFB regenerator stone is shown in Table D-4 and product analyses are in Tables D-5 and D-6. The first run was CAFB-701 and used a feed with a normal distribution (mean 130 μm, standard deviation 50 μm). This showed that the usable range of velocities for the 10-cm reactor was a four-fold range from that needed to create uniform fluidization as judged by the appearance of the bed to that at which either elutriation was judged excessive or particles were being ejected to the level of the outlet flange. At the 11.4 cm/s superficial velocity required for minimum fluidization, the gas contact time for a 15-cm (5.9-in) bed at 50-percent voids was 0.8 seconds. To increase this, a smaller mean particle size was required. As the particle size decreases, however, the flow character of the CAFB stone changes. The -177 + 125 μm fraction was observed to be free flowing, the -125 + 88 μm fraction was somewhat sticky, and the -88 + 63 μm fraction was definitely sticky. The -44 μm fraction readily compacted to a nonflowing mass. We decided to modify the particle size distribution before proceeding with the sulfation.

CAFB-702 was a modified blend of particle sizes to increase the amount of +125 μm from 53 to 64 percent, reducing the -125 + 44 μm from 42 to 31 percent and retaining the -44 μm at 5 percent. The distribution was still normal, with a mean of 147 μm and a standard deviation of 62 μm. This change reduced the U_{mf} by about 10 percent, but elutriation was noticeably greater at the maximum flow rate. The flow rates increased by about 10 percent. Using a typical analysis for CAFB-7 regenerator stone, the degree of sulfation was calculated from the total sulfur content as 44 to 68 mol %, with a trend toward higher sulfation for the smaller particle sizes.

An incidental result was obtained toward the end of the run. Droplets of liquid were observed leaving the final vent on the apparatus. The liquid was viscous and acid, as evidenced by the corrosion of the aluminum countertop where some of the droplets had deposited. Inspection

Table D4

Dwg. 1684809

TEST CONDITIONS FOR CAFB REGENERATOR STONE RUNS

Run Number	Charge		Gas Flow Rates (ℓ/min at 15°C, 1 atm)[a]					Reactor Time/Temperature Conditions		
	Weight, g	Size, μm	N_2	Air	SO_2	Total	Superficial Gas Velocity	Heating	Reacting	Cooling
CAFB-701	Fluidization observations only									
CAFB-702	250	− 420 + 0		20	1.74	21.74	19.7	44 mins at 63 − 404°C	542 mins at 404 − 904°C	52 mins at 616 − 577°C
CAFB-903	500	− 420 + 0								
Phase I			32	6.6	2.53	41.13	23.0	65 min at 260 − 404°C	165 min at 404 − 460°C	
Phase II				21	1.10	22.10	18.3	144 min at 457 − 738°C	91 min at 738 − 854°C	Overnight to 190°C
Phase III				21	1.10	22.10	18.3	150 min at 190 − 699°C	94 min at 699 − 827°C	224 min at 827 − 127°C
CAFB-904	500	− 420 + 0								
Phase I				27.5	1.45	28.95	25.6	109 min at 221 − 654°C	339 min at 654 − 871°C	30 min at 846 − 638°C
Phase II				27.5	1.54	29.04	24.1	177 min at 118 − 640°C	290 min at 640 − 832°C	34 min at 832 − 651°C
Phase III				27.5	1.54	29.04	25.7	291 min at 518 − 813°C	171 min at 813 − 895°C	Overnight to 516°C
Phase IV				20.1	1.08	21.18	18.7	53 min at 516 − 627°C	280 min at 627 − 899°C	70 min at 899 − 570°C
CAFB 905	1975	− 354 + 0								
Phase I				44	2.3	46.3	25.9	184 min at 105 − 452°C	243 min at 452 − 457°C	37 min at 450 − 340°C
Phase II				17.1	0.9	18.0	14.2	148 min at 380 − 752°C	244 min at 742 − 758°C	88 min at 749 − 365°C
Phase III				11.4	0.6	12.0	10.4	190 min at 370 − 846°C	221 min at 845 − 853°C	83 min at 850 − 485°C
CAFB 906	1000	− 500 + 0								
Phase I			30		1.5	31.5	22.5	145 min at 308 − 655°C	277 min at 643 − 655°C	84 min at 647 − 352°C
Phase II			20		1.0	21.0	17.4	187 min at 397 − 795°C	109 min at 791 − 808°C	145 min at 803 − 222°C

[a] 1 atm = 101.32501 kPa

Dwg. 1705B87

Table D-5

CHEMICAL ANALYSES OF STONE SAMPLES FROM CAFB SULFATION STUDIES

Batch	Composition, wt%		
	$S^=$	$SO_4^=$	Total Sulfur
CAFB-702			
Feed		–	–
Sulfated Product, μm			
+ 420		–	15.4
+ 250		45.1	15.9
+ 177		–	16.2
+ 125		–	16.5
+ 88		–	18.4
+ 63		–	19.7
+ 44		–	18.3
− 44		–	18.5
Filter liquid		1092 g H_2SO_4/ℓ	
CAFB-703			
Feed		–	–
Sulfated		40.2	–
CAFB-904			
Feed		–	–
Sulfated I		39.7	–
Sulfated II-IV, μm		63.5	–
+ 420		49.5	–
+ 250		60.0	–
+ 177		65.9	–
+ 125		68.8	–
+ 88		68.2	–
+ 63		58.5	–
+ 44		58.1	–
− 44		54.2	–

of this liquid showed that it contained 1092 g H_2SO_4/ℓ and had a specific gravity of 1.62, corresponding to 67 percent acid. This finding was explored further in the subsequent runs.

In CAFB-903, the amount of -44 μm particles was doubled to 10 percent. Ths distribution had the same mean, but the standard deviation was increased to 80 μm. Compared to CAFB-702, the charge had fewer particles in the midrange and more at both ends. Elutriation was found to be appreciable at a considerably lower velocity than in the previous run and the range of operable flow rates in the test reactor appreciably reduced.

Sulfation was carried out in two phases, first at 450°C and then at 700 to 850°C. No significant pickup of SO_2 was indicated by the monitor at 450°C. Although this temperature is favorable for the conversion of SO_2 to SO_3, whatever mechanism was responsible for acid production in CAFB-702 was clearly not operating in this run. Actual sulfation finally achieved was 57.0 wt % $CaSO_4$, appreciably lower than in the previous run. The reactor product was granular, although a few small lumps were present. The difference in degree of sulfation was attributed to the difference in reaction time: 542 minutes in CAFB-702 versus 350 in CAFB-903.

CAFB-904 was a variation on CAFB-903. We hypothesized that the sulfated limestone was displaying catalytic activity in converting SO_2 to SO_3. The revised approach was to sulfate the stone partially at 870°C and then explore absorption/conversion of SO_2 at 450°C. Particle size distribution was the same as in CAFB-903. The reactor product from Phase I contained 56.3 wt % $CaSO_4$. There was evidence that gas bypassing may have occurred during part of the Phase I test.

Phases II through IV were concerned with maximizing the degree of sulfation at 650 to 900°C. Total exposure time to 5 percent SO_2 was 18 hours for the run. The SO_2 monitor showed some pickup of SO_2 throughout most of this exposure. Overall, the reactor product contained 90.0 wt % $CaSO_4$. Maximum sulfation was in the -177 + 125 μm and the -125 + 88 μm fractions (97.6 and 96.6 wt % $CaSO_4$, respectively). The lowest sulfation was in the +420 μm fraction (70.1 percent) and in the -44 μm

Dwn. 1705B88

Table D-6

CHEMICAL ANALYSES OF STONE SAMPLES FROM CAFB SULFATION STUDIES

CAFB-905	Measured		Calculated		BET Surface Area, m^2/g
	$S^=$	$SO_4^=$	CaS	$CaSO_4$	
Feed					
−500 + 177	1.94	4.08	4.36	5.78	2.79
−171 + 88	0.31	7.15	0.70	10.13	2.71
−88	1.85	4.23	4.16	6.00	10.71
Sulfation I 450°/0 min					
−500 + 127	1.97	3.79	4.43	5.37	3.80
−177 + 88	1.90	3.64	4.27	5.16	6.63
−88	1.95	3.94	4.30	5.58	7.98
450°/15 min					
−500 + 177	1.09	5.16	2.45	7.31	1.98
−177 + 88	1.59	4.98	3.58	7.06	3.99
−88	0.81	6.96	1.82	9.86	8.39
450°/75 min					
−500 + 177	1.49	6.07	3.35	8.60	2.11
−177 + 88	1.14	6.07	2.56	8.60	3.00
−88	0.78	6.36	1.76	9.01	5.78
450°/135 min					
−500 + 177	0.97	6.47	2.18	9.17	1.60
−177 + 88	1.09	6.89	2.45	9.76	1.90
−88	0.70	8.29	1.58	11.74	4.93
450°/255 min					
−500 + 177	1.45	7.77	3.27	11.01	0.943
−177 + 88	1.13	7.47	2.54	10.59	1.354
−88	1.51	11.35	3.40	16.08	
Cyclone Catch					
−500 + 177	0.52		1.18		−
−177 + 88	0.64		1.43		4.97
−88	0.98		2.21		9.96
Filter Catch					
−500 + 177	0.21		0.47		−
−177 + 88	0.69		1.55		12.43
−88	0.62		1.40		7.52

Dwg. 1705B89

Table D-6 (Cont'd)

CAFB - 905	Measured		Calculated		BET Surface Area, m^2/g
	$S^=$	$SO_4^=$	CaS	$CaSO_4$	
Sulfation II					
750°/0 min					
−500 + 177	1.52	10.13	3.42	14.36	1.75
−177 + 88	1.65	9.89	3.71	14.02	2.01
−88	2.26	15.57	5.08	22.07	–
750°/15 min					
−500 + 177	1.43	13.86	3.22	19.64	–
−177 + 88	1.54	14.43	3.46	20.45	–
−88	1.39	19.14	3.13	27.12	–
750°/75 min					
−500 + 177	1.28	21.17	2.88	30.00	–
−177 + 88	1.33	21.80	2.99	30.90	–
−88	NS*	25.31	NS	35.87	–
750°/135 min					
−500 + 177	1.30	25.06	2.92	35.02	–
−177 + 88	1.19	25.49	2.68	36.12	–
−88	NS	30.88	NS	43.76	–
750°/255 min					
−500 + 177	0.97	29.65	2.18	42.02	0.996
−177 + 88	1.14	32.29	2.56	45.76	1.227
−88	NS	10.44	NS	14.80	–
Cyclone Catch					
−500 + 177	–	31.51	–	44.66	NS
−177 + 88	–	21.45	–	30.40	NS
−88	0.79	11.77	1.78	16.68	6.96
Filter Catch					
−500 + 177	–	–	–	–	NS
−177 + 88	1.80	17.44	4.05	24.72	11.73
−88	1.81	15.29	4.07	21.67	6.30
Sulfation III					
850°/0 min					
−500 + 177	1.06	29.08	2.38	41.21	1.017
−177 + 88	1.12	30.36	2.52	43.03	2.830
−88	NS	42.38	NS	60.06	–

---

*NS = Not Sufficient Sample Quantity

Dwg. 1705890

Table D-6 (Cont'd)

CAFB 905	Measured		Calculated		BET Surface Area, m^2/g
	$S^=$	$SO_4^=$	CaS	$CaSO_4$	
850°/15 min					
−500 + 177	0.95	30.80	2.14	43.65	–
−177 + 88	1.09	32.75	2.45	46.41	–
−88	NS	37.11	NS	52.59	–
850°/60 min					
−500 + 177	1.03	31.31	2.32	44.37	0.955
−177 + 88	1.04	–	2.34	–	0.961
−88	NS	39.37	NS	55.80	–
850°/120 min					
−500 + 177	0.95	32.87	2.14	46.58	–
−177 + 88	1.06	35.75	2.38	50.67	–
−88	NS	NS	–	NS	–
850°/239 min					
−500 + 177	0.88	35.46	1.98	50.26	0.505
−177 + 88	1.00	39.75	2.25	56.34	4.608
−88	NS	NS	–	–	–
Reactor Product					
+ 500	0.60	52.50	1.35	74.40	1.70
−500 + 354	1.13	37.14	2.54	52.64	1.41
−354 + 177	0.88	34.72	1.98	49.21	1.06
−177 + 88	0.96	39.78	2.16	56.38	0.90
−88	0.73	31.52	1.58	44.67	1.98
Cyclone Catch					
−500 + 177	0.46	61.94	1.04	87.78	17.88
−177 + 88	0.57	42.42	1.28	60.12	17.40
−88	0.71	13.40	1.60	18.99	8.52
Filter Catch					
−500 + 177	–	–	–	–	31.94
−177 + 88	–	–	–	–	27.00
−88	–	–	–	–	–

	Measured				
CAFB 906	$S^=$	$SO_4^=$	Total Sulfur	Ca	CO_2
Feed Sulfation I 650°C/280 min					
−500 + 354	3.28	–	7.64	58.67	8.03
Reactor Product	3.73	–	9.44	53.87	10.3

fraction (76.8 percent). This run was taken as evidence that when fluidization is achieved, the calcium can be sulfated to essentially 100 percent by contact times of the order of 20 hours. The same result was achieved in a 2.5-cm fixed bed.

CAFB-905 was intended to collect additional information to clarify the effect of particle size distribution in fluidization and to correlate the progress of sulfation in a fluidized bed with surface area and pore volume measurements made on the same fractions. As a preliminary, extensive observations were made in an existing atmospheric pressure 7.6-cm (3-in) Plexiglas column on the behavior of -420 + 125 μm spent CAFB sorbent to which were added various proportions of -63 + 0 μm powder. These showed that the addition of fines

- Increased the pressure energy needed to maintain a fluidized bed
- Increased the maximum bed pressure drop before fluidization was achieved
- Produced a larger pressure drop at a lower superficial gas velocity.

The transition from a fixed bed to a fluidized bed was also less smooth and occurred over a wider range of gas velocities. With a bed containing one-third of its weight as -44 + 0 μm particles, for example, the transition occurred over the range of 2.5 to 11.0 cm/s versus 7.5 to 8.0 cm/s for a bed without these fines.

Sulfation was carried out in three phases corresponding to the reactor temperatures of 450, 750, and 850°C. Samples were collected at five reaction times and were analyzed for sulfur content, both sulfide and sulfate, BET surface area, and pore volume as a function of particle size. Observations were made on sorbent carry-over. A summary of sorbent distribution is given in Table D-7. Figures D-1 through D-3 show the time-temperature curves.

In the meantime, the significance for dry sulfation is that the design previously worked out for the absorber provides more than enough

Dwg. 2570612

Table D-7

MATERIAL BALANCE DATA FOR TEST CAFB-905

	Sample Wt., g	Particle Size Distribution, g					Total Sample Wt., g
		+35(1)	−35 +45	−45 +80	−80 +170	−170 +0	
Phase 1 Initial Conditions							25.1
Reactor Charge	25.1	0.0	1.1	20.0	1.8	2.2	
Phase 2 Sulfation at 450° C							245.6
Sample Tube Cleanings	25.1	0.0	0.8	16.7	3.8	3.8	
Initial Sample	25.1	0.0	1.1	19.1	2.6	2.4	
15 Minutes	26.5	0.0	0.9	20.6	2.6	2.4	
75 Minutes	26.7	0.0	0.2	21.7	3.0	1.8	
135 Minutes	31.7	0.0	0.9	25.6	3.6	1.6	
255 Minutes	29.3	0.0	0.7	24.6	3.3	0.7	
Sample Purges	36.8		This sample was not sieved				
Cyclone Catch	25.8	0.0	0.030	0.1	2.8	22.9	
Filter Catch (2)	18.6	1.3	0.1	0.1	4.3	12.8	
Phase 3 Sulfation at 750° C							262.6
Initial Sample	30.7	0.0	0.9	26.8	2.9	0.1	
15 Minutes	33.7	0.0	1.0	29.2	3.3	0.2	
75 Minutes	39.1	0.0	0.9	34.2	4.0	0.042	
135 Minutes	44.5	0.0	1.1	38.8	4.6	0.014	
255 Minutes	46.8	0.0	1.1	40.9	4.8	0.022	
Sample Purges	40.0	0.0	1.1	34.3	4.1	0.5	
Cyclone Catch	24.4	0.0	0.021	0.064	0.2	24.2	
Filter Catch	3.4	0.2	0.027	0.045	0.9	2.2	
Phase 4 Sulfation at 850° C							1838.4
Initial Sample	42.0	0.0	1.0	36.6	4.4	0.028	
15 Minutes	40.3	0.0	1.1	35.1	4.1	0.011	
60 Minutes	46.8	0.0	1.5	40.8	4.5	0.012	
120 Minutes	43.1	0.0	1.3	37.6	4.2	0.004	
239 Minutes	44.8	0.0	2.3	38.9	3.6	0.012	
Sample Purges	78.7	0.0	2.9	68.2	7.6	0.026	
Cyclone Catch	216.9	9.9	1.6	2.6	4.2	198.6	
Filter Catch	2.1	0.1	0.1	0.2	0.8	0.9	
Tubing Catch	10.2	3.7	0.8	1.4	2.1	2.2	
Reactor Product	1313.5	68.0	45.0	972.0	142.5	86.0	
Total Sample Weight Recovered							2371.7

Notes

1. U. S. sieve mesh sizes
2. Includes about 3g of material found in inlet line to filter

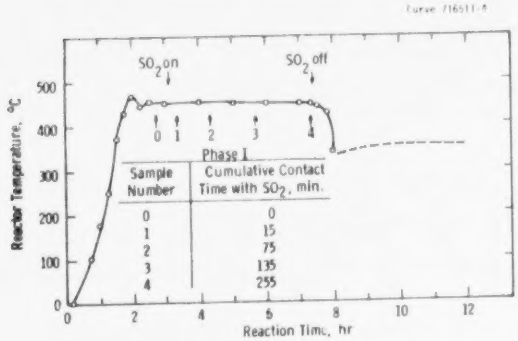

Figure D-1 - Dry Sulfation of CAFB-9 Regenerator Stone at 450°C

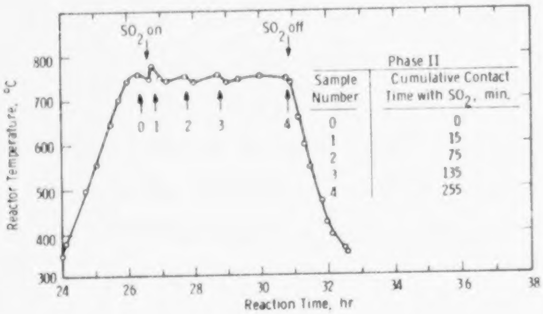

Figure D-2 - Dry Sulfation of CAFB-9 Regenerator Stone at 750°C

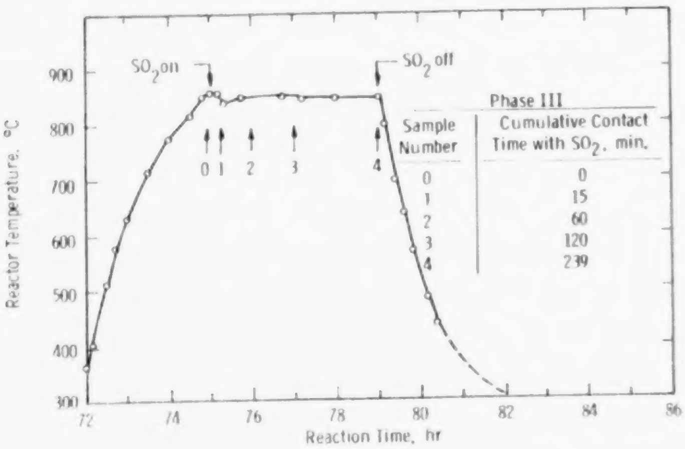

Figure D-3 - Dry Sulfation of CAFB-9 Regenerator Stone at 850°C residence time (~100 hours versus 18) for the solid. The conclusion suggests that the regenerator stone may not have to be ground, thus permitting elimination of the jet pulverizer and the associated air compression cost.

One further run was made, CAFB-906, to explore the reactivity of CAFB stone to dry SO_2 versus SO_2 in moist nitrogen. Previous TG results had shown that fresh limestone would pick up substantial amounts of SO_2.

The reactor was charged with 1000 g of -500 μm CAFB-9 stone obtained by a combination of sieving out the -500 μm fraction from the stone as received and grinding +500 μm to accumulate the desired charge.

Fluidization behavior was observed at atmospheric pressure using air, as shown in Figures D-4 and D-5. Sulfitation was then carried out in two phases. In Phase I, the charge was heated to 650°C and then treated with 5 percent SO_2 in nitrogen, with about half the nitrogen being fed through the hydrator. Samples were taken at time intervals as shown on Figure D-6. The reactor was cooled to below 300°C overnight. In Phase II the reactor temperature was 800°C; sampling was at similar intervals as shown on Figure D-7. After we had cooled the sulfited product to ambient temperature, we observed its fluidization behavior, using dry nitrogen as shown in Figures D-8 and D-9.

Table D-8 gives material balance information by particle size. Table D-9 shows that a slight change in distribution occurred as a result of attrition and sulfidation. Some particle growth occurred in the +500 μm fraction, and a reduction in the percent of -500 + 354 μm can be noted.

Chemical analysis of the reactor showed only 9.4 wt % total sulfur, essentially the sulfite sulfur, and 3.73 wt % of sulfide sulfur. Allowing for the disproportionation of calcium sulfite into sulfate and sulfide, we can calculate a theoretical SO_2 pickup. The analytical results, however, were not sufficiently consistent to permit this. If we use a typical analysis for the regenerator stone, as in the 1975 Annual Report,[D1] the 9.4-percent sulfur works out to an 18-percent conversion of the

Curve 716512-A

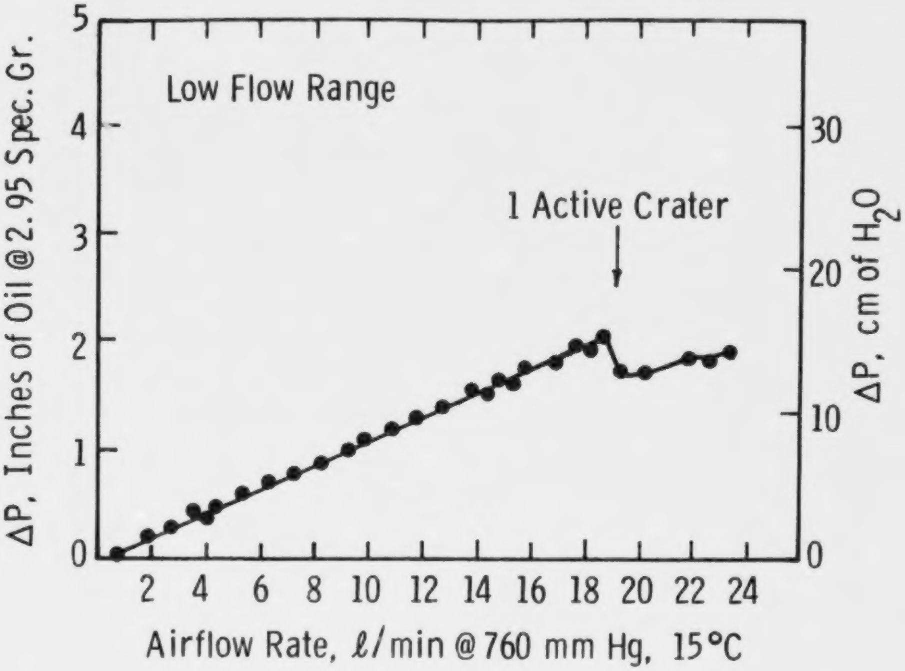

Figure D-4 - Fluidization Behavior of CAFB-9 Regenerator Stone, Run CAFB-906, prior to Sulfitation

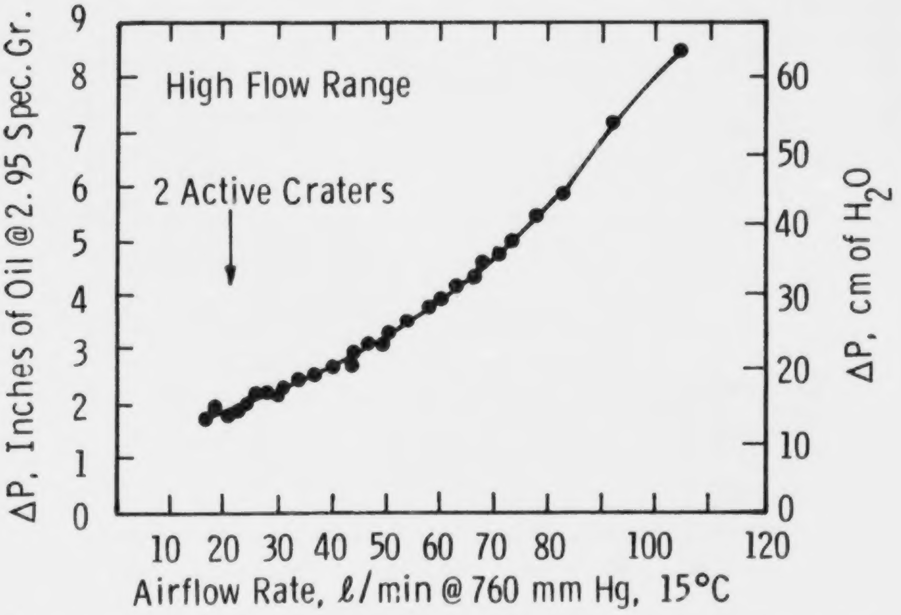

Figure D-5 - Fluidization Behavior of CAFB-9 Regenerator Stone, Run CAFB-906, prior to Sulfitation

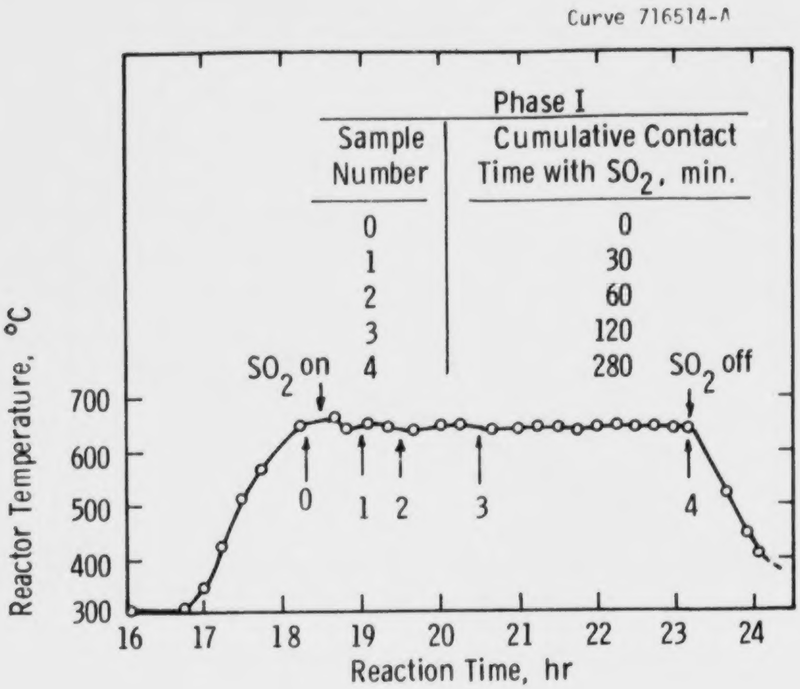

Figure D-6 - Absorption of SO_2 on CAFB-9 Stone in Absence of Air

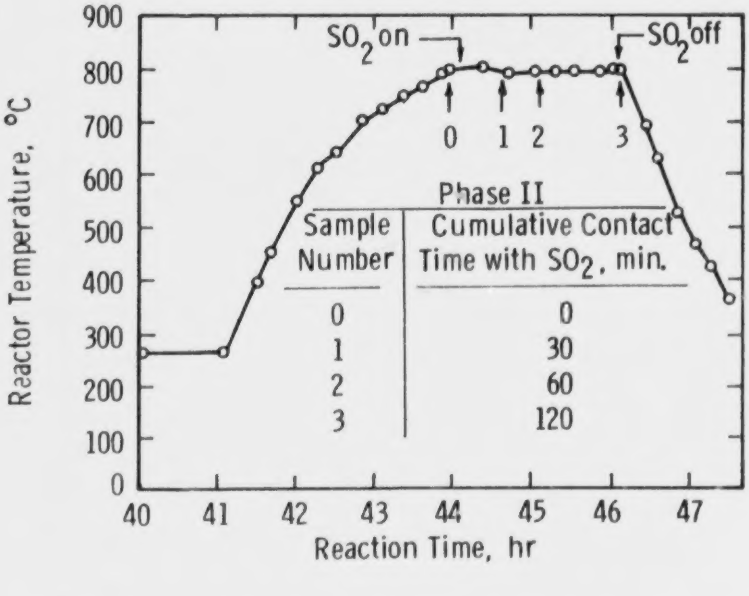

Figure D-7 - Absorption of SO_2 on CAFB-9 Stone in Absence of Air

Curve 716513-A

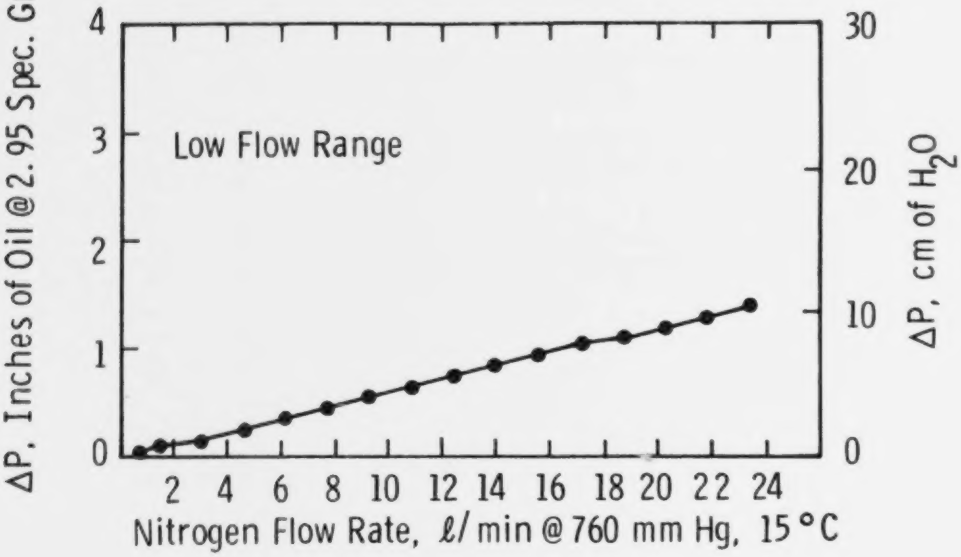

Figure D-8 - Fluidization Behavior of CAFB-9 Regenerator Stone, Run CAFB-906, after Sulfitation

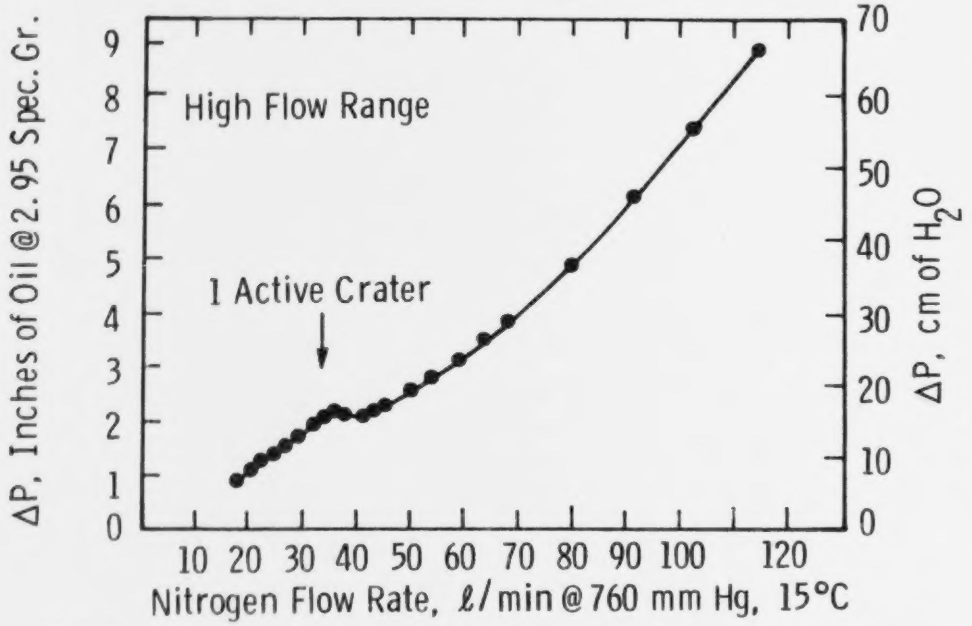

Figure D-9 - Fluidization Behavior of CAFB-9 Regnerator Stone, Run CAFB-906, after Sulfitation

Table D-8

MATERIAL BALANCE DATA FOR TEST CAFB-906

	Sample Wt, g	Particle Size Distribution, g[a]								
		+35	+45	+60	+80	+120	+170	+230	+325	-325
Phase I Sulfitation at 650°C										
Initial sample	27.0	1.1	15.8	5.7	2.6	1.3	0.4	<0.1	0	0
30 minutes	28.9	1.0	16.6	6.1	3.0	1.6	0.5	<0.1	0	0
60 minutes	38.7	1.6	22.2	8.4	4.0	2.0	0.4	<0.1	0	0
120 minutes	45.9	1.8	25.4	10.0	5.1	2.7	0.8	<0.1	0	0
280 minutes	37.5	1.9	20.4	7.7	4.3	2.3	0.8	<0.1	0	0
Subtotal	178.0									
Phase II Sulfitation at 800°C										
Initial sample	28.5	1.7	15.8	5.8	3.0	1.6	0.5	<0.1	0	0
30 minutes	38.6	2.1	21.3	8.1	4.1	2.2	0.6	<0.1	<0.1	0
60 minutes	36.0	1.1	20.3	7.7	4.0	2.2	0.6	<0.1	0	0
120 minutes	34.8	1.9	19.5	7.2	3.7	1.9	0.5	<0.1	0	0
Subtotal	137.9									
Combined Sample Purges	73.6	2.9	44.2	16.1	6.7	2.9	0.7	<0.1	0	0
Reactor Product Sample	25.0	Not sieved								
Reactor Product	745.6	23.1	379.9	147.5	81.3	67.2	39.1	6.0	1.0	0.5
Cyclone Catch	1.9	Not sieved								
Filter Catch	0.0									
Line Plugging	1.6	Not sieved								
Total output	1163.6									

---

[a] U. S. sieve mesh sizes

Table D-9

EFFECT OF SULFITATION ON PARTICLE SIZE DISTRIBUTION OF CAFB-9 REGENERATOR STONE

U. S. Screen Size	Reactor Charge		Phase I Initial Sample		Reactor Product	
	Weight, g	Wt %	Weight, g	Wt %	Weight, g	Wt %
-25 + 35	0.0	0.00	1.1	4.07	23.1	3.10
-35 + 45	587.8	57.34	15.8	58.52	379.9	50.95
-45 + 60	212.4	20.72	5.7	21.11	147.5	19.78
-60 + 80	103.6	10.11	2.6	9.63	81.3	10.90
-80 + 120	75.4	7.35	1.3	4.82	67.2	9.01
-120 + 170	38.1	3.72	0.4	1.48	39.1	5.25
-170 + 230	6.1	0.60	<0.1	0.37	6.0	0.81
-230 + 325	1.2	0.12	0.0	0.00	1.0	0.13
-325	0.4	0.04	0.0	0.00	0.5	0.07
	1025.0	100.00	27.0	100.00	745.6	100.00

available CaO. As a check, the sulfide sulfur was 2.9 percent versus the 3.73 percent found. For comparison, in the same contact time of about six hours, sulfitation in air (sulfation, i.e.) proceeded to a level at least twice as high. Apparently, the presence of oxygen enhances the ability of SO_2 to penetrate the spent stone particles.

In contrast earlier work had shown that much higher sulfur burdens could be achieved with fresh limestone, an indicator of the reduced chemical reactivity of CAFB regenerator stone but also suggesting that in sulfation the oxygen present may have more than a stoichiometric role.

A sample of CAFB-9 stone, therefore, was tested in the TG apparatus for reaction of CaO with SO_2 in the absence of oxygen. In 0.5 percent SO_2/N_2, the reaction was sluggish and corresponded to 9.7 percent of stoichiometric for formation of $CaS \cdot 3CaSO_4$, in 70 minutes at 800°C. Raising the temperature to 825°C had little effect on the rate of reaction. Previous TG tests had shown that fresh CaO reacts strongly with SO_2 in the absence of air.

These test results overall support the conclusion that dry sulfation is technically feasible. An optimum temperature for the dry sulfation of small particles (<74 μm), however, has not been shown. The model presented in the March 1975 report[1] seems to be applicable to both fixed and fluidized beds in the case of small particles but may not be applicable to a fluidized bed in the case of large particles.

ANALYSIS OF DATA FROM CAFB RUNS

Figures D-10 through D-12 present the basic information collected in CAFB-905 in terms of weight percent $CaSO_4$ versus run time for three size fractions of spent stone. Some sulfation, 5 to 10 wt %, occurred even at 450°C, but most of it occurred at 750°C (about 30 wt %). A further increment was obtained on raising the temperature to 850°C (5 to 10 percent). The maximum sulfation was obtained in the +500 μm fraction (about 75 wt %), while the -88 μm fraction showed only 45 percent sulfation. The middle fraction, -500 + 88 μm, contained 49 to 56 percent $CaSO_4$.

Figure D-13 shows the changes in BET surface area obtained for three size fractions during sulfation. The BET areas for the two larger fractions (-500 + 177 and -177 + 88 μm) were about the same, whereas the area for the -88 μm fraction was, at least initially, larger by a factor of more than 2. It is likely that the area declines gradually over the period covered by Phase II. It is also possible that, for the -88 μm fraction, the BET area in Phase I declines to about the level of 2 m^2/g, as for the other two fractions. The sulfation obtained in Phase I, which was no more than about 5 percent of the calcium, was associated with a three-fold reduction in BET area. Despite the substantial sulfation that occurred in Phase II, there did not appear to be a comparably large reduction in BET area. Continued sulfation as in Phase III appears to be associated with a resumption of the decline in BET area.

For comparison with previous work done by others, the March 1975 Annual Report, Vol. II, page 280,[D1] showed data on the sulfation of CAFB-7 stone ground to less than 148 μm (100 mesh). In 5 percent SO_2, TG

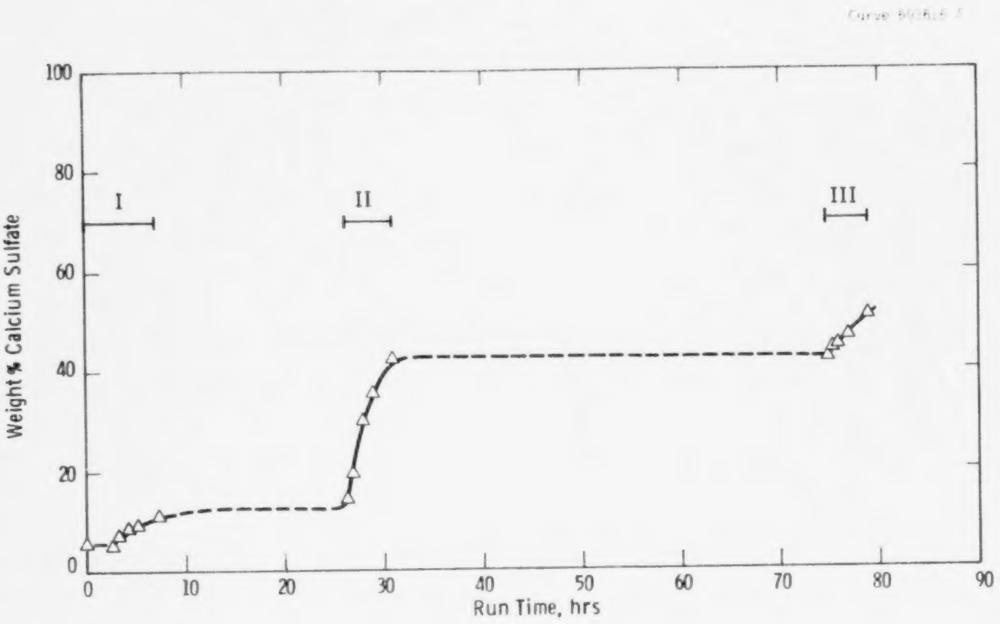

Figure D-10 - Dry Sulfation of -500 + 177 μm Fraction of CAFB-9 Regenerator Stone

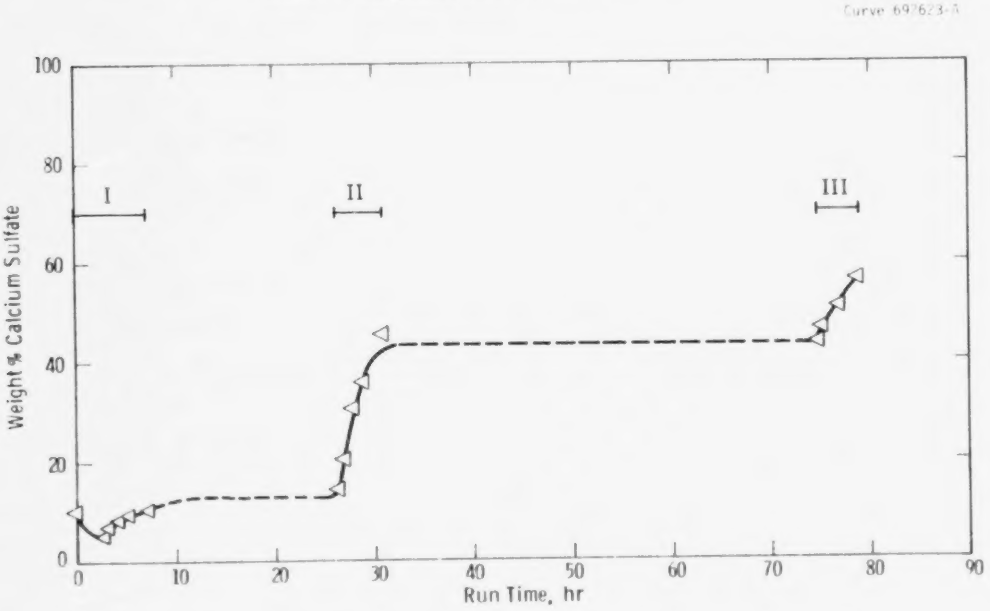

Figure D-11 - Dry Sulfation of -177 + 88 μm Fraction of CAFB-9 Regenerator Stone

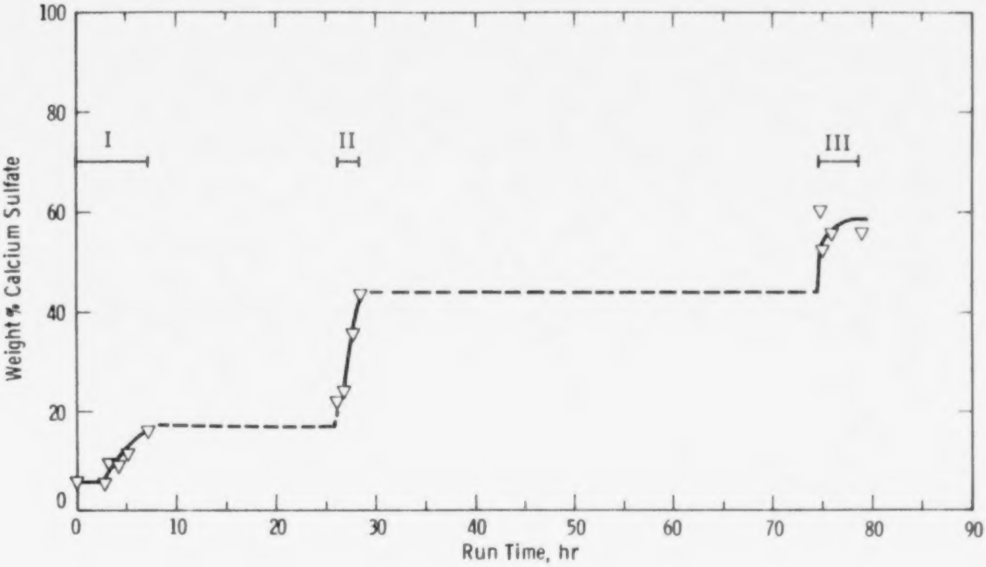

Figure D-12 - Dry Sulfation of -88 μm Fraction of CAFB-9 Regenerator Stone

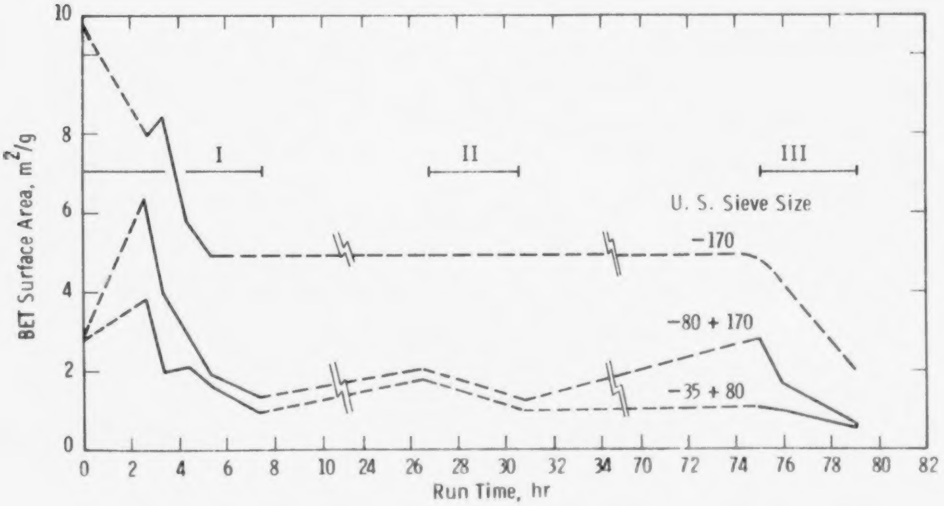

Figure D-13 - Effect of Dry Sulfation on BET Surface Area of CAFB-9 Regenerator Stone sulfation experiments showed two hours was sufficient to achieve 95 percent sulfation for -149 + 125 μm particles at 920°C or for -74 μm particles at 825°C. No more than about 5 minutes was required for 35 percent sulfation (56 wt % $CaSO_4$). In contrast, the results from the 10-cm fluidized unit show the increase in $CaSO_4$ from 14 wt % to about 46 wt % required 255 minutes at 750°C for -177 + 88 μm particles. This corresponds to a conversion of CaO from 6.5 to 26.0 mol %. Thus, there is a discrepancy of a factor of 50 in reaction rate to be rationalized. First, the 10-cm unit results do not appear to have been limited by stoichiometry. At 5 percent SO_2 in air, the oxygen available was 8 times theoretical. The total SO_2 supplied was 1.27 times theoretical. About 18 percent of the supplied SO_2 was absorbed. This amount was determined by noting that the $CaSO_4$ content of the final product was about 53 wt % more than initial value.

Next, the 1 to 5 percent conversion of calcium at 450°C might have been responsible for the low reaction rate. The BET data, strictly speaking, show that the number of sites capable of adsorbing nitrogen was greatly reduced in Phase I. Although this interpretation is consistent with the inference that chemical reactivity for SO_2/O_2 was also reduced, the BET area was essentially constant in Phase II, when most of the sulfation occurred. Thus, one sequence is initial reduction of available pores, either by pore blockage or by lining the internal pore area with a less reactive $CaSO_4$ layer. Calculations show that a very small amount of conversion is sufficient to create a monolayer of $CaSO_4$, so the first phase of sulfation at any temperature can be seen as converting all surface CaO to $CaSO_4$. Thereafter, SO_2 and oxygen must diffuse through this and subsequent layers of $CaSO_4$ to achieve the demonstrated levels of conversion. The constancy of the BET values in Phase II supports this view and thus implies that the reaction with subsurface calcium leaves the surface area essentially constant over a considerable portion of the reaction. We consider it unlikely that the observed effects can be explained by blockage of pore mouths except, perhaps, in the later stages, as in Phase IV.

Another possibility is inadequate fluidization or, more basically, inadequate contact between the fines and the gas. Such failure of contact could happen if segregation occurred in the bed so that the bulk of the fines was out of the gas path or if fines were elutriated to reduce their concentration in the bed. The final product had 6.5 percent of -88 μm material, so at least half of the original fines charged were elutriated. Also, the fines content of the samples withdrawn during the course of the test began at about 10 percent of -88 μm and dropped to less than 0.1 percent. This also resulted in very small samples for chemical analysis, although we do not believe that the sulfate contents found are unrepresentative. Therefore, despite the evidence that fluidization occurred, it does appear likely that the combination of elutriation and segregation could be responsible for the low sulfation of the fines. The low sulfation of the coarse particles is in line with the previous work and the literature.

Superficial gas velocities in each of the three phases are summarized in Table D-10. We had found previously that in some cases velocities to 200 times minimum fluidization velocity were needed to elutriate fines. Only the -44 μm particles at 450°C and 750°C met or surpassed this criterion. More than 90 percent of the +88 μm material was retained in the bed. Thus, to retain -44 μm fines in a bed of -354 + 125 μm particles requires the superficial gas velocity at 750°C to be less than 13.6 cm/s, whereas to fluidize -354 μm particles would require it to be 4.5 cm/s.

Further analysis of the data was accomplished by use of the shrinking core model for reaction of a gas with a nonporous solid developed in the literature.[2] Several assumptions are required.

1. Particles remain spherical during the reaction.
2. Reaction occurs only at the boundary between the reaction product and the unreacted core.
3. Temperature is uniform.
4. Density of solid remains constant.

5. There is no gaseous region between the reaction product and the unreacted core.
6. The diffusion rate of the gaseous reactant is large relative to the rate of decrease of unreacted core radius.

Table D-10

GAS VELOCITIES IN THE DRY SULFATION OF REGENERATOR STONE IN RUN CAFB-905, cm/s

	Phase		
	I	II	III
Temperature Level, °C	450	750	850
U_o, Superficial Velocity	24.66	13.56	9.94
U_{mf}, Minimum Fluidization Velocity			
Particle Size, μm			
44 (325 mesh)	0.0896	0.0701	0.0661
88 (170 mesh)	0.358	0.286	0.265
354 (45 mesh)	5.77	4.54	4.19
500 (35 mesh)	11.40	9.02	8.53
U_o/U_{mf}			
44 μm	275	193	150
88 μm	69	47	38
354 μm	4.3	3.0	2.4
500 μm	2.2	1.5	1.2

Where the diffusion rate of the reacting gas through the product layer is controlling, the equation developed is expressible as:

$$r_s[1 + (1 - X_B)^{1/3} - 2(1 - X_B)^{2/3}] = A + B \frac{t}{r_s[1 - (1 - X_B)^{1/3}]}$$

where

r_s = particle radius, cm
X_B = (initial mass - mass of unreacted core)/ initial mass
t = reaction time, minutes

A = constant = $-6\ D_e/k$, cm

D_e = effective diffusivity of reacting gas through the product layer, cm^2/min

k = first-order reaction rate constant, cm/min

B = constant = $6\ D_e\ b\ M_B\ (C_A)_b/\rho_B$, cm^2/min

M_B = molecular weight of solid reactant

$(C_A)_b$ = concentration of reactant gas in the bulk of the gas, $moles/cm^3$

b = moles of solid reacting per mole of reactant gas

ρ_B = density of solid reactant, g/cm^3.

Chemical analysis of the sorbent samples yields y, the weight fraction of $CaSO_4$ in the sample, which is related to X_B as follows:

$$X_B = \frac{(y - y_o)/(1 - y_o)}{1 + (1 - y)\left(\frac{80.06}{56.08}\right)}$$

where

y_o = weight fraction $CaSO_4$ at the beginning of sulfation

and

y = weight fraction $CaSO_4$ at time t.

This model neglects the small corrections due to CaS and impurities. For $y_o = 0$ and $y = 0.50$, $X_B = 0.2917$; for $y = 0.90$, $X_B = 0.7876$. For $y_o = 0.50$ and $y = 0.75$, $X_B = 0.3685$; for $y = 0.95$, $X_B = 0.8400$.

Data from Run CAFB-905 for the dry sulfation of CAFB-9 regenerator stone are summarized in Tables D-11 through D-13 and are plotted in Figures D-14 through D-16. The correlating lines are least-squares representations of the form $Y = A + BX$. The constants A and B are given in Table D-14. To extract values of D_e and k, use is made of pore volume data. The pore volume distributions are condensed on Figures D-17 through D-19, plotted to show the cumulative percent of pore volume above 6×10^{-3} μm pore diameter. The values of pore volumes shown on the figures are estimates of intraparticle pore volume, the balance of cumulative volume above pore diameters of 8.8 μm being attributed to interparticle voids.

Table D-11

DRY SULFATION OF CAFB-9 REGENERATOR STONE, PHASE I - 450°C

Time, min	Wt % $CaSO_4$	X_B	$X \times 10^{-6}$	$Y \times 10^4$
-35 + 80 U. S. Sieve Size				
0	5.37	0.000000	-	-
15	7.31	0.008824	0.301	1.493
75	8.60	0.014809	0.894	2.508
135	9.17	0.017484	1.362	2.961
255	11.01	0.026251	1.709	4.451
-80 + 170 U. S. Sieve Size				
0	5.16	0.000000	-	-
15	7.06	0.008610	0.787	0.571
75	8.60	0.015737	2.147	1.044
135	9.76	0.021196	2.864	1.408
255	10.59	0.025151	4.552	1.671
-170 U. S. Sieve Size				
0	5.58	0.000000	-	-
15	9.86	0.019822	1.025	0.437
75	9.01	0.015801	6.438	0.348
135	11.74	0.028867	6.315	0.637
255	16.08	0.050593	6.756	1.119

Table D-12

DRY SULFATION OF CAFB-9 REGENERATOR STONE, PHASE II - 750°C

Time, min	Wt % $CaSO_4$	X_B	$X \times 10^{-5}$	$Y \times 10^3$
-35 + 80 U. S. Sieve Size				
0	14.36	0.000000	-	-
15	19.64	0.028713	0.917	0.488
75	30.00	0.091343	1.410	1.562
135	35.52	0.128144	1.785	2.201
255	42.02	0.176712	2.401	3.053
-80 + 170 U. S. Sieve Size				
0	14.02	0.000000	-	-
15	20.45	0.035017	1.917	0.233
75	30.90	0.098831	3.321	0.662
135	36.12	0.134437	4.337	0.905
255	45.76	0.208053	5.145	1.413
-170 U. S. Sieve Size				
0	22.07	0.000000	-	-
15	27.12	0.031759	6.372	0.070
75	35.87	0.092446	10.715	0.206
135	43.76	0.154378	11.288	0.334
255	14.80	-	-	-

Table D-13

DRY SULFATION OF CAFB-9 REGENERATOR STONE, PHASE III - 850°C

Time, min	Wt % $CaSO_4$	X_B	X x 10^{-5}	Y x 10^4
-35 + 80 U. S. Sieve Size				
0	41.21	0.000000	-	-
15	43.65	0.023001	1.147	3.903
60	44.37	0.029958	3.514	5.807
120	46.58	0.051822	4.033	8.822
239	50.26	0.090017	4.562	15.392
-80 + 170 U. S. Sieve Size				
0	43.03	0.000000	-	-
15	46.41	0.033613	1.998	2.235
60	NA[a]	-	-	-
120	50.67	0.078690	6.721	5.260
239	56.34	0.143925	7.146	9.695
-170 U. S. Sieve Size				
0	60.06	-	-	-
15	52.59	0.000000	-	-
60	55.80	0.041513	19.434	0.918
120	NA	-	-	-
239	56.34	0.048726	65.788	1.078

[a] NA = Not available.

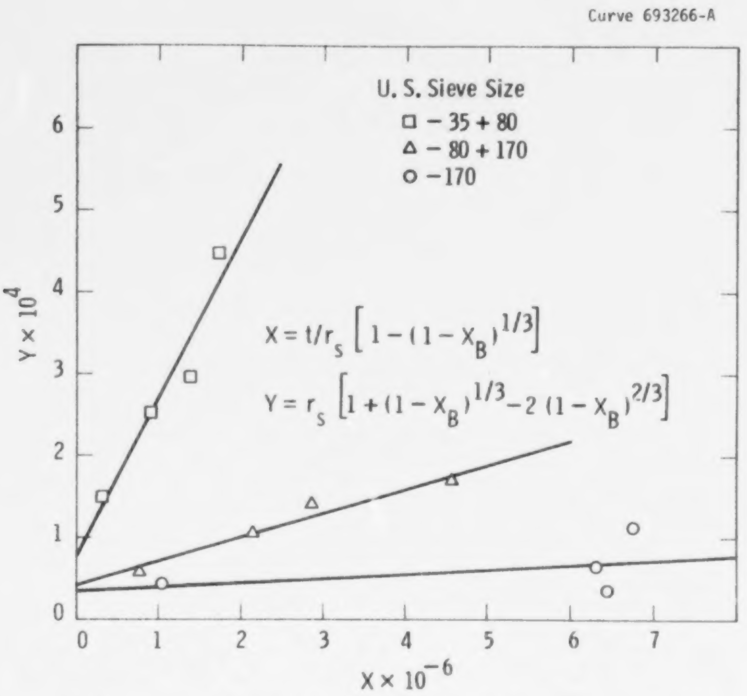

Figure D-14 - Dry Sulfation of CAFB-9 Regenerator Stone in a Fluidized Bed at 450°C

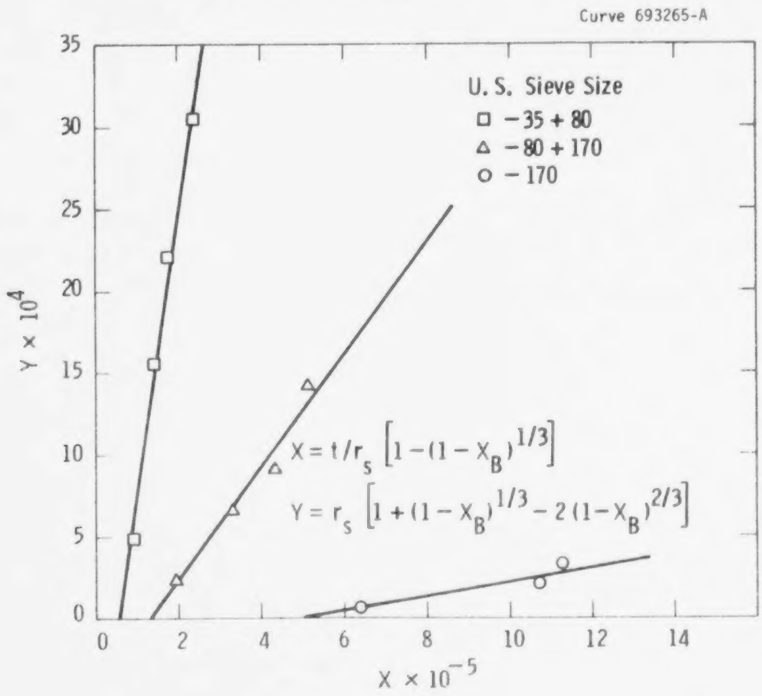

Figure D-15 - Dry Sulfation of CAFB-9 Regenerator Stone in a Fluidized Bed at 750°C

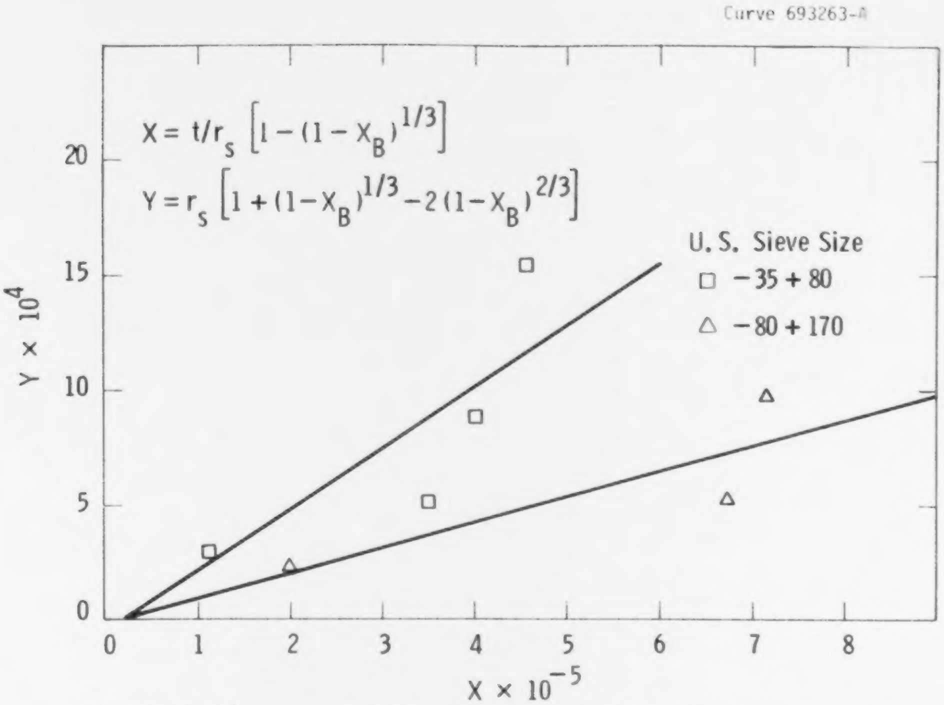

Figure D-16 - Dry Sulfation of CAFB-9 Regenerator Stone in a Fluidized Bed at 850°C

Figure D-17 shows that the -177 + 88 μm fraction had a broader distribution of pore diameters than did the other two fractions inspected. From Table D-15 the total pore volume in the fresh feed can be related to the arithmetic average particle diameter by the equation:

$$V_p = 2.63\ D^{-1/2}$$

where V_p is in cm^3/g and D is in μm. This suggests that smaller particles as obtained by grinding are more porous, and presumably their calcium content can be more fully utilized.

With respect to the distribution of the intraparticle pore volume, the 50 percent points are at 0.50, 0.16, and 0.85 μm for the three fractions in decreasing order of particle size. Thus, the intermediate size fraction (-177 + 88 μm) had fewer of the larger pores than did the other two sizes and might, therefore, be expected to be less reactive because of a less open structure. Opposed to this is the fact that its total

Table D-14

CONSTANTS IN THE LINEARIZED CORRELATION OF CONVERSION VS REACTION TIME IN THE DRY SULFATION OF CAFB-9 REGENERATOR STONE

Constant	U. S. Sieve Size		
	-35 + 80	-80 + 170	-170
Phase I - 450°C			
A	7.898E-05	4.071E-05	3.568E-05
B	1.935E-10	2.962E-11	5.429E-10
Phase II - 750°C			
A	-9.691E-04	-4.723E-04	-2.239E-04
B	1.717E-08	3.466E-09	4.515E-10
Phase III - 850°C			
A	-5.124E-05	-1.612E-05	NA[a]
B	2.660E-09	1.114E-09	NA

[a] NA = Not available.

pore volume was twice that of the -500 + 177 μm fraction. Table D-13 shows that a somewhat higher degree of sulfation was obtained with the -177 + 88 μm fraction than with the -500 + 177 μm, but there is a suggestion that even more sulfation was obtained with the -88 μm fraction. Thus, the initial distribution of pore volumes does not appear to be a predictor of the degree of sulfation.

Figure D-18 shows the effect of dry sulfation on the -500 + 177 μm fraction. Phase I yielded a product with about 10 percent less pore volume. This was reduced by 50 percent in Phase II, but further sulfation in Phase III from 40 to 50 wt % $CaSO_4$ was not accompanied by a further change in pore volume. Table D-16 shows how the distribution of pore volume was affected by sulfation. Pores larger than 0.4 μm in the -500 + 177 μm fraction were essentially eliminated, while volume due to smaller pores was roughly unchanged.

Figure D-19, however, shows Phase I sulfation reduced pore volume for the -177 + 88 μm fraction by 50 percent in going from 5 to 10 wt %

Table D-15

POROSITY AND PARTICLE DENSITY OF SAMPLES FROM CAFB-905

Sample No.	Identification	U. S. Sieve Size	Pore Volume, cm^3/g	Wt % $CaSO_4$	Calculated Density, g/cm^3
176B	Reactor Feed	-500 + 177 μm	0.1358	5.37	2.278
176C		-177 + 88	0.2443	5.16	1.827
176D		-88	0.3887	5.58	1.445
186B	Product I	-500 + 177 μm	0.1203	11.01	2.350
186C		-177 + 88	0.1316	10.59	2.890
186D		-88	NA[a]	16.08	NA
196B	Product II	-500 + 177 μm	0.0688	42.02	2.595
196C		-177 + 88	0.0717	45.76	2.566
196D		-88	NA	NA	NA
200B	Feed III	-500 + 177 μm	0.0571	41.21	2.678
200C		-177 + 88	0.0502	43.03	2.724
200D		-88	NA	60.06	NA
204B	Product III	-500 + 177 μm	0.0689	50.26	2.576
204C		-177 + 88	0.0413	56.34	2.754
204D		-88	NA	NA	NA

[a] NA = Not available.

$CaSO_4$. Phase II reduced pore volume by another 50 percent as for the -500 + 177 μm fraction. Phase III reduced it again in half, contrary to the behavior of the -500 + 177 μm fraction. Table D-13 shows pore volume was reduced by 80 to 85 percent in all pore diameter ranges. Unfortunately, sample sizes available for the -88 μm fraction were too small to permit pore volume measurements. These results show that in large particles (-500 + 177 μm) the large pores are nearly completely utilized in preference to small pores, whereas in small particles all pores are utilized to about the same degree. The manner in which the BET surface area changes during sulfation appears inconsistent with loss of pore volume. This point needs further study.

Table D-16

EFFECT OF DRY SULFATION ON THE DISTRIBUTION OF PORE VOLUME, cc/g

Pore Diameter, µm	Feed	Products Phase I	Products Phase II	Products Phase III
-500 + 177 µm Fraction				
Above 0.4	0.08498	0.08131	0.03389	0.00253
0.04 to 0.4	0.02852	0.02302	0.01160	0.03132
Below 0.04	0.02235	0.01598	0.02330	0.03481
Total	0.13585	0.12031	0.06879	0.06866
-177 + 88 µm Fraction				
Above 0.4	0.06856	0.08958	0.00962	0.01261
0.04 to 0.4	0.08099	0.01917	0.03248	0.01151
Below 0.04	0.09479	0.02287	0.02964	0.01718
Total	0.24434	0.13162	0.07174	0.04130

Table D-17

AVERAGE PARTICLE DENSITY OF SAMPLES FROM CAFB-905

Particle	U. S. Sieve Size -35 + 80	U. S. Sieve Size -80 + 170	U. S. Sieve Size -170
Average particle radius, µm	169.25	66.25	22.00
Particle density			
Phase I - 450°C	2.314	2.058	1.842
Phase II - 750°C	2.472	2.428	2.388
Phase III - 850°C	2.622	2.739	2.762

Particle densities were calculated from the pore volume data summarized in Table D-15 and plotted on Figure D-20. Finally, average particle densities for each phase of the experiment were calculated as in Table D-17. For these calculations the density of $CaSO_4$ and CaO were taken as 2.96 and 3.32, respectively.

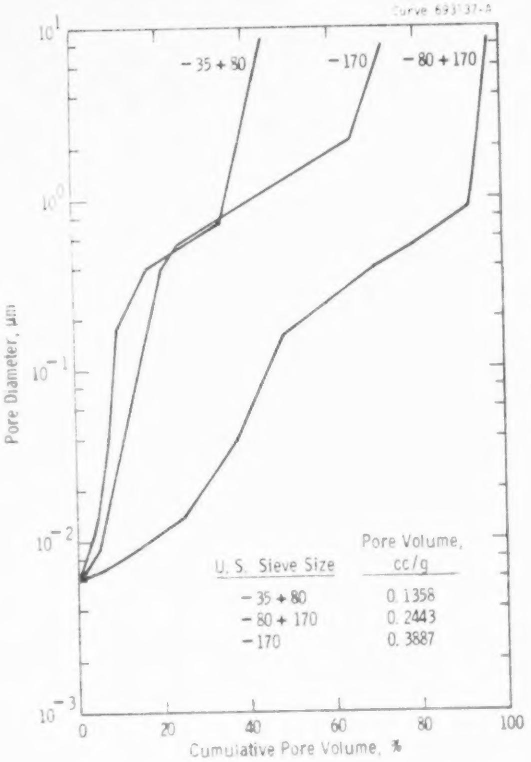

Figure D-17 - Distribution of Pore Volumes in CAFB-905 Sample Phase I Feed

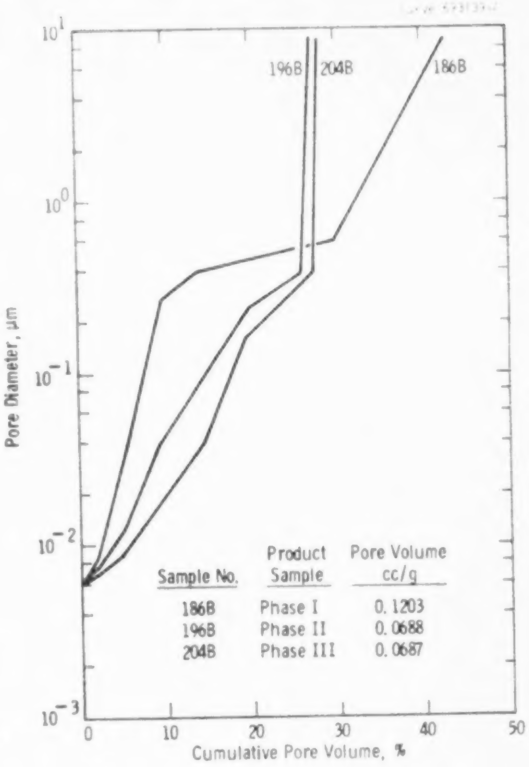

Figure D-18 - Distribution of Pore Volumes in CAFB-905 Product Samples, -35 + 80 U. S. Sieve Size Fraction

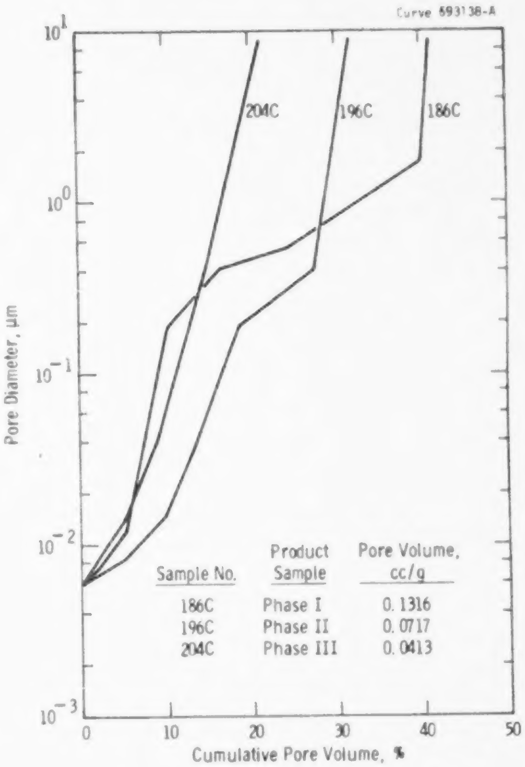

Figure D-19 - Distribution of Pore Volumes in CAFB-905 Product Samples, -80 + 177 U.S. Sieve Size Fraction

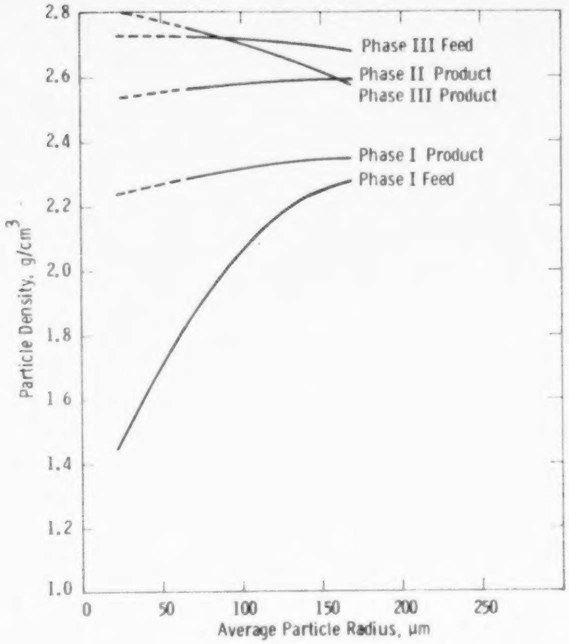

Fig. D-20 - Particle Density of Samples from Dry Sulfation of CAFB-9 Regenerator Stone

Diffusion coefficients were calculated for Phases II and III by using M_B = 56.08 and $(C_A)_b$ = 5 percent, corrected to temperature. Comparable values for Phase I could not be calculated because the graphs had positive instead of negative Y-intercepts. This might mean that diffusion was not controlling at low conversions. The results are in Table D-18 from which the following statements with respect to the effect of temperature may be made:

- Increasing the temperature from 750°C to 850°C increases k, the reaction rate constant, for -500 + 177 μm particles by a factor of greater than 3 versus nearly 12 for the -177 + 88 μm fraction.
- Increasing the temperature as above reduces D_e, the diffusion coefficient per particle, by a factor of 5.5 for the -500 + 177 μm versus 2.5 for the -177 + 88 μm fraction.

Thus, increasing temperature to at least 850°C is favorable in that the reaction rate is increased, but the effect of temperature on the diffusion

Table D-18

PARAMETERS FOR DRY SULFATION OF CAFB-9

Parameters	U. S. Sieve Size		
	-35 + 80	-80 + 170	-170
Phase II			
D_e, cm^2/min/particle[b]	2.118E-04	4.199E-05	5.380E-06
k, cm/min/particle	1.311	0.533	0.144
Phase III			
D_e, cm^2/min/particle	3.819E-05	1.671E-05	NA[a]
k, cm/min/particle	4.472	6.223	NA
Activation Energy			
Q_D, cal/g mole	-39,200	-21,100	NA
ΔH, cal/g mole	28,000	56,100	NA

[a] NA = Not available.

[b] The dimensions used are intended to remind the reader that the theory was derived for a single particle, while the observations were made on a bed of particles, thus requiring the assumption that every particle was exposed to the same average conditions.

coefficient may be obscured by the different sulfation levels in Phases II and III.

Additional insight can be obtained by calculating activation energies: Q_D for D_e and ΔH for k in accord with the equations

$$\ln = \frac{k_2}{k_1} = -\frac{\Delta H}{R}\left(\frac{1}{T_2} - \frac{1}{T_1}\right) \tag{1}$$

and

$$\ln \frac{(D_e)_2}{(D_e)_1} = \ln \frac{T_1}{T_2} - \frac{Q_D}{R}\left(\frac{1}{T_2} - \frac{1}{T_1}\right) . \tag{2}$$

The latter is derived from Barrer and includes consideration of entropy of activation. As shown in Table D-18, the activation energies for k

Table D-19

CALCULATION OF BULK VALUES OF PARAMETERS

	Size Fraction		
	-35 + 80	-80 + 170	-170
Size Range, μm	-500 + 177	-177 + 88	-88
Average Radius, μm	169.25	66.25	22.00
Particle Density, g/cm^3			
Phase II	2.472	2.428	2.388
Phase III	2.622	2.739	2.762
N, Particles/g			
Phase II	1.9919E+04	3.3815E+05	9.3888E+06
Phase III	1.8780E+04	2.9975E+05	8.1174E+06
Reaction Rate, kN, cm/min/g			
Phase II	2.611E+04	1.802E+05	1.352E+06
Phase III	8.398E+04	1.865E+06	NA[a]
Diffusion Rate, D_eN, cm^2/min/g			
Phase II	4.218	14.199	50.512
Phase III	0.717	5.009	NA

[a] NA = Not applicable.

appear reasonable but suggest that grinding the spent sorbent is not desirable since the smaller particles have a higher activation energy. This higher energy may also aid in the unfavorable changes, such as modification of pore structure. The Q_D values are negative, reflecting the decrease in D_e with increase in temperature, possibly coupled with the increase in degree of sulfation.

The role of particle size is further clarified in Table D-19, in which the parameters are calculated per gram of sorbent. Grinding to smaller sizes increases the reaction rate per gram of sorbent nearly two orders of magnitude in both phases. This also increases the diffusion coefficient. We conclude that grinding to at least -177 μm is advantageous.

- A peak surface area appears at the completion of calcination, followed by a sharp decrease in surface area on continued calcination. This change is essentially complete, irrespective of the size, when the calcination is continued for about four hours.
- The effect of particle size is noticeable only at the early stage of calcination prior to the completion of decomposition.

The results indicate two competing mechanisms during calcination. A loss of CO_2 increases the area while continued exposure at high temperature decreases it. Surface area can be increased by increasing the number of particles/g or by creating more pores or larger pores within each particle.

Table E-1

WEIGHT LOSS OF LIMESTONE 1359 DURING CALCINATION AT 1070°C

U. S. Mesh Size	Particle Diameter, μm	Weight Loss (%) at 1070°C	
		After 1 hr	After 2 hr
-6 + 10	-3360 + 2000	12.7	43.5
-30 + 40	-595 + 420	43.3	42.8
-140 + 200	-105 + 74	42.9	43.5

Theoretical weight loss = [illegible]4 percent.

Table E-2

BET SURFACE AREA OF LIMESTONE 1359, m^2/g

Particle Diameter, μm	Calcination Time at 1070°C, hr						
	0	1	2	4	9	17	32
3360 - 2000	0.09	2.29	5.91	1.64	1.07	0.80	0.79
595 - 420	0.23	5.19	5.07	1.38	1.12	0.87	0.88
105 - 74	0.81	6.47	4.42	1.58	1.16	0.98	0.92

Curve [illegible]

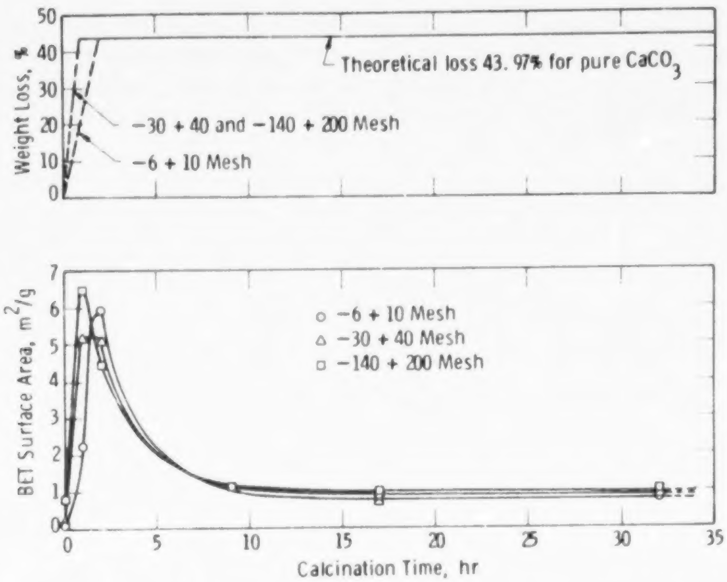

Figure E-1 - Effect of Calcination Time at 1070°C on the Surface Area of Limestone 1359

Curve 697255-A

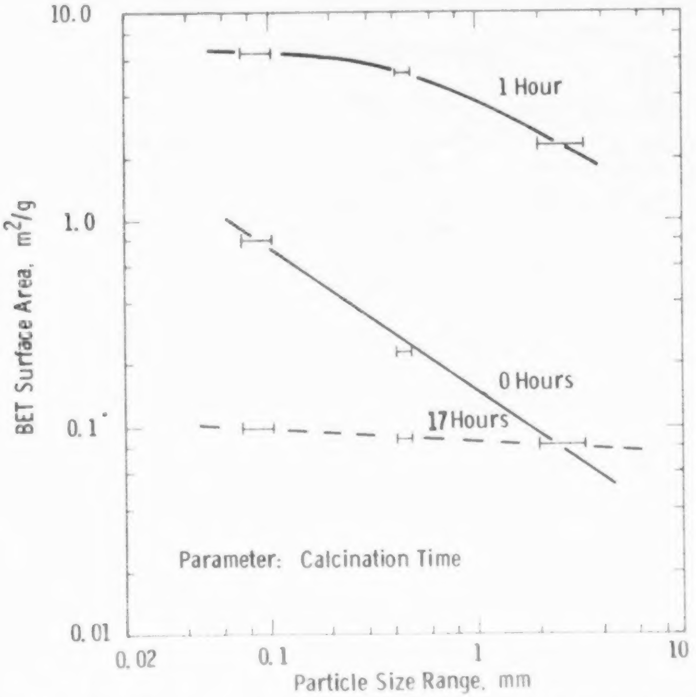

Figure E-2 - BET Surface Area of Limestone 1359 Calcined at 1070°C

REFERENCES

1. Keairns, D. L., et al., Fluidized Bed Combustion Process Evaluation, Phase 1 - Residual Oil Gasification/Desulfurization Demonstration at Atmospheric Pressure, Vols. I and II, Report to EPA, Westinghouse Research Laboratories, Pittsburgh, PA, March 1975, EPA 650/2-75-027 a and b, NTIS PB 241-834 and 241-835.

2. Smith, J. M., Chemical Engineering Kinetics, New York: McGraw-Hill Book Co.; Ch. 2, 14.

3. Jost, W., Diffusion in Solids, Liquids and Gases, New York: Academic Press, Inc.; 1952, Ch. VII.

APPENDIX E

PORE VOLUME STUDIES

In support of the dry sulfation and the dead-burning studies, parallel work on pore volumes and surface areas of Limestone 1359 and CAFB regenerator stone was carried out. The upper limit on processing temperature for the CAFB stone might be taken as that at which thermal decomposition of the $CaSO_4$ it contains occurs. If the SO_2 released can be recycled to the gasifier or to a sulfur recovery plant, then the upper limit might be set higher by other considerations, such as process economics. The lower limit is set by the rate of reaction, either for SO_2/O_2 pickup or for migration of the constituents of the crystal lattices leading to inactivation. Either limit may be modified from that for pure $CaSO_4$ by the presence of other elements in the matrix.

Initial studies used three size fractions of Limestone 1359: -3360 + 2000, -595 + 420, and -105 + 74 μm. Approximately 10 g of each fraction was placed in an alumina boat covered with platinum foil. The boat was inserted in a furnace heated to 1070°C in air. The samples were held at that temperature for 1, 2, 9, 17, and 32 hours, then quickly cooled, and placed in a desiccator. Surface areas were measured by BET using nitrogen as the absorbed gas. Similar measurements were made on the as-received powder. The data are presented in Tables E-1 and E-2 and Figure E-1 along with weight loss measurements.

The following observations can be made from the table and the figure.

- The calcination is accompanied by an increase in surface area as the decrease in weight proceeds to the theoretical value of 44 percent.
- For each size fraction, calcination is complete in about one to two hours as determined by weight loss data. The large particles take nearly twice as long for complete calcination as do the small particles, which is reflected both in weight loss and BET surface area data.

The absolute values of surface area are uncertain due to possible reabsorption of moisture and CO_2 after calcination, yet the data seem to support the view that some process resulting in reduction of surface area is occurring along with the calcination. This is probably the well-known dead-burning process, but what is also of interest here is how long do the particles continue to have a reasonable surface area, and does this reflect directly on the capacity of the stone to absorb SO_2? The calcination is extended to 32 hours because preliminary design work on the dry sulfation system indicated that a retention time in the absorber of at least 20 hours would be required.

Figure E-2, plotted from Table E-2, shows that the surface area for the uncalcined stone is nearly a straight line with a slope of -0.693. To evaluate the reasonableness of this result, consider dividing a spherical particle of diameter d_0 into n spherical particles, all of diameter d_1. The number of particles is the ratio of volumes:

$$n = \frac{1}{6} \pi d_0{}^3 / \frac{1}{6} \pi d_1^3 \quad \text{or} \quad d_0^3/d_1^3 \quad . \tag{1}$$

The ratio of the external spherical surfaces is

$$S_1/S_0 = \pi d_1^2 n / \pi d_0^2 = d_0/d_1 \quad . \tag{2}$$

The total BET area found may be taken as the sum of the external spherical surface (S_0 or S_1) and the internal surface of the pores in the particles: $(Si)_0$ or $(Si)_1$. Thus,

$$BET = S_1 + (Si)_1 \quad . \tag{3}$$

Now, if $S_1 >> (Si)_1$, then the BET will vary inversely as d_1 and the log-log plot will have a slope of -1. If $(Si)_1 >> S_1$, then a slope of -1 means Si varies the same way as S_1: inversely with d_1. Since the slope obtained is less than 1 (in absolute value), the internal surface area must vary as a smaller power of particle diameter, regardless of the relative magnitudes of S_1 and $(Si)_1$.

After 17 hours of calcination, the exponent on diameter dropped to -0.0608, meaning that the residual BET area was then nearly independent of particle diameter.

After one hour of calcination, the BET area increased at all three particle diameters. For small particles, the BET area had already attained the limiting condition of independence of diameter.

PORE VOLUME STUDIES ON LIMESTONE

We sought further information by measuring pore volumes of four of the calcined limestone samples. The data we obtained are summarized in Tables E-3 and E-4. The apparatus used was a Micromeritics Instrument Corporation Model 900 Series Mercury Penetration Porosimeter. We determined pore volumes by forcing liquid mercury at ambient temperature into the sample at pressures in the range 0.9 to 30,000 psia. Pore diameters are calculated from the surface tension formula if one assumes the surface tension of mercury to be 474 dynes/cm and the contact angle to be 130°.

An existing computer program was modified to produce Figures E-3 through E-10. One modification normalized the pore volume data by dividing each value by the largest value found. A second generated differential normalized volume curves by plotting the incremental volume between successive measurements against the arithmetic average of the corresponding pore diameters.

Both size fractions showed significant pore volumes in the range 0.02 to 0.2 µm: 0.0568 (50% of 0.1136) versus 0.1746 (19% of 0.9191) cc/g for the 1-hour samples 92-1 and 94-1, respectively. Peak volumes in these ranges occurred at 0.08 and 0.15 µm, respectively. At 32 hours, pores in this diameter range are absent.

Samples 92-1 and 93-1 have lower total pore volumes than the other two samples. This difference is in line with BET surface area measurements reported previously, showing that calcination of large particles of limestone was not completed under the conditions used in one hour.

All of the samples show that a significant fraction of the total volume (10 to 15 percent) occurs in the average diameter range of 8 to

Table E-3

PORE VOLUME DATA ON LIMESTONE SAMPLES CALCINED AT 1070°C

Sample No.	U. S. Mesh Size	Calcination Time, hr	Total Pore Volume, cc/g	Pore Volume below 8 μm, cc/g[a]
92-1	-6 + 10	1	0.1136	0.0772
93-1	-6 + 10	32	0.3336	0.2669
94-1	-140 + 200	1	0.9191	0.4044
95-1	-140 + 200	32	0.8283	0.3893

[a] Discussed later in text.

Table E-4

DISTRIBUTION OF SIGNIFICANT CONTRIBUTIONS TO INTRAPARTICLE PORE VOLUME

Sample No.	Contributions to Intraparticle Pore Volume		Location of Significant Contributions	
	Average Pore Diameter Range, μm	% of Total Volume in This Range[a]	% of Total Volume[b]	Pore Diameter, μm
92-1	0.02 - 0.2	50	8.0	0.09
93-1	0.3 - 2.0	73	6.0	1.1
94-1	0.02 - 0.2	19	6.0	0.15
	1.0 - 8.0	14	2.9	7.0
			2.0	4.0
			2.0	2.2
			1.9	1.5
			1.8	1.2
95-1	0.3 - 1.8	24	7.0	8.0
	1.8 - 6	11	4.0	3.0
			3.0	5.0

[a] Total volume is cumulative normalized volume, including interparticle voids

[b] Refers to the ordinate on a plot of differential normalized volume versus average pore diameter.

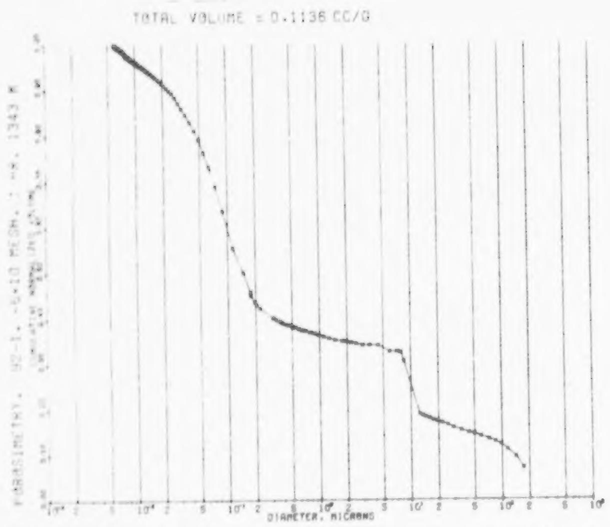

Figure E-3 - Cumulative Pore Volume for Calcined Limestone 1359 (See ordinate for calcination conditions)

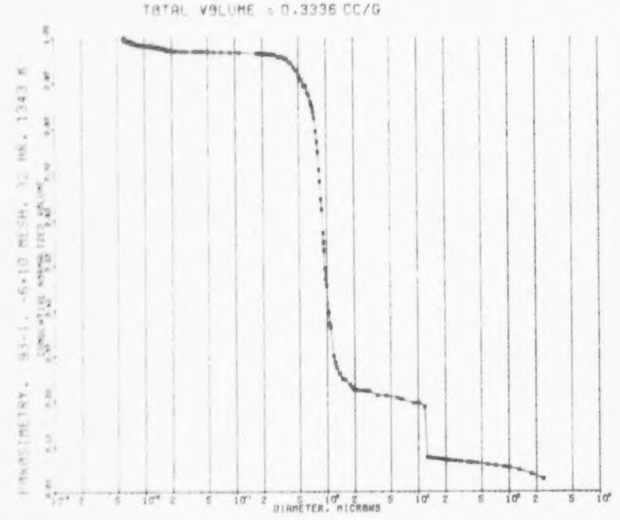

Figure E-4 - Differential Pore Volume for Calcined Limestone 1359 (See ordinate for calcination conditions)

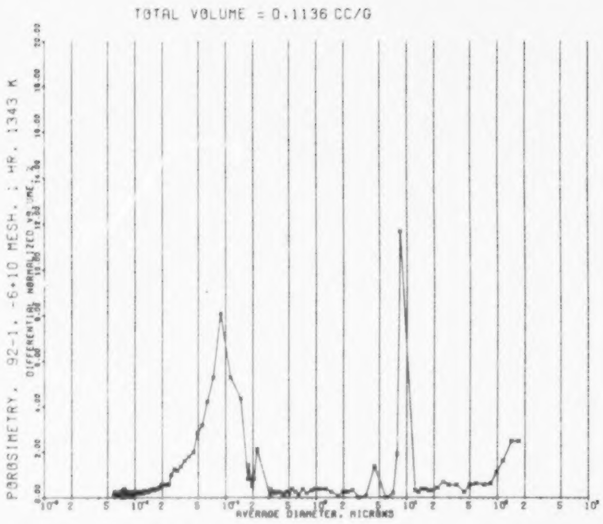

Figure E-5 - Differential Pore Volume for Calcined Limestone 1359 (See ordinate for calcination conditions)

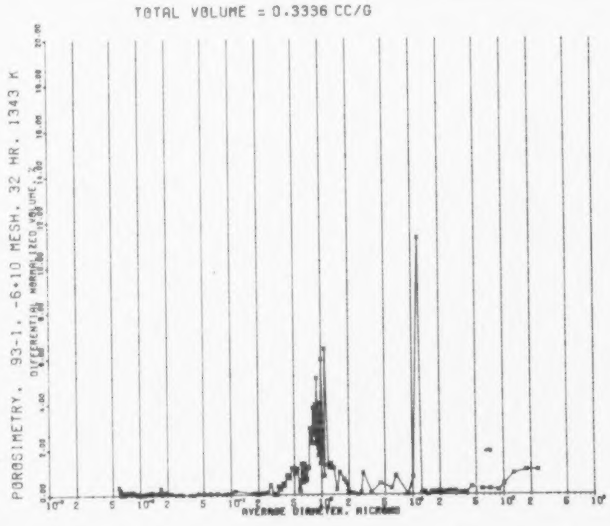

Figure E-6 - Differential Pore Volume for Calcined Limestone 1359 (See ordinate for calcination conditions)

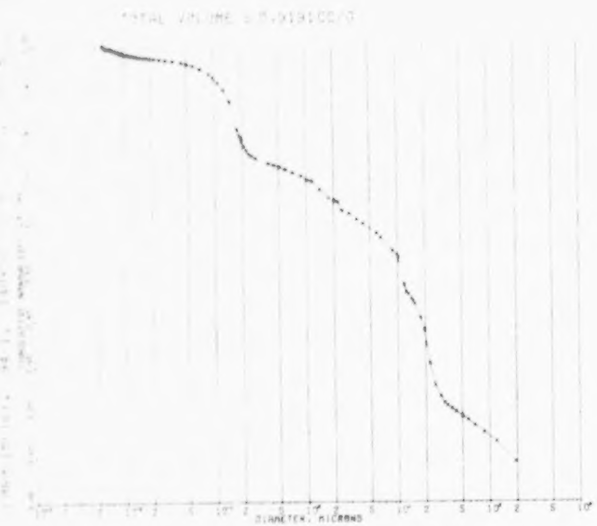

Figure E-7 - Cumulative Pore Volume for Calcined Limestone 1359 (See ordinate for calcination conditions)

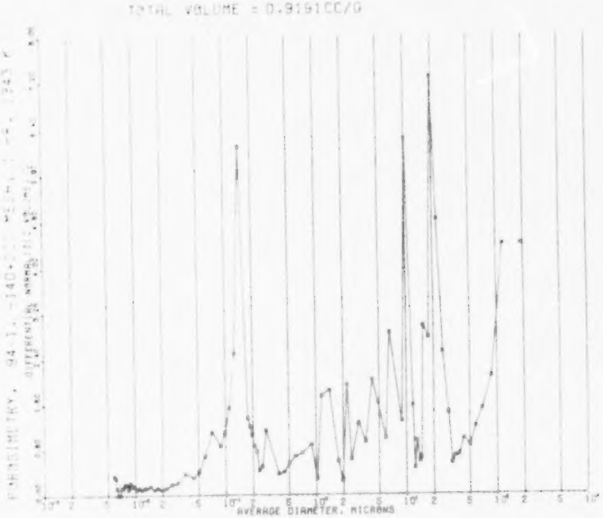

Figure E-9 - Differential Pore Volume for Calcined Limestone 1359 (See ordinate for calci ation conditions)

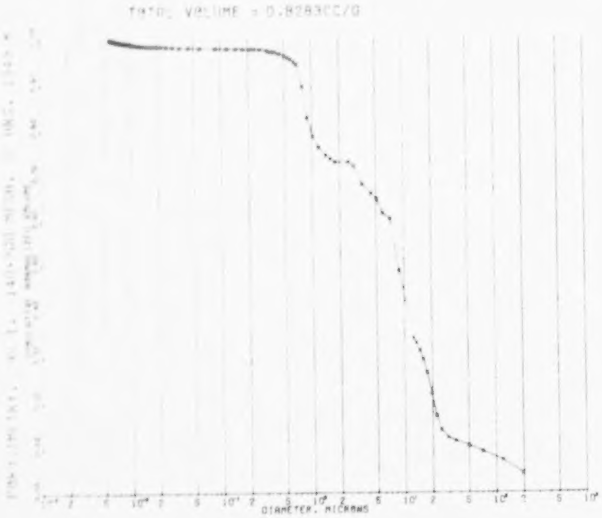

Figure E-8 - Differential Pore Volume for Calcined Limestone 1359 (See ordinate for calcination conditions)

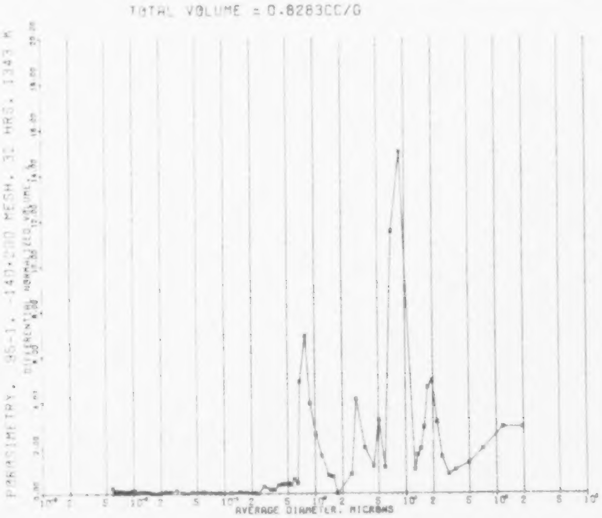

PAI

Figure E-10 - Differential Pore Volume for Calcined Limestone 1359 (See ordinate for calcination conditions)

20 μm. This is considered to be volume between the particles. The value of 8 μm as the largest intraparticle pore is obtained by further analyses described below.

Samples with smaller particle sizes (-105 + 74 μm) have higher total pore volumes and higher intraparticle pore volumes than the samples with larger particle sizes (-3360 + 2000 μm). This finding is in contrast with the nearly equal surface area recorded for these samples, allowing for the time lag for the larger particles.

The data support the conclusion that short-time calcination develops significant pore volume in the 0.02 to 0.2 μm pore diameter range, whereas exposure to 107[illegible]C for more than 2 to 4 hours essentially eliminates these pores. Pore volume also develops in the 0.5 to 2.0 μm size range. It is likely that these have consolidated from the smaller pores found initially.

ANALYSIS OF PORE DATA BY MODEL

To examine these data more intensively, a model was developed from which the number distribution of pores, the pore surface area, the pore mouth area, and the pore volume could be estimated. Development of the model is given at the end of this section in an addendum.

Pores are present in the sorbents in a variety of sizes and configurations. The purpose of a model is to provide a simplified way of describing the essential relationships among the variables involved. Klinkenberg[E1] proposed straight cylindrical, not interconnected, capillaries but concluded that pore sizes in sandstone calculated from miscible displacement data were smaller than those obtained by mercury porosimetry. Dullien and Azzam[E2] proposed modifying this model to a network of cylindrical capillaries with step changes in diameters. Their model would require information on the sum of the lengths of the necks and bulges in the capillaries, an effective length of the capillaries, and the radii of the necks and bulges.

Instead of such a model we took a more direct approach. The pores are visualized as right circular cones with their apices at the center of spherical particles and their mouths on the spherical surfaces of the particles. Such a structure might permit application of a single factor, derived from experimental data, to yield an effective surface area.

Three physical characteristics of the pores are of interest: pore volume, pore surface area, and pore mouth area. The primary data required are the particle diameter, the porosimetry data, and the particle density. The porosimetry data are in the form of cumulative volume of mercury added to the sample versus pressure, from which a distribution of pore diameters versus pore volume can be calculated. The model developed permits estimation of the number distribution of pores by pore diameter, permitting, in turn, calculation of the three quantities of interest as distributions by pore diameter.

Number of Pores/Particle

The number of pores per particle in the ith pore diameter interval is given by

$$(N_p)_i = 4f_i(\rho V_T)\left(\frac{d}{d_p}\right)_i^2 \frac{1}{\left[1-\left(\frac{d_p}{d}\right)_i^2\right]^{1/2}} \qquad (4)$$

where

f_i = the fraction of the pore volume in the i^{th} pore diameter interval

ρ = the particle density, g/cm^3

V_T = the total measured pore volume, cm^3/g

d = the particle diameter, μm

$(d_p)_i$ = the average pore diameter for the i^{th} interval, μm.

The data for the fine powder (-105 + 74 μm) were used to calculate $(N_p)_i$. The results are plotted in Figure E-11. We found that the number of pores in each pore diameter interval increased at an accelerating rate as the pore diameter decreased. This behavior continued down to the smallest diameter measurable, corresponding to the maximum pressure of 206.8 MPa (30,000 psi) attainable in the porosimeter. Consequently, the absolute total number of pores cannot be inferred from these data.

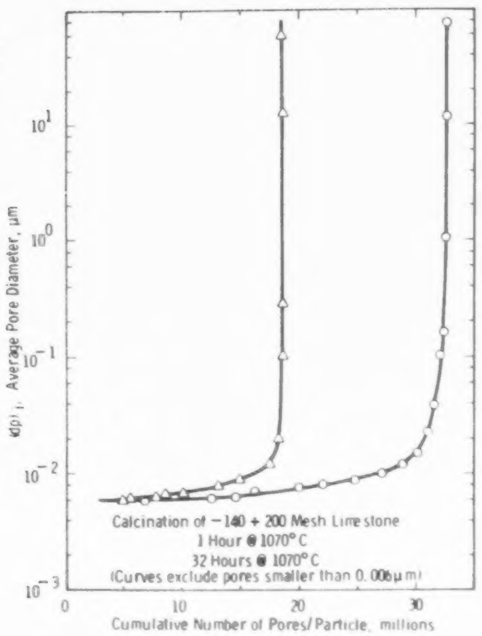

Figure E-11 - Effect of Calcination Time on Number of Pores/Particle

There is a further problem in interpreting the results. The porosimeter measures all voids as pores, whether they are inside the particles or between them. The former are the pores of interest in this investigation and are referred to as internal pores or simply as pores. The latter are called interparticle pores where it is necessary to discuss them.

To determine how much of the "pore" volume obtained was in internal pores, the data were cumulated from the lower end of the pore diameter range, as shown in Figure E-11. Calcination for 32 hours reduces the total number of "pores" from 32.6 million to 18.7 million/particle. It is evident that above a certain pore diameter, there is no significant increase in the number of pores in either case. For both samples, about 85 percent of the total "pores" are below about 0.01 µm in diameter. The distribution of pores, however, is apparently different from the two samples, since when the pore diameter is increased the 99 percent level is reached at 0.025 μm for 32 hours of calcination but not until 0.2 μm for 1 hour of calcination.

Pore Mouth Area/Particle

If the area of the pore mouth for each diameter interval is multiplied by the number of pores in that interval and the results cumulated, again from the lower end of the diameter range, the total will be limited by the spherical surface area of the particle. Figures E-12 and E-13 show the results of this calculation. First, note that the end points are very nearly the same: 5.02×10^{-8} for calcination for 1 hour versus 5.35×10^{-8} m^2 for 32 hours of calcination. Second, the curves do not differ much until one considers diameters smaller than about 1 μm. In the range of 0.15 to 0.5 μm, as is more clearly shown in Figure E-13, the pore mouth area is nearly an order of magnitude higher for particles calcined for 1 hour compared to those calcined for 32 hours. Extended calcination apparently results in a loss of pore mouth area in this range of diameters. This decreases the probability that a gas molecule striking the particle will find itself at a pore mouth and, therefore, in a position to continue into the particle.

The limits shown on Figure E-12 are from Table E-5, giving the particle characteristics. It may be a coincidence, but the curves of Figure E-12 cross at the theoretical value for spherical surface/particle of 2.38×10^{-8} m^2. Since the pore diameter at this point is about 6 μm, larger pores are concluded to be outside the particles and are, therefore, interparticle pores. Compare this conclusion with deductions from the volume fraction of pores as summarized in Table E-6. Both approaches yield about the same limit. These calculations say in effect that, if the pore volume/particle approached the particle volume estimated on the basis of spherical particles, the maximum pore diameter to be considered as an internal pore corresponds to that for which the cumulative pore volume equals the particle volume. This pore diameter is identified

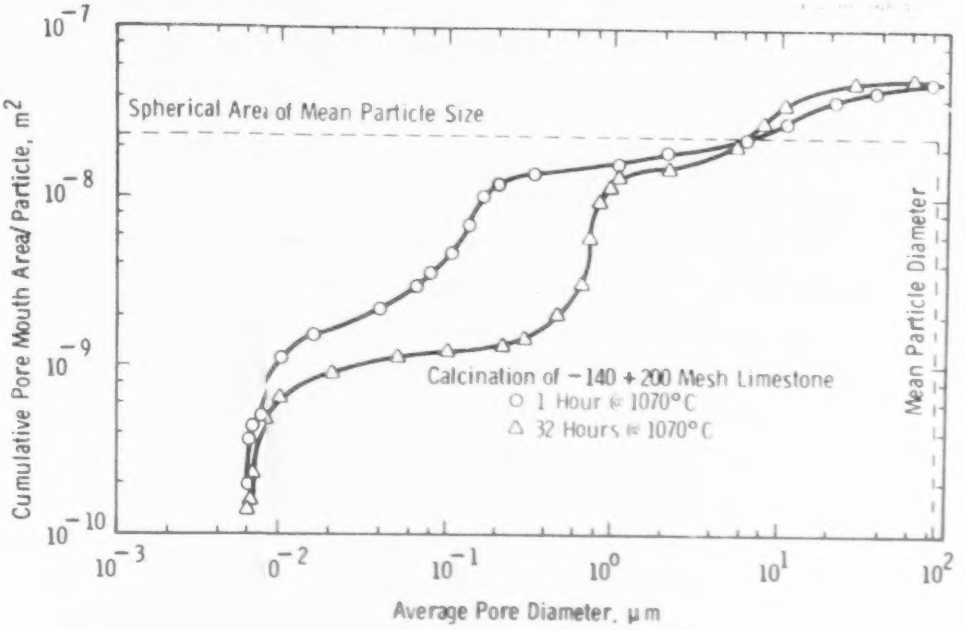

Figure E-12 - Effect of Calcination Time on Pore Mouth Area/Particle

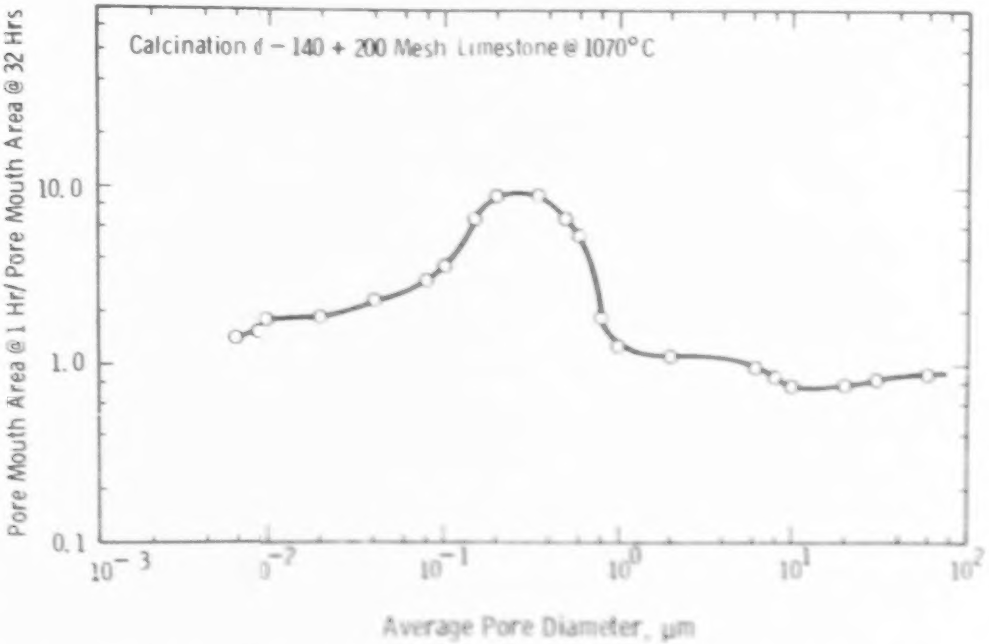

Figure E-13 - Effect of Calcination Time on Pore Mouth Area Ratio

Table E-5

SUMMARY OF CHARACTERISTICS OF -140 + 200 MESH SPHERICAL PARTICLES

Particle diameter, μm	
Range	74 to 105
Harmonic mean	86.8
Surface area/particle, m^2	2.36695×10^{-8}
Volume/particle, cm^3	3.42419×10^{-7}
Particle density, g/cm^3	2.6
Particle volume, cm^3/g	3.84615×10^{-1}
Mass of one particle, g	8.90289×10^{-7}
Number of particles/g	1.12323×10^{6}

Table E-6

ESTIMATE OF MAXIMUM AVERAGE INTERNAL PORE DIAMETER FOR CALCINED LIMESTONE 1359

Sample Identification		
Number	94-1	95-1
Mesh size	-140 + 200	-140 + 200
Calcination time at 1070°C	1 hour	32 hours
Measured total "pore" volume, cm^3/g	0.9191	0.8283
Calculated no. of spherical particles/g	1.123×10^{6}	1.123×10^{6}
"Pore" volume/particle, cm^3	8.133×10^{-7}	7.374×10^{-7}
Volume of spherical particle, cm^3	3.424×10^{-7}	3.424×10^{-7}
Particle volume/"pore" volume	0.4185	0.4643
Average pore diameter, μm	7.69	9.59

from the original data as that corresponding to the fraction in Table E-6 labeled particle volume/pore volume. This approach yields about the same limits as Figure E-12.

In summary, the pores may be considered intraparticle pores if their average diameters are less than 8 ± 2 μm, based on the criteria that the pore mouth area does not exceed the spherical surface area of the particle and the pore volume does not exceed the particle volume. The number of pores, however, is essentially negligible down to about 0.2 μm for even short-term calcination.

Surface Area/Gram

The calculated pore surface areas are shown in Figure E-14. After 1 hour of calcination, the particles show a total area of 30.4 m^2/g. Calcining for 32 hours reduces this to 13.7 m^2/g. Of the total area, in each case 84 percent is in pores smaller than about 0.13 μm. An additional 12 percent occurs in the range of 0.4 to 2.0 μm for the 32-hour calcination, while the 1-hour case shows a continuous increase in area amounting to an additional 15 percent in the interval from 0.13 to 2.0 μm.

The surface areas calculated from the model may be compared with measured values (Table E-7). Values derived from porosimetry are also given. The surface area changes inferred from mercury porosimetry are

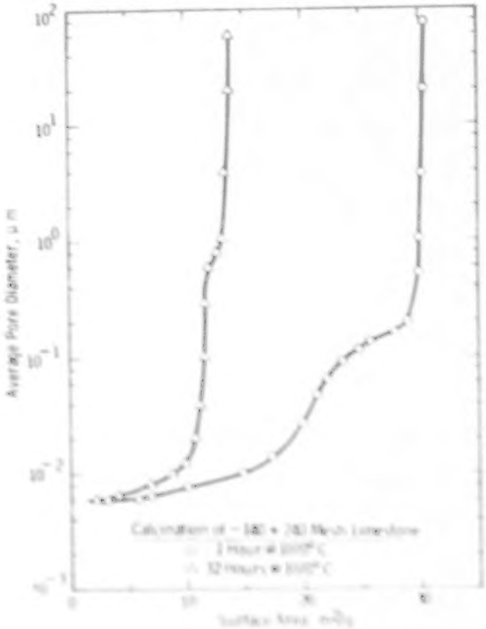

Figure E-14 - Effect of Calcination Time on Total Surface Area/Gram

Table E-7

SURFACE AREAS OF LIMESTONE 1359

Sample Number	94-1	95-1
Calcination time at 1070°C	1 hour	32 hours
Calculated area, m^2/g		
Below 8 μm	30.3	13.7
Below 0.2 μm	28.7	11.6
50% point	0.0105 μm	0.00802 μm
Measured area, m^2/g		
Total by BET	6.47	0.92
Below 8.8 μm by porosimetry	19.8	8.1
Reduction in area		
By BET	---	85.8%
By porosimetry	---	59.1%
By model	---	54.8%

in good agreement with those predicted by the model. The BET values, however, show a much larger reduction. These values may be low due to a decrease in the absorptive power of CaO for nitrogen after calcination Another possibility is that the model overestimates the surface area since not all of the pores extend deeply into the particles.

If C is the fraction of altitude of the conical pore measured from the apex, then the surface area for a given pore varies as C^2, and the volume of the pore varies as C^1. If C is 25 percent of the cone altitude, meaning the pore extends from the surface of the particle to 75 percent of a particle radius of the center, then truncating this much of the cone reduces the surface area by only 6.25 percent and the volume by 1.56 percent. Clearly, the reduction in calculated area would have to come from a substantial adjustment in the model near the surface of the particle. If the pores were more compact than a cone, the calculated surface area for a given pore volume would be decreased. If, for example, the volume attributed to one conical pore were assigned to a cylindrical pore, the ratio of surface areas would be

$$\frac{S_c}{S_p} = \frac{2}{3}\left[1 - \left(\frac{d_p}{d}\right)^2\right]^{1/2} + \frac{d_p}{d} ,$$

which for 0.1 μm pores in 100 μm particles is about 2/3. One may conclude that a significant number of the pores are more cylindrical than conical, but elaboration of the model to reflect this finding is outside the scope of the present work.

Relative Distribution of Pores before and after Calcination

The progress of the calcination can be further illuminated by comparing the number of pores left after 32 hours of calcination for each interval of pore diameter with the number produced by 1 hour of calcination. This comparison is shown in Figure E-15 which reveals three important consequences of extended calcination:

- Pores in the diameter range of 0.088 to 0.36 μm are essentially eliminated (97+%).
- Pores in the interval from 0.36 μm to the upper end of the diameter range show either retentions of essentially 100 percent or increases of up to 700 percent.
- About half the pores with diameters smaller than 0.04 μm survive 32 hours at calcination of 1070°C.

Thus, there is a critical pore diameter range of, say, 0.04 to 0.4 μm in which pores essentially disappear on extended calcination. Above this range larger diameter pores are generated, and below it about half the pores are somehow able to survive calcination. In Figure E-14 the critical diameter range accounts for about 30 percent of the surface area present at 1 hour of calcination and only 3 percent of that at 32 hours.

The increase in the number of pores in the large diameter range is considered part of the same process responsible for eliminating pores in the middle range of diameters. Similar results have been observed in sintering other oxides like MgO, ZnO, and UO_2.[E3,E4] This process is believed to depend on the free surface energy which is minimized by reducing the area in the approach to equilibrium.

The survival of very small pores suggests an additional mechanism is operative. One possibility is that the gas present in the fine pores somehow stabilizes their dimensions, a theory that could be tested by sintering in a vacuum.

Figure E-15 shows two discontinuities. The one between 6.4 and 7.2×10^{-3} μm is because no incremental pore volume was measured at this diameter interval for the 1-hour calcination. No significance is attached to this fact; another sample would probably have had a nonzero increment here. The other discontinuity between 1.7 and 2.1×10^{-2} μm is produced by a zero increment to pore volume for the 32-hour sample. This information may be significant, but no explanation is apparent for a zero at this diameter followed by a 40 to 60 percent retention of pores in the interval of 2.4 to 3.2×10^{-2} μm.

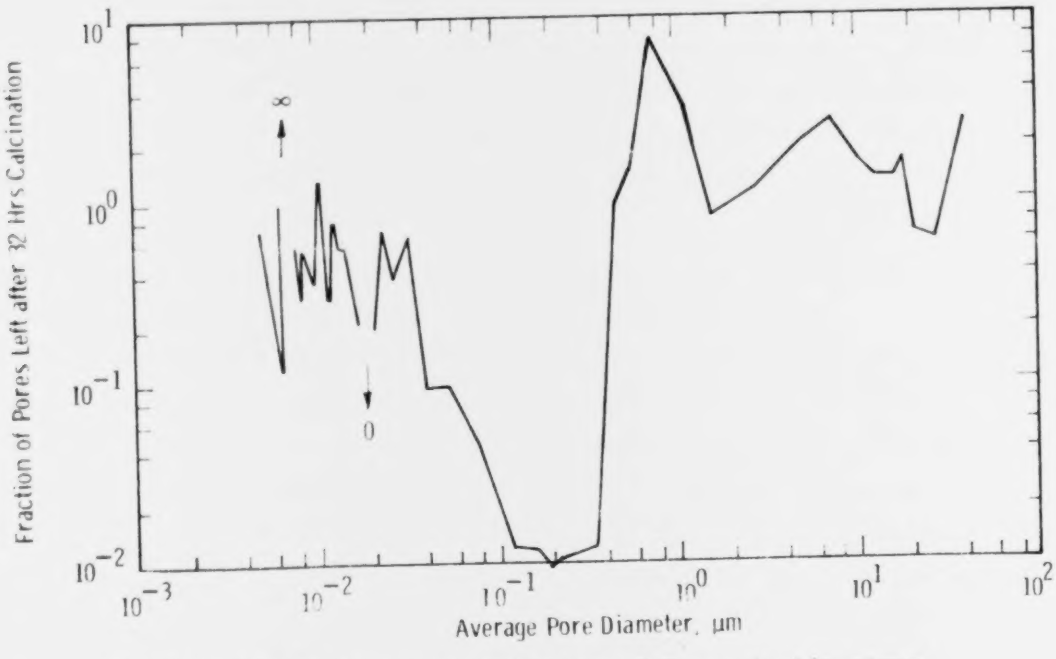

Figure E-15 - Relative Distribution of Pores in Limestone Calcined at 1070°C

One additional aspect of the data merits comment. The BET areas for large, and small particles over the 32 hours of calcination are similar, agreeing with the model. The pore volume of the large particles, however, is considerably smaller than that for small particles. Longer calcination time did not result in comparable pore volumes. The model predicts that the pore volume should be independent of the particle diameter for the case where the particles have the maximum pore volume. The 1-hour sample of the -3360 + 2000 μm fraction was not fully calcined, but the 32-hour sample, as noted in Table E-3, showed only 0.27 cc/g versus about 0.40 for the -105 + 74 μm fraction. It may be that the lattice structure is mechanically more rigid in large particles than in small, and the CO_2 evolved on calcination has time to diffuse through the lattice into the pores formed initially before additional pores can develop.

Active Pores

From the preceding analysis one sees that pores in a midrange of diameters essentially disappear on continued calcination (sintering). The width of this range depends on the criterion used. If one uses pore mouth area, as in Figure E-13, this range is 0.008 to 0.8 μm, corresponding to a factor of at least 1.5 between the area at 1 hour and that at 32 hours. In the narrower range of 0.12 to 0.62 μm, the factor is at least 5.

If one uses relative survival of pores, however, as shown in Figure E-15, the range is 0.04 to 0.4 μm, over which less than 10 percent of the pores survive extended calcination. Table E-8 summarizes the calculated pore distribution by pore diameter range. Large pores (those over 0.4 μm in diameter) increase in number by a factor of 3.5. About 60 percent of the small pores (those smaller than 0.04 μm in diameter) survive calcination and after 32 hours are about 500 times as numerous as the pores in the midrange of 0.04 to 0.4 μm.

Table E-8

NUMBER OF PORES PER GRAM OF LIMESTONE IN SELECTED PORE DIAMETER RANGE

	Sample Number		
Diameter range, μm	94-1	95-1	Ratio
8 - 0.4	8.20×10^{9}	2.86×10^{10}	3.49
0.4 - 0.04	1.17×10^{12}	4.49×10^{10}	0.0385
0.04 - 0.005	3.54×10^{13}	2.09×10^{13}	0.591

Similar results are obtained by comparing total surface area as in Table E-9., pore mouth area as in Table E-10, or pore volume as in Table E-11. This table shows that the small pores contribute less than 4 percent of the total pore volume after 1 hour of calcination and less than 2 percent after 32 hours.

One may speculate that the disappearance of pores in the range of 0.04 to 0.4 μm and the conversion of the limestone to a dead-burned or inactive stone are related. Pores in this diameter range are, therefore, called active pores. The increase in the number of large pores is insufficient to maintain activity, so these are termed inactive pores. The very small pores apparently contribute little to activity.

Table E-9

SURFACE AREA, m^2/g OF LIMESTONE, IN SELECTED PORE DIAMETER RANGES

	Sample Number		
Diameter range, μm	94-1	95-1	Ratio
8 - 0.4	0.584	1.783	3.05
0.4 - 0.004	8.89	0.369	0.0415
0.04 - 0.005	20.85	11.44	0.549

Table E-10

PORE MOUTH AREA, m^2/g OF LIMESTONE, IN SELECTED PORE DIAMETER RANGES

Diameter range, μm	Sample Number 94-1	Sample Number 95-1	Ratio
8 - 0.4	1.181×10^{-2}	3.04×10^{-2}	2.57
0.4 - 0.04	1.412×10^{-2}	8.53×10^{-4}	0.0604
0.04 - 0.005	2.259×10^{-3}	1.246×10^{-3}	0.487

Table E-11

PORE VOLUME, cm^3/g LIMESTONE, IN SELECTED PORE DIAMETER RANGES

	Sample Number				
	94-1		95-1		
Diameter Range, μm	Volume Fraction	Volume	Volume Fraction	Volume	Ratio
8 - 0.4	0.1608	0.1478	0.3661	0.3032	2.051
0.4 - 0.04	0.2223	0.2043	0.0102	0.00849	0.04156
0.04 - 0.005	0.0354	0.03249	0.0192	0.01594	0.4908
Total	0.4185		0.3955		
Bed voidage	0.5815		0.6045		

Further insight is obtained by noting that the active pores account for about 22 percent of the "pore" volume after 1 hour of calcination and only 1 percent after 32 hours. If one takes into account the previous deductions about internal pores and interparticle pores, the former amount to 41.85 percent and 39.55 percent of the "pore" volume measured, respectively.

It is interesting that the interparticle pore volume fractions of 0.582 and 0.604 agree well with general estimates of voidage in packed beds. The agreement is an indirect support of the choice of 8 μm as the largest diameter pore to be considered as an internal pore.

Why this diameter range (0.04-0.4 μm) should be critical is uncertain, but an explanation can be offered in terms of the mean free path of gas molecules estimated from Maxwell's equation:

$$L = 3/4\ \pi\sigma^2 N \quad , \qquad (5)$$

where

σ = molecular diameter

and

N = number of molecules per unit volume.

Gases like SO_2, CO_2, and N_2 are about 4Å in diameter. At standard conditions the mean free path is 560Å, versus 400 to 4000 Å for the critical diameter range. At 870°C the mean free path will be about 2300 Å. A given molecule of gas will collide with up to two other molecules before striking the pore wall. For larger pores the frequency of collision with other gas molecules increases the probability that a given molecule will be deflected back from the pore mouth into the bulk gas. For smaller pores the entrance to the pore will quickly become saturated or spent by adsorption or chemical reaction. If we consider only mechanical transport, a gas molecule would have a lower probability of penetrating the full depth of a narrow pore.

Sulfation of Limestone

These observations on surface area and pore volume are helpful in understanding the sulfation of limestone. After an initial period during which essentially 100 percent of the SO_2 passing through a fluidized bed of limestone particles is absorbed, the percentage of absorption falls off, but not immediately, to zero. Rather, there is a period during which absorption continues but at a significantly reduced rate. The literature frequently mentions that sulfating limestone either directly or by oxidizing CaS produces a layer of sulfate that effectively prevents the reaction from going to completion. This notion can be examined in the light of the present work.

In studies of calcite[E5,E6] the high degree of reactivity of the oxide following calcination has been shown to be due to the difference in structure of the original calcite and the CaO. The change from calcite structure to cubic CaO has been noted as accompanied by a linear shrinkage of 23.7 percent, meaning that either an unstable CaO lattice is formed, in which the calcium and oxygen atoms retain their original position, or pores are formed between CaO units.

Studies conducted by several workers[E5-E8] indicate that rearrangement of oxygen atoms takes place immediately following removal of CO_2 and that the decomposition begins at the surface.[E9]

Calcium oxide has a face-centered cubic structure with a lattice spacing of 4.81 Å, while $CaSO_4$ is orthorhombic, with spacings as shown in Table E-12. If one visualizes a monolayer of $CaSO_4$ on the surface of a spherical particle of calcined limestone, one may estimate the area occupied by one molecule of $CaSO_4$ as 3.5 Å x 7.0 Å, or 2.45×10^{-15} cm^2. If one assumes a particle diameter of 100 µm, one may make the following calculations:

Particle weight, g	1.361×10^{-6}
Number of particles/g	7.346×10^{5}
Particle surface area, cm^2	3.14×10^{-4}
Number of molecules of $CaSO_4$/particle	1.28×10^{11}
Number of g-mols of $CaSO_4$/particle	2.13×10^{-13}
Weight of $CaSO_4$, g/particle	2.90×10^{-11}
Wt % $CaSO_4$	2.13×10^{-3}, or 21.3 ppmw

This amount of $CaSO_4$ is very much lower than that attainable, so more than the spherical surface of the particles must become sulfated.

If the total surface area available because of the pore structure is taken into account, a higher percent of sulfation can be explained. BET measurements have shown areas of the order of 5 m^2/g. This is 6.807×10^{-6} m^2/particle, or a factor of 217 times the spherical surface of the particle. Hence, the sulfate in a monolayer is 0.461 wt %, which is still low.

Table E-12

CRYSTAL LATTICE PARAMETERS

		a_o	b_o	c_o
$CaCO_3$	Orthorhombic	4.96	7.97	5.74
CaO	Cubic	4.81	4.81	4.81
CaS	Cubic	5.6948	5.6948	5.6948
$CaSO_4$	Orthorhombic	6.238	6.991	6.996

Note: All dimensions are in Ångstroms.

The calcium ion is relatively small compared to SO_3 or SO_2: 2 Å versus at least 5 Å. In addition, the crystal lattice of $CaSO_4$ is large compared to other calcium compounds, as shown in Table E-12. Sulfur in any of its forms would thus appear to have difficulty diffusing through even the first layer of $CaSO_4$.

During calcination, the lattice of the carbonate must undergo shrinkage in all three directions. Sulfidation of the oxide then requires an expansion of the lattice in all three directions, whereas if sulfidation of the carbonate can occur directly, it should proceed more readily because two of the dimensions are larger than those of the sulfide lattice. Sulfation, either by oxidation of the sulfide or by direct sulfation of the oxide, requires expansion of all three lattice dimensions. Direct sulfation of the carbonate should proceed somewhat more readily because one of the dimensions is larger than those of the sulfate.

These comments cast some light upon the nature of the sulfation problem. Unless the SO_2 and O_3 molecules can reach the calcium lattice before it shrinks from the dimensions of the carbonate to those of the oxide, the sulfation rate should be reduced. Sufficient energy must be available to permit calcination and yet not permit so much ion mobility as to result in lattice shrinkage. The sulfation itself is exothermic and, conceivably, before the energy of reaction can be dissipated, some of it will be utilized in permitting lattice shrinkage of the calcined but unsulfated calcium.

To achieve 100 percent sulfation for the assumed 100 μm particles, the SO_2 has to penetrate 5×10^5 Å/7.97 Å or 6.27×10^4 layers of lattice structure. An extensive pore structure clearly is helpful in exposing surface, but it would appear that a substantial portion of the sulfation must occur by penetration of the lattice structure. Hence, any conditions that tend to maximize the size of the lattice will aid sulfation.

The foregoing analysis suggests that to use limestone as a sorbent for a gas at 1070°C, the absorption should be carried out simultaneously with the calcination. A critical question is the rate of pore loss versus the rate at which the gas can be brought to the site of the pore. One technique would preheat the limestone to just below the calcination temperature desired. As a variation, using fine particles, the rate at which the particle temperature equilibrates to the gas temperature may be sufficiently fast as to make short contact times feasible. Hence, with fine particles, it may not be necessary to preheat the stone. There is a flux of CO_2, however, from the interior of the particles that tends to sweep out any gas diffusing into the pores. An improved version of the process would, thus, appear to involve calcination at an optimum combination of time and temperature so as to maximize the reactivity of the stone. The latter might be directly proportional to some portion of the pore volume, as for example, that which lies in the diameter range of 0.15 to 0.50 μm. The precalcined stone would then be used either in a fluidized bed or in an entrained flow reactor, according to the contact time needed, with the temperature level similarly optimized to achieve maximum utilization of the sorbent.

STUDIES WITH SPENT CAFB REGENERATOR STONE

The preceding work was extended to cover sulfation of spent CAFB regenerator stone as in the dry sulfation process. A detailed test was made in the 10-cm laboratory fluidized bed, as described in Appendix D. Samples were collected at various times during the reaction and inspection for sulfur content, BET area, and pore volume distribution.

Figures E-16 through E-28 show the primary data obtained by porosimetry for selected samples from Run CAFB-905. The last four figures show that the apparatus was yielding reproducible results over the several weeks required to process the samples.

Figure E-29 shows the cumulative pore volume distribution in three size fractions of spent CAFB regenerator stone from Run 9. Figures E-30 through E-32 show the effect of dry sulfation. For simplicity in making comparisons, the -500 + 177 μm fraction will be referred to as the B fraction, the -177 + 88 μm fraction as the C fraction, and the -88 μm fraction as the D fraction. Table E-13 contains comparative data. We have assumed that pores larger than 8.8 μm are interparticle voids. (The slight change from the value of 8 μm used earlier in this report was a matter of convenience in reading data from the computer printouts.) Since the curves appear to break at about 2 μm, the pore volume below 1.8 μm was also noted, as was the diameter range in which the major fraction of this volume was found. The lower limit of this diameter range was 0.1 to 0.4 μm, so a second break point at 0.18 μm was selected. The following observations are obtained from Table E-13.

- Feed
  - The internal pore volume increases as particle size decreases

    (B:C:D = 1:1.8:2.9) .
  - Small pores (<0.18 μm) account for 17 and 18 percent of the intraparticle pores in the B and D fractions, respectively, but 52 percent in the C fraction.
  - Most of the pores are smaller than 1.8 μm.
- Sulfated product
  - The total pore volume remaining is about the same for the B and C fractions; no data were available for the D fraction.
  - The C fraction lost 83 percent of its pore volume versus 49 percent for the B fraction.
  - The middle range of pore diameters (0.18 to 1.8 μm) experienced a loss of 84 and 94 percent for the B and C fractions, respectively.
  - The small pores volume increased 2.3-fold for the B fraction but decreased 81 percent for the C fraction.

- Although the value of pore volume for the large pores (1.8 to 8.8 μm) may be uncertain because they are small in magnitude, they were nearly eliminated in the B fraction but increased by a factor of 4.3 in the C fraction.

Table E-13

EFFECT OF DRY SULFATION ON THE PORE VOLUME DISTRIBUTION IN SPENT CAFB REGENERATOR STONE

Fraction U. S. Mesh Size Particle Size, μm	B -35 + 80 -500 + 177		C -80 + 170 -177 + 88		D -177 -88
	Feed	Sulfated Product	Feed	Sulfated Product	Feed
Total Pore Volume, cc/g	0.3055	0.2416	0.2508	0.1926	0.5329
Distribution, cc/g					
- 8.8 + 1.8 μm	0.0070	0.0003	0.0023	0.0099	0.0526
- 1.8 + 0.18 μm	0.1060	0.0168	0.1155	0.0069	0.2740
- 0.18 μm	0.0228	0.0517	0.1265	0.0245	0.0712
Total internal volume	0.1358	0.0688	0.2443	0.0413	0.3978
Percent of feed		50.7		16.9	
Distribution, %					
- 8.8 + 1.8 μm	5.2	0.4	0.9	24.0	13.2
- 1.8 + 0.18 μm	78.0	24.4	47.3	16.7	68.9
- 0.18 μm	16.8	75.2	51.8	59.3	17.9

These observations support the view that more pore volume is present in the -177 + 88 μm fraction than in the -500 + 177 μm fraction, and it apparently is more available for whatever processes occur during dry sulfation. These include sulfation, pore coalescence, and pore formation. Since the C fraction was more highly sulfated, it appears advantageous to grind spent regenerator stone at least to -80 mesh (177 μm).

Figure E16a

Cumulative Pore Volume for Sulfated CAFB Regenerator Stone
(see ordinate for sulfation conditions)

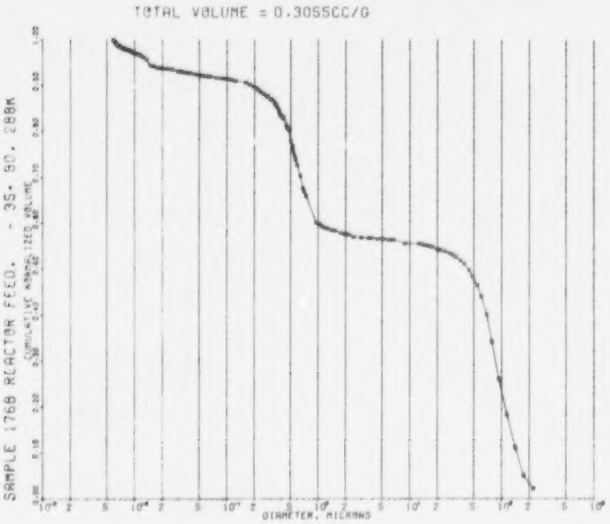

Figure E16b

Differential Pore Volume for Sulfated CAFB Regenerator Stone
(see ordinate for sulfation conditions)

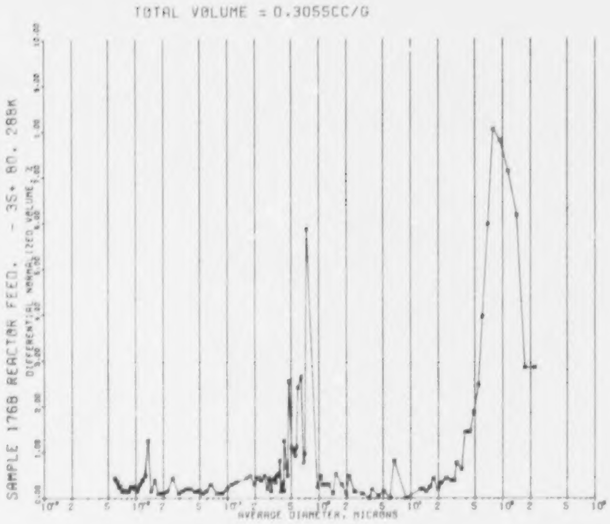

Figure E17a

Cumulative Pore Volume for Sulfated CAFB Regenerator Stone
(see ordinate for sulfation conditions)

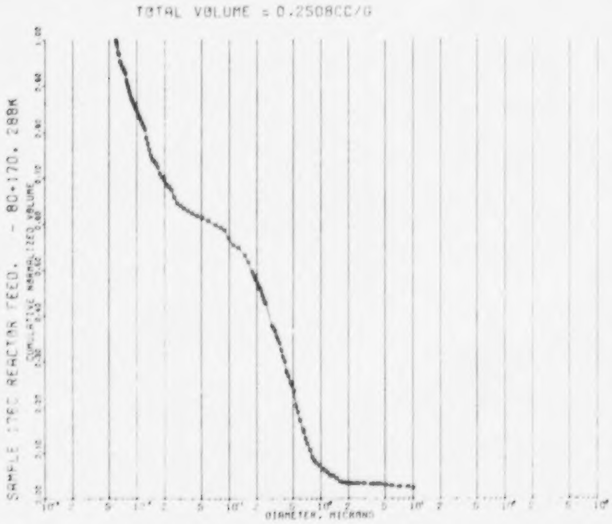

Figure E17b

Differential Pore Volume for Sulfated CAFB Regenerator Stone
(see ordinate for sulfation conditions)

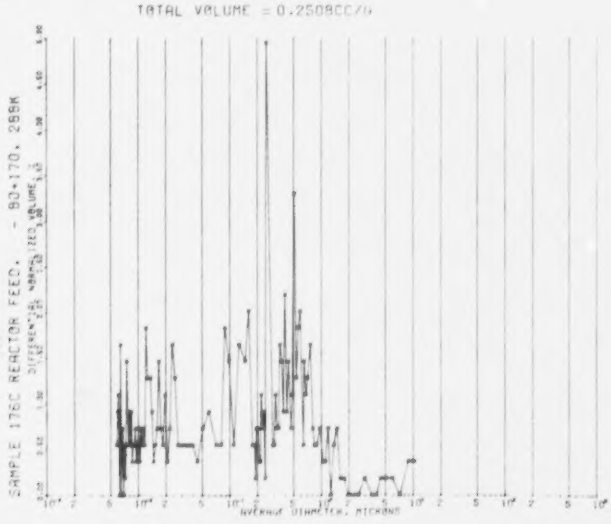

Reproduced from
best available copy.

Figure E18a

Cumulative Pore Volume for Sulfated CAFB Regenerator Stone
(see ordinate for sulfation conditions)

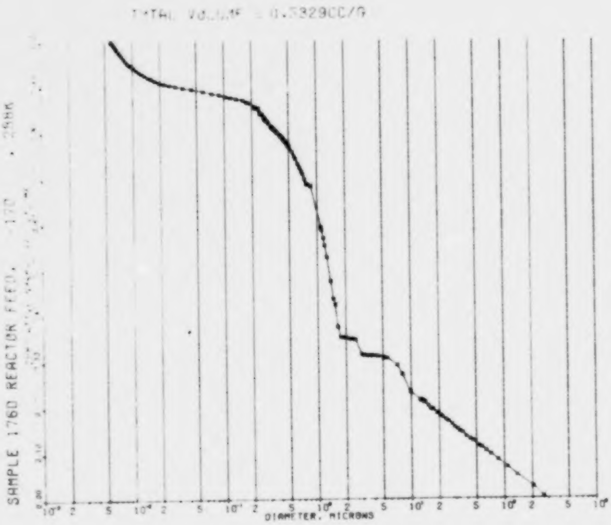

Figure E18b

Differential Pore Volume for Sulfated CAFB Regenerator Stone
(see ordinate for sulfation conditions)

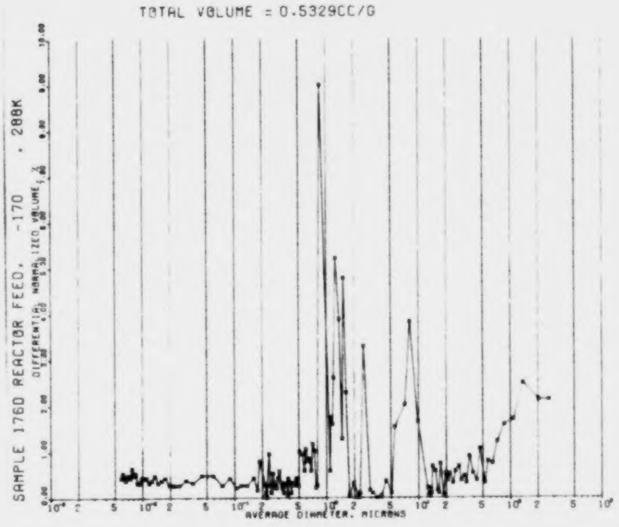

Figure E19a

Cumulative Pore Volume for Sulfated CAFB Regenerator Stone
(see ordinate for sulfation conditions)

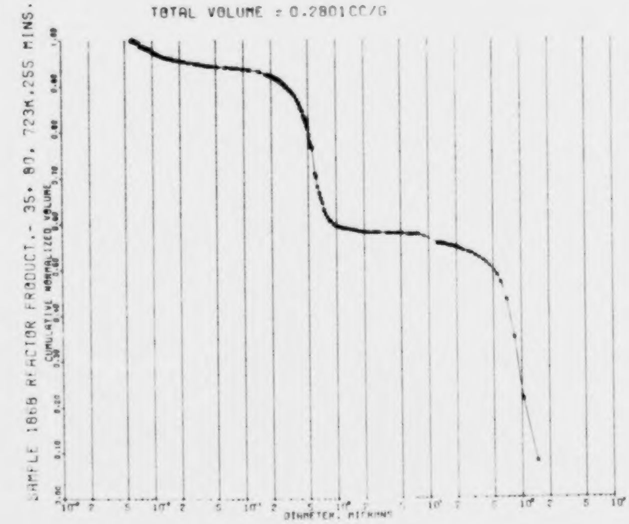

Figure E19b

Differential Pore Volume for Sulfated CAFB Regenerator Stone
(see ordinate for sulfation conditions)

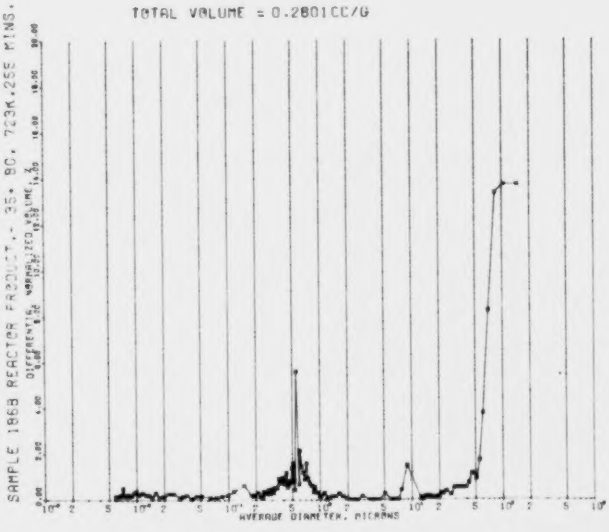

Figure E20a

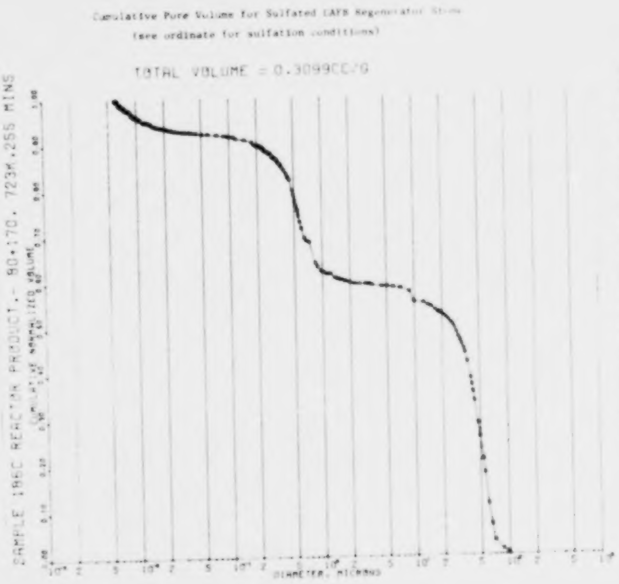
Cumulative Pore Volume for Sulfated CAFB Regenerator Stone
(see ordinate for sulfation conditions)

Figure E20b

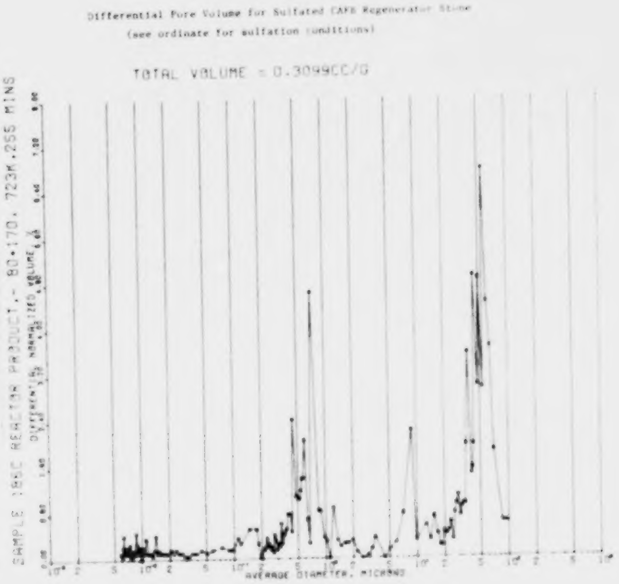
Differential Pore Volume for Sulfated CAFB Regenerator Stone
(see ordinate for sulfation conditions)

Figure E21a

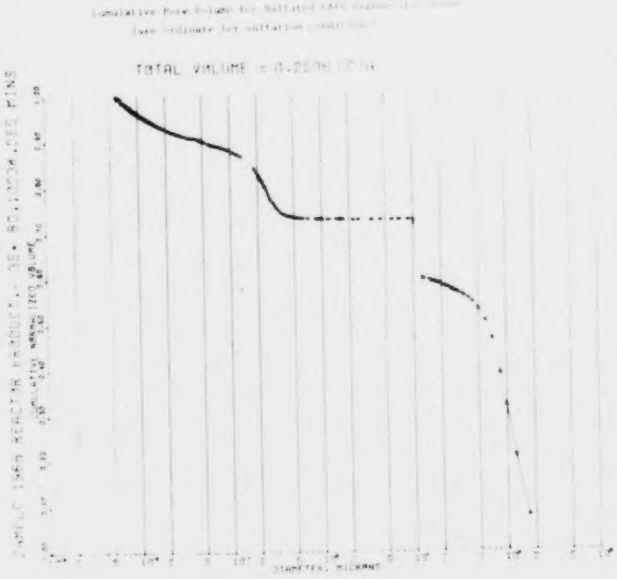
Cumulative Pore Volume for Sulfated CAFB Regenerator Stone
(see ordinate for sulfation conditions)

Figure E21b

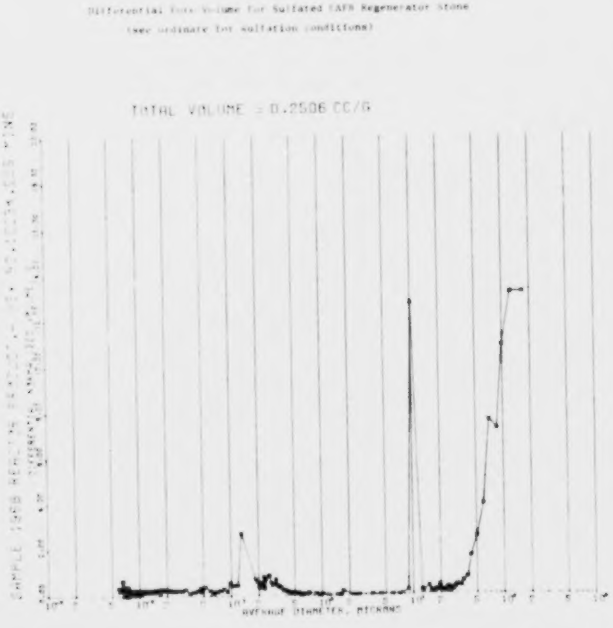
Differential Pore Volume for Sulfated CAFB Regenerator Stone
(see ordinate for sulfation conditions)

Reproduced from
best available copy.

Figure E22a

Cumulative Pore Volume for Sulfated CAFB Regenerator Stone
(see ordinate for sulfation conditions)

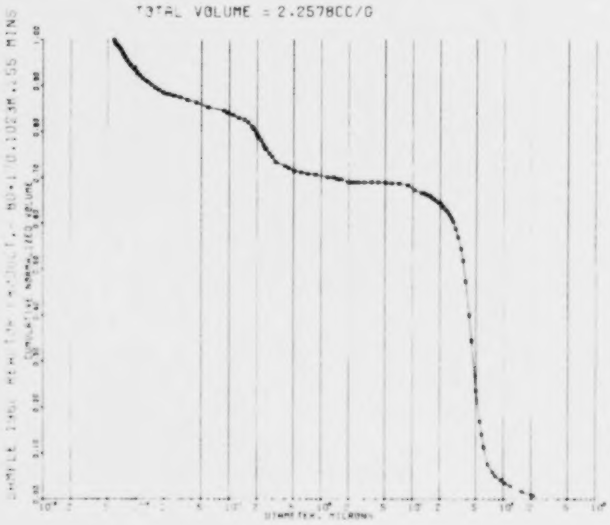

Figure E22b

Differential Pore Volume for Sulfated CAFB Regenerator Stone
(see ordinate for sulfation conditions)

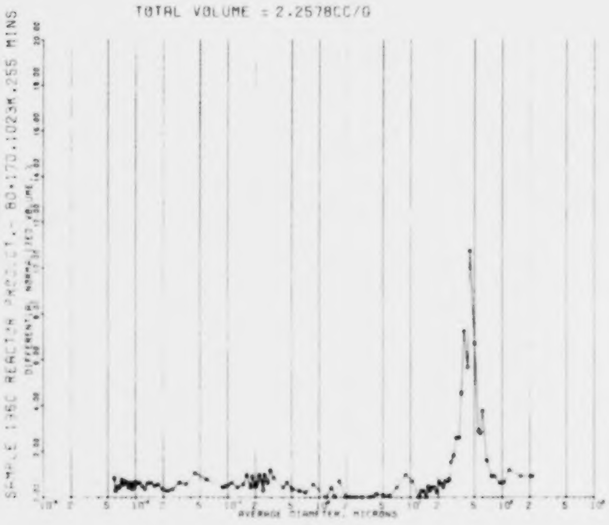

Figure E23a

Cumulative Pore Volume for Sulfated CAFB Regenerator Stone
(see ordinate for sulfation conditions)

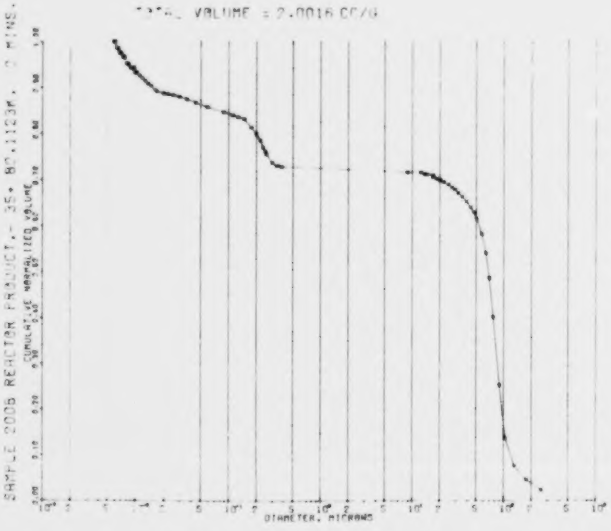

Figure E23b

Differential Pore Volume for Sulfated CAFB Regenerator Stone
(see ordinate for sulfation conditions)

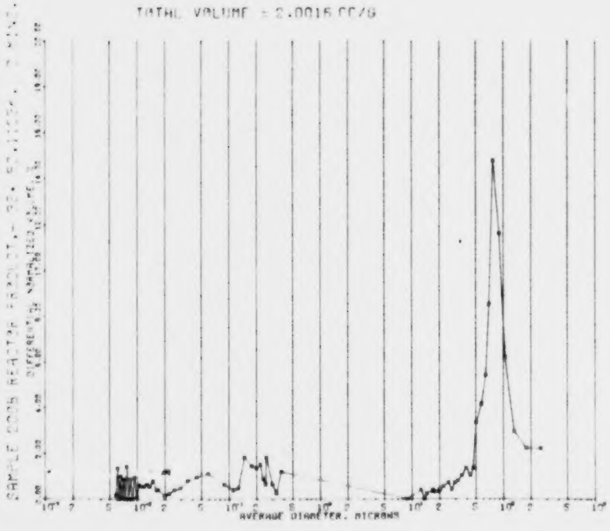

Figure E24a

Cumulative Pore Volume for Sulfated CAFB Regenerator Stone
(see ordinate for sulfation conditions)

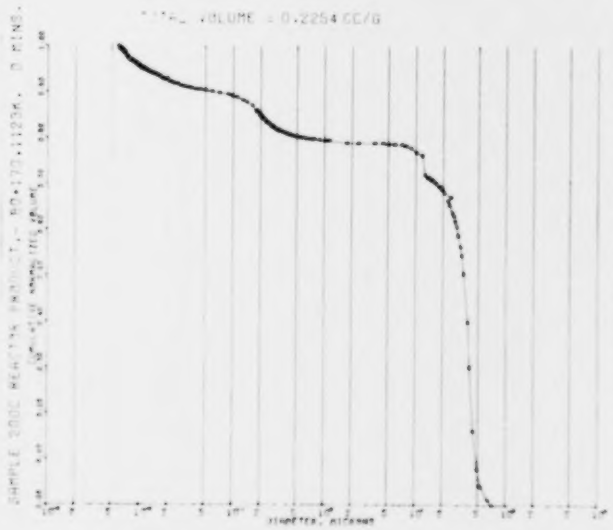

Figure E24b

Differential Pore Volume for Sulfated CAFB Regenerator Stone
(see ordinate for sulfation conditions)

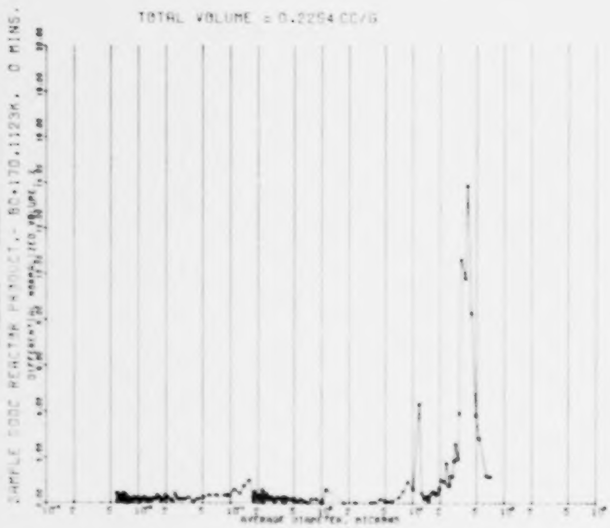

Figure E25a

Cumulative Pore Volume for Sulfated CAFB Regenerator Stone
(see ordinate for sulfation conditions)

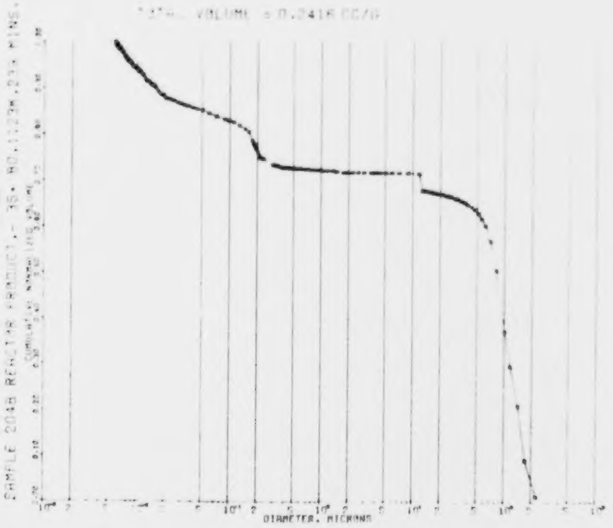

Figure E25b

Differential Pore Volume for Sulfated CAFB Regenerator Stone
(see ordinate for sulfation conditions)

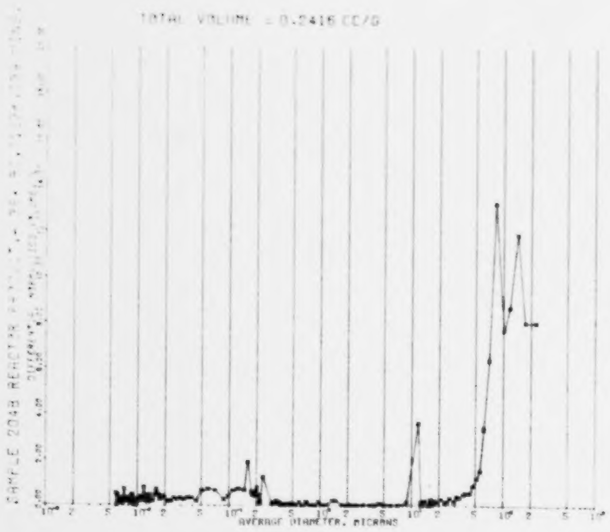

Reproduced from
best available copy.

Figure E26a

Differential Pore Volume for Sulfated CAFB Regenerator Stone
(see ordinate for sulfation conditions)

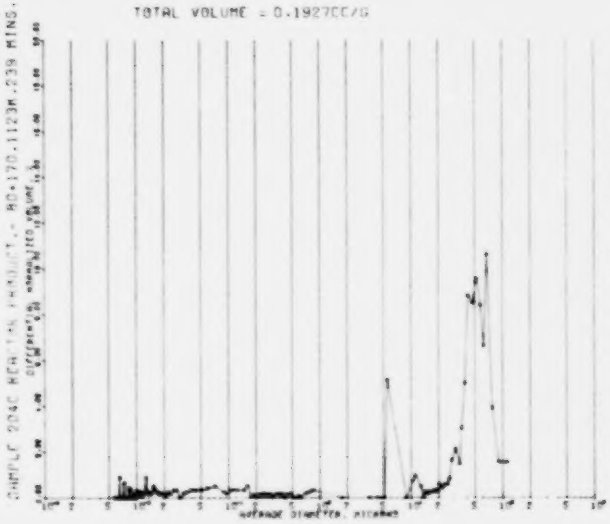

Figure E26b

Cumulative Pore Volume for Sulfated CAFB Regenerator Stone
(see ordinate for sulfation conditions)

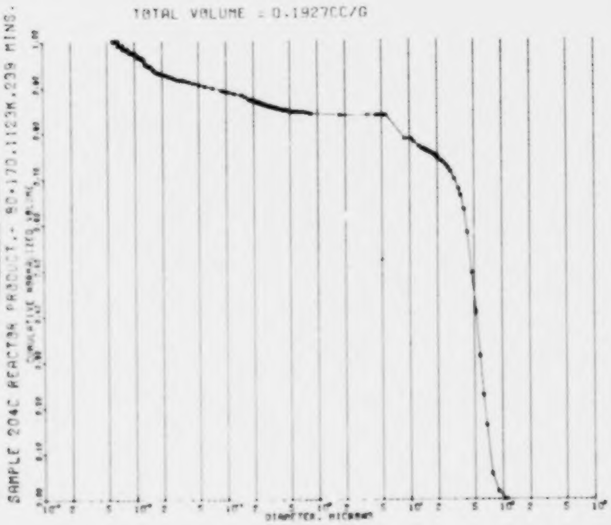

Figure E27a

Cumulative Pore Volume for Check Sample at Start of Series

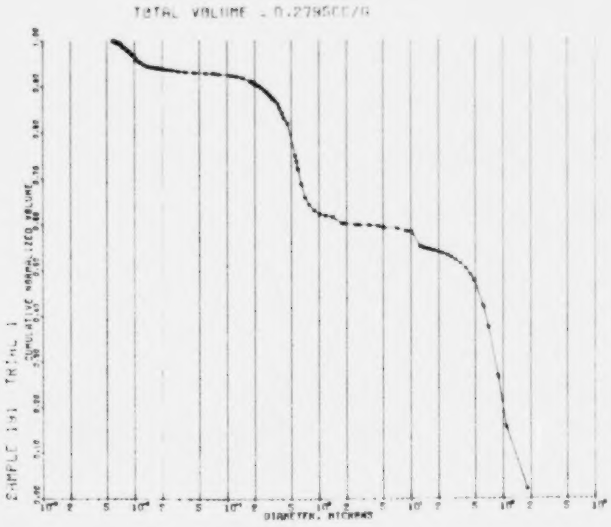

Figure E27b

Differential Pore Volume for Check Sample at Start of Series

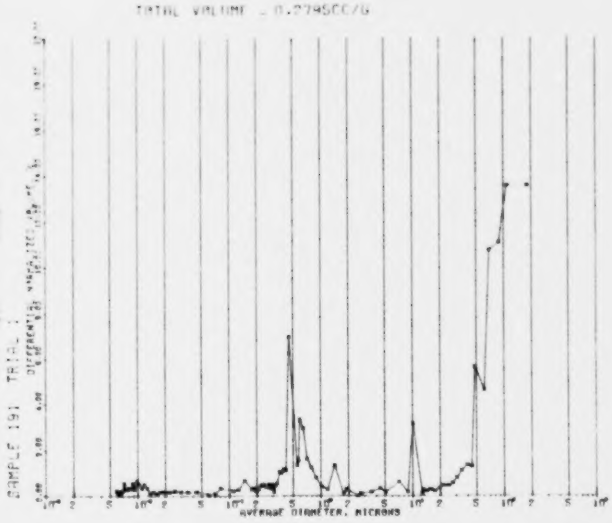

Reproduced from
best available copy.

Figure E28a

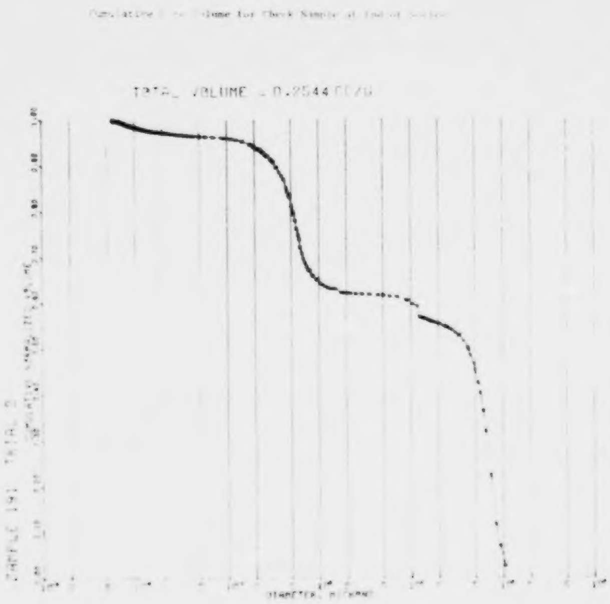

Figure E28b

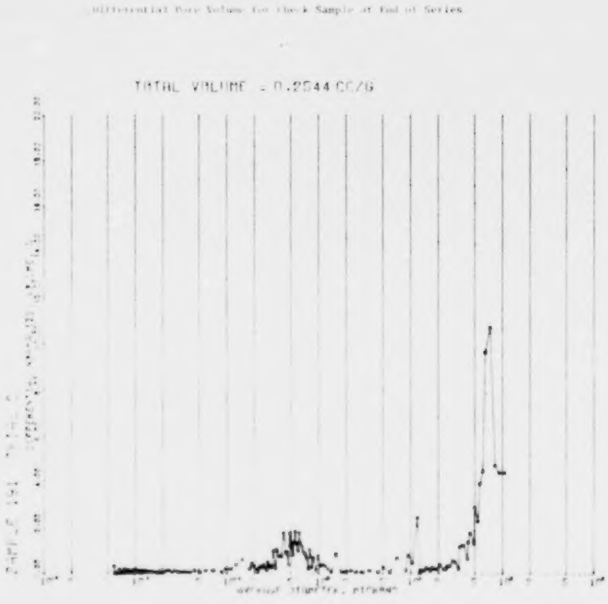

The data were examined further with the aid of the pore volume model developed earlier. Figures E-33 through E-35 show the cumulative distribution of pore diameters in terms of numbers of pores per particle. As in the case of calcination of limestone without sulfation, most of the pores are smaller than 0.01 μm in diameter. Sulfation increased the number of pores/particle from 288 to 432 million for the B fraction but reduced the number for the C fraction from 180 to 27 million/particle.

Figures E-36 and E-37 show the incremental number of pores/particle versus pore diameter. These clarify the meaning of the pore volume changes for diameters less than 0.18 μm. For the C fraction, the number of pores/particle is less for all diameters shown after sulfation, whereas for the B fraction, at nearly every diameter interval, the number of pores is increased. Prior to sulfation the sorbent particles may be considered as having a distribution of pores covering the external surface of the particles. If sulfation proceeds at an initially constant rate, one may postulate that a monolayer of $CaSO_4$ is laid down on the exposed surface of the particles and the pores. Since the crystal

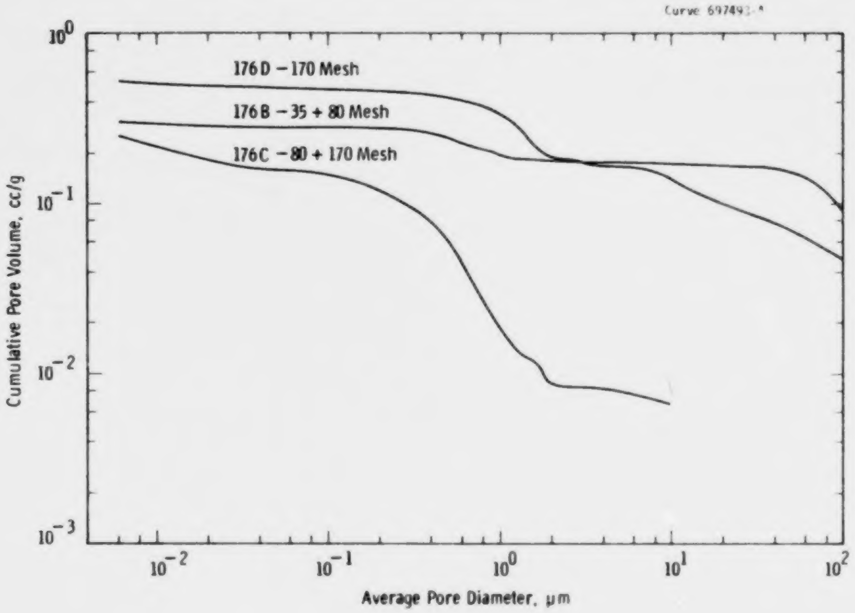

Figure E-29 - Pore Volume Distribution in Spent CAFB Regenerator Stone

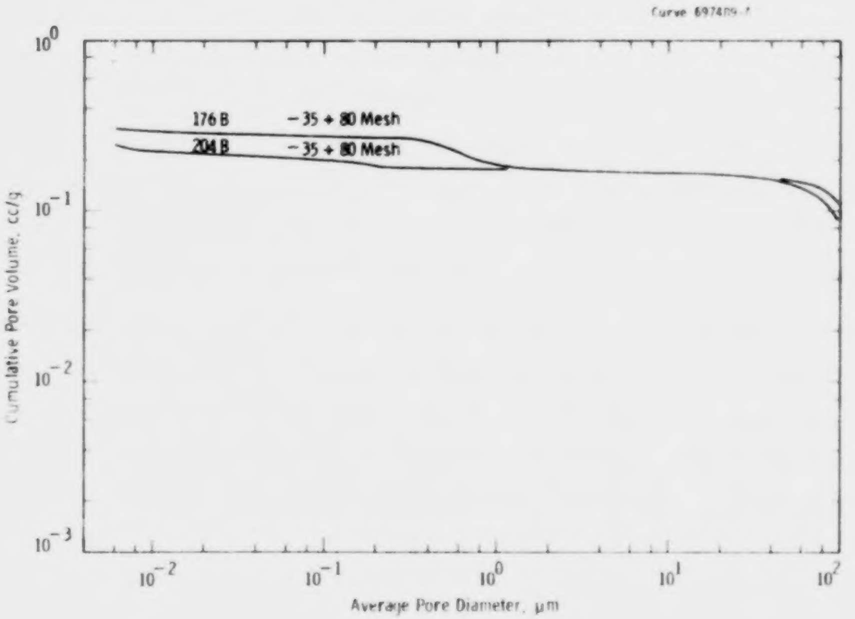

Figure E-30 - Effect of Dry Sulfation on Pore Volume Distribution of Spent CAFB Regenerator Stone

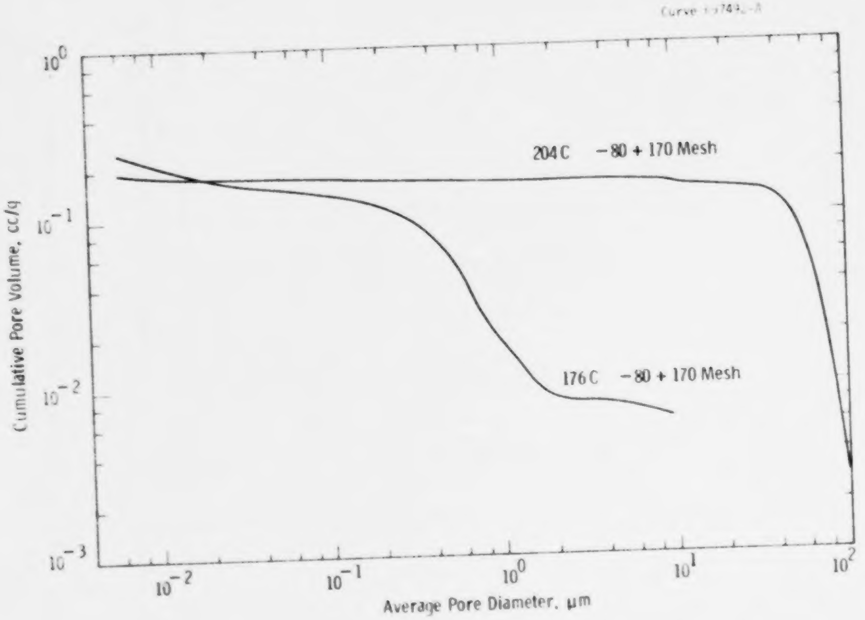

Figure E-31 - Effect of Dry Sulfation on Pore Volume Distribution of Spent CAFB Regenerator Stone

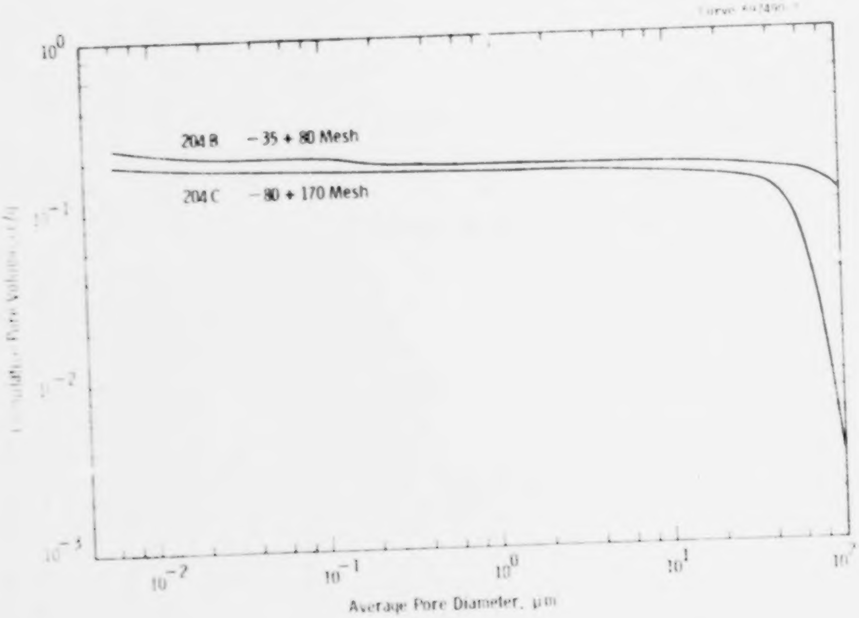

Figure E-32 - Effect of Dry Sulfation on Pore Volume Distribution of Spent CAFB Regenerator Stone

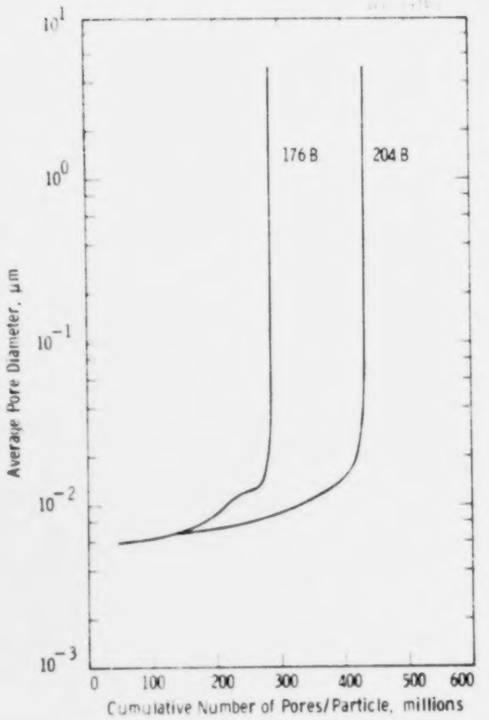

Figure E-33 - Effect of Dry Sulfation on Pore Diameter Distribution of -35 + 80 Fraction of Spent CAFB Regenerator Stone

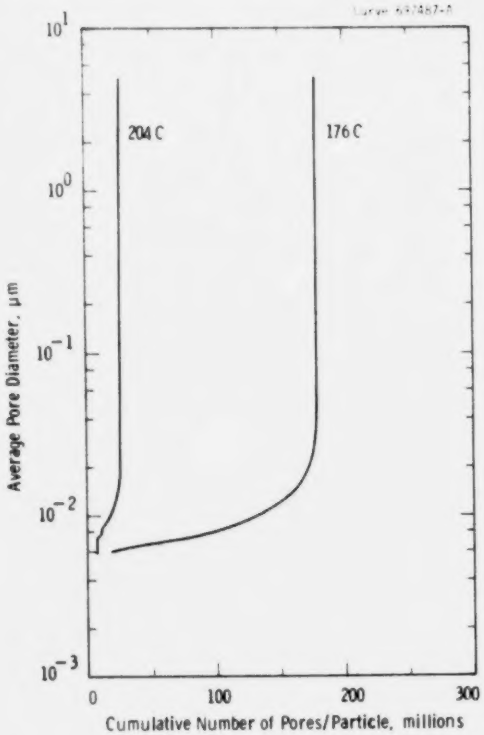

Figure E-34 - Effect of Dry Sulfation on Pore Diameter Distribution of -80 + 170 Fraction on Spent CAFB Regenerator Stone

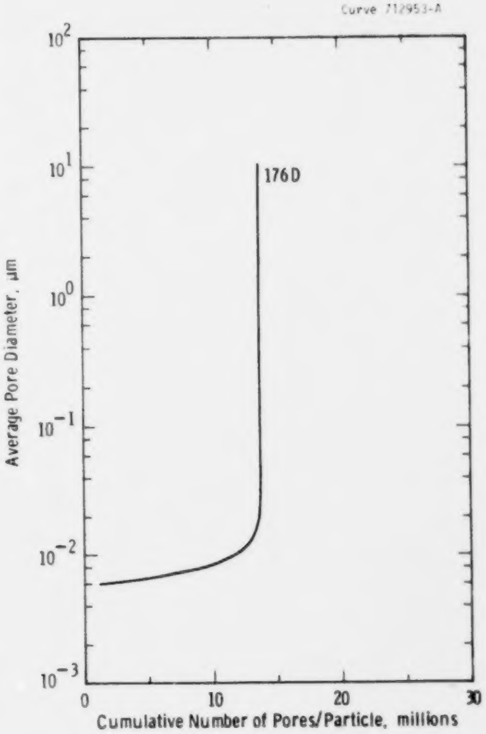

Figure E-35 - Pore Diameter Distribution in -170 Fraction of Spent CAFB-9 Regenerator Stone

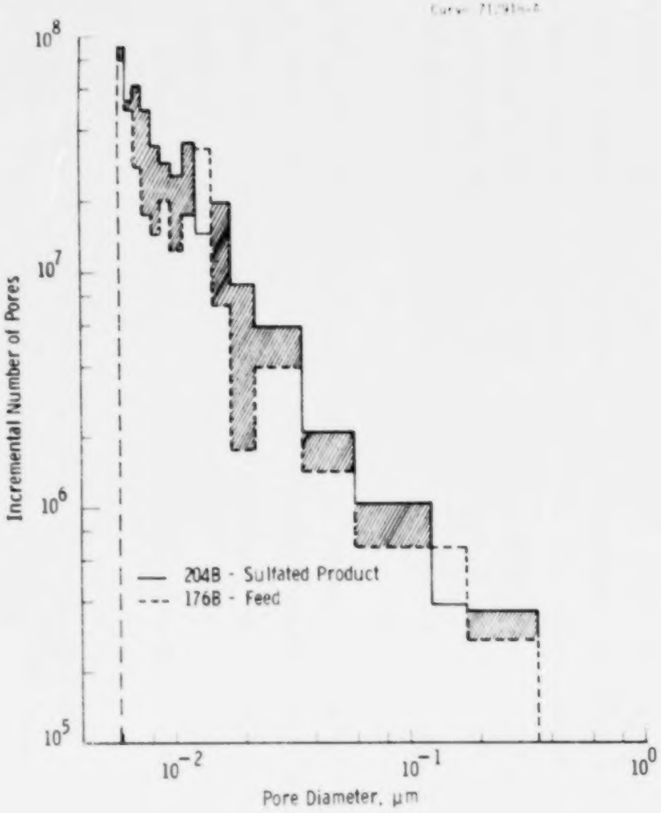

Figure E-36 - Effect of Dry Sulfation on Pore Diameter Distribution in -35 + 80 Fraction of Spent CAFB Stone

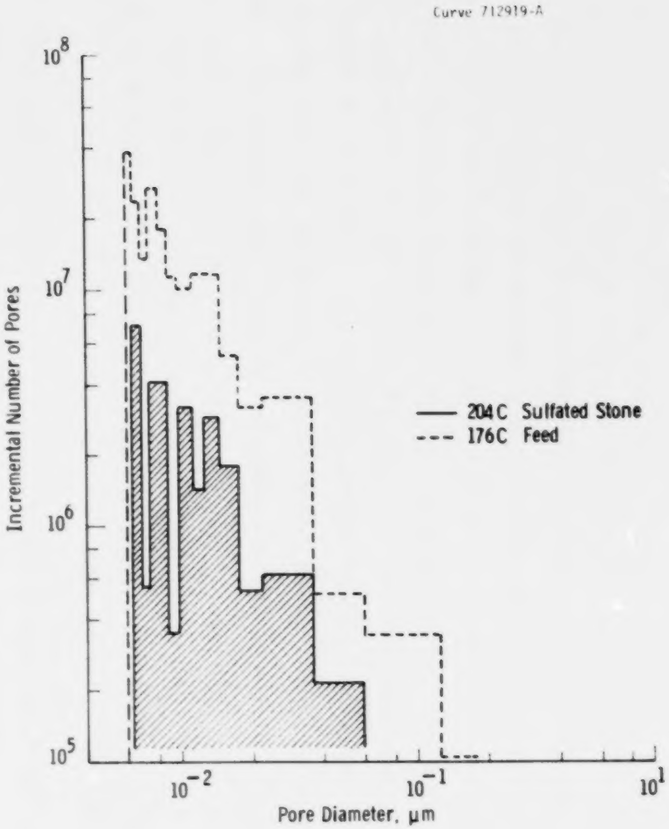

Figure E-37 - Effect of Dry Sulfation on Pore Diameter Distribution in -80 + 170 Fraction of Spent CAFB Stone lattice of $CaSO_4$ is larger than that of CaO, and since one may assume that exposure of the sorbent to 1070°C in the CAFB regenerator permitted the lattice structure to shrink from the dimensions of $CaCO_3$ and CaS to those of CaO, sulfation therefore forces a stretching of the atomic bond lengths. The $CaSO_4$ formed does not necessarily detach from the lattice, but it does tend to fill up the pore volume. It also can lead to lattice dislocations, which means creation of pores. The results with the C fraction can be explained by saying that pores at the 0.18 μm end of the range shown on the figures are reduced in diameter and that pores at the lower end of the range are rapidly closed. The results with the B fraction can be explained by saying either that pores larger than 0.18 μm are reduced to pores smaller than 0.18 μm or that pores are created. It is likely that both effects occur, but the creation of pores is the more important mechanism.

Calculations from the model as reported in Table E-14 show the total number of pores in the various diameter ranges. Regarding the B fraction, although there is a loss of 575 pores/particle in the -8.8 + 1.8 μm range, if these were merely reduced through sulfation, for example, they would represent an insignificant increment to the number of pores in any lower size range. Hence, there is a real loss of pores corresponding to a major loss of pore volume in the intermediate range of -1.8 + 0.18 μm. There is, however, a 50 to 100-percent increase in the number of pores in the two smaller ranges that is considered to indicate creation of pores.

For the C fraction, again there is an almost complete loss of pores in the intermediate range. In contrast to the B fraction, there is also a loss of pores in the smaller diameter ranges. The pores in the C fraction, therefore, appear more reactive than those in the B fraction, and grinding the spent regenerator stone to at least -177 μm appears advantageous.

Two other characteristics may be inspected: pore mouth area and pore surface area. Table E-15 summarizes certain geometric properties

Table E-14

EFFECT OF DRY SULFATION ON THE DISTRIBUTION OF PORE DIAMETERS IN SPENT CAFB REGENERATOR STONE

Fraction	B		C		D
U. S. Mesh Size	-35 + 80		-80 + 170		-170
Particle Size, μm	-500 + 177		-177 + 88		-88
Quantity	Feed	Sulfated Product	Feed	Sulfated Product	Feed
Total Pores/Particle	287.73+06	432.24+06	179.49+06	26.94+06	138.10+06
Size Range, μm					
+ 8.8	89+00	110+00	-	21+00	6+00
-8.8 + 1.8	590+00	15+00	44+00	64+00	85+00
-1.8 + 0.18	504+03	282+03	154+03	11+03	17+03
-0.18 + 0.018	6.17+06	13.01+06	6.06+06	1.13+06	0.26+06
-0.018	281.06+06	418.96+06	171.58+06	25.79+06	135.31+06

Note: Exponential notation is used: 278.73 +06 means 278.73 x 10^6.

of spherical particles. Note that the "average" diameter of a particle has several values according to the definition used. For examination of the results of the area calculations, the surface area mean was used. Figures E-38 through E-40 show the pore mouth area per particle for the three fractions of unsulfated stone and, in some cases, limits on diameter and area taken from Table E-15. Only for the -88 μm (C) fraction were these limits helpful in distinguishing between intraparticle pores and interparticle pores. Fortunately, the curves level off in the range of 1 to 10 μm so a choice of 10 μm as the largest internal pore does not appear unreasonable.

Table E-16 shows the distribution of pore mouth areas. Before sulfation most of the pore mouth area for intraparticle pores is in the diameter range 0.18 to 1.8 μm for the B and D fractions. For the C fraction, the pore mouth area is more evenly distributed by pore diameters. This is interpreted in terms of the probability of an SO_2 (and an O_2) molecule striking and entering a pore. For the C fraction, the probability is relatively independent of pore diameter below 1.8 μm, but it is much

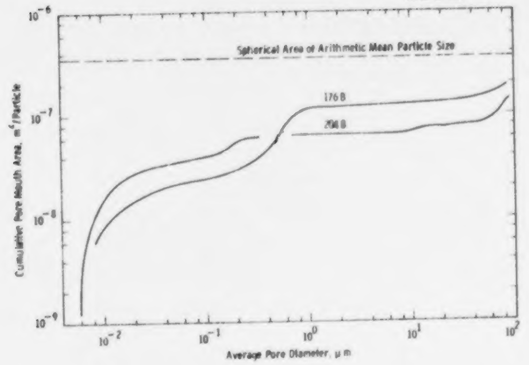

Figure E-38 - Effect of Dry Sulfation on the Pore Mouth Area in -35 + 50 Fraction of Spent CAFB Regenerator Stone

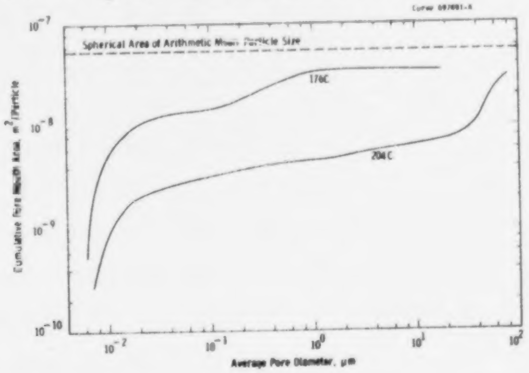

Figure E-39 - Effect of Dry Sulfation on the Pore Mouth Area in -80 + 170 Fraction of Spent CAFB Regenerator Stone

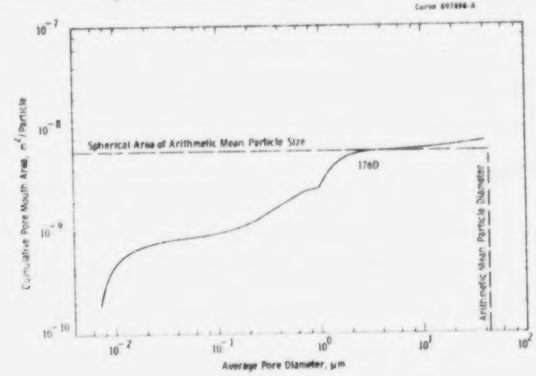

Figure E-40 - Distribution of Pore Mouth Area in -170 Fraction of Spent CAFB Regenerator Stone

Table E-15

SUMMARY OF CHARACTERISTICS OF SPHERICAL PARTICLES

Quantity	U. S. Mesh Size -35 + 80	 -50 + 170	 -170
Particle Diameter, μm			
Range	-500 + 177	-177 + 88	-88
Harmonic mean	261.45	117.56	--
Arithmetic mean	338.5	132.5	44
Surface area mean[a]	375.0	139.8	62.2
Particle Density, g/cm^3 [b]	2.278	1.827	1.445
Spherical Surface Area, m^2/particle[c]	3.600×10^{-7}	5.515×10^{-8}	6.082×10^{-9}
Volume, cm^3/particle	2.031×10^{-5}	1.218×10^{-6}	4.460×10^{-8}
Mass, g/particle	4.626×10^{-5}	2.225×10^{-6}	6.445×10^{-8}
Number of particles/g	2.162×10^{4}	4.494×10^{5}	1.552×10^{7}
Surface area, m^2/g	7.782×10^{-3}	2.478×10^{-2}	9.437×10^{-2}
Volume, cm^3/g	0.4390	0.5473	0.6920

[a] $d_{sm} = \left[\left(d_1^2 + d_2^2\right)/2\right]^{1/2}$

[b] Table D-27, Appendix D

[c] Based on arithmetic mean diameter.

higher for the 0.18 to 1.8 μm range for the B and C fractions. After sulfation, the distributions for both B and C fractions appear more even, implying that those pores that are available by reason of size or frequency are sulfated sooner.

Figure E-41 shows the ratio of pore mouth area after sulfation to that before sulfation for the B and C fractions. This more clearly shows the loss of pore mouth area for the C fraction at all pore diameters contrasted with an increase in pore mouth area at nearly all diameter intervals smaller than 0.14 μm.

Table E-16

EFFECT OF DRY SULFATION ON THE DISTRIBUTION OF PORE MOUTH AREA IN SPENT CAFB REGENERATOR STONE

Fraction U. S. Mesh Size	B -35 + 80		C -80 + 170		D -170
Quantity	Feed	Sulfated Product	Feed	Sulfated Product	Feed
Total pore mouth area, 10^{-9} m^2/particle	278.46	213.40	35.04	29.39	7.49
Size Range, μm					
+ 8.8	151.33	148.98	NA	23.47	1.14
-8.8 + 1.8	6.60	0.30	0.34	1.43	0.90
-1.8 + 0.18	92.60	15.40	16.56	0.99	4.33
-0.18 + 0.018	10.46	23.10	7.65	1.60	0.40
-0.018	17.47	25.62	10.49	1.90	0.72

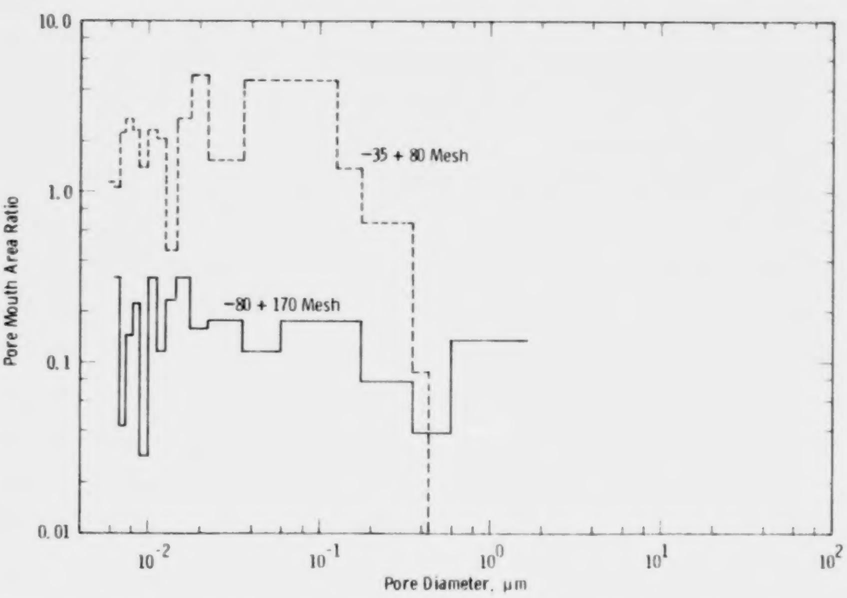

Figure E-41 - Ratio of Pore Mouth Area/Particle after Dry Sulfation to Initial Area

Finally, Figure E-42 shows the cumulative distribution of the total surface area in m^2/g before and after sulfation. Table E-17 shows the distribution of pore diameter interval. On totals, the B fraction showed a 50 percent increase from 14 to 21 m^2/g, while the C fraction showed an 84 percent decrease from 57 to 9.5 m^2/g. The B fraction also had more surface area initially than the other two fractions. Incrementally, both the B and the C fractions after sulfation had most of their surface area in pores smaller than 0.018 μm.

Table E-17

EFFECT OF DRY SULFATION ON THE DISTRIBUTION OF SURFACE AREA IN SPENT CAFB REGENERATOR STONE

Fraction U. S. Mesh Size	B -35 + 80		C -80 + 170		D -170
Quantity	Feed	Sorbent Product	Feed	Sorbent Product	Feed
Total Surface Area, m^2/g	14.456	20.946	56.610	9.445	37.399
Distribution, μm					
+ 8.8	0.015	0.017	NA	0.024	0.036
-8.8 + 1.8	0.012	0.000	9.004	0.011	0.072
-1.8 + 0.18	1.183	0.407	1.762	0.126	2.325
-0.18 + 0.018	1.362	2.914	7.359	1.494	3.480
-0.018	11.884	17.608	47.485	7.790	31.986

Overall, while we do not claim that the pore model used is an accurate description of actual pores, we feel that the model is helpful in thinking about what aspects of pore geometry are important for chemical reaction. First, gas molecules must have access to the interior of the sorbent particles; hence, pore mouth area is important. Once the reacting molecules have entered the pores, large surface area should enhance reactivity. Finally, since in this case the reaction product has a larger molecular volume than the solid sorbent, large pore volume is desirable. We conclude that all of these criteria are best met by grinding the sorbent from the CAFB process to about -177 μm. Whether the fines

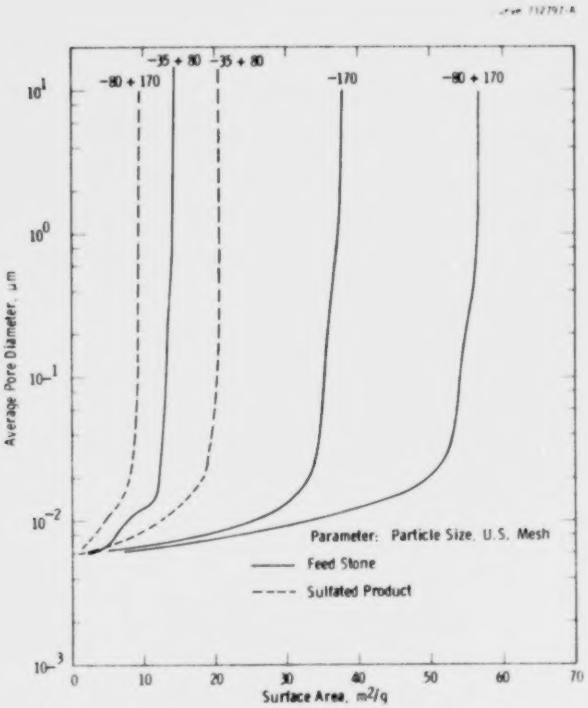

Figure E-42 - Cumulative Distribution of Total Surface Area in CAFB-9 Regenerator Stone

(-88 μm) should be handled differently is not clear from the current data, but, for the present, processing this fraction along with the -177 + 88 μm appears satisfactory.

REFERENCES

1. Klinkenberg, L. J., Pore Size Distribution of Porous Media and Displacement Experiments with Miscible Liquids, American Institube of Mining, Metallurgical and Petroleum Engineers Transactions, 210: 366-69; 1957.
2. Dullien, F. A., and M. I. S. Azzam, Comparison of Pore Size as Determined by Mercury Porosimetry and by Miscible Displacement Experiment , Industrial and Engineering Chemistry Fundamentals, 15 (2): 147; 1976.
3. Gupta, T. K., J. Mat. Sc., 6 (25); 1971

4. Coble, R. L., and T. K. Gupta, On Sintering and Related Phenomena, ed. G. C. Kuczynski et al, New York: Gordon and Breach; 1967, p. 423.
5. Fischer, H. C., J. Am. Ceram. Soc. 38 (7): 245; 1955, and 38 (8): 284; 1955.
6. Hartman, M., and R. W. Coughlin, Ind. Eng. Chem., 13 (3): 248; 1974.
7. Farnsworth, M., Ind. Eng. Chem., 19 (5): 583; 1927.
8. Clark, G. L., W. F. Bradley and V. J. Azbe, Ind. Eng. Chem., 32: 9; 1940.
9. Norton, F. H., Fine Ceramics, New York: McGraw-Hill; 1970.

ADDENDUM TO APPENDIX E

PORE VOLUME MODEL

NUMBER OF PORES PER PARTICLE

Studies involving absorption of gases on solid particulate sorbents often include attempts to interpret the data in terms of pores and diffusion through these pores to the interior of the particles. This paper looks at a simple model of such a pore structure and compares the results with experimental measurements of surface area and pore volume.

The volume of a spherical particle is

$$V_1 = \pi d^3/6 \quad , \tag{AE-1}$$

where

d = the particle diameter
V_1 = the particle volume.

The number of particles per gram of sorbent is

$$N = 1/V_1\rho \quad , \tag{AE-2}$$

where ρ is the particle density.

Note that this is not the number of particles in a bed of such particles, for this would depend on the bulk density, not the particle density. The spherical surface area of one particle is

$$S_1 = \pi d^2 \quad , \tag{AE-3}$$

and the area of each pore mouth is

$$A_p = \pi d_p^2/4 \quad , \tag{AE-4}$$

where d_p is the pore diameter.

Visualize a pore structure consisting of only conical pores with the mouths of the pores all opening on the outer surface of the spherical particles and with the apex of the cone at the center of the particle. A cross-section through a diametral plane is shown in Figure AE-1. The mouths of the pores are assumed to be on the equivalent of an equilateral triangular spacing with some finite ligaments between the adjacent pores.

From spherical trigonometry are obtained the following formulae. If a, b, and c are the lengths of the sides of a spherical triangle in radians, the area of the spherical triangle is given by

$$A = S_1 \ E/4\pi \tag{AE-5}$$

where E is the excess spherical angle over π radians in the triangle. E in turn is given by

$$\tan^2(E/4) = \tan(s/2)\tan((s-a)/2)\tan((s-b)/2) \tan((s-c)/2) \tag{AE-6}$$

in which

$$s = (a + b + c)/2 \ . \tag{AE-7}$$

If the angles between the sides of the triangle are known,

$$E = A + B + C - \pi \ . \tag{AE-8}$$

To illustrate the use of these formulae to calculate the area of one octant of a sphere, set a, b, and c each equal to $\pi/2$. The value of s is then $3\pi/4$ and

$$\tan^2(E/4) = \tan(3\pi/8)\tan^3(\pi/8) \tag{AE-9}$$

$$E = 1.57079637 \tag{AE-10}$$

$$= \pi/2 \ .$$

The area of an octant is then $S_1(\pi/2)(1/4\pi)$ or $S_1/8$.

From Figure AE-1, the length of the arc connecting the centers of two adjacent pores is d_s. This subtends an angle of $(\theta_p + \alpha)$ radians. The angle α is given by

$$\alpha = w/(d/2) \ , \tag{AE-11}$$

Dwg. 6445A46

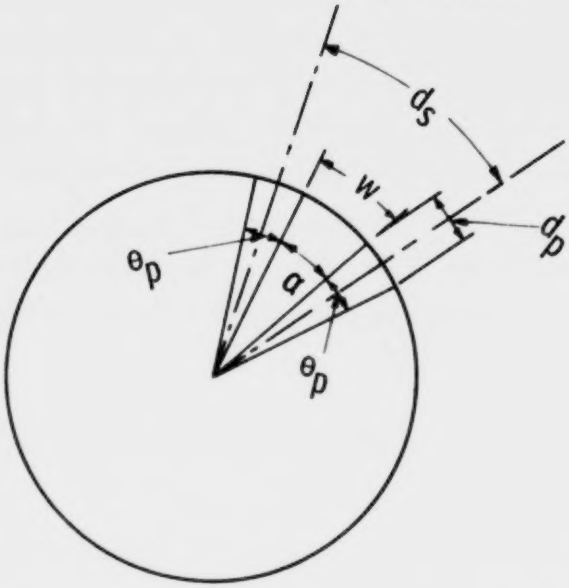
d_s
w
d_p
θ_p
a
θ_p

Figure AE-1 - Diametral Plane Section Showing Two Adjacent Pores

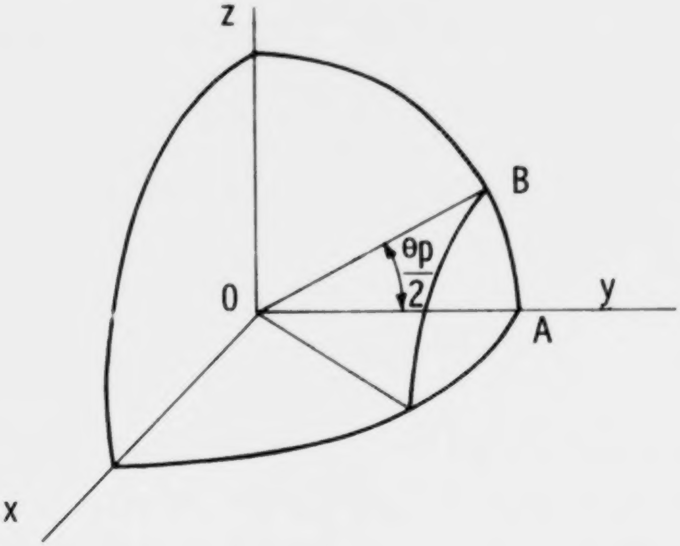
Z
B
$\frac{\theta p}{2}$
0
y
A
X

Figure AE-2 - Intersection of a Right Circular Cone and a Sphere where w is the width of the ligament between adjacent pores as measured along the spherical surface.

The pore included angle is

$$\theta_p = 2 \arcsin (d_p/d) \quad . \qquad \text{(AE-12)}$$

Applying the above formulae:

$$a = \theta_p + \alpha$$

$$s = (3/2)(\theta_p + \alpha) \qquad \text{(AE-13)}$$

$$s - a = (\theta_p + \alpha)/2$$

$$\tan^2 (E/4) = \tan ((3/4)(\theta_p + \alpha)) \tan^3 (\theta_p + \alpha)/4) \quad . \qquad \text{(AE-14)}$$

Consider a 100 μm particle with all of its pores 0.1 μm in diameter. The width of the ligament may be taken for purposes of illustration as 0.01 μm. Then α is 0.01/50 or 0.0002 radian and the pore included angle is

$$\theta_p = 2 \arcsin (0.1/100) \quad \text{or} \quad 0.002000 \text{ radians} \quad .$$

Both these angles are very small so we may take advantage of an approximation:

$$\sin x = x = \tan x \quad . \qquad \text{(AE-15)}$$

Equation (AE-12) reduces to

$$\theta_p = 2\, d_p/d \quad . \qquad \text{(AE-16)}$$

Equation (AE-14) becomes

$$(E/4)^2 = (3/4)(1/4)^3(\theta_p + \alpha)^4 \qquad \text{(AE-17)}$$

$$E = (\sqrt{3}/4)(\theta_p + \alpha)^2 \quad . \qquad \text{(AE-18)}$$

Substituting from equations (AE-16) and AE-11)

$$E = \sqrt{3}(d_p/d)^2(1 + (w/d_p))^2 \quad . \qquad \text{(AE-19)}$$

Finally,

$$A/S_1 = \frac{\sqrt{3}}{4\pi} (d_p/d)^2(1 + (w/d_p))^2 \quad . \tag{AE-20}$$

The number of pores per particle is

$$N_p = (1/2)(S_1/A) \tag{AE-21}$$

because each of the S_1/A equilateral spherical triangles has half of a pore. Also the number of pores per gram is

$$NN_p = \frac{1}{2V_1\rho}\frac{S_1}{A}$$

$$= \frac{4\sqrt{3}}{d}\frac{1}{(d_p + w)^2} \quad . \tag{AE-22}$$

SURFACE AREA PER PARTICLE

Next, expressions may be written for the surface area per particle. Since each pore is visualized as a right circular cone, the lateral area of one such cone is

$$s_p = \pi r l \tag{AE-23}$$

where

r = the radius of the pore mouth

and

l = the slant height of the pore

$$s_p = \pi(d_p d/4) \quad . \tag{AE-24}$$

To this is added the residual surface area of the particle represented by the ligaments between the pores. To calculate this quantity, certain auxiliary relations are needed.

The portion of the spherical surface subtended by one pore depends on the solid angle ω that can be related to the included angle θ_p. In Figure AE-2, a right circular core is shown positioned with its apex at the origin and its altitude coincident with the y-axis. The portion of the spherical surface cut out by the intersection of the core with the sphere can be generated by rotating the arc AB about the y-axis

$$S = 2\pi \int_A^B r\,ds$$

$$S = 2\pi \int_{R \cos (\theta_p/2)}^{R} z \left[1 + \left(\frac{dz}{dy}\right)^2\right]^{1/2} dy \tag{AE-25}$$

$$R^2 = y^2 + z^2 \tag{AE-26}$$

$$S = 2\pi \int_{R \cos (\theta_p/2)}^{R} (z) \frac{R}{z} dy = 2\pi R^2 \left(1 - \cos \frac{\theta_p}{2}\right) , \tag{AE-27}$$

and the fraction of the spherical surface subtended by one pore is

$$f = \frac{1}{2} \left(1 - \cos \frac{\theta_p}{2}\right) . \tag{AE-28}$$

The solid angle ω is defined by

$$\omega = \frac{S}{4\pi R^2} (4\pi) = \frac{S}{R^2} \tag{AE-29}$$

$$\omega = 2 \left(1 - \cos \frac{\theta_p}{2} \right. . \tag{AE-30}$$

The residual surface area of one particle having N_p pores is

$$s_r = \pi d^2 (1 - N_p f)$$

$$= \pi d^2 \left[1 - \frac{\left(1 - \cos \frac{\theta}{2}\right)}{2} N_p\right] . \tag{AE-31}$$

The total surface area per particle is

$$S_p = s_p + s_r \tag{AE-32}$$

$$S_p/S_1 = \frac{N_p}{4}\left(\frac{d_p}{d}\right) + 1 - \frac{N_p}{2}\left(1 - \cos\frac{\theta_p}{2}\right) \ . \tag{AE-33}$$

We may now calculate illustrative numerical values for these various quantities, using a 100 μm particle with 0.1 μm pores. From equation (AE-20), A/S_1 is 1.66777×10^{-7} and N_p is 2.99802×10^6 pores per particle. From equation (AE-33), the total surface area per particle is

$$\begin{aligned} S_p/S_1 &= 749.505 + 1 - 0.749502 \\ &= 749.758 \ . \end{aligned}$$

Since the surface area of the sphere is $S_1 = 3.14159 \times 10^{-8}$ m^2, S_p is 2.35719×10^{-5} m^2.

These values show that we can drop the last two terms in equation (AE-33); combining with equations (AE-20) and (AE-21),

$$\begin{aligned} S_p/S_1 &= \frac{\frac{2\pi}{\sqrt{3}}\left(\frac{d}{d_p}\right)^2}{\left(1 + \frac{w}{d_p}\right)^2}\left(\frac{1}{4}\right)\left(\frac{d_p}{d}\right) \\ &= \frac{\pi\sqrt{3}}{6}\left(\frac{d}{d_p}\right)\frac{1}{\left(1 + \frac{w}{d_p}\right)^2} \ . \end{aligned} \tag{AE-34}$$

This says that for a given pore diameter and w/d_p ratio, the surface area due to porosity varies as the cube of the particle diameter. This is for one particle. Combining with equations (AE-1) and (AE-2)

$$NS_p = \text{surface area/gram of sorbent}$$

$$= \frac{1}{V_1\rho}\left(\pi d^2\right)\left(\frac{\pi\sqrt{3}}{6}\right)\left(\frac{d}{d_p}\right)\frac{1}{\left(1 + \frac{w}{d_p}\right)^2}$$

$$= \frac{\pi\sqrt{3}}{\rho d_p} \frac{1}{\left(1 + \frac{w}{d_p}\right)^2} . \qquad \text{(AE-35)}$$

Thus, the surface area/gram varies inversely as the pore diameter, and is nearly independent of the particle diameter.

PORE VOLUME PER PARTICLE

Turning next to pore volume, the volume of one pore is

$$v_p = \frac{\pi}{3} \frac{d_p^2}{4} \left(\frac{d}{2}\right) \left[1 - \left(\frac{d_p}{d}\right)^2\right]^{1/2} \qquad \text{(AE-36)}$$

and the pore volume per particle is

$$V_p = N_p v_p . \qquad \text{(AE-37)}$$

The fraction of the volume of each particle occupied by pores is

$$\frac{V_p}{V_1} = \frac{N_p}{4} \left(\frac{d_p}{d}\right)^2 \left[1 - \left(\frac{d_p}{d}\right)^2\right]^{1/2} . \qquad \text{(AE-38)}$$

Substituting from equations (AE-20) and (AE-21)

$$\frac{V_p}{V_1} = \frac{\pi}{2\sqrt{3}} \frac{\left[1 - \left(\frac{d_p}{d}\right)^2\right]^{1/2}}{\left(1 + \frac{w}{d_p}\right)^2} . \qquad \text{(AE-39)}$$

Since $d_p \ll d$, a close approximation is

$$\frac{V_p}{V_1} = \frac{\pi}{2\sqrt{3}} \frac{1}{\left[1 + \frac{w}{d_p}\right]^2} . \qquad \text{(AE-40)}$$

This says the pore volume/particle varies as d^3 for a given w/d_p ratio. Combining equations (AE-1), (AE-2), and (AE-39)

$$NV_p = \text{Pore volume/gram of sorbent}$$

$$= \frac{1}{V_1\rho}(V_1)\frac{\pi}{2\sqrt{3}}\frac{1}{\left[1+\frac{w}{d_p}\right]^2}\left[1-\left(\frac{d_p}{d}\right)^2\right]^{1/2}$$

$$= \frac{\pi}{2\sqrt{3}\rho}\frac{1}{\left[1+\frac{w}{d_p}\right]^2}\left[1-\left(\frac{d_p}{d}\right)^2\right]^{1/2} \quad . \qquad \text{(AE-41)}$$

Thus, the pore volume/gram is independent of the size of the particles and only somewhat dependent on the pore diameter. This means that if the maximum number of pores of the type visualized in the model is present, then it does not matter whether the particles are large or small. The total pore volume will be the same per gram of sorbent.

Using the numerical values above,

$$V_p/V_1 = 0.74950 \quad .$$

One more relationship is obtained by combining equations (AE-40) and (AE-34):

$$\frac{S_p/S_1}{V_p/V_1} = \frac{d}{d_p} \quad . \qquad \text{(AE-42)}$$

Pore Mouth Area Per Particle

An expression for the pore mouth area is obtained by combining equations (AE-20), (AE-21), and (AE-4)

$$\Sigma A_p = \frac{\pi^2}{2\sqrt{3}}\frac{d^2}{\left[1+\frac{w}{d_p}\right]^2} \quad . \qquad \text{(AE-43)}$$

Thus, the pore mouth area/particle varies as the square of the particle diameter. Combining with equation (AE-2)

$$N\Sigma A_p = \frac{\pi\sqrt{3}}{\rho d} \frac{1}{\left[1 + \frac{w}{d_p}\right]^2} \quad . \qquad \text{(AE-44)}$$

Hence the pore mouth area/gram of sorbent increases as the particle size is reduced.

MODIFICATIONS FOR DISTRIBUTION OF PORE DIAMETERS

These relationships apply for the case of uniform diameter spheres with pores of equal diameter. For the practical case, a given spherical particle will have a distribution of pore sizes. By porosimetry the fraction of pore volume within a given diameter range can be obtained by measurement and then the number of such pores estimated from equation (AE-38) as applied to the i^{th} pore diameter interval:

$$\left(\frac{V_p}{V_1}\right)_i = \frac{1}{4}\,(N_p)_i \left(\frac{d_p}{d}\right)_i^2 \left[1 - \left(\frac{d_p}{d}\right)_i^2\right]^{1/2} \quad . \qquad \text{(AE-45)}$$

In porosimetry, both the "pore" volume outside the particles as well as that within the particles is measured. Let the total measured "pore" volume be V_T cm^3/g and let N be the number of particles/g. Then V_T/N is the "pore" volume/particle and

$f_i = N(V_p)_i/V_T$ = Fraction of pore volume in the i^{th} pore diameter interval

$$= \frac{(V_p)_i}{V_1} \cdot \frac{V_1}{V_T/N} \qquad \text{(AE-46)}$$

$$(V_p/V_1)_i = (f_i V_T/N)/V_1 = \rho f_i V_T \quad . \qquad \text{(AE-47)}$$

Combining equations (AE-47) and (AE-45)

$$(N_p)_i = 4 f_i (\rho V_T)\left(\frac{d}{d_p}\right)_i^2 \frac{1}{\left[1 - \left(\frac{d_p}{d}\right)^2\right]^{1/2}} \quad . \qquad \text{(AE-48)}$$

Similarly, from equation (AE-33), by dropping the last terms

$$(S_p/S_1)_i = \frac{(N_p)_i}{4}\left(\frac{d_p}{d}\right)_i \qquad \text{(AE-49)}$$

and

$$\frac{(S_p/S_1)_i}{(V_p/V_1)_i} = \left(\frac{d}{d_p}\right)_i \frac{1}{\left[1 - \left(\frac{d_p}{d}\right)_i^2\right]^{1/2}}$$

$$\sim \left(\frac{d}{d_p}\right)_i \quad . \qquad \text{(AE-50)}$$

Substituting from equation (AE-47)

$$\left(\frac{S_p}{S_1}\right)_i = \left(\frac{d}{d_p}\right)_i \left(\frac{f_i V_T}{N}\right) \frac{1}{V_1} \qquad \text{(AE-51)}$$

and

$$(S_p)_i = 6\left(\frac{f_i}{(d_p)_i}\right)\frac{V_T}{N} \quad . \qquad \text{(AE-52)}$$

This is the lateral surface area of the conical pores in the i^{th} diameter interval for one particle. The surface area for N particles, exclusive of the residual surface area of the ligaments between the pores is

$$S = N(S_p)_i = 6\,\frac{f_i}{(d_p)_i}\,V_T \quad . \qquad \text{(AE-53)}$$

The total surface area is

$$S_T = \Sigma S = 6V_T\Sigma\,\frac{f_i}{(d_p)_i} \qquad \text{(AE-54)}$$

Also, the pore mouth area for a distribution of pore diameter can be derived by combining equation (AE-48) with (AE-4)

$$\Sigma(A_p)_i(N_p)_i = \Sigma \frac{\pi(d_p)_i^2}{4} 4f_i \rho V_T \left(\frac{d}{d_p}\right)_i^2 \frac{1}{\left[1 - \left(\frac{d_p}{d}\right)_i^2\right]^{1/2}}$$

$$= \Sigma \frac{\pi f_i \rho V_T d^2}{\left[1 - \left(\frac{d_p}{d}\right)_i^2\right]^{1/2}} \quad . \qquad \text{(AE-55)}$$

Per gram of sorbent, the pore mouth area is

$$N\Sigma(A_p)_i \, (N_p)_i = \frac{6V_T}{d} \Sigma \frac{f_i}{\left[1 - \left(\frac{d_p}{d}\right)_i^2\right]^{1/2}} \quad . \qquad \text{(AE-56)}$$

So, as for uniform pore diameter, the total pore mouth area/gram of sorbent increases as the average particle diameter decreases.

These relations are summarized in Table AE-1 to show how the various particle parameters per gram of sorbent vary with particle dimensions. For the case where d_p is much less than the width of the ligament between the pores, if grinding results only in size reduction and does not create pores, then pore mouth area is increased but surface area and pore volume are not. This would make the interior of the particles more accessible to a reactant and would favor increased utilization. It would increase reaction rate only if transport rate to reacting surface of the sorbent rather than reaction rate were controlling.

Table AE-1

DEPENDENCE OF PARTICLE PARAMETERS ON PARTICLE DIMENSIONS[a]

	Functional Dependence	Practical Dependence		
		$d_p >> w$	$d_p \sim w$	$d_p << w$
Number of Pores/g	$\frac{1}{d(d_p + w)^2}$	$\frac{1}{d_p^2 d}$	$\frac{1}{4d_p^2 d}$	$\frac{1}{dw^2}$
Surface Area/g	$\frac{d_p}{(d_p + w)^2}$	$\frac{1}{d_p}$	$\frac{1}{4d_p}$	$\frac{d_p}{w^2}$
Pore Volume/g	$\frac{d_p^2}{(d_p + w)^2}$	1	$\frac{1}{4}$	$\left(\frac{d_p}{w}\right)^2$
Pore Mouth Area/g	$\frac{d_p^2}{d(d_p + w)^2}$	$\frac{1}{d}$	$\frac{1}{4d}$	$\frac{1}{d}\left(\frac{d_p}{w}\right)^2$

[a] Basis:

1. Spherical particles of diameter d
2. Maximum number of conical pores of pore mouth diameter $d_p \ll d$ separated by ligaments of width w.

NOMENCLATURE

A	Area of spherical triangle
A_p	Area of mouth of one pore
d	Diameter of a particle
d_p	Diameter of a pore
d_s	Arc length between adjacent pore centers
f_i	Fraction of pore volume in i^{th} diameter interval
N	Number of particles/gram
N_p	Number of pores/particle
s_p	Lateral area of one pore
s_r	Residual spherical surface corresponding to the ligaments between pores
S_1	Spherical surface area of one particle
S_p	Total surface area in one particle
V_p	Volume of one pore
V_1	Volume of one particle
V_T	Total measured pore volume
w	Arc length of ligament between adjacent pore
α	Projected angle subtended by the ligament between adjacent pores
θ_p	Projected angle between pore walls
ρ	Particle density

APPENDIX F

LOW-TEMPERATURE FLY ASH BLENDING

Exploration of fly ash blending began with bench-scale feasibility tests using oxidized sulfated limestone from Batch L-1 as a simulated spent sorbent. Mix details are in Table F-1. This stone contained 34.0 wt % $CaSO_4$ composition. Details are given in Appendix I.

Table F-1

EFFECT OF ADDITION OF SIMULATED SPENT SORBENT ON THE COMPRESSIVE STRENGTH OF 2-INCH PORTLAND CEMENT CUBES

Mix Composition, g	
Type I Portland cement	250.0
White sand	687.5
Simulated spent sorbent	30.0
	967.5
Water	121.2
Ratios	
Water/cement	0.485
Sand/cement	2.75
Sorbent/cement	0.12
Compressive Strength, MPA (psi)	
7 days	14.1 (2050)
26 days	25.4 (3690

The mix was placed in 2-in. cube molds, well vibrated and tamped. The cubes were stripped 24 hours after casting and cured in wet paper. The compressive strengths obtained at 7 and 26 days are in the range for normal structural concrete, 13.79 to 42.37 MPa (2000 to 6000 psi). Figure F-1 shows the strength development curve compared to that of

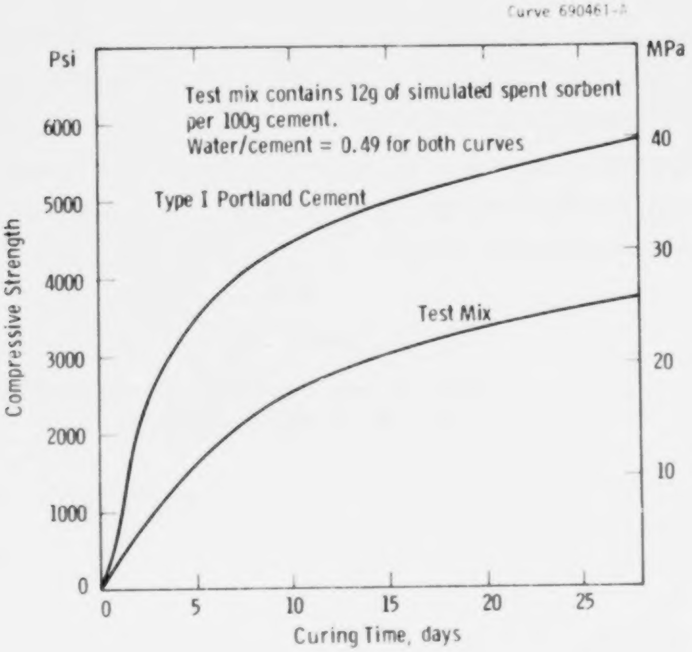

Figure F-1 - Effect of Spent Sorbent on Compressive Strength of Type I Portland Cement

normal Type I cement. The use of the spent sorbent apparently led to a substantial reduction (30-50%) in compressive strength, not attributable solely to the presence of 3.6 percent $CaSO_4$ in the spent sorbent/cement mix.

The effect of $CaSO_4$ was explored further in mixes containing reagent grade gypsum. The test specimens were cylinders 7.6 cm diameter and 15.2 cm high (3 in. x 6 in.), and the mixes contained 10 percent of either gypsum or simulated spent sorbent (oxidized sulfided limestone). To test the oxidized sulfided limestone addition, we first placed the material in water, and when the exothermic slaking reaction was complete, we removed the solids and used them in the mortar. The 7- and 14-day compressive strength data (see Table F-2) indicate that the addition of pure gypsum resulted in a significant strength reduction at 7 days, whereas the addition of the oxidized sulfided limestone, which had been reacted with water prior to its utilization in the mortar mix, did not result in any initial loss of strength. Further, there appears to be a gain in strength between 7 and 14 days. At 44 days, strengths for all three mixes reached a common value of about 55 MPa (about 8800 psi), as shown in Figure F-2. The effect of gypsum is, thus, to delay development of compressive strength, while $CaSO_4$ in the form and amount present in the simulated spent sorbent was without noticeable effect.

Table F-2

EFFECT OF CALCIUM SULFATE ADDITION ON THE COMPRESSIVE STRENGTH OF CEMENT MORTARS

Addition	Age Days		
	7	14	44
None	43.0 (6250)	-	53.6 (7780)
Oxidized Sulfided Limestone	42.9 (6240)	49.6 (7210)	54.3 (7860)
Gypsum	30.9 (4490)	28.2 (4100)	57.6 (8370)

Notes:

1. Test specimens were cylinders 7.6 cm diameter x 15.2 cm high (3 in. x 6 in.)
2. The oxidized sulfided limestone was slaked with water before blending with mortar.
3. The basic mortar was a sand-Type I Portland cement mortar. Additives were 10 percent by weight of the cement.
4. Compressive strengths are in MPa (psi).

The cylinder tests were extended to higher gypsum/cement ratios. In these, 7.6 cm by 15 cm (3 in. by 6 in.) cylinders were cast, moist cured for 7 days, cured in air for 14 days, and checked for axial compressive strength. The sand/cement ratio was as per ASTM 109-73 "Compressive Strength of Hydraulic Cement Mortars." The compressive strength increased linearly with the gypsum/cement ratio. The actual values of compressive strength were about half those of the previous test. The difference was attributed to the method of curing (air versus immersion). These data support the view that the gypsum/cement ratio can be as high as 0.5, as shown in Figure F-3.

Table F-3

EFFECT OF GYPSUM/CEMENT RATIO ON COMPRESSIVE STRENGTH

Mix	1	2	3
Type I Portland Cement, g	1000	1000	1000
Reagent Grade Gypsum, g	100	300	500
White Sand, g	2750	2750	2750
Water, ml	500	500	500
Compressive Strength, psi	3305	3735	4190
MPa	22.8	25.8	28.9

Other tests at even higher gypsum/cement ratios are summarized in Table F-4

Table F-4

GYPSUM/CEMENT MIXES USED TO COMPARE COMPRESSIVE STRENGTHS

Mix	1	2	3	4
Type I Portland Cement, g	1000	50	30	10
Gypsum, g	0	50	70	90
White Sand	500	500	500	500
Water, ml	125	125	125	125

Although all of the mixes set completely within 48 hours, mixes 3 and 4 were rather weak at the end of 10 days. Mix 4 could be crushed by hand. Except for mix 1, these were extremely lean mixes relative to normal concrete compositions.

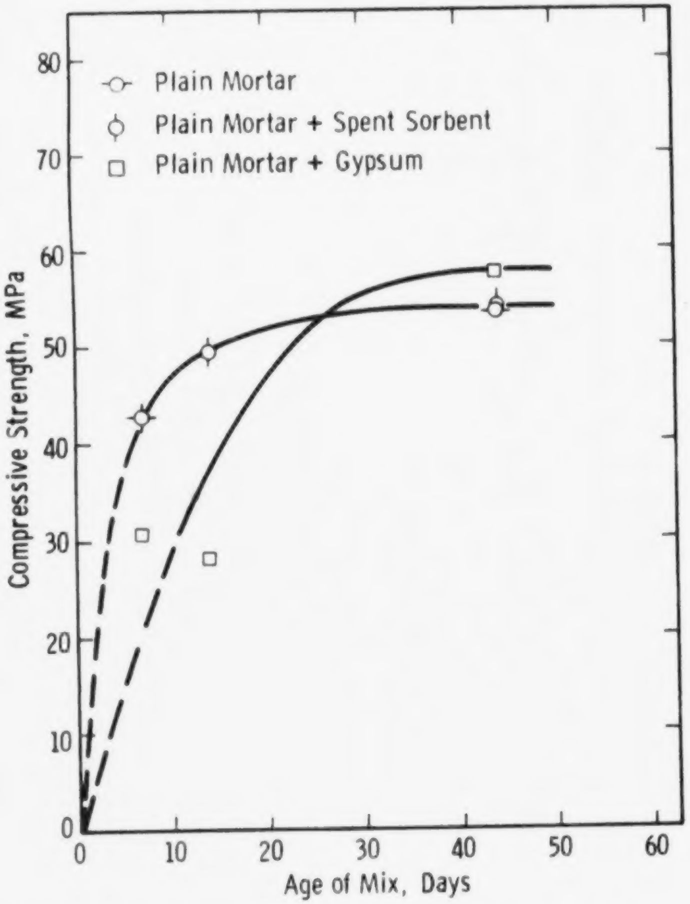

Figure F-2 - Effect of Simulated Spent Sorbent on the Compressive Strength of Cement Mortars

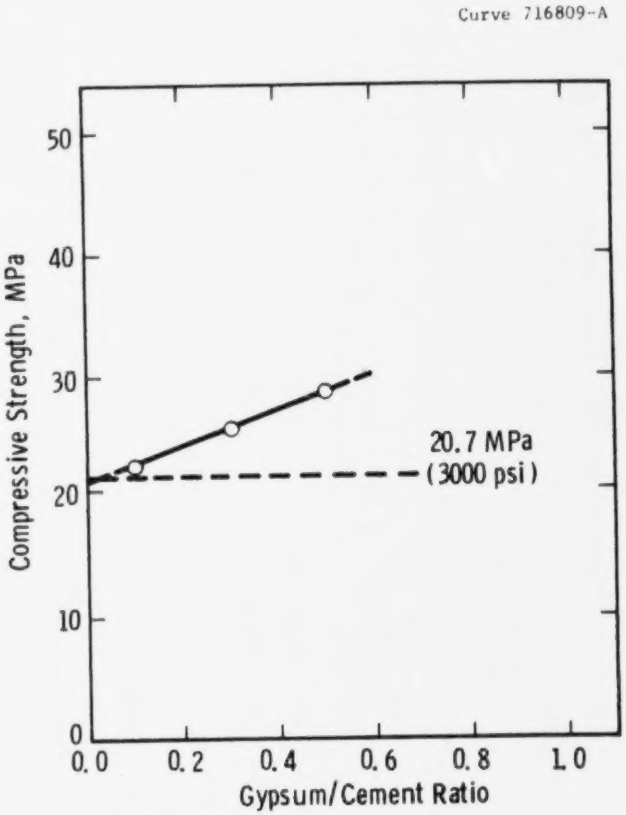

Figure F-3 - Effect of Aging on the Compressive Strength of Gypsum Mortars

A comparison was made of the compressive strengths of 7.6 cm by 15 cm (3 in. by 6 in.) cylinders made with and without spent stone. The mix composition was as follows:

Type I Portland cement, g	1000
White sand, g	2750
Fly ash, g	200
Water, ml	700

To one batch of the above mix was added 100 g of spent stone (oxidized sulfided limestone from test L-1) after it had been slaked in 200 ml of water. The total water content of the two batches of mix was the same at the beginning of the test. The average compressive strength of three cylinders containing spent stone was 18.1 MPa (2627 psi) versus 16.0 MPa (2323 psi) for the cylinders of plain mix. This is an increase of 11 percent, which shows that fly ash/spent sorbent compacts are possible. This test may be regarded as the first of the tests of utilizing spent sorbent as part of the aggregate in normal concrete.

Subsequent tests to explore the effect of mix composition on compressive strength are summarized in Tables F-5 and F-6. Mixes including CAFB stone were made by first slaking the stone and allowing the product to cool to ambient temperature. Slaking was vigorously exothermic, reaching temperatures of 105°C. The test specimens were 5.08 cm (2 in.) cubes. Figure F-4 shows the relative locations of the mixes on a triangular diagram from which the sand has been omitted inasmuch as it was held at a constant ratio to the cement.

All of the mixes showed a general trend toward increased compressive strength as they aged. This is shown in Figure F-5. Mix A, the normal cement mortar mix, developed a 28-day strength of 45 MPa (6530 psi). Adding fly ash to the level of 31.2 wt % on cement while keeping other ratios constant resulted in an increase in 28-day strength to 50 MPa (7250 psi). However, adding spent stone to the level of 66.7 percent on cement while keeping the sand/cement rates constant at 2.75 resulted in a sharp drop in 3-day compressive strength. The trend on aging indicated a 28-day strength of 14 MPa (2030 psi). The drop may be due to the sharp increase in water content as discussed below.

Table F-5

COMPRESSIVE STRENGTH OF 5.08 cm (2 in.) CUBES MADE WITH THE MIXES IN TABLE F-6

Age at Test, days	Compressive Strengths, kPa (psi)							
	Mix A	Mix B	Mix C	Mix D	Mix E	Mix F	Mix F_1	Mix F_2
1	-	-	-	1520 (220)	790 (115)	240 (35)	-	-
3	22850 (3314)	27850 (4040)	7690 (1115)	5760 (835)	930 (135)	210 (30)	-	-
7	26890 (3900)	36040 (5227)	-	8030 (1165)	1620 (235)	-	930 (135)	2390 (346)
11	35420 (5137)	37440 (5430)	11340 (1645)	9240 (1340)	-	-	-	-
14	44200 (6410)	48310 (7007)	12060 (1750)	-	2520 (365)	-	1100 (160)	2965 (430)
27	41070 (5957)	49900 (7238)	-	-	-	-	-	-
28	-		-	12340 (1790)	3520 (510)	-	1450 (210)	3170 (460)

Mixes D to F, in which the cement/fly ash ratio was held constant at 3.2 and the sand/cement ratio at 2.75, showed a continued drop in strength with the increase in the relative amount of spent stone. Mix D was observed at 90 days to have developed a strength of 22 MPa (3190 psi). The ultimate strength of the other mixes appeared to be no more than 4 MPa (580 psi).

Table F-6

Dwg. 1680B1

WATER DISTRIBUTION IN PREPARED MIXES

Mix	A	B	C	D	E	F	F_1	F_2
Amount of Component, g								
Spent Stone	0	0	400	320	480	640	864	518
Cement	1000	800	600	480	320	160	216	130
Water @ 0.5 × Cement	500	400	300	240	160	80	108	65
Slaking Water	0	0	600	520	750	1000	1209	638
Water for Reaction(1)	0	0	118	95	142	189	256	153
Free Water	–	–	482	425	608	811	953	485
Decantable Water	–	–	150	80	90	60	25	0
Slurry Water	–	–	332	345	508	751	928	485
Water Added for Mix	0	0	150	160	70	20	0	0
Total Water Added	500	400	750	680	820	1020	1209	638
Total Free Water	500	400	632	585	678	831	953	485
Sand Added	2750	2200	1650	1320	880	440	594	356
Flyash Added	0	250	0	150	100	50	68	41
Total Solids in Mix	3750	3250	2650	2270	1780	1290	1742	1015
Ratios								
Total Water/Total Solids	0.133	0.123	0.283	0.300	0.461	0.791	0.694	0.628
Total Water/Cement	0.500	0.500	1.250	1.417	2.562	6.375	5.597	4.908
Total Free Water/Cement	0.500	0.500	1.053	1.219	2.119	5.194	4.412	3.731
Slurry Water/Spent Stone	–	–	0.830	1.078	1.079	1.173	1.074	0.936
Spent Stone/Cement	0	0	0.667	0.667	1.500	4.000	4.000	3.985
Flyash/Spent Stone	–	–	0	0.469	0.208	0.078	0.079	0.079
Cement/Total Solids	0.267	0.246	0.226	0.211	0.180	0.124	0.124	0.128
Cement/Flyash	–	3.200	–	3.200	3.200	3.200	3.200	3.200

Dwg. 6358A31

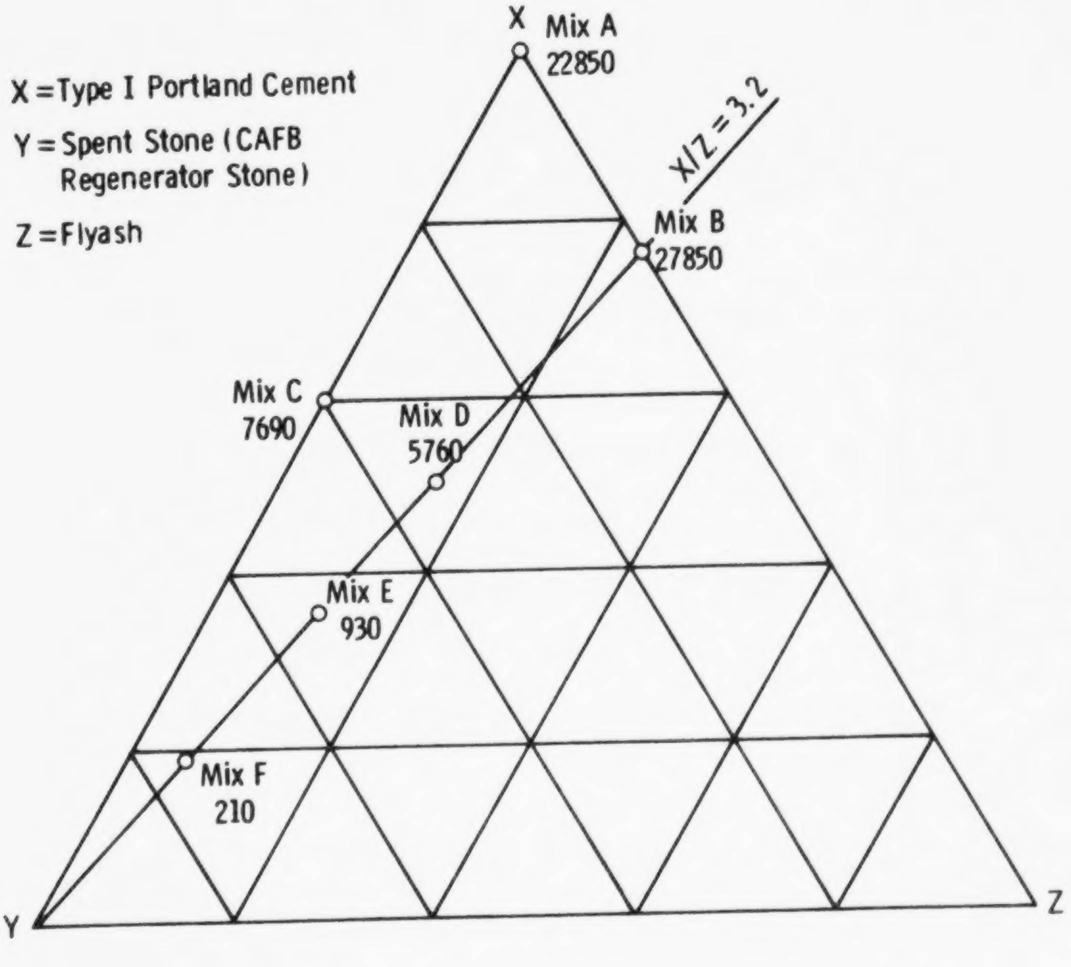
X
Mix A
22850
X = Type I Portland Cement
Y = Spent Stone (CAFB Regenerator Stone)
Z = Flyash
X/Z = 3.2
Mix B
27850
Mix C
7690
Mix D
5760
Mix E
930
Mix F
210
Y
Z

Notes:
1. Compositions are in weight % of primary mix (X + Y + Z)
2. Numbers on the graph are 3-day compressive strengths of 2" cubes in kilopascals
3. Sand/cement ratio is 2.75

Figure F-4 - Effect of Mix Design on 3-day Compressive Strength

Curve 716808-A

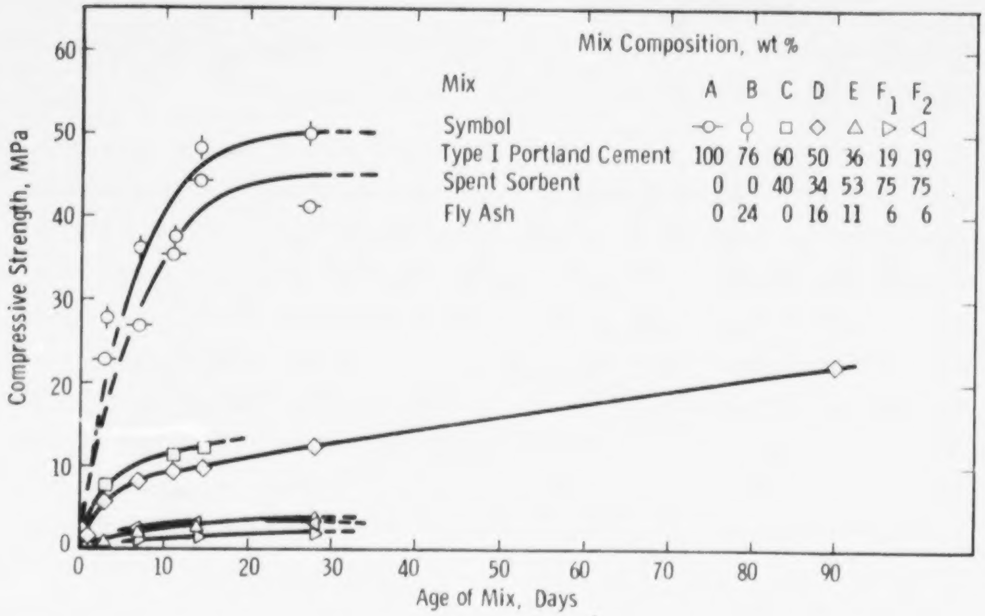

Figure F-5 - Effect of Pilot Plant Spent Sorbent on the Compressive Strength of Fly Ash/Cement Mortars

Specimens of composition F, after soaking in water three days, cracked into several pieces, and the color of the water became yellowish. A repeat batch was made and, instead of being cured in water, this batch was kept in the mold and covered with wet cloth. When the strength was found still to be low (0.210 MPa or 30 psi) at 3 days, observations on mix F were terminated in favor of mixes with a lower total water content. The specimens were also cured differently from mix F. Instead of ponding the specimens in water, specimens of mix F_1 and F_2 were air cured after their removal from the mold. Air curing enhanced the compressive strength at the reduced water content.

Normally, hydration of cement paste proceeds best when the capillary spaces in the paste are water filled. Curing by ponding works well for the high cement content mixes, but for very low cement content the hydraulic pressure created in the capillaries exceeds the early mechanical strength of the specimens, causing them to fall apart.

Table F-5 shows that mix F_2 developed a compressive strength 18 percent greater at 14 days than did mix E, even though the stone/cement ratio was increased from 1.5:1 to 4:1. This result was obtained by simple changes in process technique: lower total water/cement ratio plus air curing rather than water curing. Table F-6 shows the distribution of the water added between slaking water and free water. Normally, a total of 0.5 part of water/part of cement is used. Some water, however, is needed for plasticity. With the low cement/stone ratio, the amount of water needed to achieve a plastic slurry greatly exceeds that needed for hydration of the cement. Even so, the apparently slight reduction from 5.2 for mix F to 3.7 for mix F_2 in free water/cement may be credited with at least some of the strength gain. Mixes E and F_2, incidentally, developed about the same 28-day strength, 3.5 versus 3.2 MPa (510 versus 460 psi), suggesting that increasing spent stone in the total of stone + cement + fly ash from 53 to 75 percent did not change the inherent strength of the mix.

The next step was to explore the other end of the composition range, namely, zero cement content.

Mixes of CAFB stone and coal fly ash were made as per the proportions shown below:

	Mix 1	Mix 2	Mix 3
CAFB stone, g	100	100	100
Fly ash, g	100	50	25
Water, ml	120	115	105

The mixes were air cured and were found not only to attain final set but also to possess sufficient handling strength when the specimens had dried. Qualitatively, mix 3 was adjudged the least permeable to water. Compressive strengths on these specimens were not determined because they were too irregular. The effect of using stone ground to 63 μm (-230 mesh) was tested in three 5.08-cm (2-in.) cubes of the following compositions on a weight basis:

Mix 4A	100 Stone + 23 Fly ash
Mix 4B	100 Stone + 10 Fly ash
Mix 4C	100 Stone + 36 Fly ash

Mix 4A was based on calculations from the typical composition of fly ash and that of CAFB-9 stone. The object was to have the free CaO content the same as that of the total calcium in Portland cement. This put the Al_2O_3 also in the correct range but left the SiO_2 much lower than in cement. Mix 4B was arbitrarily set for half this proportion of fly ash while 4C was 50 percent greater. The stone was first slaked in water, using a water/total solids ratio of 1.125. After cooling, the slaked stone was blended thoroughly with the desired amount of fly ash. Water content was increased to 1.14 to improve plasticity. The specimens were cured in a humidifier at 95 percent R.H. and 21°C. Compressive strengths are in Table F-7.

Table F-7

COMPRESSIVE STRENGTH OF CAFB-9 REGENERATOR STONE/FLY ASH MIXES, kPa (psi)

Mix	Age, Days		
	7	14	28
4A	758 (110)	889 (129)	1144 (166)
4B	1131 (164)	1413 (205)	1689 (245)
4C	648 (94)	869 (126)	1034 (156)

These data show that mix 4B, containing 10 percent fly ash, continued to develop higher compressive strength on aging than did mixes containing more or less fly ash.

The values were still low but suitable for landfill. These same samples were subjected to leaching tests in chunk and in powder form. Sulfate levels in the leachate from 10 g in 100 ml after 256 hours, which were in the range 2000 to 3400 ppm, approached the saturation value for $CaSO_4$. Use of Student's t test on the means for the chunk data versus the powder data show that the probability of finding as large a difference in means (1944 versus 1747 ppm) by chance was about 5 percent, supporting the view that processing the spent sorbent into large blocks should reduce the leach rate of sulfate ions.

The next experiment was a detailed investigation of the effect of particle size using narrow cut fractions. The mix composition was 765 g stone, 85 g fly ash, and 1000 g H_2O, except for the -60 + 80 mixes, which used 950 g. The amount of water used was based on the plasticity of the mix. Duplicate measurements were made to permit statistical analysis of the variance of the results. The data are in Table F-8, the analysis of variance in Table F-9.

Table F-8

COMPRESSIVE STRENGTH OF 5.08 cm (2 in.) CUBES MADE WITH CAFB-9 REGENERATOR STONE AND COAL FLY ASH

	Curing Time, Days			
Size Range, μm	7	14	21	66
-250 + 177	100;113	234;260	188;161	193;213
-177 + 175	45;43	170;168	205;313	340;370
-125 + 88	20;25	220;258	210;210	398;405
-88	70;40	160;148	125;148	208;235

Notes:

1. Coal fly ash is from Duquesne Light Company's Phillips Plant.
2. Mix composition is 765 g stone, 85 g fly ash, 1000 g water, except for -250 + 177 μm mixes, where only 950 g water was used.
3. Compressive strengths in psi.

Table F-9

ANALYSIS OF VARIANCE FOR COMPRESSIVE STRENGTH DATA ON CAFB STONE/FLY ASH CUBES

	Sum of Squares	Degrees of Freedom	Mean Square	F. Ratio
Main Effects				
Size	27522.8		9174.3	16.28
Age	231210.3	3	77040.1	136.73
		3		
Interaction				
Size & Age	67926.5	9	7547.4	13.39
Remainder	9018.5	16	563.6	
TOTAL	335678.1	31		

Table F-8 presents the data on the effect of particle size range on the compressive strength of compacts made from CAFB regenerator stone and coal fly ash. Table F-9 contains a statistical analysis of these data. Curing time was, as expected, highly significant, but the effect of partical size range and the interaction of curing time and particle size were also significant at better than the 99-percent level.

Closer examination of these findings revealed that the contribution of the effect of replication to the total sum of squares of deviations from the grand mean is relatively small. This is a formal way of stating that the replicates in general were in close agreement (within 0 to 20 percent), and this agreement prevailed over a wide range of compressive strengths. In only two of the 16 pairs of results was the difference greater than 20 percent, nor was there any trend to greater differences with a decrease in particle size or curing time.

The grand mean of the compressive strengths was 1.290 MPa (187.2 psi). Both early and late strength data deviated widely from the grand mean and, therefore, made large contributions to the total sum of squares. The statistical analysis was repeated after deleting the 7-day data to determine whether they were responsible for the effect of particle size range.

In commercial use the early strength of concrete determines how soon forms can be removed and load placed on the concrete. The strengths obtained at 7 days were in all cases far below those for normal weight concrete: 5.52 to 14.48 MPa (800 to 2100 psi). All three effects were still found to be significant at better than the 95 percent level.

The original data support the view that intermediate particle sizes -170 + 88 μm gave higher compressive strengths, of the order of 2.76 MPa (400 psi), about twice the strength of compacts made with -250 + 177 μm material. The gain is not sufficient, however, to justify processing spent sorbent to -177 + 88 μm, but grinding to at least 100 percent less than 177 μm appears worthwhile.

It is also interesting that all four size ranges showed a drop in strength at an intermediate age, followed by a recovery to generally higher levels.

Since relatively low 60-day compressive strengths were obtained, use of narrow particle size ranges of CAFB spent sorbent in blends with coal fly ash appears unattractive. Other variations, however, need to be explored. The large amount of water needed for plasticity is considered a major contributor to the low strengths. Two methods available for reducing water content are the use of a surfactant and the use of isostatic pressing. We plan to employ these techniques in later tests.

Following the thought of producing synthetic aggregate from spent sorbent, cubes previously made from -250 + 177 and -125 + 88 μm CAFB stone were crushed to -1.27 cm (-1/2 in.) for testing as a synthetic aggregate. The mix composition was 100 g of Type I Portland cement, 175 g sand, and 100 g crushed CAFB composite. Compressive strengths of single specimens at 14 days were 8.69 MPa (1260 psi) and 5.38 MPa (780 psi), respectively. These values are 2 to 5 times those for the original stone/fly ash compacts but still below the normal concrete range.

APPENDIX G

HIGH-TEMPERATURE FLY ASH BLENDING

Feasibility experiments were conducted whose object was to determine whether stable solid compacts could be made by sintering mixes of sulfated limestone with fly ash and clay. The initial tests used -595 + 420 μm oxidized sulfided limestone from Batch L-1 made in the 10-cm laboratory fluidized bed. Data for these tests are in Table G-1.

Three levels of additive -- 20, 40, and 60 wt % of the blend -- and four levels of sintering temperature -- 800, 900, 1000, and 1200°C -- were used. The mixes were heated for two hours in a stream of 3.3 ℓ nitrogen/min (7 cfh).

In the case of the fly ash additive, CF-3, the composition containing 40 percent OSL* + 60 percent fly ash, yielded a clinkerlike product when sintered at 1000°C. With other compositions and sintering temperatures the product was either a powder or a melt.

With clay additives all the compositions sintered to a solid mass at all temperatures, but when these products were aged for three to five days in the laboratory, they crumbled to powder without exception.

The results indicate that, within the experimental range studied, compositions containing fly ash need to be heated to at least 1000°C before sintering occurs.

Chemical analyses for sulfide and sulfate sulfur are also in Table G-1 and presented graphically in Figures G-1 and G-2. In all cases most of the sulfate sulfur was lost. An unexpected result was the increase in sulfide sulfur with increased fly ash content. In contrast, the residual sulfide content did not vary with ball clay content.

---

*OSL is oxidized sulfided limestone.

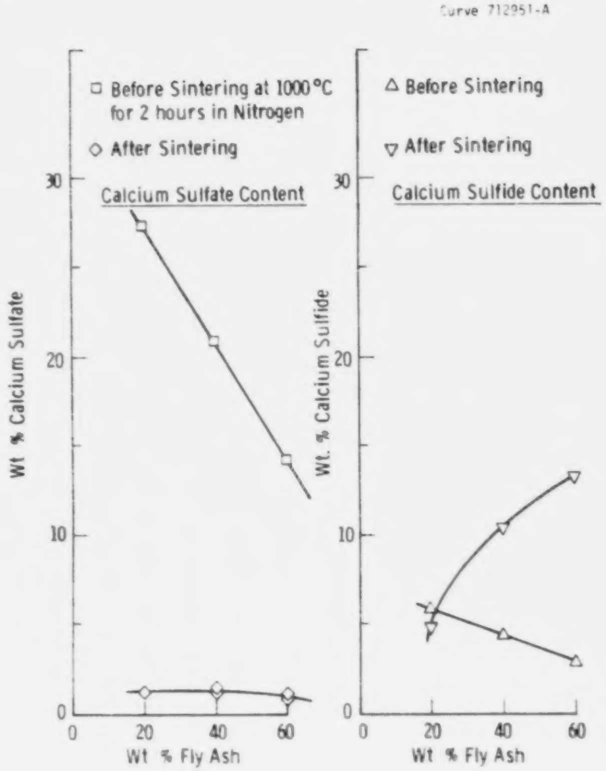

Figure G-1 - Sulfur Retention in Sintered Spent Sorbent/Fly Ash Mixes

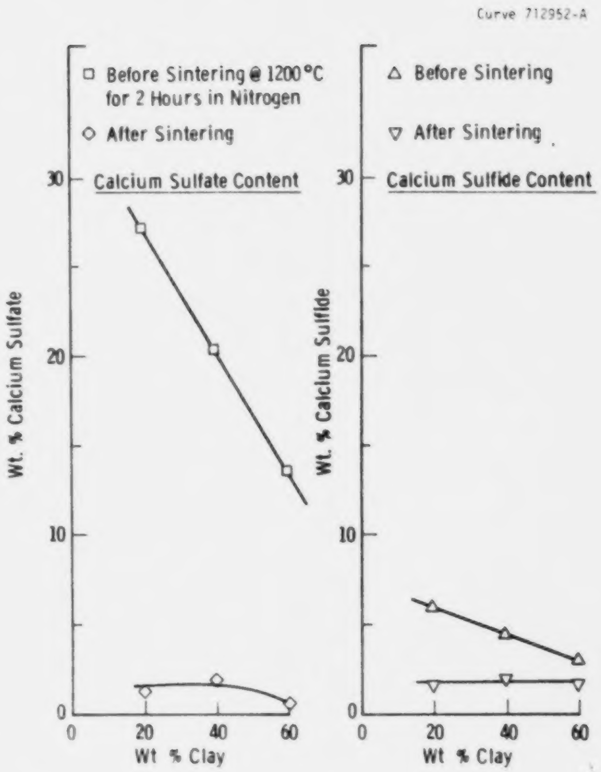

Figure G-2 - Sulfur Retention in Sintered Spent Sorbent/Clay Mixes

The sulfur retention was examined, as shown in Table G-2. The calculations include an allowance for the SO_3 content of the fly ash used, which was 0.00874 g moles SO_3/100 g fly ash. The average sulfate retention was 6.3 percent. This is high by an amount unknown because the yield of product per 100 g charge was not measured. The maximum weight loss if all the sulfur were evolved as SO_2 and no other changes occurred, however, would work out to 21.6 g/100 g sorbent. For mix CF-2 with 60 percent sorbent, the maximum loss possible was 13.0 percent plus 0.3 percent from the SO_3 in the fly ash.

Table G-2

SULFUR RETENTION IN SINTERED SPENT SORBENT/ADDITIVE MIXES

	Specimen					
	CF-1	CF-2	CF-3	CF-4	CF-5	CF-6
Wt % Sorbent	80	60	40	80	60	40
Input, moles/100 g mix						
Total $SO_4^=$	0.2015	0.1533	0.1051	0.1998	0.1498	0.0999
Total $S^=$	0.0822	0.0616	0.0411	0.0822	0.0616	0.0411
Total S	0.2837	0.2149	0.1462	0.2820	0.2115	0.1410
Output, moles/100 g product						
Total $SO_4^=$	0.0090	0.0116	0.0087	0.0095	0.0140	0.0037
Total $S^=$	0.0683	0.1444	0.1852	0.0224	0.0274	0.0224
Total S	0.0773	0.1560	0.1939	0.0319	0.0414	0.0261
Ratios, Output/Input						
Total $SO_4^=$	0.0448	0.0760	0.0824	0.0478	0.0931	0.0368
Total $S^=$	0.832	2.344	4.507	0.273	0.445	0.546
Total S	0.273	0.726	1.326	0.114	0.196	0.185

Calculations show further that the sulfur levels found in CF-2 can be interpreted as follows:

- The overall weight loss was 10.4 percent (which is within the maximum above).

- There was a 54 percent conversion of $CaSO_4$ to CaS.
- There was a 25 percent loss of sulfur from the original CaS present.
- There was a 39 percent decomposition of $CaSO_4$ to CaO.

The identity of the reductant was a matter of speculation earlier. It would appear that something in the fly ash was responsible, and at this point, although the earlier thought of FeO involvement might still be a contributor, it appeared more likely that the carbon content of the fly ash was the source. The NEES fly ash showed a 7.6 percent LOI, and 3.5 percent CO_2. The difference of 4.1 percent may be interpreted as carbon. Mix CF-2, therefore, contained only 82 percent of the carbon needed for the $CaSO_4$ reduction calculated.

A second set of sintering experiments was conducted on mixtures of fly ash and gypsum and fly ash and CaS. These two calcium compounds are potential end products of fuel desulfurization processes. The tests were aimed at narrowing down the effective field of investigation of blends of fly ash with actual spent stones.

Five compositions, three sintering temperatures, one to three sintering times, and two kinds of ambient atmospheres were used. Discs were pressed in a 1-in diameter die at about 2100 MPa (3000 psi) and then sintered. Data are presented in Table G-3 for the gypsum mixes and Table G-4 for the CaS mixes.

Colors developed in the specimens showed a gradation from light to dark (gray, yellow, brown, black) with increasing temperature. The specimens were characterized as fragile, coherent, or strong in accordance with their behavior when handled. There was a trend toward greater cohesiveness as the sintering temperature increased.

The density data did not present a clear picture graphically so a statistical analysis was made. The data matrix is unbalanced (i.e., incomplete) because of our desire to minimize the number of tests. The complete matrix would have required 360 tests (2 sorbent types x 5 fly ash contents x 3 sintering times x 3 sintering temperatures x 2 atmosphere

Dwg. 2622C70

Table G-3

EFFECT OF FLY ASH CONTENT ON SULFUR RETENTION IN SINTERED $CaSO_4$ MIXES[a]

	Composition, wt%					Product				
Sample No.	Gypsum	Fly Ash	Temp., °C	Time, hrs	Nitrogen Flow, scfh	Character	Color	Density, g/cm^3	Composition, wt %	
									$Ca SO_4$	Ca S
75-CF-7	80	20	1000	1	4	Coherent	White	1.761	77.99	1.35
				2		Coherent	White	1.770	–	–
				4		Coherent	White	1.400	–	–
			1100	2		Coherent	Light gray	2.118	71.85	0.36
				4		Coherent	Light gray	2.094	–	–
			1200	2		Strong	Yellow white	2.091	58.42	0.45
			1000	2	0	Coherent	Gray	1.489	–	–
				4		Fragile	Yellow gray	1.393	61.65	–
			1100	4		Fragile	Light brown	1.644	59.20	–
			1200	2		Strong	Dark gray	1.103	2.38	26.24
75-CF-8	70	30	1000	1	4	Coherent	White	1.735	–	–
				2		Coherent	White	1.741	71.64	0.45
				4		Coherent	White	1.226	–	–
			1100	2		Coherent	Light gray	1.992	60.76	1.44
				4		Coherent	Light gray	1.835	57.52	1.26
			1200	2		Strong	Brown	1.783	23.48	0.27
			1000	2	0	Coherent	Gray	1.364	–	–
				4		Powdered	Yellow white	1.265	–	1.26
			1100	4		Powdered	Light brown	1.254	–	1.44
			1200	2		Coherent	–	0.978	–	–
75-CF-9	60	40	1000	1	4	Coherent	White	1.552	–	–
				2		Coherent	Light gray	1.509	–	–
				4		Coherent	Light gray	1.044	–	–
			1100	2		Coherent	Light gray	1.797	–	–
				4		Coherent	Yellow gray	1.345	–	–
			1200	2		Strong	Dark brown	2.318	–	–
			1000	2	0	Fragile	Gray	1.128	–	–
				4		Powdered	Yellow gray	1.036	–	–
			1100	4		Powdered	Light brown	0.998	–	–
			1200	2		Fragile	Black	0.917	–	–
75-CF-10	50	50	1000	1	4	Fragile	Light gray	1.386	–	–
				2		Fragile	Light gray	1.248	–	–
				4		Fragile	Light gray	0.977	–	–
			1100	2		Coherent	Light gray	1.667	–	–
				4		Fragile	Yellow gray	1.151	–	–
			1200	2		Strong	Yellow brown	1.572	–	–
			1000	2	0	Fragile	Dark gray	0.996	–	–
				4		Powdered	Yellow gray	1.018	–	–
			1100	4		Powdered	Light brown	0.962	–	–
			1200	2		Strong	Dark gray	1.664	0.85	0.36
75-CF-11	40	60	1000	1	4	Fragile	Light gray	1.202	–	–
				2		Fragile	Light gray	1.184	–	–
				4		Fragile	Light gray	0.999	–	–
			1100	2		Coherent	Light gray	1.449	22.85	0.63
				4		Fragile	Yellow gray	1.142	–	–
			1200	2		Strong	Dark brown	Melted	1.70	0.72
			1000	2	0	Fragile	Dark gray	1.016	–	–
				4		Fragile	Dark gray	0.978	–	–
			1100	4		Coherent	Light brown	1.045	3.54	0.54
			1200	2		Strong	Black	Sintered	0.34	0.45

---

[a] Fly Ash was from the New England Electric System.[1]

Table G-4

EFFECT OF FLY ASH CONTENTS ON SULFUR RETENTION IN SINTERED CaS MIXES

Composition, wt %						Product				
									Composition, wt %	
Sample No.	CaS Calcium Sulfide	Fly Ash	Temp., °C	Time, hrs	Nitrogen Flow, scfh	Character	Color	Density, g/cm^3	Ca SO$_4$	CaS
75-CF-12	80	20	1000	2	4	Strong	Gray	1.575	1.19	66.32
				4		Coherent	Gray	1.555	–	–
			1100	2		Strong	Gray	1.612	1.53	70.86
				4		Strong	Gray	1.578	0.85	44.96
			1200	2		Strong	Gray, tinge of yellow	1.799	1.02	75.80
			1000	2	0	Strong	Gray	1.652	–	–
				4		Strong	Gray	1.626	–	–
						Strong	Gray, tinge of yellow	1.534	1.02	71.04
			1100	4		Strong	Light brown	1.576	11.06	42.34
						Strong		1.603	–	–
			1200	2		Strong	Dark gray	1.834	1.02	53.89
75-CF-13	70	30	1000	2	4	Coherent	Gray	1.534	2.55	63.23
				4		Coherent	Gray	1.485	–	–
			1100	2		Coherent	Gray	1.772	0.85	62.60
				4		Coherent	Dark gray	1.521	–	–
			1200	2		Strong	Gray, yellow tinge	1.554	1.36	62.69
			1000	2	0	Coherent	Gray	1.502	–	–
				4		Strong	Gray	1.537	–	–
						Coherent	Gray, yellow tinge	1.475		
			1100	4		Coherent	Brown	1.526	6.13	41.67
						Strong	–	1.554	–	–
			1200	2		Strong	Dark gray	1.566	2.72	30.99
75-CF-14	60	40	1000	2	4	Coherent	Gray	1.499	–	–
				4		Coherent	Gray	1.449	–	–
			1100	2		Coherent	Dark gray	1.513	–	–
				4		Coherent	Dark gray	1.429	–	–
			1200	2		Strong	Gray, (yellow tinge)	1.365	–	–
			1000	2	0	Coherent	Dark gray	1.260	–	–
				4		Coherent	Gray	1.467	–	–
						Strong	Gray, (yellow tinge)	1.473	–	–
			1100	4		Coherent	Brown	1.306	–	–
						Strong	–	1.499	–	–
			1200	2		Coherent	Black	1.021	–	–
75-CF-15	50	50	1000	2	4	Coherent	Gray	1.461	–	–
				4		Coherent	Gray	1.386	–	–
			1100	2		Coherent	Dark gray	1.446	–	–
				4		Coherent	Dark gray	1.412	–	–
			1200	2		Coherent	Gray, tinge of yellow	1.394	–	–
			1000	2	0	Coherent	Dark gray	1.359	–	–
				4		Coherent	Dark gray	1.402	–	–
						Coherent	Dark gray	1.430	–	–
			1100	4		Fragile	Brown	1.159	–	–
						Strong	–	1.409	–	–
			1200	2		Coherent	Black	1.087	–	–
75-CF-16	40	60	1000	2	4	Coherent	Dark gray	1.423	2.04	34.63
				4		Fragile	Gray	1.343	–	
			1100	2		Coherent	Dark gray	1.413	1.11	34.10
				4		Coherent	Dark gray	1.354	–	–
			1200	2		Coherent	Dark gray, tinge of yellow	1.300	1.70	39.25
			1000	2	0	Fragile	Dark gray	1.214	–	–
				4		Fragile	Dark gray	1.384	–	–
						Fragile	Gray,	1.390	–	–
			1100	4		Fragile	Brown	1.088	0.94	0.75
						Strong	–	1.357	–	–
			1200	2		Coherent	Dark gray	0.984	0.52	0.36

Notes

1. Fly ash was from the New England Electric System.

types x 2 replicates). The actual number of density determinations available was 103. A series of F-tests were made by extracting balanced submatrices from Tables G-3 and G-4. The level of significance chosen was 5 percent, meaning that if the ratio of the variance of the effect under test to the error variance exceeded the applicable standard F-value, the effect would be termed significant since this result would be obtained by chance less than 5 percent of the time. All such results are marked with an asterisk in the ANOVA (analysis of variance) tables.

The first step in the analysis was to obtain an estimate of the error variance. This is best obtained where tests were replicated. One such set was available, as shown in Tables G-5a and G-5b, covering CaS/fly ash mixes sintered in static nitrogen for four hours. Here, fly ash content was shown to be significant while temperature was not. Since the fly ash and temperature interaction was also insignificant it can be combined with the error variance to get a revised error estimate. The value obtained was 0.00878 with 14 degrees of freedom (d.f.). This does not change the conclusions on significance since the numerical values for the F-ratios are changed only slightly. For fly ash content, F becomes 6.18 versus a table value of 3.11.

Table G-5a

EFFECT OF SINTERING TEMPERATURE AND FLY ASH CONTENT ON THE DENSITY OF CaS/FLY ASH MIXES SINTERED IN STATIC NITROGEN FOR FOUR HOURS

Weight % Fly Ash	Temperature, °C		Mean Density
	1000	1100	
20	1.626; 1.534	1.576; 1.603	1.585
30	1.537; 1.475	1.526; 1.554	1.523
40	1.467; 1.473	1.306; 1.499	1.436
50	1.402; 1.430	1.159; 1.409	1.350
60	1.383; 1.390	1.088; 1.357	1.304
Mean Density	1.472	1.408	1.440

Table G-5b

ANOVA FOR DATA IN TABLE G-5a

Source of Variation	Sum of Squares	Degrees of Freedom	Mean Square	Calculated F-Ratio	F-Ratio @ 5% Level
Fly Ash Content, W	0.2173	4	0.0543	5.82*	3.48
Temperature, T	0.0205	1	0.0205	2.19	4.96
W x T	0.0296	4	0.0074	0.79	3.48
Error	0.0934	10	0.00934		
Total	0.3608	19			

To pursue further the question of the significance of temperature, Table G-6a was assembled and analyzed as in Table G-6b. The four main effects (fly ash content, type of sorbent, temperature, and sintering atmosphere) were all significant. The fly ash effect on density actually was expected, so the effect of the other factors is of greater interest. In contrast to the data on Table G-5, temperature was significant. This suggests that the gypsum data were responsible for the reversal of significance. Discussion of significance is, therefore, better done by treating the CaS and the gypsum results separately.

None of the four-factor or three-factor interactions was significant. Combining these interactions into an error estimate yielded 0.0094 with 17 d.f., again supporting use of the original value.

Continuing with the CaS data, Tables G-7a and G-7b show the effect of temperature when sintering was carried one for 2 hours in flowing nitrogen. Temperature continued to be insignificant for the CaS mixes. The temperature x weight % fly ash interaction also was insignificant and was used to obtain a third estimate of the error variance: 0.0095 with 8 d.f. Mean values of density were calculated and included in Table G-7a.

Table G-6a

EFFECT OF MIX COMPOSITION, TEMPERATURE, AND TYPE OF SINTERING ATMOSPHERE ON THE DENSITIES OF MIXES SINTERED FOR FOUR HOURS

Weight % Fly Ash	Gypsum				Calcium Sulfide			
	Flowing Nitrogen		Static Nitrogen		Flowing Nitrogen		Static Nitrogen[a]	
	1000°C	1100°C	1000°C	1100°C	1000°C	1100°C	1000°C	1100°C
20	1.400	2.094	1.393	1.644	1.555	1.578	1.580	1.590
30	1.226	1.835	1.265	1.254	1.485	1.521	1.506	1.540
40	1.044	1.345	1.036	0.998	1.449	1.429	1.470	1.403
50	0.977	1.151	1.018	0.962	1.386	1.412	1.416	1.284
60	0.999	1.142	0.978	1.045	1.343	1.354	1.387	1.223

NOTE:

[a] The values for calcium sulfide-static nitrogen are averages of the repeats shown in Table G-5.

Tables G-8a and G-8b explore the significance of sintering time for the CaS mixes. Neither time nor temperature was significant, and the effect of fly ash content was shown to be limited to a linear relationship.

Compositing the four interaction terms led to a smaller estimate of the error variance: 0.0026 with 13 d.f. Use of this value made the effect of time significant at the 1 percent level: 10.4 versus 9.07. This result means further tests are needed to define the contribution of sintering time.

One further effect on the case of the CaS mixes can be checked - the effect of atmosphere - using the data for four hours of sintering time. Tables G-9a and G-9b present this analysis. We concluded that only the weight % fly ash was significant.

Table G-6b

ANOVA FOR DATA IN TABLE G-6a

Source of Variation	D.F.	Sum of Squares	Mean Square	Calculated F-Ratio	F-Ratio @ 5% Level
Temperature, T	1	0.0894	0.0894	9.6*	4.96
Atmosphere, A	1	0.0751	0.0751	8.1*	4.96
Mixture, M[a]	1	0.4213	0.4213	45.3*	4.96
Weight %, W[b]	4	1.050	0.2624	28.0*	3.48
T x A	1	0.1106	0.1106	11.9*	4.96
T x M	1	0.1413	0.1413	15.2*	4.96
A x M	1	0.0568	0.0568	6.1*	4.96
T x W	4	0.0902	0.0226	2.4	3.48
A x W	4	0.0075	0.0019	0.2	3.48
M x W	4	0.2383	0.0596	6.4*	3.48
T x A x M	1	0.0431	0.0431	4.6	4.96
T x A x W	4	0.0091	0.0023	0.2	3.48
T x M x W	4	0.0356	0.0089	0.96	3.48
A x M x W	4	0.0318	0.0080	0.86	3.48
T x A x M x W	4	0.0403	0.0101	1.1	3.48
Total	39	2.4404			
Error	10	0.0934	0.0093		

[a] Refers to type of sorbent.
[b] Refers to fly ash content.

Compositing interaction terms led to 0.0022 as the internal estimate of error, with 13 d.f. Use of this smaller error did not change any of the conclusions on significance.

Turning next to the gypsum results, Tables G-10a and G-10b contain an analysis of the effect of sintering temperature and weight of fly ash on density. In contrast to the CaS results, and, as suspected from the analyses of Tables G-5b and G-6b, temperature had a significant effect

Table G-7a

EFFECT OF SINTERING TEMPERATURE AND FLY ASH CONTENT ON THE DENSITY OF CaS/FLY ASH MIXES SINTERED IN FLOWING NITROGEN FOR TWO HOURS

		Temperature, °C			
		1000	1100	1200	Mean Density
Weight Percent Fly Ash	20	1.575	1.612	1.799	1.662
	30	1.534	1.772	1.554	1.620
	40	1.499	1.513	1.365	1.459
	50	1.461	1.446	1.394	1.434
	60	1.423	1.413	1.300	1.579
Mean Density		1.498	1.551	1.482	1.510

Table G-7b

ANOVA FOR THE DATA OF TABLE G-7a

Source of Variation	Degrees of Freedom	Sum of Squares	Mean Square	Calculated F-Ratio	F-Ratio @ 5% Level
Temperature, T	2	0.0130	0.0065	0.7	4.10
Weight % Fly Ash, W	4	0.1826	0.0457	4.91*	3.48
T x W	8	0.0759	0.0095	1.02	3.07
Total	14	0.2715			
Error	10	0.0934	0.0093		

on the density of gypsum/fly ash sinters. The temperature x weight % fly ash interaction was also significant. The actual effect of fly ash content on density is shown in Table G-10a.

Examination of the data in Table G-10a reveals that the data point at 1200°C for 40 percent fly ash is out of line with the rest of the table. At each level of fly ash, density at 1100°C is greater than at

Table G-8a

EFFECT OF SINTERING TIME ON THE DENSITY OF CaS/FLY ASH MIXES SINTERED IN FLOWING NITROGEN

Weight % Fly Ash	Sintering Time, hr				Mean Density
	2		4		
	Temperature, °C		Temperature, °C		
	1000	1100	1000	1100	
20	1.575	1.612	1.555	1.578	1.580
30	1.534	1.772	1.485	1.521	1.578
40	1.499	1.513	1.449	1.429	1.472
50	1.461	1.446	1.386	1.412	1.426
60	1.423	1.413	1.343	1.354	1.383
Mean density	1.498	1.551	1.444	1.459	1.488

Table G-8b

ANOVA FOR DATA IN TABLE G-8a

Source of Variation	Degrees of Freedom	Sum of Squares	Mean Square	Calculated F-Ratio	F-Ratio @ 5% Level
Time, t	1	0.0271	0.0271	2.91	4.96
Temperature, T	1	0.0058	0.0058	0.6	4.96
Weight % Fly Ash, W	4	0.1264	0.0316	3.4	3.48
Linear	1	0.1187	0.1187	12.8*	4.96
Remainder	3	0.0077	0.0026	0.28	3.71
t x T	1	0.0018	0.0018	0.2	4.96
t x W	4	0.0084	0.0021	0.2	3.48
T x W	4	0.0139	0.0035	0.4	3.48
t x T x W	4	0.0093	0.0023	0.2	3.48
Total	19	0.1927			
Error	10	0.0934	0.0093		

Table G-9a

EFFECT OF TYPE OF SINTERING ATMOSPHERE ON THE DENSITY OF CaS/FLY ASH MIXES SINTERED FOR FOUR HOURS

Weight % Fly Ash	Type of Sintering Atmosphere				Mean Density
	Flowing Nitrogen		Static Nitrogen[a]		
	Temperature, °C		Temperature, °C		
	1000	1100	1000	1100	
20	1.555	1.578	1.580	1.590	1.574
30	1.485	1.521	1.506	1.540	1.513
40	1.449	1.429	1.470	1.403	1.438
50	1.386	1.412	1.416	1.284	1.374
60	1.343	1.354	1.387	1.223	1.327
Mean Density	1.444	1.459	1.472	1.408	1.445

[a] The entries under static nitrogen are all averages of the two repeats which were shown in Table G-4.

Table G-9b

ANOVA FOR THE DATA OF TABLE G-9a

Source of Variation	Degrees of Freedom	Sum of Squares	Mean Square	Calculated F-Ratio	F-Ratio @ 5% Level
Temperature, T	1	0.0028	0.0028	0.3	4.96
Atmosphere, A	1	0.0006	0.0006	0.06	4.96
Weight %, W	4	0.1616	0.0404	4.34*	3.48
T x A	1	0.0080	0.0080	0.86	4.96
T x W	4	0.0093	0.0023	0.2	3.48
A x W	4	0.0046	0.0011	0.1	3.48
T x A x W	4	0.0065	0.0016	0.2	3.48
Total	19	0.1934			
Error	10	0.0934	0.0093		

Table G-10a

EFFECT OF SINTERING TEMPERATURE AND FLY ASH CONTENT ON THE DENSITY OF GYPSUM/FLY ASH MIXES SINTERED FOR TWO HOURS IN FLOWING NITROGEN

Weight % Fly Ash	Temperature, °C			Mean Density
	1000	1100	1200	
20	1.770	2.118	2.091	1.993
30	1.741	1.992	1.783	1.839
40	1.509	1.797	2.318	1.875
50	1.248	1.667	1.572	1.496
Mean Density	1.567	1.894	1.941	1.801

Table G-10b

ANOVA FOR THE DATA OF TABLE G-10a

Source of Variation	Degrees of Freedom	Sum of Squares	Mean Square	Calculated F-Ratio	F-Ratio @ 5% Level
Temperature, T	2	0.3316	0.1658	17.83*	4.10
Weight %, W	3	0.4108	0.1369	14.7	3.71
T x W	6	0.2123	0.0354	3.81*	3.22
Total	11	0.9547			
Error	10	0.0934	0.0093		

1000 or 1200°C. At 40 percent fly ash the density trend from 1000 to 1100°C is the same but then shows a marked increase, rather than a decrease, in going to 1200°C. A repeat measurement at these conditions is needed to determine whether the density increase is real.

Tables G-11a and G-11b examined the effect of sintering time on the density of gypsum/fly ash mixes sintered in flowing nitrogen at 1000°C.

Table G-11a

EFFECT OF SINTERING TIME ON THE DENSITY OF GYPSUM/FLY ASH MIXES SINTERED AT 1000°C IN FLOWING NITROGEN

Weight % Fly Ash	Sintering Time, hr			Mean Density
	1	2	4	
20	1.761	1.770	1.400	1.644
30	1.735	1.741	1.226	1.567
40	1.552	1.509	1.044	1.368
50	1.386	1.248	0.977	1.204
60	1.202	1.184	0.999	1.128
Mean	1.527	1.490	1.129	1.382

Table G-11b

ANOVA FOR DATA IN TABLE G-11a

Source of Variation	Degrees of Freedom	Sum of Squares	Mean Square	Calculated F-Ratio	F-Ratio @ 5% Level
Time, t	2	0.4837	0.2419	26*	4.10
Weight %, W	4	0.5975	0.1494	16*	3.48
t x W	8	0.0507	0.0063	0.7	3.07
Total	14	1.1319			
Error	10	0.0934	0.0093		

Time had a greater effect than fly ash content. The density decreases or prolonged sintering may be attributed to the evolution of H_2O, SO_2, and oxygen on decomposition of gypsum.

Tables G-12a and G-12b present an analysis of the effect of type of sintering atmosphere on density. All three main effects were significant, as was the interaction on temperature and atmosphere.

Table G-12a

EFFECT OF TYPE OF SINTERING ATMOSPHERE OR THE DENSITY OF GYPSUM/FLY ASH MIXES SINTERED FOR FOUR HOURS

Weight % Fly Ash	Type of Sintering Atmosphere				Mean Density
	Flowing Nitrogen		Static Nitrogen		
	Temperature, °C		Temperature, °C		
	1000	1100	1000	1100	
20	1.400	2.094	1.393	1.644	1.633
30	1.226	1.835	1.265	1.254	1.395
40	1.044	1.345	1.036	0.998	1.106
50	0.977	1.151	1.018	0.962	1.027
60	0.999	1.142	0.978	1.045	1.041
Mean Density	1.129	1.513	1.138	1.181	1.240

Table G-12b

ANOVA FOR DATA IN TABLE G-12a

Source of Variation	Degrees of Freedom	Sum of Squares	Mean Square	Calculated F-Ratio	F-Ratio @ 5% Level
Temperature, T	1	0.2277	0.2277	24.5*	4.96
Atmosphere, A	1	0.1312	0.1312	14.1*	4.96
Weight %, W	4	1.125	0.2813	30.2*	3.48
T x A	1	0.1459	0.1459	15.7*	4.96
T x W	4	0.1168	0.0292	3.1	3.48
A x W	4	0.0349	0.0087	0.9	3.48
T x A x W	4	0.0427	0.0107	1.2	3.48
Total	19	1.8242			
Error	10	0.0934	0.0093		

Another response to sintering on which data were obtained was residual sulfide and sulfate content. Figures G-3 through G-6 show the change in sulfur content as a function of fly ash content, which may be summarized as follows:

- For gypsum in flowing nitrogen, at 1100°C/2 hr the residual $CaSO_4$ decreased linearly with an increase in fly ash content. At 1200°C/2 hr, there was a sharp decrease in $CaSO_4$ even at 30 percent fly ash and over 95 percent loss of sulfate at 60 percent fly ash.
- For gypsum in static nitrogen, sulfur losses were greater at all levels of fly ash content than were those for flowing nitrogen.
- Sulfide content reached levels to 1.5 percent, but there was no clear effect of fly ash content.
- For CaS in flowing nitrogen, there was a decrease of about 12 percent in sulfide sulfur, independent of fly ash content in the range of 20 to 60 percent. There appeared to be a small increase in sulfate content with increase in fly ash content to the level of 1.7 percent CaS.
- For CaS in static nitrogen there was a sharp decrease in sulfide sulfur with an increase in fly ash content with over 99 percent rejection at 60 percent fly ash. The 1100°C/4 hr data showed about 9 percent $CaSO_4$.

One can only speculate at this point on the gypsum results. If there were to be any $CaSO_4$ decomposition, use of flowing nitrogen to sweep away the SO_2/O_2 formed should have favored it. The loss of sulfate sulfur was not via reduction to sulfide and must, therefore, have been as SO_2. One possibility is that in static nitrogen the temperature of the sinter may have been higher than the thermocouple indication. This reasoning is supported by cross plots in Figures G-7 and G-8 showing the effect of temperature on the sulfur retention of gypsum fly ash mixes versus CaS/fly ash mixes. Increasing temperature from 1000 to 1100°C led to a small loss of sulfate sulfur from the gypsum mixes, but on

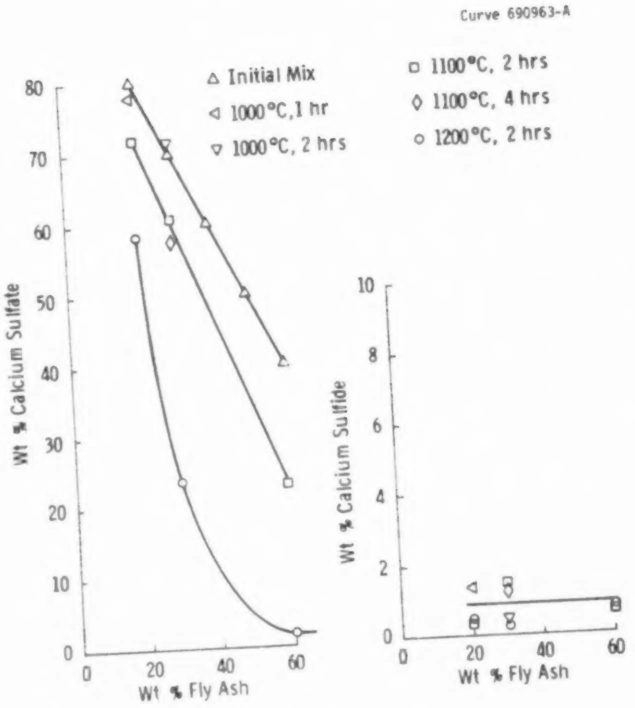

Figure G-3 - Sulfur Retention in Gypsum/Fly Ash Mixes Sintered in Flowing Nitrogen

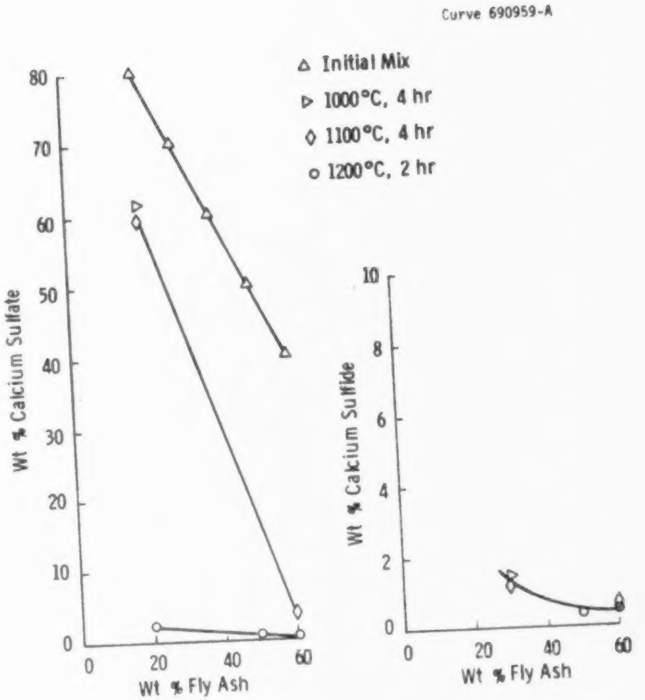

Figure G-4 - Sulfur Retention in Gypsum/Fly Ash Mixes Sintered in Static Nitrogen

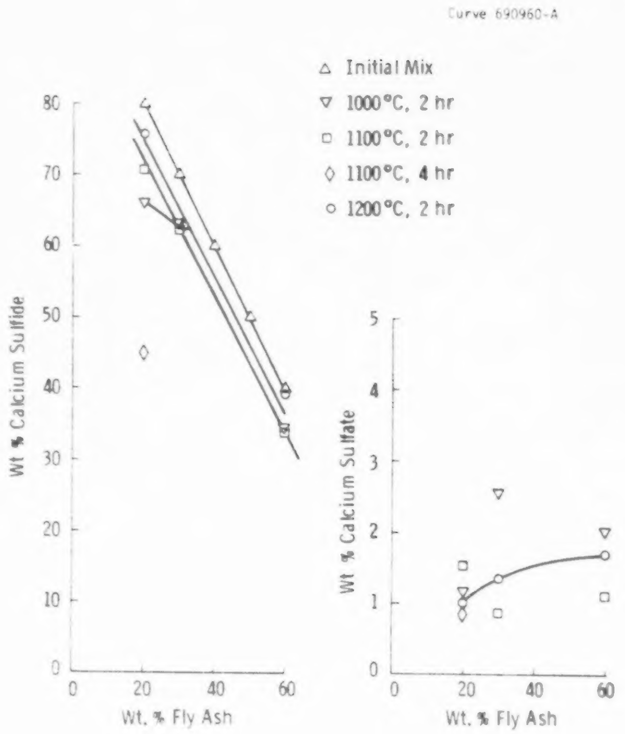

Figure G-5 - Sulfur Retention in Calcium Sulfide/Fly Ash Mixes Sintered in Flowing Nitrogen

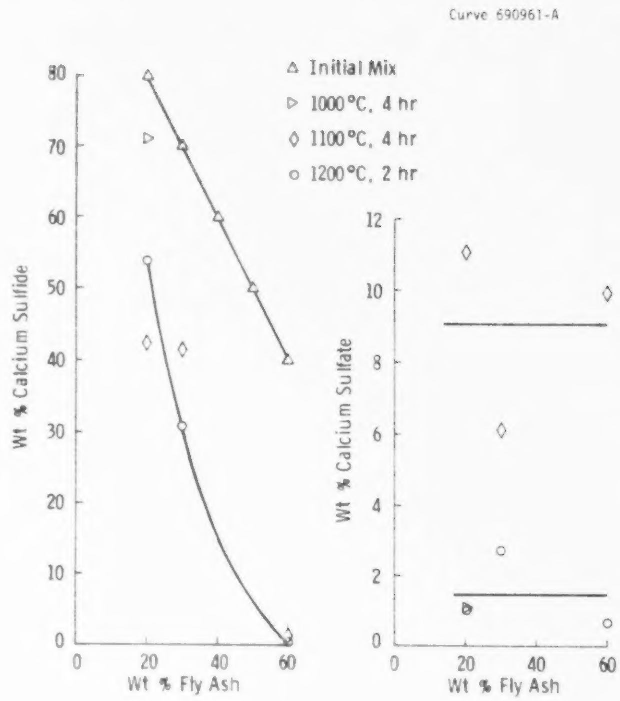

Figure G-6 - Sulfur Retention in Calcium Sulfide/Fly Ash Mixes Sintered in Static Nitrogen

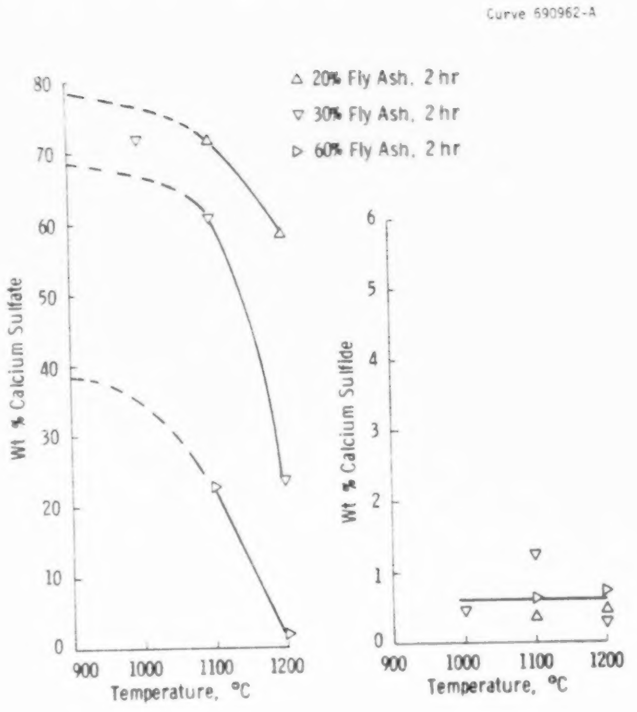

Figure G-7 - Effect of Temperature on Sulfur Content of Gypsum/Fly Ash Mixes Sintered in Flowing Nitrogen

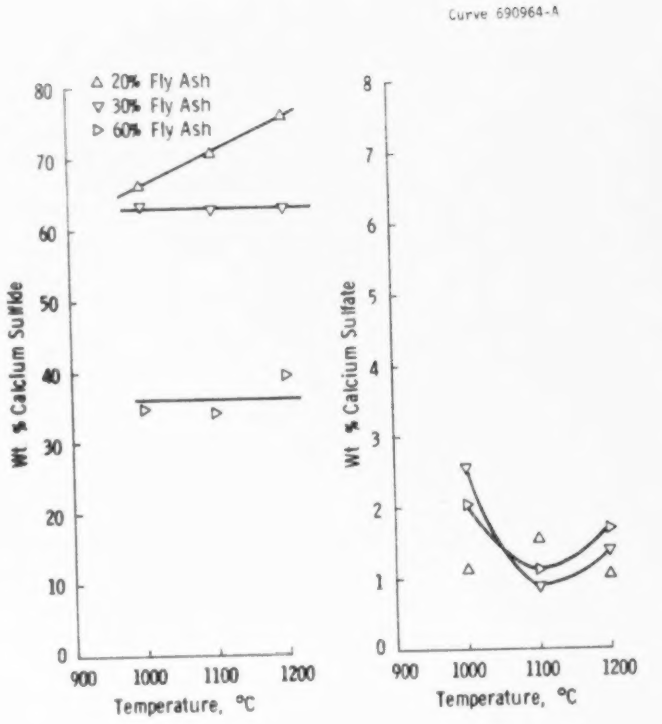

Figure G-8 - Effect of Temperature on Sulfur Content of Calcium Sulfide/Fly Ash Mixes Sintered in Flowing Nitrogen further increase to 1200°C, major to over 95 percent loss of sulfate sulfur occurred. In contrast, temperature was without effect on the CaS mixes except at the lowest level (20%) of fly ash. Here a linear increase with temperature was demonstrated. This might better be regarded as a loss at 1000°C, decreasing with an increase in temperature. Since no effect of temperature on CaS was demonstrated for 20 percent fly ash, the losses in the case of gypsum are attributed to decomposition.

Another technique for carrying out the spent sorbent/fly ash reaction is hot pressing, a modified sintering operation in which the specimen is subjected simultaneously to heat and pressure. A higher density was expected with this technique than with conventional atmospheric pressure sintering. Figure G-9 is a sketch of the apparatus. A reducing atmosphere is probably created at the surface of the pellet being made, permitting a test of the hypothesis that air leakage in the first set of sintering tests was responsible for the loss of sulfide sulfur. The sketch shows a top plunger of graphite; in subsequent work, this was changed to an aluminum rod.

Two compositions were evaluated:

- 80 percent CaS plus 20 percent fly ash (75-CF-17 series)
- 80 percent gypsum plus 20 percent fly ash (75-CF-18 series).

Each powder sample was thoroughly mixed, placed in the die, and heated while pressure was applied to the upper plunger. Specimens were held at selected temperatures and pressures for 30 minutes. The whole assembly was then cooled, and measurements were made on the specimens from which their density was calculated. These results are in Tables G-13 and G-14 and plotted in Figures G-10 and G-11.

The specimens were obtained in the form of cylinders, 1.27 cm (1/2 in) diameter and about 2.54 cm (1 in) long, with a graphite coating outside. They appeared well compacted and sintered and did not disintegrate with aging as had specimens made by conventional sintering. Both compositions showed an increase in density with an increase in hot-pressing temperature. The effect of temperature, however, is more

Dwg. 6358A32

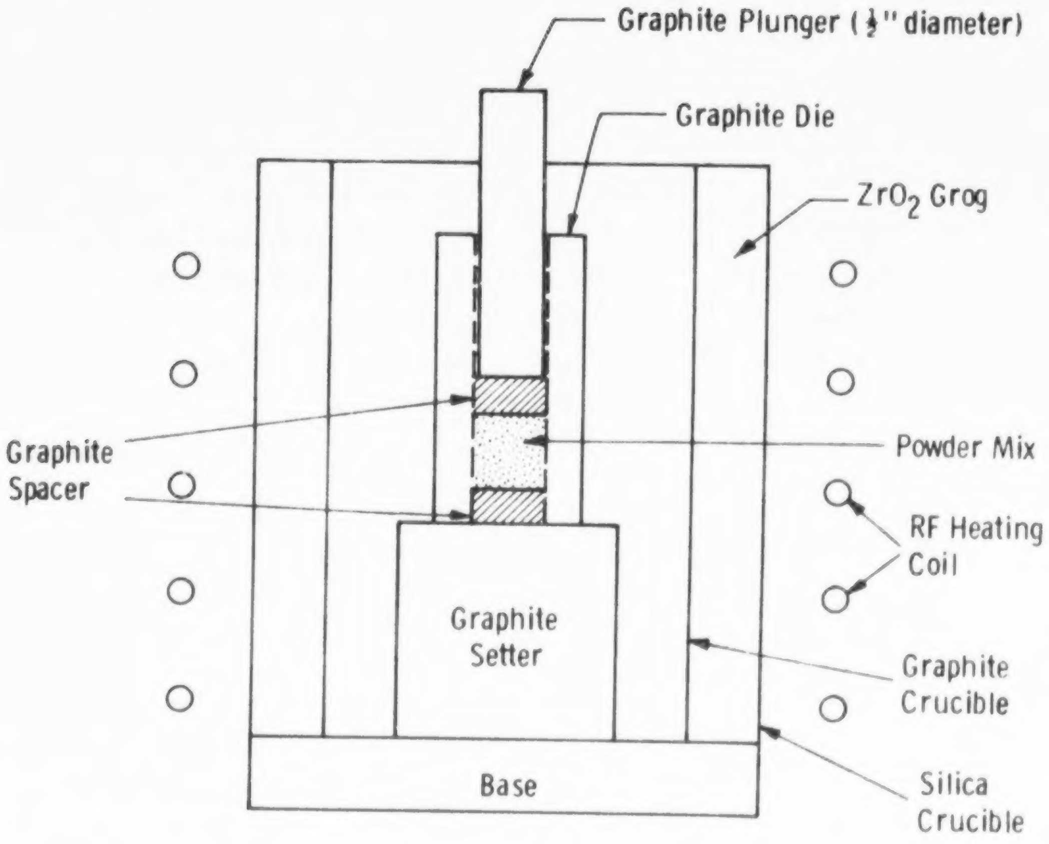
Graphite Plunger ($\frac{1}{2}$" diameter)
Graphite Die
ZrO_2 Grog
Graphite Spacer
Powder Mix
RF Heating Coil
Graphite Setter
Graphite Crucible
Base
Silica Crucible

Figure G-9 - Schematic of Hot Pressing Unit

Table G-13

Dwg.1706B06

CHARACTERISTICS OF HOT-PRESSED 80% CALCIUM SULFIDE/20% FLY ASH MIXES. SERIES 75-CF-1

Hot Pressing Conditions			Product		Composition, wt %				
Force, N (lb)	Nominal Pressure, MPa (psi)	Temperature, °C	Density, g/cc	Compressive Strength, MPa (psi)	Total Sulfur	Sulfide	Sulfate	Calcium	Calculated Total Sulfur Wt % [a]
3559 (800)	28.1 (4074)	850	1.76	–	17.98	0.11	54.03 ; 54.28	–	18.18
						0.16	55.05	–	18.53
		950	2.43	–	17.86	0.48;0.71	50.42	–	17.31
			2.47	65.2 (9450)	–	0.24	58.90	–	19.90
		1050	2.74	–	15.64	2.47;2.77	41.21	30.06	16.37
		1200[b]	2.67	122.4(17750)	–	6.06	27.45	35.27	15.22
4448 (1000)	35.1 (5093)	850	1.89	37.2 (5400)	–	11.41	20.85	–	18.37
		950	2.30	23.4 (3400)	–	0.56	50.40	–	17.38
			2.54	34.1 (4950)	–	0.52	57.34	–	19.66
		1050	2.78	–	–	–	–	–	–
5338 (1200)	42.1 (6112)	850	2.01	–	25.54	18.70;17.85	20.11;20.80	–	25.11
						19.68;18.82	22.02	–	26.60
		950	2.47	–	18.65	0.40;0.56	50.90	–	17.46
		1050	2.74	54.8(7950)	16.04	1.55;1.12	49.10	–	17.72

Notes:

a Initial value 35.59 wt %

b Specimen hot pressed for 15 minutes; all others, 30 minutes

Dwg. 1706807

Table G-14

CHARACTERISTICS OF HOT-PRESSED 80% GYPSUM/20% FLY ASH MIXES. SERIES 75-CF-18[a]

Hot Pressing Conditions			Product		Composition, wt %				
Force, N (lb)	Nominal Pressure, MPa (psi)	Temperature, °C	Density, g/cc	Compressed Strength, MPa (psi)	Total Sulfur	Sulfide	Sulfate	Calcium	Total Sulfur, wt %[b]
3559 (800)	28.1 (4074	850	2.03	–	15.73	0.24	56.90;54.26	–	18.78
		1050	2.70	–	16.39	1.75	46.23;43.95	29.66	16.80
5338 (1200)	42.1 (6112)	850	2.21	–	17.34		57.76 56.08;56.89 54.77[c]	–	18.99
		1050	2.85		16.72	1.56	42.88;45.08		16.24

[a] All specimens hot pressed for 30 minutes

[b] Initial value 14.94 wt%

[c] Gravimetric determination

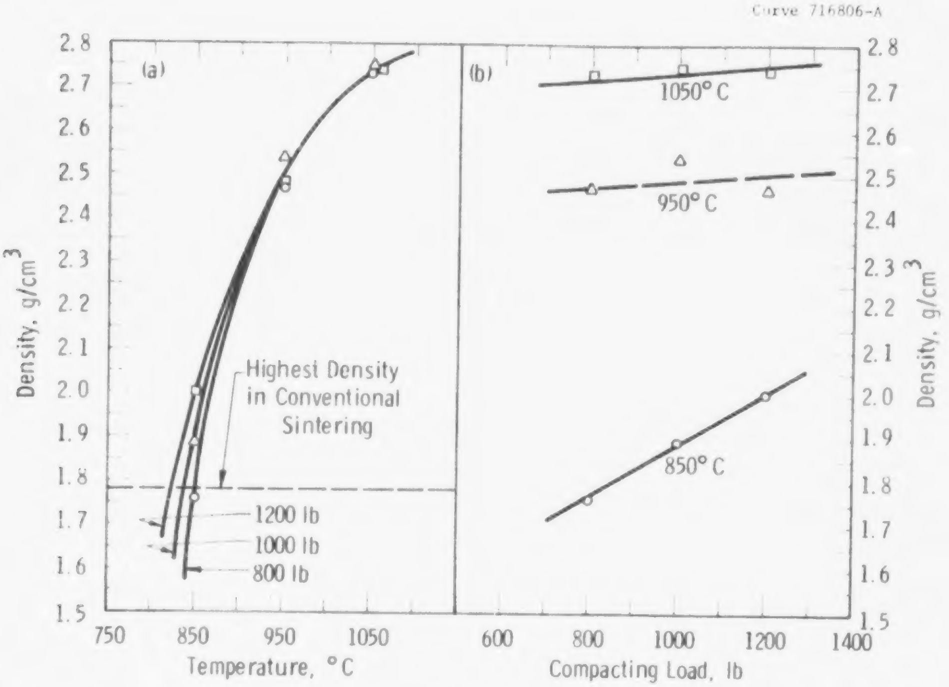

Figure G-10 - Density Data of the Hot-Pressed Specimens Having the Composition of 80% CaS and 20% Fly Ash

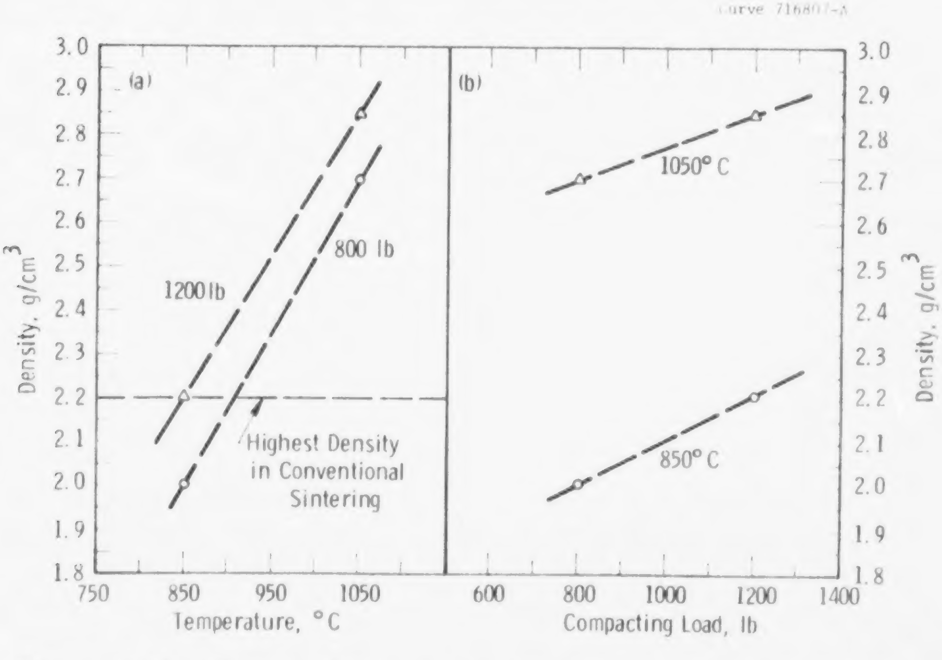

Figure G-11 - Density Data of the Hot-Pressed Specimens Having the Composition of 80% $CaSO_4$ and 20% Fly Ash pronounced than the effect of pressure. Figure G-10 indicates that for the CaS/fly ash composition the effect of pressure is negligible when the temperature is high, 950 to 1050°C, but significant at 850°C.

Figure G-11 for the $CaSO_4$/fly ash compositions again shows a strong effect of temperature. The effect of pressure is somewhat greater at 1050°C and somewhat smaller at 850°C than for CaS/flv ash.

For comparison the highest densities obtained by conventional sintering are included in both the figures. Note that hot pressing yields higher density when conducted at high temperature, for example, 850°C.

The specimens showed no degradation upon aging for several weeks, in contrast with sintered specimens, which crumbled on aging. Table G-13 shows compressive strength data for one composition: 80 wt % CaS plus 20 percent fly ash. The values obtained are comparable to those of typical cement composites. The data show considerable scatter but the combined effect of higher temperature and pressure appears to be increased compressive strength. The value of 122.4 MPa (17,750 psi) obtained at 800 lb/ 1200°C may not be representative. Compressive strengths on the gypsum/fly ash specimens were not measured; a comparison is made below in a subsequent experiment.

Chemical analyses for some of the specimens were obtained as shown also in Tables G-13 and G-14. The four gypsum/fly ash specimens showed total sulfur contents in the range of 15.7 to 17.3 wt %, corresponding to 66.8 to 73.6 wt % $CaSO_4$ versus 80 percent initially. The CaS/fly ash specimens showed total sulfur contents in the range of 15.6 to 25.5 percent, or 35.2 to 57.5 percent CaS versus 80 percent initially. Sulfide was determined by an iodometric method, while sulfate was determined by an ion-exchange method. As a check on the validity of these methods, the total sulfur was calculated from these values and compares well with the total sulfur determined by a bomb method. As a further check, the sulfate was determined gravimetrically for one specimen (Table G-14, (c)). While the gravimetric value was somewhat lower than the ion-exchange values, the relative agreement indicates no serious interferences from the anions.

The sulfur data are plotted in Figures G-12 through G-14. The gypsum results are as expected: low CaS content and decreasing $CaSO_4$ content with an increase in temperature. The CaS results were unexpected. The 78 wt % $CaSO_4$ found at 850°C/5.52 MPa (800 psi) corresponds to 41.3 wt % CaS or about 52 percent of the original CaS content, so despite the expectation that hot pressing would exclude atmospheric oxygen, about half the CaS was oxidized to the sulfate and the rest of the sulfide sulfur was lost.

For explanations of the above changes, atmospheric oxygen seems most likely compared to hydrolysis loss by moisture or reduction of ferric oxide (Fe_2O_3) as per the following equations:

$$4\ Fe_2O_3 \rightarrow 8\ FeO + 2\ O_2$$

$$CaS + 2\ O_2 \rightarrow CaSO_4 \quad .$$

These appear thermodynamically possible, since the net free energy change at 1000°C is -7782 J/g mole of CaS. Stoichiometry, however, limits the conversion to less than 1 percent.

In another test, 75-CF-32, CaS was hot pressed with Fe_2O_3. The cylindrical specimen produced was magnetic, confirming the ability of CaS to reduce Fe_2O_3. Additional observations should be made to clarify what chemical changes are occurring.

Further experiments were conducted to explore the effect of particle size. Pure CaS/fly ash and $CaSO_4 \cdot 2H_2O$/fly ash mixes were compared with the CAFB regenerator stone/fly ash mixes. Three compositions were made with each system, as shown in Table G-15. Each composition was ball milled for two hours, screened to -125 μm, and subjected to hot pressing for one hour in a 1.9-cm (3/4 in) graphite die at approximately 3310 MPa (4800 psi) and 1050°C. A flowing nitrogen atmosphere was

Curve 690933-A

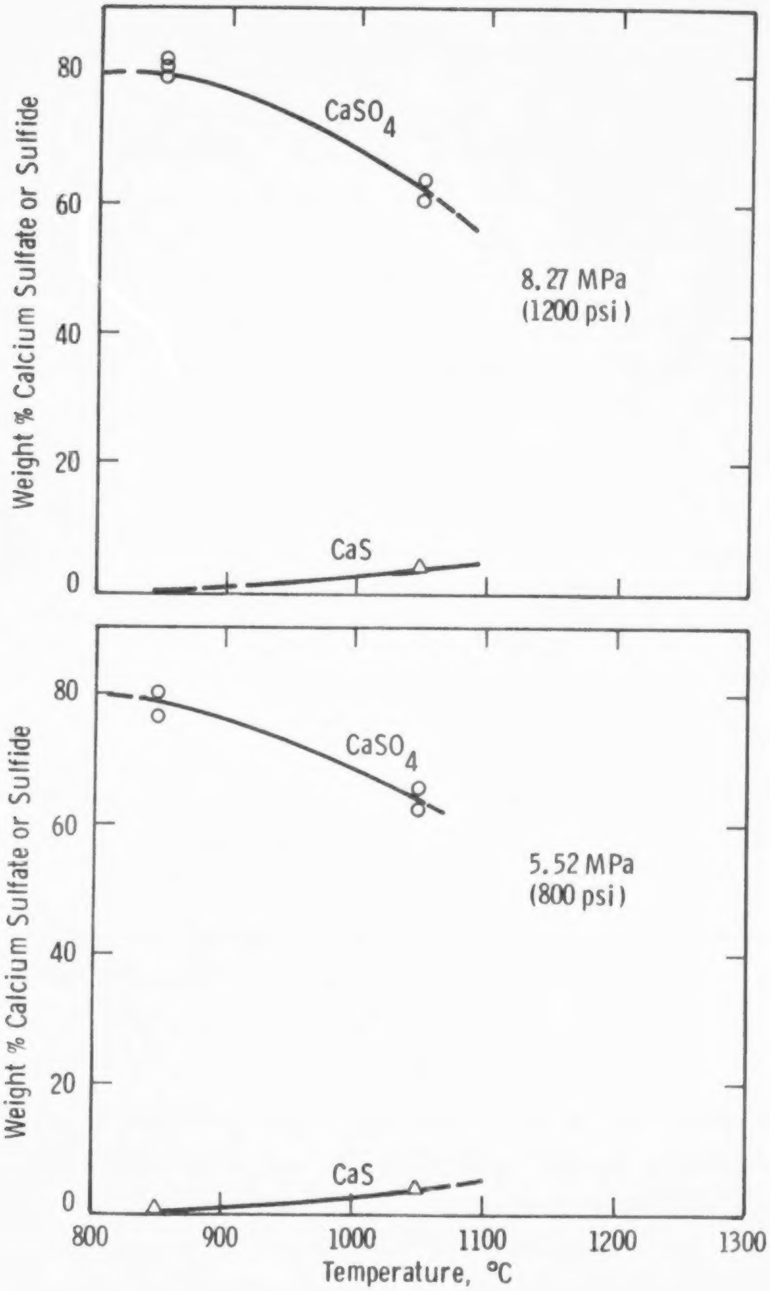

Figure G-12 - Residual Sulfur Content of Hot-Pressed Gypsum/Fly Ash Mixes. Series 75-CF-18

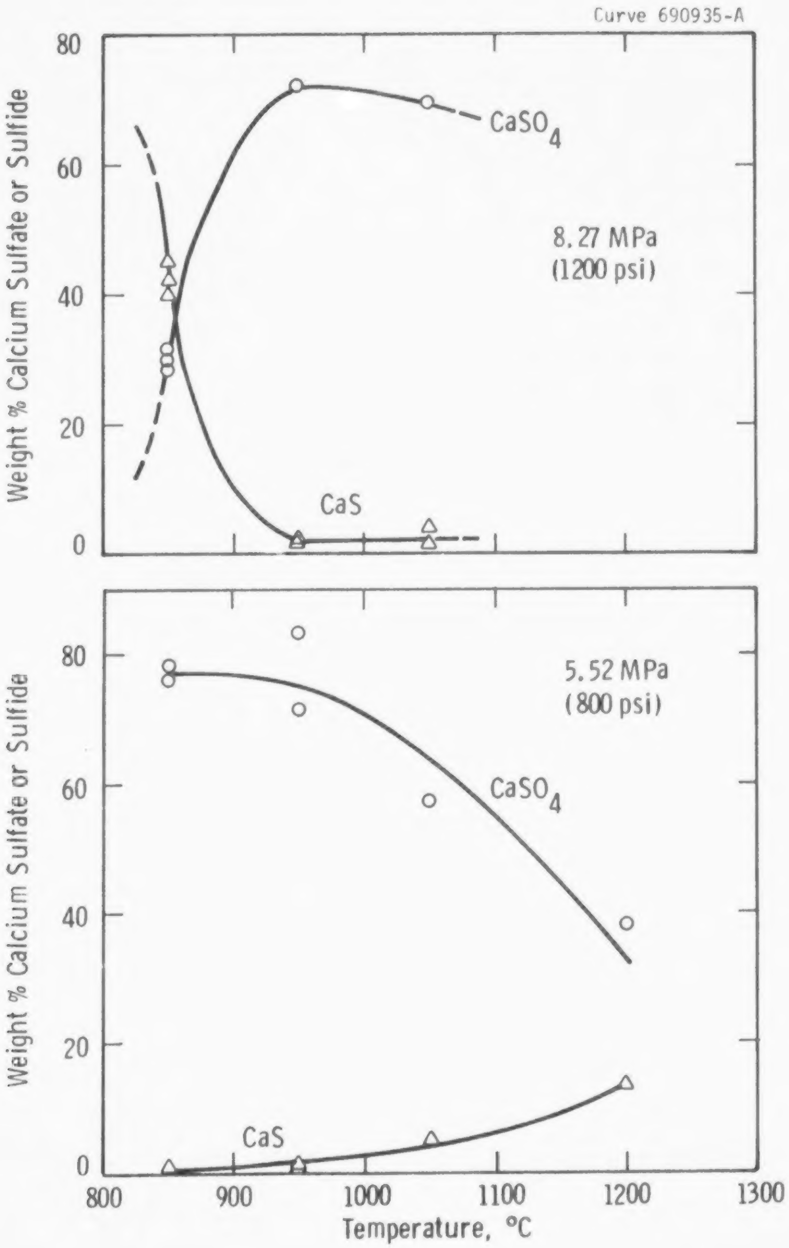

Figure G-13 - Residual Sulfur Content of Hot-Pressed Calcium Sulfide/Fly Ash Mixes. Series 75-CF-17

Curve 690934-A

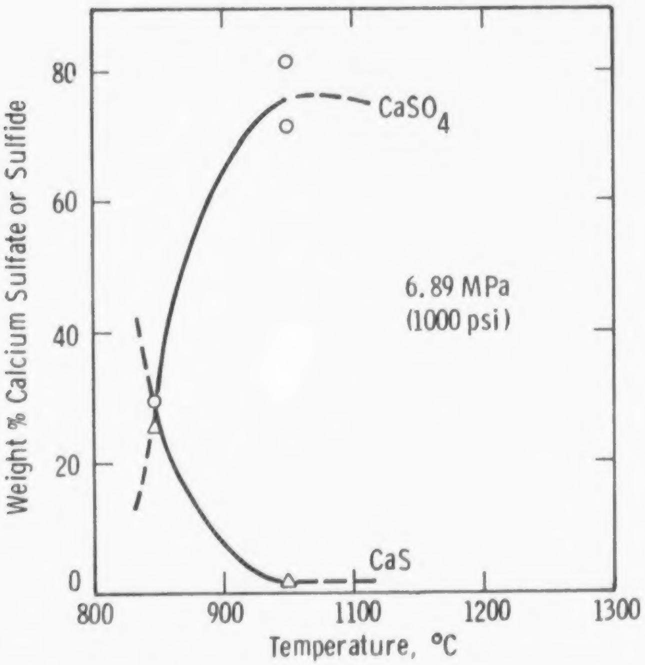

Figure G-14 - Residual Sulfur Content of Hot-Pressed Calcium Sulfide/Fly Ash Mixes. Series 75-CF-17

maintained during the experiment. After the samples were hot pressed, they were calipered and weighed. The calculated densities of the CAFB/ fly ash specimen were slightly higher than those of the other two systems.

All three systems show a decrease in density as the fly ash content increases from 20 to 80 wt %, consistent with the fact that the density of fly ash is lower than that of the other three components.

While all of the mixes were successfully hot pressed, when aged in air two of the specimens crumbled within 30 days. Table G-15 also presents compressive strength data on the hot-pressed mixes. The values were much higher than expected so a further test was devised.

Six of the specimens were pulverized by a combination of methods, including ball milling. The samples were first hand crushed to -841 μm (-20 mesh) and then ball milled with Al_2O_3 balls in an aluminium-lined mill. Dry milling did not produce any significant size reduction, so a liquid vehicle was added, as noted in Table G-16. Except for one

Table G-15

COMPRESSIVE STRENGTH OF HOT-PRESSED MIXES OF FLY ASH[2] AND VARIOUS CALCIUM COMPOUNDS

Specimen Identification	Composition, wt %		Condition after Aging[b]	Compressive Strength		Density, g/cc
	CaS	Fly Ash		MPa	psi	
75-CF-22	80	20	Good	195.8	28,400	2.55
75-CF-23	50	50	Good	243.4	35,300	2.46
75-CF-24	20	80	Good	199.0	28,860	2.40
	$CaSO_4 \cdot 2H_2O$	Fly Ash				
75-CF-25	80	20	Crumbled	--	--	2.43
75-CF-26	50	50	Good	45.2	6,550	2.35
75-CF-27	20	80	Good	120.0	17,400	2.22
	CAFB Stone	Fly Ash				
75-CF-28	80	20	Crumbled	--	--	2.57
75-CF-29	50	50	Good	--	--	2.55
75-CF-30	20	80	Good	261.2	37,880	2.46

---

[a] Fly Ash was from the Duquesne Light Co., Phillips Plant, Pittsburgh, PA.

[b] Minimum aging time about one month.

gypsum/fly ash mix, methanol was used to avoid setting in the presence of water. A 240 cm^3 (1/2 pt) capacity ball mill was used to grind approximately 15 g of the sample. The grinding was done overnight, following which the slurry was passed through a 44 μm (325 mesh) screen. There was a mild smell of sulfur after grinding in some cases.

The powders were filtered and dried and then mixed with Ottawa sand and water. The sand-to-powder ratio was 2.67 and the water-to-powder ratio 0.5. A control specimen was made with Portland cement and Ottawa sand. The pastes were allowed to set in 1.9 cm diameter by 1.27 cm high (3/4 in diameter by 1/2 in high) Teflon cylindrical molds. After 24 hr the specimens were taken out of the mold so we could see whether they remained as solid blocks or crumbled to powder. This result is recorded in Table G-16, along with the composition of the hot-pressed powder. The powder compositions containing CaS and fly ash showed a cementlike setting property. The strongest block qualitatively was obtained with 50 percent CaS + 50 percent fly ash.

Compressive strengths for the CaS/fly ash mixes and the Portland cement controls after curing in air for 7 days are given in Table G-16. While the values obtained were lower than those for Portland cement, the CaS/fly ash hot-pressed specimens do have a cementlike setting property.

Table C-16

SETTING CHARACTERISTICS OF MIXES OF SAND AND POWDERED HOT-PRESSED MATERIALS[a,b]

Specimen Identification	Powder Composition,[c] Wt %		Observation After 24 Hrs	7-Day Compressive Strength	
	CaS	Fly Ash		kPa	psi
75-CF-22	80	20	Solid block, strong	965	140
75-CF-23	50	50	Solid block, very strong	1723	250
75-CF-24	20	80	Solid block, moderately strong	620	90
	$CaSO_4 \cdot 2H_2O$	Fly Ash			
75-CF-26	50	50	Crumbled to powder	--	
75-CF-27	20	80	Crumbled to powder	--	
	CAFB-9 Stone	Fly Ash			
75-CF-30	20	80	Crumbled to powder	--	
Control	Portland cement		Solid block, strong	5860	850

---

[a] The mixes contained 22 g of Ottawa sand and powdered specimens of hot-pressed materials in weight ratio of 2.67/1 plus 3 cc of water. The pastes were allowed to set in Teflon molds for 24 hours.

[b] The hot-pressed specimens were all ground in methanol except for 75-CF-27, which was ground in water prior to being mixed with sand and water.

[c] The "powder composition" is before hot pressing.

APPENDIX H

CALCIUM SULFIDE STUDIES

The first run made in the 10-cm laboratory fluidized-bed test unit, Batch L-1, served to check operability and to produce a test quantity of sulfated limestone. Supplies of spent sorbent from the CAFB pilot plant regenerator were extremely limited, and the initial tests were therefore planned around use of a simulated stone produced by sulfiding calcined limestone and then oxidizing this to the sulfate.

In L-1, 1600 g of -595 +420 μm Limestone 1359 were calcined, sulfided, and air oxidized in separate operations. Tables H-1 and H-2 contain the operating conditions for the run while Table H-3 contains product analyses. Table H-4 presents an analysis of the performance, based on the chemical compositions of the samples in various stages. We assumed that no material was lost by elutriation, since we had found less than 1 g of solids in the cyclone and essentially nothing in the final filter. This was a sintered metal filter with a mean pore size of 65 μm and rated at 100 percent removal of 20 μm particles and 98 percent of 8 μm particles in gas service. The active filtering area was 334 cm^2 (0.36 ft^2). The filter pressure drop normally was essentially zero.

Calcination was high but incomplete in the first step and essentially completed during sulfidation. Oxidation (70.8% of the CaS) was also high but significantly less than the complete conversion desired.

Figures H-1 and H-2 show photomicrographs of sulfided and oxidized particles. The particles were embedded in plastic and then ground and polished to expose the interior of the grains. The outer layer is plastic while the darker layer inside is CaS. There was no evidence of pores containing CaS that had penetrated deep into the particles. Further, there was no evidence of CaS deep within the particles of oxidized stone.

Table H-1

MATERIAL BALANCE DATA FOR LIMESTONE SULFIDATION STUDIES

	Gas Flow Rates (ℓ/min) 15°C, 1 atm				Batch Charge, g
	N_2	H_2S	H_2	Air	
BATCH L-1					
Fluidization	89				800
	134				1600
Calcination	43				
Sulfidation	43	0.90	4.08		
Oxidation	37			6.1	
BATCH L-4					
Fluidization	194				1000
	202				2000
Calcination	45				
Sulfidation	55	1.2	3.0		1100
Oxidation	52-18			9.4-5.5	
BATCH L-6					
Calcination	36				1476
Sulfidation	18	2.51	5.15		
Oxidation	22			8.8	300[a]

---

[a] Sulfided limestone. Bulk density - 1.276 g/cc.

Thus it appeared that in the fluidized bed most of the sulfide sulfur was laid down initially close to the surface of each particle, at least to the level of 21 percent sulfidation. This suggested that if the CaS were present in a sufficiently thin layer, it might be possible to oxidize it completely to $CaSO_4$.

Table H-2

TIME/TEMPERATURE DATA FOR LIMESTONE SULFIDATION STUDIES

	Heating	Reacting	Cooling
BATCH L-1. Particle Size -595 + 420 μm			
Calcination	125 min @ 600-730°C	195 min @ 730-760°C	
Sulfidation	170 min @ 659-766°C	120 min @ 766°C	40 min @ 766-589°C
Oxidation	130 min @ 651-810°C	150 min @ 810-795°C	40 min @ 795-520°C
BATCH L-4. Particle Size -1190 + 500 μm			
Calcination	1260 min @ 600-730°C	315 min @ 730-906°C	40 min @ 906-600°C
Sulfidation	300 min @ 25-762°C	20 min @ 762°C	50 min @ 762-457°C
Oxidation	345 min @ 480-870°C	155 min @ 870-935°C	15 min @ 935-835°C
BATCH L-6. Particle Size -595 + 149 μm			
Calcination	60 min @ 548-743°C	255 min @ 743-904°C	-
Sulfidation	-	125 min @ 864-880°C	15 min @ 866-760°C
Oxidation	Standby overnight @ 378°C		
	200 min @ 370-859°C	180 min @ 859-872°C	120 min @ 872-349°C

Environmentally, there would still be a problem because the core of the particles would be CaO. On the other hand, if the calcium could be completely sulfided, it might be possible to encapsulate a CaS core with a relatively impermeable $CaSO_4$ shell. A process material balance on a no-loss basis is shown in Table H-5.

The next run in this series was L-4, in which -1190 +500 μm mesh particles of Limestone 1359 were calcined, sulfided to a low degree, and then oxidized with air. Sulfidation was set by stoichiometry. The data in Table H-3 indicate that the sulfidation achieved was uniform across the bed at about 5.1 mol % of the calcium, as planned. The reactor product after oxidation wtih 3.2 percent oxygen showed 1.6 to

Table H-3

CHEMICAL ANALYSIS OF STONE SAMPLES FROM LIMESTONE SULFIDATION STUDIES

Batch	Component wt %				
	Ca	$S^{=}$	$SO_4^{=}$	ΣS	CO_2
Batch L-1					
Calcined	61.7	-	-	-	11.9
Sulfided	64.6	10.9	0.15	-	2.1
Oxidized	55.0	3.3	24.0	-	-
Batch L-4					
Feed	40.19	-	-	-	43.38
Calcined	68.48	-	-	-	4.19
Sulfided, center of bed	65.93	2.70	-	2.45	4.93
Sulfided, edge of bed	-	2.65	-	-	-
Oxidized					
+1190 μm	65.32	-	-	0.86	4.84
+841 μm	67.39	-	-	1.04	-
+595 μm	66.69	0.05	-	1.90	-
+500 μm	67.27	0.05	-	1.12	-
-500 μm	67.00	0.05	-	1.32	-
Batch L-6					
Feed	38.76	-	-	-	43.41
Sulfided, powder	48.61	32.69	-	28.09	-
Sulfided, sinter	42.23	30.65	-	-	-
Oxidized	49.74	27.95	4.01	27.80	-

3.6 mol % of the calcium was sulfated. The highest sulfation was in the -841 +595 μm fraction. These results showed that the thin layer of CaS was not readily oxidizable under the conditions used without losing a substantial amount of sulfur (30-70%). The SO_2 monitor on the

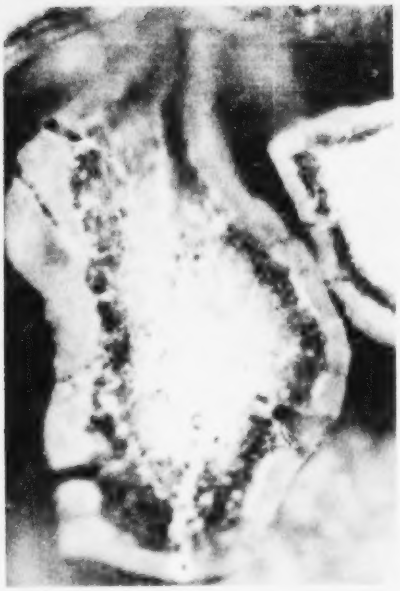

Figure H-1 - Sulfided Limestone, -595 +420 μm

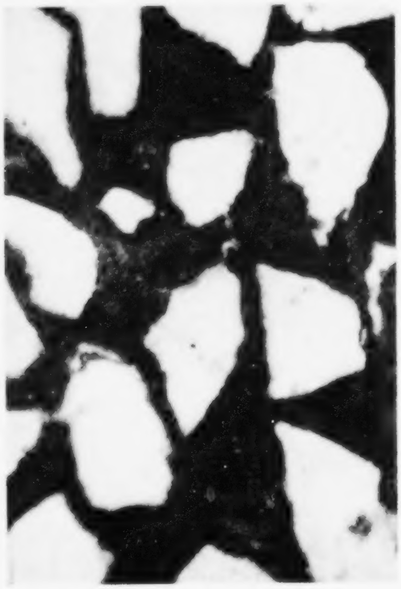

Figure H-2 - Oxidized Sulfided Limestone, -595 +420 μm

Table H-4

CALCULATED RESULTS FOR BATCH L-1

	Calcined Stone	Sulfided Stone	Oxidized Stone
Composition, wt %			
$CaCO_3$	27.05	4.77	---
CaO	71.23	68.67	57.25
CaS	---	24.48	7.41
$CaSO_4$	---	0.21	34.00
Inerts	1.72	1.87	1.34
	100.00	100.00	100.00
Ratios			
Inert content, g/g mol Ca	1.116	1.158	0.974
% of $CaCO_3$ calcined	82.5	97.04	---
% of Ca sulfided	---	21.0	7.48
% of CaS oxidized	---	---	70.8
Stoichiometry			
Mols of H_2S fed		4.57	---
Mols of CaS made, theor.		3.32	---
Mols of O_2 fed		---	8.13
Mols of $CaSO_4$ made, theor.		---	2.87

off-gas during oxidation showed about 0.5 percent SO_2 within 5 minutes after cutting in the air stream, rising to about 1 percent, and then dropping to 0.1 percent within 20 minutes.

Following the completion of the oxidation based on quantity of air fed, an attempt was made to simulate exposure to the CAFB regenerator conditions of 1070°C in a mildly oxidizing atmosphere. Flow rates were cut back to minimize possible carry-over. The total excess oxygen used

Table H-5

PROCESS MATERIAL BALANCE FOR BATCH L-1

	Raw Stone	Calcined Stone	Sulfided Stone	Oxidized Stone
Material Balance, g mols				
$CaCO_3$	15.822	2.774	0.468	---
CaO	---	13.048	12.012	11.765
CaS	---	---	3.327	1.183
$CaSO_4$	---	---	0.015	2.874
Totals	15.822	15.822	15.822	15.822
Material Balance, g				
$CaCO_3$	1582.19	277.41	46.76	---
CaO	---	730.68	672.68	658.86
CaS	---	---	239.88	85.29
$CaSO_4$	---	---	2.08	391.12
Inerts	17.81	17.81	17.81	17.81
Totals	1600.00	1026.00	979.21	1153.08
Composition, wt %				
Calcium	39.55	61.68	64.63	54.89
Carbon dioxide	43.51	11.90	2.10	---
Sulfide	---	---	10.91	3.29
Sulfate	---	---	0.15	23.95
Inerts	1.11	1.74	1.82	1.54

was 10.1 moles at a concentration ranging from 3.2 to 4.9 percent. The maximum temperature attainable with the equipment appeared to be 935°C after two hours, so the run was terminated.

Some change in particle size distribution was also noted. The final oxidized product contained 1 percent +1190 μm and 4 percent -500 μm versus none of these fractions in the original limestone charge. The total cyclone catch was 15.8 g or 0.08 percent of the original charge. The filter catch was 0.2 g.

Limestone batch L-6 was aimed at 100 percent sulfidation of -595 +149 μm stone followed by 100 percent oxidation to $CaSO_4$. Significant corrosion attack was observed for the first time. The reactor bed thermocouple Inconel sheath had been penetrated and had to be replaced. Some hard deposits on the reactor wall had formed and, by scraping, a small amount of scale was removed. The concentration of H_2S used was 10 percent versus 2 percent in previous runs. The temperature level was 870 to 900°C versus 760°C. The hydrogen concentration was also increased to 20 percent versus 5 to 8.5 percent to continue suppression of the dissociation of H_2S.

The average sulfide content found was 30.48 wt % versus an average calcium of 45.42 percent. On a mole basis, there were 0.951 moles of sulfur, 1.133 moles of calcium, corresponding to 84 mole % sulfidation.

The oxidation level achieved with 6 percent oxygen was lower than had been expected or desired: 3.4 mole % of the calcium sulfated. The retention of sulfur was about 83 percent. There was no problem of controlling bed temperature with the conditions used. Further exploration of CaS production was deferred in favor of dry sulfation studies.

APPENDIX I

TEST PROCEDURES FOR IN SITU LEACHING OF SPENT SORBENTS WITH SEAWATER

TEST I

This test is to determine the leaching of spent stone by mixing with natural seawater under field winter conditions at an offshore mid-Atlantic location. Two hundred grams of material are placed in 2 liters of seawater in a 4 liter container and placed on a magnetic stirrer for 24 hours. Temperature and pH are recorded for every 15 minutes in the first hour and every 6 hours after the start of the test for 24 hours. After 6 hours of the test, 1 liter is removed and sealed in a glass jar for analysis. After 24 hours, the remaining liter is sealed for analysis. (Note: When removing the samples of water, stop the stirrer and allow the particles to settle out before removing the water samples.) Perform this test on all three chemicals. A control sample must be kept for each different seawater type used.

TEST II

This test is to determine the leaching of spent stone as a function of concentration in natural seawater. Four concentrations (20, 100, 200, and 400 g) are placed in 1 liter of seawater in 2-liter breakers. Pour each packet of material in such a way as to form a mound of spent stone in each beaker. Do not stir. Any rolling of the ship will provide all the mixing necessary. Temperature and pH are recorded every 15 minutes in the first hour and every 6 hours after the start of the test for 24 hours. After 24 hours, the water is decanted off to be sealed for analysis, a scraping of the surface of each mount is placed in a vial for analysis, and a core of each mound is removed for analysis. Ten grams are needed of each for analysis. A control sample of seawater must be taken for analysis.

Table I-1

CHEMICAL ANALYSES OF SPENT SORBENT SAMPLES

Source	ANL	ERCA	Westinghouse R&D
Type of stone sorbent	Dolomite	Limestone CAFB 9	Dolomite D-2
Composition, wt %			
$CaSO_4$	57	4.35	53.83
$CaCO_3$	9	--	--
CaO	2	84.26	13.83
CaS	<0.05	5.04	0.91
MgO	20	--	25.99
Inerts	12	6.35	5.44
	100	100.00	100.00

Table I-2

TEST I. EFFECT OF LEACHING TIME ON LIQUOR TEMPERATURE AND pH

Stone	CAFB-9	Argonne	Westinghouse D-2
Initial Seawater Conditions			
Temperature, °C	14.5 ± 2.1	18.45 ± 1.1	18.45 ± 1.1
pH	8.5	7.95	7.95

Time, hr	Temperature Rise, °C	pH	Temperature Rise, °C	pH	Temperature Rise, °C	pH
0	0.0	9.0	0.70	9.0	1.0	10.4
0.25	0.3	9.3	1.95	10.1	1.85	10.5
0.50	0.7	9.5	3.50	10.1	2.50	10.5
0.75	1.1	10.2	4.00	10.1	2.80	10.9
1.0	1.4	10.3	4.90	10.1	3.20	11.8
6.0	4.6	10.3	6.20	9.9	4.50	12.0
12.0	5.3	10.0	6.70	9.9	5.00	12.0
18.0	5.2	9.9	6.70	10.0	5.50	12.0
24.0	5.3	9.9	7.30	10.0	5.80	11.9

Table I-3

TEST II. EFFECT OF TREAT RATIO ON LEACHING OF SPENT SORBENTS

Treat Ratio, g/	Stone	CAFB-9		Argonne		Westinghouse D-2	
	Time, hrs	ΔT, °C	pH	ΔT, °C	pH	ΔT, °C	pH
20	0.00	0.0	8.5	0.25	7.7	0.8	7.7
	0.25	0.25	8.75	1.45	8.05	0.95	8.6
	0.50	0.80	8.9	3.10	8.13	1.6	8.8
	0.75	1.19	8.95	3.50	8.15	1.8	8.9
	1.00	1.47	9.05	4.40	8.18	2.3	9.0
	6.0	2.42	9.65	6.20	8.3	4.1	9.85
	12.0	2.69	9.70	7.90	8.6	5.3	9.97
	18.0	2.37	10.0	7.80	8.62	5.9	10.12
	24.0	2.30	10.0	7.60	8.6	5.3	9.95
100	0.00	*	*	0 05	7.7	0.6	7.7
	0.25	*	*	1.35	8.58	1.25	9.65
	0.50	*	*	3.0	8.65	1.9	10.05
	0.75	*	*	3.40	8.68	2.2	10.13
	1.00	*	*	4.4	8.70	2.7	10.15
	6.0	*	*	6.3	8.70	4.0	9.91
	12.0	*	*	7.5	9.20	5.1	10.4
	18.0	*	*	7.7	9.20	5.7	10.55
	24.0	*	*	7.4	9.15	5.2	10.2
200	0.00	2.51	9.9	0.0	7.7	†	†
	0.25	23.9	9.6	1.45	8.92	†	†
	0.50	26.43	9.5	3.0	9.0	†	†
	0.75	25.36	9.5	3.4	9.0	†	†
	1.00	23.47	9.55	4.4	9.3	†	†
	6.0	22.93	10.10	6.3	9.08	†	†
	12.0	22.84	10.10	7.5	9.5	†	†
	18.0	22.26	10.20	7.7	9.55	†	†
	24.0	22.2	10.20	7.5	9.48	†	†
400	0.00	70.25	--	0.0	7.7	0.7	7.7
	0.25	51.92	11.3	1.55	9.5	2.65	10.28
	0.50	41.64	11.25	3.1	9.52	3.6	10.29
	0.75	36.5	11.25	3.5	9.55	4.0	10.25
	1.00	33.38	11.35	4.3	9.58	4.5	10.2
	6.00	33.39	11.8	5.6	9.3	4.2	9.92
	12.00	32.98	11.8	9.3	10.05	5.2	10.7
	18.0	32.19	11.9	8.6	10.1	5.7	11.2
	24.0	32.22	11.9	7.6	9.72	5.4	11.82

*Sample lost
†Insufficient sample for test

APPENDIX J

ANALYTICAL PROCEDURES USED ON SAMPLES FROM OCEAN DUMPING TESTS

SAMPLE PREPARATION

Solids

A representative fraction of the sample was transferred to a platinum vessel and dried at 110°C in excess of 12 hours (overnight). It was reduced in a tungsten carbide mortar and pestle to a <100 mesh size and finally diluted with high-purity graphite prior to spectrochemical determination.

Liquids

Samples of the liquids were obtained by agitating the bottle or jar until all sediment was uniformly distributed whence a known volume was removed and immediately filtered through a millipore. The filtrate was transferred to a 100 ml tared plastic beaker and evaporated to dryness over low heat on an electric hot plate.

The insoluble fraction was transferred to a tared platinum crucible and dried at 110°C. The dried weight corrected for the filter was used in calculating the solid to liquid relationship. This dried residue was diluted with graphite in the same manner as for solids.

SPECTROSCOPY

All of the spectrochemistry was done on a Jarrell Ash 3.4 meter, Ebert mount spectrograph. Direct current arc excitation was employed in an argon-oxygen atmosphere supplied by a modified Stallwood type jet. The samples were compared against standards made by adulterating at various levels high purity calcium carbonate or sodium chloride with the elements of interest. Visual comparisons were made against these standards with an estimated accuracy of 1/2 to 2X the determined value. Determination of selenium was done by flameless atomic absorption.

A preliminary analysis of some of the samples had been made to generally characterize them. Impurities incorporated in graphite were used in this instance.

Table J-1

EXTRACTION OF TRACE ELEMENTS FROM CABF REGENERATOR STONE BY SEAWATER

Sample Identification (1)		Element Concentration, ppm						Solids Concentration g/ℓ	Sample Volume, liters
		Cr	Ni	Sn	V	Cu	Pb		
II S L2	**Background**	<0.5	0.05	<0.5	<0.1	0.1	<0.15	-	-
I C 6 LM	Filtrate	<0.2	<0.2	<0.7	<1	0.2	<0.2	3.3	1.0
	Floc	<30	500	<100	3000	<30	<30	7.9	-
I C 24 LM	Filtrate	<0.2	<0.2	<0.7	<1	0.2	<0.2	3.4	1.0
	Floc	<30	330	<100	2000	30	<30	11.9	-
I C 6 L1	Filtrate	<1	<1	<1	<0.5	<1	<1	-	1.0
	Floc	10	50	20	200	20	10	1.2	0.28
I C 24 L1	Filtrate	<0.3,<1	<0.3,<1	<0.7,<1	<1,<0.5	<0.3,<1	<1	3.6	1.0
	Floc	<30,10	100,100	<100,<20	1000,600	30,20	<30,10	1.8	0.30
II C 20 L1	Filtrate	<0.5	0.05	<0.5	<0.1	<0.05	<0.15	-	-
	Floc	<30	50	<10	100	30	10	0.3	0.28
II C 100 L1	Filtrate	<0.5	0.05	<0.5	<0.1	0.05	<0.15	3.2	-
	Floc	<30	20	10	50	10	<10	0.9	0.26
II C 200 L1	Filtrate	<0.3	<0.3	<0.8	<1	0.8	<0.2	3.8	-
	Floc	<30	30	<100	500	30	<30	1.4	-
II C 400 L1	Filtrate	<0.5	0.5	<0.5	<0.1	0.1	<0.15	-	
	Floc	<30	30	<10	50	10	<10	3.4	0.23
II C 20 CS		<20	800	<6	>2000	<10	<20	-	-
II C 100 CS		<30	330	<100	2000	30	<30	-	-
II C 200 CS		<30	330	<100	2000	30	<30		
II C 400 CS		<20	800	<6	>2000	<10	<20	-	-

Table J-1 (Cont)

EXTRACTION OF TRACE ELEMENTS FROM ARGONNE SPENT SORBENT BY SEAWATER

Sample Identification (1)		Element Concentration, ppm Cr	Ni	Sn	V	Cu	Pb	Concentration g/ℓ	Sample Volume, liters
I A 6 L	Filtrate	<1	<1	<1	<0.5	<1	<1	-	1.0
	Floc	100	20	<20	70	30	10	2.7	1.0
I A 24 L	Filtrate	<1	<1	<1	<0.5	<1	<1	-	1.0
	Floc	100	20	<20	70	30	10	12.4	0.92
II A 20 L	Filtrate	1	0.1	<0.5	<0.1	0.1	<0.15	-	-
	Floc	300	200	20	100	1000	30	0.03	1.0
II A 100 L	Filtrate	<0.5	0.05	<0.5	<0.1	<0.05	<0.15	-	-
	Floc	<30	20	20	30	20	10	0.2	1.0
II A 400 L	Filtrate	<0.2,<1	<0.2,<0.3	<0.7,<0.3	0.3,<1	0.2,0.3	<0.2,<0.3	3.4	-
	Floc	100	50	<100	100	100	<30	1.1	0.82
II A 20 CS		70	20	<6	40	10	<20	-	-
II A 400 CS		70	20	<6	40	10	<20	-	-

EXTRACTION OF TRACE ELEMENTS FROM WESTINGHOUSE SIMULATED SPENT SORBENT BY SEAWATER

Sample Identification (1)		Element Concentration, ppm Cr	Ni	Sn	V	Cu	Pb	Concentration g/ℓ	Sample Volume, liters
I D 6 L	Filtrate	<1	<1	<1	<0.5	<1	<1	-	1.0
	Floc	150	200	<20	5	50	10	2.6	1.0
I D 24 L	Filtrate	<1	<1	<1	<0.5	<1	<1	-	1.0
	Floc	150	200	<20	5	50	10	11.7	0.86
II D 20 L	Filtrate	<0.5	0.05	<0.5	<0.1	<0.05	<0.15	-	-
	Floc	<30	20	<10	<10	20	<10	1.0	0.90
II D 100 L	Filtrate	<0.5	0.05	<0.5	<0.1	0.1	<0.15	-	-
	Floc	<30	50	<10	<10	50	<10	2.6	1.0
II D 400 L	Filtrate	<0.5	<0.05	<0.5	<0.1	0.05	<0.15	-	-
	Floc	<30	30	<10	<10	100	10	4.0	1.0
II D 20 CS		20	800	<6	10	10	<20	-	-
II D 400 CS		70	800	<6	10	10	<20	-	-

NOTES TO TABLE J-1.

1. Sample code numbers have the following meanings:

First character	I or II	Refer to test conditions I or II
Second character	C	CAFB regenerator stone (limestone)
	A	Argonne dolomite
	D	Dolomite from Westinghouse test unit
Third group	6,24	Applies to Test I and designates the time at which the sample was taken
	20,100,200, 400	Applies to Test II and designates the grams of sorbent used per liter of sea water
Fourth group	L1, L2, L3	Indicates liquid sample 1, 2, and 3
	LM	Indicates liquid sample using Maryland offshore water
	CS,SS	Indicates core solids or surface solids
	SM	Indicates solids from test with Maryland offshore water

APPENDIX K

EXTRACTION OF SELECTED TRACE ELEMENTS BY SEAWATER FROM SPENT SORBENTS

	Mercury, ppb	Selenium, ppm	Fluorine, ppm
II SL 1	<1	ND (1)	0.68
II A 400 L	<1	ND (1)	0.23
II C 400 L	-	-	0.41
II A 400 CS	<10	ND (2)	34
II C 400 CS	-	-	46

(1) Not detected by flameless atomic absorption: level is < 0.1 ppm
(2) Not detected by flameless atomic absorption: level is < 1 ppm